THE UNIVERSITY
of EDINBURGH

A Novel Organ Culture Model

For a Complete Synovial Joint:

Creation and Application

Yi-Cheng Lin

Presenting for The Degree of Doctor of Philosophy

The University of Edinburgh – 2014

Contents

Tables and Figures

DECLARATION

I declare that all the material presented in this thesis is my own work and I composed this thesis. The thesis has not been submitted in part or in whole for any other degree or professional qualification in other academic institutes.

Yi-Cheng Lin

Edinburgh

20th June 2014

ACKNOWLEDGEMENTS

I would like to express my profound gratitude to my supervisor, Professor Hamish Simpson, for his kindness and thoughtfulness throughout the period when I am in Edinburgh. His creative thinking in various fields of orthopaedic research and effective strategies to solve encountered experimental problems deeply influence me that change me from an orthopaedic surgeon to a good scientific researcher. I also wish to thank Dr Andrew Hall for his generous support of the use of confocal laser scanning microscope and for his limitless patience in discussion, from which several marvellous ideas could be additionally included in the thesis. I also want to thank Professor Donald Salter for his clever point of view to interpret my experimental results that enables me to think in different directions.

I would like to thank the following people: Dr Innes Smith at the Centre for Integrative Physiology – Without his help, the very beginning success of the joint model cannot be confirmed and the following works cannot be continued; Dr Trudi Gillespie at the Centre for Integrative Physiology – for teaching me the advanced techniques of the confocal laser scanning microscope; Mrs Anne Pryde at the Department of Hepatology – for helping me operating the spectrophotometer and ensuring every analysis of the cartilage matrix proteoglycan being done under her strict science principles; Mr Anotnello Spadaccino – for his management of every stuff in our laboratory; and The Scotbeef Company in Stirling – for freely providing the bovine feet in every experiment.

To suspend my clinical work and to pursue the postgraduate study in an unfamiliar environment is not easy for me. I deeply appreciate all the assistance from Taiwan before and after we come to UK, including the financial support by Taipei Medical University – Shuang Ho Hospital and the considerable encouragement from Professor Wen-Ta Chiu, Professor Chih-Hsiung Wu and Professor Yang-Hwei Tsuang. The warm support from my family and friends also gives me much confidence to walk persistently along this different way.

Finally, I would like to thank my wife, *Josephine*, who always gives me her the most complete support and honest suggestions from her love.

AWARD

This novel organ culture model has been awarded the scientist prize at The Laboratory Animal Welfare Symposium 2014, held by the University of Edinburgh's Biological Services and the Jeanne Marchig International Centre for Animal Welfare Education (JMICAWE).

This award is for an original scientific or technological initiative that has been shown to have a positive impact on the welfare of animals used in research or has led to the development of an alternative non-animal research model.

ABSTRACT

Disorders affecting articular cartilage are amongst the most common problems in orthopaedics. Osteoarthritis, the end stage of the disease of articular cartilage, reduces the quality of life for tens of millions of people in the world, and has a profound impact on the economics of industrialized countries. Despite progress in articular cartilage research, the problem is still far from being defeated. Various models e.g. *in vitro* cartilage explants and *in vivo* animal models, have been established for cartilage research, but each has its own limitations. Thus, a novel *ex vivo* isolated joint organ culture model was developed.

Bovine metatarsophalangeal joints were chosen as a suitable synovial joint because it consists of a hinge-type joint that is similar to the human knee joint, and has a large cartilage surface that provides enough space for multiple sampling in the same joint. The joints were isolated aseptically and placed into culture media. The viability of chondrocytes, glycosaminoglycan (GAG) content of cartilage matrix, cartilage morphology and water content of matrix were evaluated under different culture conditions, i.e. static, static with flowing media, and dynamic with different durations of the movement period.

The model was used to investigate the effect on the sharp scalpel cartilage injury of adding serum to the culture medium by culturing the whole joint explants in serum-supplied or serum-free media. The feasibility of investigating the early phases of chondrocyte implantation in this model was also studied: circular holes of 2.5 mm diameter were created by making a pilot hole with a 2.0 mm drill followed by using a fresh 2.5 mm biopsy punch. Allogeneic isolated chondrocytes at different passages were aggregated as cell pellets and implanted in the holes to evaluate their integration ability and the response from the recipient cartilage.

Results from the static model showed that, after 28 days culture, the chondrocytes were still alive with 66.5%, 80.9% and 46.9% viability in the superficial, middle and deep zones, respectively. The GAG content of the static model decreased 19.2% after the first week of culture and then lost another 15.0% during the third week.

Paradoxically, at end of the 4th week the GAG level rebounded to some extent and increased 19.0% relative to the previous week.

Interestingly, the cell viability of all three zones improved if the culture fluid was flowing as seen with the experiments carried out with stirred media or dynamic movement of the articular surfaces. (e.g. for the stirred media after 28 days of culture the chondrocyte viability was 80.6%, 92.4% and 70.4% for the superficial, middle and deep zones respectively.)

The GAG content was maintained at a constant level in the contact area of the dynamic model, but decreased as in the media-stirred model and non-contact area of the dynamic model to a similar extent to that observed with the static model.

In the injury model, the GAG content fell approximately 10.8% straight after the scalpel cut, but no further loss was observed if the joint was cultured in the serum-supplied media. In contrast, if the injured joint was cultured in the serum-free media, the GAG content continued to fall week by week and finally dropped by 41.7% at the end of the 4th week. In the chondrocyte implantation model, the majority of the host chondrocytes around the circular defect were alive (78.5 % viability). Viewed from the surface, the dead cells were all within 20 μm from the cut edge. The implanted chondrocytes, which were aggregated as cell pellets, began to transform their shapes and spread to the surrounding surface of the recipient cartilage, but did not appear to integrate with the host tissue during the first 2 weeks of culture.

The results supported the validity of this *ex vivo* joint model and demonstrated that the chondrocytes subjected to flow of the media or dynamic loads survived well over a 4 week period. Of importance was the finding that there was no measured loss of the matrix GAG content when the joints were under dynamic load compared to all of the non-loaded conditions. This whole joint model could be of value in providing a more natural and controllable platform where research involving the normal processes or pathologic mechanisms of articular cartilage can be investigated, as well as the early response to newly developed pharmacological agents and cartilage tissue engineering constructs.

ABBREVIATIONS

ACI	Autologous chondrocyte implantation
ADAMTS	A disintegrin and metalloproteinase with thrombospondin motifs
AMP	Adenosine monophosphate
ATP	Adenosine triphosphate
BMP	Bone morphogenetic proteins
CLSM	Confocal laser scanning microscopy
CMFDA	5-Chloromethylfluorescein diacetate
COMP	Cartilage oligomeric matrix protein
CPM	Continuous passive motion
CS	Chondroitin sulphate
DMEM	Dulbecco's Modified Eagle Medium
DMMB	Dimethylmethylene blue
DNA	Deoxyribonucleic acid
DZ	Deep zone
ECM	Extracellular matrix
FGF	Fibroblast growth factor
GAG	Glycosaminoglycan
H&E	Haematoxylin and Eosin
IGD	Interglobular domain
IL	Interleukin
KS	Keratan sulphate
MACI	Matrix-induced autologous chondrocyte implantation
MMP	Metalloproteinase
mRNA	Messenger ribonucleic acid

MSC	Mesenchymal stem cell
MZ	Middle zone
NBF	Neutral buffered formalin
OCT	Optimum cutting temperature
PBS	Phosphate buffered saline
Pen/Strep	Penicillin and streptomycin
PI	Propidium iodide
ROI	Region of interest
SCB	Subchondral bone
STD	Standard deviation
SZ	Superficial zone
TIMP	Tissue inhibitor of metalloproteinases
TNF	Tumour necrosis factors

SECTION A – LITERATURES & INTRODUCTION

Including

Chapter 1: Literature Review and Introduction

Chapter 1: Literature Review and Introduction

1.1 Osteoarthritis

Osteoarthritis affects the quality of life of tens of millions of people in the world (Buckwalter, *et al.* 2000; Martel-Pelletier & Pelletier 2010). In western populations it is the second major cause of work disability in men over 50 years of age. The increased burden on the cost of health care as a consequence of this disease and the loss of labour productivity have had a great impact on the economics in both the developing and developed countries (Arden & Nevitt 2006).

Although, in most patients, the causes of osteoarthritis remain unknown, some factors have been shown to increase the risk of joint degeneration, such as obesity, advancing age, high-impact and torsional loads, abnormality of joint anatomy, joint instability, inadequate muscle strength, and disturbance of joint innervation (Martin & Buckwalter 2002b; Lotz & Loeser 2012). If the reasons of osteoarthritis can be identified, treatments should if possible be focused on the correction of risk factors or prevention of their recurrence.

Even though most of the causes of osteoarthritis remain unknown, some universal phenomena can be identified. Clinically, osteoarthritis results in symptoms such as joint pain and loss of joint function, which occur in almost every patient suffering from osteoarthritis. Microscopically, disruption of the cartilage integrity that leads to wear and fissuring on the cartilage surface, and, biochemically, the loss of matrix tensile strength and stiffness due to decreased size and aggregation of proteoglycan aggrecans can also be observed (Martin & Buckwalter 2001). In a more detailed investigation of the cell biology, it was found that the mitotic and synthetic activity of chondrocytes, as well as the responsiveness of chondrocytes to anabolic growth factors, was decreased in the degenerative joint (Martin & Buckwalter 2002b). The reasons in part might be associated with the finding of degeneration of oxidatively damaged mitochondria and the erosion of telomere length inside the chondrocyte of osteoarthritic cartilage (Li, *et al.* 2012a; Lotz 2012).

Therapeutic decisions mainly depend on the cause and the stage of osteoarthritis and divide into non-surgical and surgical treatment. Non-surgical treatment includes body weight control, activity modification, pharmacologic treatment or rehabilitation therapy (Davis & MacKay 2013). Surgical treatment of osteoarthritis includes a variety of operations under different indications, such as surface debridement, penetration of subchondral bone, osteochondral transplantation, chondrocyte implantation, realignment osteotomies and total joint replacement. If the risk factor for osteoarthritis can be identified, e.g. mal-alignment of the limb or ligament insufficiency, surgical correction of the mechanical abnormality is likely to be the best policy for treating the disease (Buckwalter, *et al.* 2000). It should be emphasised that the aim of surgery is not only to reconstruct a new joint surface but must make the joint function better than it would be expected if the disease was left untreated or treated non-surgically (Buckwalter 2002).

There is a huge range of research fields in osteoarthritis, but in terms of the tissues involved, articular cartilage is of prime importance.

1.2 Articular cartilage

Articular cartilage, known as hyaline cartilage, is a highly differentiated tissue with distinctive hypocellular, aneural, alymphatic and avascular characteristics. It provides the contact interface between two comparatively hard bones. The smoothness of articular surface, which is classified as 'smooth' according to the international standard for machined and polished metal surfaces (Bloebaum & Radley 1995), provides an extremely low friction interface for the movement of synovial joints. Its remarkable mechanical properties depend on the structural integrity of cartilage tissue, which is maintained by the interaction between the chondrocytes, the only cell type in the articular cartilage, and the extracellular matrix. Nevertheless, the structure of cartilage, in contrast to its simplistic compositions, is considerably complex and heterogeneous.

1.2.1 Structure of articular cartilage

Histologically, the articular cartilage extends from the articular surface to the osteochondral junction. It is loosely divided into 4 zones – the superficial (tangential) zone, the middle (transitional) zone, the deep (radial) zone, and the calcified zone (**Figure 1.01**). A wavy and irregular line, which is known as the tide mark, can be found between the deep zone and the calcified zone, and is most prominent in peripheral non-weight-bearing areas of joints (Brower & Hsu 1969).

The morphology of chondrocytes, cell density, mechanical properties, and the composition of the contents of the extracellular matrix differ from each zone. In addition, the thickness of each zone varies within the same joint, between joints of the same individual, between individuals of the same species, and between species (Brower & Hsu 1969; Huber, *et al.* 2000).

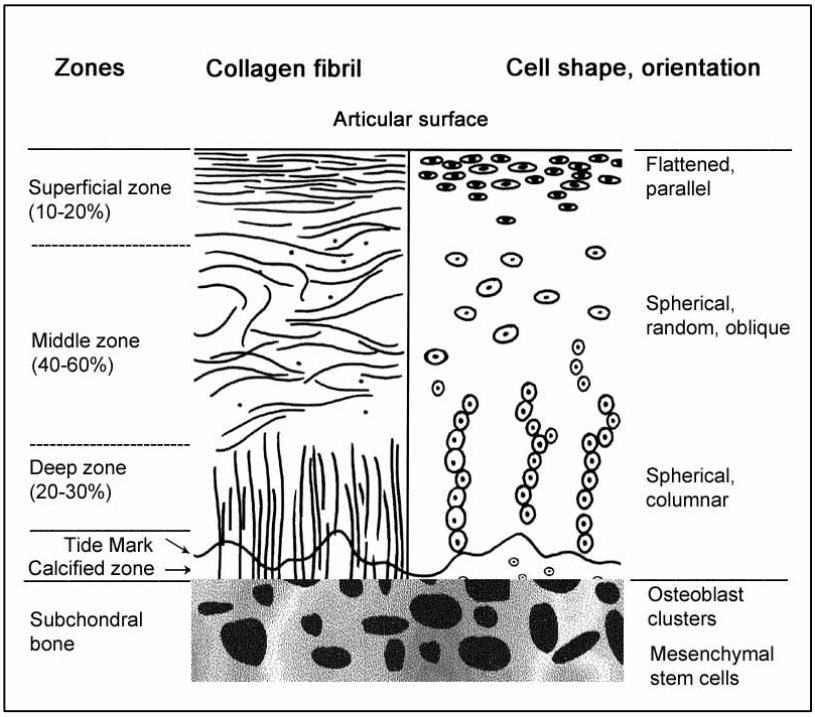

Figure 1.1 Articular cartilage morphology

The morphology of articular cartilage can be loosely divided into 4 zones according to the orientation of collagen fibrils and the shape and alignment of the chondrocytes. However, except the tide mark that separates the deep zone and calcified zone, borders among each zone cannot be easily differentiated because of their gradual alteration.

Superficial zone. The superficial zone is composed of flattened chondrocytes, the highest content of water, low proteoglycan content, and the highest collagen content. The superficial zone is further divided into two layers according to the orientation of collagen fibres. The first layer (known as the lamina splendens) is an acellular sheet that covers the articular surface with parallel-oriented thick collagen bundles. The second layer consists of flattened chondrocytes with the highest cell density, and the orientation of most collagen fibres are more oblique to the articular surface than those in the lamina splendens (Minns & Steven 1977; Huber, *et al.* 2000).

The surface of articular cartilage consists of sheets of tightly woven collagen fibrils. This specific organization of collagen fibre provides two important properties – the mechanical tensile strength and the barrier function (Mow, *et al.* 1984). The tensile strength of superficial collagen fibres protects cartilage from dissociation because of the shearing force from joint movement. The barrier phenomenon describes the function of cartilage matrix that allows exchange of small molecules, e.g. nutrients, growth factors and metabolites, with synovial fluid but obstructs large molecules, e.g. antibodies, to come in and damage chondrocytes (Buckwalter & Mankin 1998). This is because the average size between glycosaminoglycan chains of collagen network is 30-40 Å that is less than the size of immunoglobulins or serum albumin, whereas the cytokines or growth factors are 0.1-0.3 Å (Maroudas 1979; Maroudas, *et al.* 1992).

Middle zone. The middle zone of articular cartilage is made up of spherical chondrocytes, a low water content, a high concentration of proteoglycan, and a low collagen content. The collagen fibres appear randomly oriented and homogenously dispersed. They conjugate with proteoglycans that provide the resistance to compressive forces. This character confers the property of resilience to cartilage and acts as a ‘shock absorber’.

Deep zone. The deep zone of articular cartilage is formed by columns of spherical or elongated chondrocytes, the lowest concentration of water, the highest concentration of proteoglycan, and the widest diameter collagen fibres. The collagen fibres are aggregated together to form larger, radially oriented fibre bundles. These bundles

enter the calcified zone, crossing the tidemark, to form an interlocking network that anchors the tissue to the subchondral bone. The main function of this zone is similar to the middle zone and is to provide resistance against compression forces.

Tide mark. The tide mark, which separates the deep zone from the calcified zone, is a compacted fibril band that acts as a tethering mechanism. It tethers collagen fibres of the above non-calcified zones in order to prevent them from being sheared at their point of anchorage to the calcified zone. Small gaps were found in the tide mark that might provide the channels for nutrients or metabolites exchange between the subchondral bone and the deep non-calcified zone of articular cartilage (Redler, *et al.* 1975).

Calcified zone. The deepest layer of articular cartilage is the calcified zone, which is a transitional layer between the non-calcified articular cartilage and the subchondral bone. It is characterized by a sparse population of spherical chondrocytes surrounded by uncalcified lacunae in a calcified matrix. The matrix is devoid of proteoglycan.

1.2.2 Extracellular matrix

The extracellular matrix of cartilage is essentially a fibre-reinforced gel consisting of tissue fluid and three classes of molecules – collagens, proteoglycans, and non-collagenous proteins.

Collagen. The collagen composes 10-30% wet weight of the cartilage matrix. It forms a network as the endoskeleton of cartilage. The main collagen type of articular cartilage is type II collagen that accounts for 80%-90% of total collagen. It is constituted by a right-handed triple helix, which is composed of three α1(II)-chains with high content of hydroxylysine, glucosyl and galactosyl residues that mediate the interaction with proteoglycans (Gelse, *et al.* 2003). Type IX and type XI collagens are cross-linked together with type II collagen, and are thought to limit the fibril diameter to approximately 15-50 nm (Mendler, *et al.* 1989). Type II, IX and XI are cartilage-specific collagens and only can be found in the articular cartilage.

There are other collagen types that are found in the articular cartilage such as type X, which is present around hypertrophic chondrocytes in the growth plate and in the calcified zone of cartilage (Schmid & Linsenmayer 1985). Type VI collagen, which is located in the matrix immediately surrounding the chondrocyte (known as pericellular matrix), may help chondrocytes to attach to the macromolecular framework of the matrix (Buckwalter & Mankin 1998). Type III collagen can be detected in a diffuse area around the chondrocytes and throughout the depth of the cartilage (Wotton & Duance 1994).

Proteoglycan. Proteoglycans are proteins that are heavily glycosylated. In the articular cartilage, they consist of 3-10% wet weight of the matrix. The cartilage proteoglycan can be classified into two groups according to their molecular weights – the large proteoglycan and the small proteoglycan groups. The large proteoglycan group can be further categorised into two types – the aggregated proteoglycan, known as aggrecan, and the non-aggregated proteoglycan monomers. In fact, the aggrecan consists of numerous proteoglycan monomers non-covalently bonded to the hyaluronic acid chain to form large aggregates, which have molecular weight of up to 2×10^8 Daltons (D), and the length of approximately 2 μm (Vanwanseele, *et al.* 2002). The proteoglycan monomer consists of a chain of core protein with a quantity of glycosaminoglycan (GAG) chains attached, and its length is approximately 200-400 nm (**Figure 1.2**).

Glycosaminoglycans (known as the mucopolysaccharides) are long unbranched polysaccharides composing a repeating disaccharide unit. According to the difference of core disaccharide structures, GAG are classified into four groups, which are heparin/heparan sulphate, chondroitin/dermatan sulphate, keratan sulphate and hyaluronic acid. Due to the sulphate groups, glycosaminoglycans are negatively charged molecules that potentially attract large amount of water and cations (Lindahl & Hook 1978).

Aggrecan, the large aggregated proteoglycan, is the most important proteoglycan type in the cartilage. Its core protein chain contains three globular domains (G1, G2 and G3) and three extended domains (IGD, KS and CS) (**Figure 1.2A**). The G1

domain is the N-terminus of the core protein, which interacts with hyaluronic acid and link protein. Functionally, it holds the aggrecan together with the hyaluronic acid. The binding is stabilised by the link protein. Although the interaction between the proteoglycan monomer and the hyaluronic acid chain can occur independently, stability of the aggregate to alteration in ionic concentration, pH, centrifugal pressure and temperature is enhanced by the presence of link proteins (Ryu, *et al.* 1982).

Between the G1 and G2 domains is the interglobular domain (IGD) that contains small amounts of keratan sulphate (KS) chains (**Figure 1.2A**). This segment consists of some proteolytic cleavage sites for a variety of proteinases, such as matrix metalloproteinases (MMPs) or aggrecanases (e.g. ADAMTS). These two enzymes are believed to be involved in the turnover of aggrecan molecules in the aging or pathological conditions. The keratan sulphate (KS) domain and the chondroitin sulphate (CS) domain are located between the G2 and G3 domains, and they provide the attaching sites for KS and CS chains. The KS or CS glycosaminoglycan chain is composed of repeating disaccharide subunits that contain at least one sulphate group per disaccharide subunit. These sulphate groups are negatively charged and attract a cation flow into the cartilage matrix. The accumulation of ions into the matrix results in elevation of matrix osmolality that further leads to water influx from outside cartilage to balance the osmolar difference. Under these conditions, the matrix tissue is inclined to swell, but the expansion is restricted by the dense collagen network. As a result of these interactions, cartilage has a high hydrostatic pressure inside its matrix that provides great resistance to compressive force (Ulrich-Vinther, *et al.* 2003).

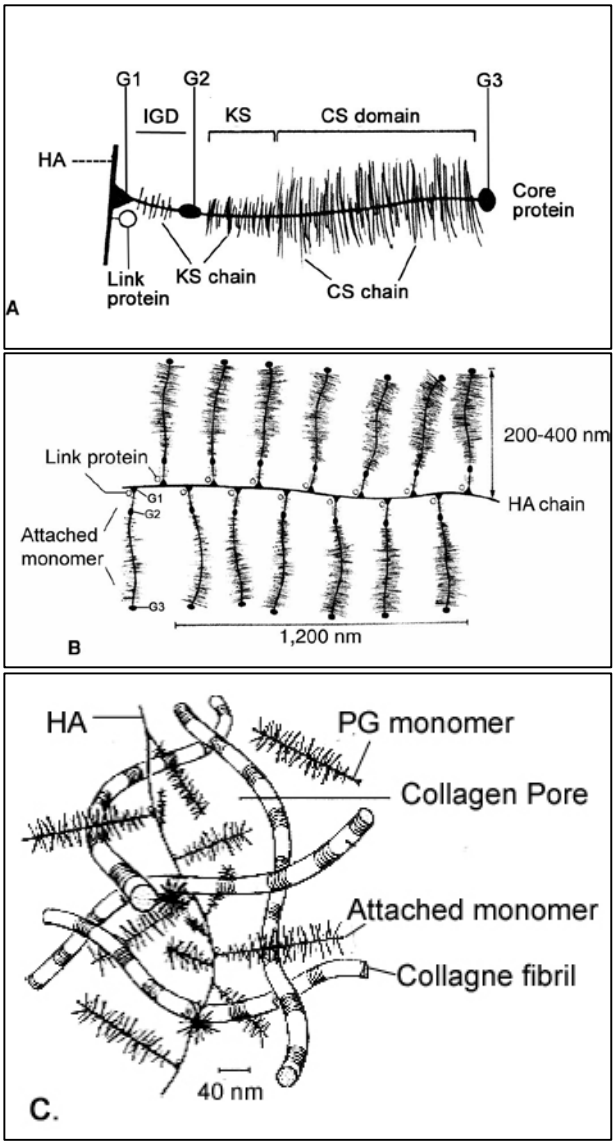

Figure 1.2 Proteoglycan structure of the articular cartilage

A. The basic unit of the cartilage proteoglycan is the proteoglycan monomer. It looks like a bottle brush, and can be differentiated into 6 segments, which in sequence from the N-terminus are G1, IGD, G2, KS domain, CS domain and G3. The G1 segment has the ability to bind with the hyaluronic chain non-covalently and also to interact with link protein. **B.** A number of proteoglycan monomers aggregated with the hyaluronic acid chain constitute aggrecan. **C.** The aggrecan and collage fibril network are interlaced together to consist of the major structure of cartilage matrix.

In mature cartilage, there are approximately 30 KS chains and 100 CS chains attached to the KS and CS domain, respectively. Nevertheless, the KS chains attach not only to the KS domain but also the CS domain or IGD, whereas the CS chains can only be found in the CS domain of core protein. The CS domain is the largest domain of aggrecan that accounts for the major function of aggrecan, i.e. to hold a large amount of water in the extracellular matrix (Kiani, *et al.* 2002).

The synthesis and degradation of aggrecan are being investigated for their roles in cartilage deterioration during joint injury, disease, and aging. It has been found that the amount of the KS and protein content increase significantly with age, which leads to an increase in the molar concentration of aggrecan and a decrease in their molecular size and weight (Martin & Buckwalter 2002b). These changes might be due to degradation of the aggrecans in the matrix, alteration in the biosynthesis within aged chondrocytes, or both. Nevertheless, the turnover rate of different sites of aggrecan in aged cartilage was found to be dissimilar since the G1 domain had a half-life of 25 years, while the half-life of CS-rich fractions was only 3.4 years (Maroudas, *et al.* 1998). These findings imply that the large proteoglycan molecules are able to be modified after they were synthesised by the chondrocyte, and different segments of proteoglycan have different rates of modification, which results in different component ratios of the cartilage matrix between the young and aged individuals.

In addition to the large proteoglycans, there are some small proteoglycans in the cartilage matrix, such as decorin, biglycan, and fibromodulin. They consist of approximately 3% of the total proteoglycan mass. They are distributed throughout whole layers of cartilage but most of them are concentrated in the surface layer (Poole, *et al.* 1982). Functionally, they are involved in the stabilisation of the matrix, and may act as signalling molecules that regulate the inflammatory response of chondrocytes to microbial invasion (Nastase, *et al.* 2012).

Non-collagenous proteins. Some proteins, other than collagens, can also be found in the matrix such as anchorin CII, tenascin, fibronectin, and cartilage oligomeric matrix protein (COMP). Anchorin CII helps to anchor the chondrocytes to the

collagen fibrils (Mollenhauer, *et al.* 1984). Tenascin and fibronectin influence the interaction between chondrocytes and the matrix, and play a role in the process of arthritis and osteoarthritis (Saxne & Heinegard 1992). Cartilage oligomeric matrix protein has the functions of binding other ECM proteins, catalysing polymerization of type II collagen fibrils and regulation of chondrocyte proliferation. It is also a marker for the joint destruction associated with osteoarthritis, rheumatoid arthritis, joint trauma, and intense activity (Posey & Hecht 2008).

Subregions of matrix. According to different distance of the matrix to chondrocytes, the extracellular matrix can be approximately subdivided into three regions – the pericellular, territorial, and interterritorial regions. The proteoglycan constituents of each region are different. The pericellular region is a thin, transparent layer just surrounding the chondrocyte. It contains a high concentration of proteoglycans and type VI collagen that provides chondrocytes hydrodynamic protection against physiological loads. The interactions between the chondrocyte and the pericellular matrix are so close that they are considered together as a unit named the 'chondron'. Recently, the pericellular region has attracted more attention because it is involved in the regulation of transmissions of biochemical and mechanical signals. The early changes of osteoarthritis can be detected in this region (Youn, *et al.* 2006; Wilusz, *et al.* 2013).

The territorial region is the basophilic matrix around groups of cartilage cells. It consists of large type II collagen fibrils arranged in radial bundles. It has a higher concentration of chondroitin sulphate-rich proteoglycans. The interterritorial region is a paler staining region between the darker territorial zones that comprises the bulk of articular cartilage. It consists of larger diameter type II collagen fibrils and a higher concentration of keratan sulphate-rich proteoglycans (Youn, *et al.* 2006).

1.2.3 Chondrocyte

The chondrocytes are the only cell type in the articular cartilage. They are highly differentiated mesenchymal cells. They are isolated from each other, enclosed with a

voluminous extracellular matrix, and occupy about 10% of the total tissue volume (Stockwell 1967).

Articular chondrocyte develop from a group of non-committed stem cells in the mesodermal elements of the limb in an embryo. During ontogenesis, these cells differentiate into chondroprogenitor cells and produce an immature foetal type of articular cartilage that provides a temporary scaffold for skeletal development through endochondral ossification. During the early postnatal phase, these chondroprogenitor cells of the cartilage, especially those in the superficial zone, continue to produce foetal type tissues to expand the epiphyseal bone. The immature cartilage does not undergo remodelling but is resorbed gradually. During puberty these precursor cells are reprogrammed to become mature chondrocytes that produce an adult type of articular cartilage (Pacifici, *et al.* 2006; Hunziker, *et al.* 2007; Hunziker 2009).

The lifespan of the mature articular chondrocytes can last as long as the host life. Those chondrocytes in the calcified cartilaginous matrix become hypertrophic, which is the terminally differentiated state of the chondrocyte and then die by apoptosis. Some hypertrophic chondrocytes do not die but transdifferentiate or metaplase into osteoblasts that continue to convert the cartilage into bone tissue by depositing bone matrix inside their lacunae (Roach 1997; Archer & Francis-West 2003).

After skeletal maturity, the chondrocytes of the articular cartilage stop cell division except in a few pathological situations (e.g. cloning/clustering in OA). The environment of the chondrocytes in the cartilage of mature individuals is hypoxic because articular cartilage is not vascularized and its supply of nutrients and oxygen mainly depends on diffusion from synovial fluid. Thus the oxygen tension decreases from the cartilage surface from 10% to <1% at the deep zone (Marcus 1973). Anaerobic glycolysis, as a result, is the major metabolic mechanism by which the chondrocytes develop their energy. For this reason, chondrocytes normally do not contain abundant mitochondria in their cytoplasm. Instead, they have a large amount of rough endoplasmic reticulum, juxtanuclear Golgi apparatus and glycogen deposits,

which all indicate that the cells are still metabolically active (Archer & Francis-West 2003).

Synthesis and maintenance of the components of the extracellular matrix are the primary functions of the chondrocyte. These functions are regulated by many signals coming from the interaction between the extracellular matrix and chondrocytes.

1.2.4 Interactions between chondrocytes and the matrix

Interactions between the chondrocytes and the extracellular matrix are extremely close and complex. For the matrix, all of the components and structures are produced by chondrocytes, and, for chondrocytes, all signals of synthesis or degradation of the components of extracellular matrix are transmitted through the matrix. The transmitted signals can be generally classified as mechanical, electrical, osmotic or physicochemical signals. Nevertheless, most of these transmission mechanisms are not clearly understood.

More attention has been paid to the signalling pathway of mechanical loading because the chondrocytes, physiologically, are the cells under pressure (Urban 1994). Mechanical loading is produced naturally by joint movement, and it results in complex changes within the cartilage tissue. The mechanism of compression on the cartilage has been thoroughly studied. First, the compression force deforms the matrix and leads to a rise of hydrostatic pressure. As a consequence, fluid flows out of the compressed area within milliseconds (Broom & Myers 1980). Secondly, because the water content of the matrix decreases, the concentration of proteoglycan increases, which raises the density of anions since the proteoglycan molecules are highly negatively charged by their multiple sulphated groups. Finally, inflow of cations, e.g. Ca^{2+} and K^{+}, continues until electric equilibrium is restored (Mow, *et al.* 1984).

Changes of the local ion constitution and concentration around the chondrocyte, as well as deforming the chondrocyte directly (Urban, *et al.* 1993) are detected by mechanoreceptors on the cell surface, which include mechanosensitive ion channels

and integrins (Wright, *et al.* 1996; Wang & Thampatty 2006). The influx of ions crossing the mechanosensitive ion channels, e.g. slow conductance Ca^{2+} channel, transfers the physical stimulus into a chemical signal. It activates an intracellular signalling cascade that regulates gene expression, and results in the production of matrix protein (anabolism) or proteases (catabolism) (Ramage, *et al.* 2009). Balance between the catabolic and the anabolic activity of the chondrocyte is fundamental to maintain the integrity of cartilage. Pathology of cartilage can be regarded as the result of disturbance of this homeostasis (Huber, *et al.* 2000).

There are several complex factors involved in determining whether the anabolic or catabolic pathway is activated. Nevertheless, the triggering point is the loss of matrix fluid. The load pattern, e.g. frequency, duration, and magnitude, has different effects on the extent, amount or rate of fluid loss, and the response of the chondrocyte varies (Urban 1994). For example, normal walking produces 4-5 MPa in the joint that results in 1-5% fluid loss on the pressured cartilage (Hodge, *et al.* 1986), and it is considered anabolic for maintenance of the integrity of the articular cartilage. However, if the loading pressure rises to 20 MPa, which can be observed during some active sports, the cytoskeletal elements of the chondrocyte will be dissociated, and that leads to a reduction in protein synthesis and an inhibition of membrane transport (Hall, *et al.* 1991). These results indicates that different ranges of loading pressure induce divergent outcomes, which may be due to the different rate or amount of fluid loss triggering different pathways.

Not only the load pattern but also the matrix compositions and structures have influences on the fluid flow inside the pressured cartilage. It was observed that the degenerative cartilage lost its fluid faster than the healthy cartilage, as well as with larger degree of deformation of cartilage shape (Mizrahi, *et al.* 1986). This can be explained by the fact that there is a low proteoglycan concentration in the matrix of osteoarthritic cartilage and therefore there is an increase in the rate and amount of fluid loss. This phenomenon can also be observed in the different zones within the same cartilage explant as the cartilage of superficial zone is more compliant than the deeper zones due to its lower proteoglycan concentration compared to the other zones (Urban 1994).

Other factors that are discussed less frequently, yet may also play an important role on the metabolism of chondrocytes, include cytokines, growth factors, hormones or reactive oxygen metabolites (free oxygen radicals). Catabolic cytokines, e.g. interleukin-1 (IL-1), tumor necrosis factor-α (TNF-α) or γ-interferon (γ-IFN), and catabolic hormone, e.g. glucocorticoids, degrade the matrix molecules by producing and activating proteolytic enzymes, such as collagenase, proteinase or proteoglycanase. For example IL-1, released from chondrocytes acts as autocrine regulator, but when it is released from synoviocytes or leukocytes acts in a paracrine fashion and induces the expression of matrix proteinases such as stromelysin (known as matrix metalloproteinase) that degrades aggrecan and type IX collagen (McGuire-Goldring, *et al.* 1984; Roughley, *et al.* 1991; Sztrolovics, *et al.* 2002).

In contrast, anabolic effects of the chondrocytes can be observed with some types of growth factors, e.g. platelet-derived growth factor (PDGF), fibroblast growth factor (FGF), insulin growth factor (IGF), transforming growth factor-β (TGF-β) and bone morphogenetic proteins (BMPs), and with several hormones, e.g. growth hormone, insulin, calcitonin and androgens (Osborn, *et al.* 1989; Mankin, *et al.* 1991). Chondrocyte proliferation and/or synthesis of matrix macromolecules can be stimulated by these elements.

Proper balance between anabolic and catabolic activities of chondrocytes is crucial for maintenance of cartilage integrity and repair of molecular damages by daily usage. If the balance is compromised and the catabolic activity is predominant over the anabolic activity – breakdown of matrix components begins. The fragmented matrix molecules induce the chondrocyte to produce more degenerative enzymes, such as IL-1 and TNF-α, which initiate a vicious cycle of catabolic and degradative events in the cartilage (Chikanza & Fernandes 2000; Wieland, *et al.* 2005). This progressive breakdown of articular cartilage results in osteoarthritis.

1.2.5 Nutrition of articular cartilage

Because the articular cartilage lacks blood and lymph vessels, there are only two possible pathways supplying nutrients – either from the cartilage surface via the synovial fluid, or from the underlying cancellous bone.

The route through synovial fluid is more straightforward and most of the nutrients are provided through this route. The nutrients in the synovial fluid alone were proven to be sufficient for the survival of articular cartilage (Strangeways 1920). The solutes transported by blood vessels to synovium diffuse into the synovial fluid, and then infiltrate into the cartilage matrix. There are two barriers – the synovial membrane and the cartilage matrix – blocking the solutes passage (Brower, *et al.* 1962). This double diffusion system sieves most of the harmful molecules and protects the distinctive chondrocytes from being attacked by the circulating antibodies of the immune system.

The other possible route for nutrients to reach the cartilage is via the subchondral bones, however its importance is still uncertain (Mital & Millington 1970; Arkill & Winlove 2008). A study using non-human primates demonstrated that separation of articular cartilage from its vascularised subchondral bone with polymethylmethacrylate cement resulted in degenerative change of cartilage, which required very long periods (3 years) to become obvious and detectable (Malinin & Ouellette 2000). This indicates that the subchondral route may play a role in maintaining the long-term cartilage health. However, a long-term observation (from 6 to 16 years) of 9 patients, who suffered from the giant-cell tumour of knee joint and received curettage and cementing to fill the bone marrow space up to less than 1 mm from the bone-cartilage interface, revealed that no evidence of degenerative osteoarthritis developed despite their subchondral structures being different (von Steyern, *et al.* 2007). Thus, the role of the subchondral bone for maintenance of cartilage health is still debated.

The transportation of nutrients in the articular joint mainly depends on the joint movement. Compression of the cartilage by joint movement makes the matrix fluid flows in and out of cartilage that simultaneously exchanges solutes and wastes with

synovial fluid. Therefore, immobility of the joint, which causes stasis of synovial fluid and lack of mechanical stimulation to chondrocytes, results in the reduction of matrix components production that leads to loss of cartilage integrity (Imhof, *et al.* 1999).

1.2.6 Subchondral bone and articular cartilage

Subchondral bone and the articular cartilage can be seen as one functional unit (Imhof, *et al.* 1999). Anatomically, the subchondral bone provides a base for articular cartilage to sit on, but the interface is not as smooth as the surface of cartilage. The subchondral bone plate, which is also called the cortical endplate or articular bone plate, is the interfacing structure of subchondral bone that connects with the deepest layer of cartilage (calcified zone). It has a wavily irregular 3-D surface. Compared to a smooth interface, this rough configuration provides a much stronger contact strength and protects against shear force during joint movement, which prevents the articular cartilage sliding on the subchondral bone (Imhof, *et al.* 1999).

In the subchondral region, there is a surprisingly rich vascularization, which is known as the articular vascular plexus. Within this, there is 3 to 10 times more blood flow than that in the cancellous bone region (Nakano, *et al.* 1986). It was found that there were direct vascular contacts to the calcified and (some of) the uncalcified zones of cartilage in approximately 5% of the deep zone of articular cartilage (Holmdahl & Ingelmark 1951).

In addition to the nutrients that have already been discussed, there are also some soluble factors, which are released from subchondral bone itself, that have an influence on the articular cartilage. It was observed that progressive chondrocyte death occurred in the cartilage explants excised from subchondral bone, but not found if cartilage was left attached to subchondral bone or co-cultured with subchondral bone (Amin, *et al.* 2009b). Accordingly, it could be inferred that the maintenance of the health of articular cartilage relied not only on the synovial fluid

but also on the subchondral bone, which was providing important signals for chondrocyte survival.

1.3 Mechanical influence on articular cartilage

Mechanical stimuli have significant influence on the development and maintenance of the integrity of the articular cartilage. Non-physiological mechanical loadings, e.g. overuse/disuse (frequency) and excessive mechanical loading (intensity), damages the cartilage tissue (Bader, *et al.* 2011).

1.3.1 Influence of non-physiological mechanical loading

Joint overloading, e.g. overuse or high impact trauma, leads to softening, fibrillation, ulceration, and loss of articular cartilage (Mankin & Buckwalter 1996). Sports activities that subject joints to repetitive high levels of impact and torsional loading increase the risk of articular cartilage degeneration (Buckwalter & Lane 1997). An *in vivo* canine model has shown that strenuous exercise by running 20 or 40 km/day for up to 15 weeks reduced the matrix proteoglycan content in the superficial zone, increased the water content and decreased the collagen concentration in the load-bearing region (Kiviranta, *et al.* 1992; Arokoski, *et al.* 1993). *In vitro* studies have identified a critical stress threshold of 15-20 MPa (153-204 Kg/cm^2) in bovine cartilage explants. Single impacts above this range induce significant matrix destruction with cell death (Jeffrey, *et al.* 1995). Another *in vitro* study demonstrated the chondrocyte apoptosis occurred at peak stresses as low as 4.5 MPa (46 Kg/cm^2), collagen degradation at 7-12 MPa (71-122 Kg/cm^2) and nitrite accumulation at 20 MPa (204 Kg/cm^2) on bovine cartilage explants (Loening, *et al.* 2000).

However, the *in vitro* results should be considered carefully because the type and extent of damage are affected by both the source of the tissue and the nature of the impact. It was found that human cartilage explants had more resistance to a single impact than bovine cartilage explants (Jeffrey & Aspden 2006). Different strain rates of the compression force were shown to have different effects on the reduction of proteoglycan synthesis in bovine cartilage explants (Kurz, *et al.* 2001).

In addition to joint overloading, reduced joint burden, e.g. immobilisation, leads to cartilage degeneration. In clinical studies, patients with spinal cord injuries

demonstrated progressive thinning of knee cartilage (atrophy) because of the absence of normal joint loading and movement (Vanwanseele, *et al.* 2002). In animal studies, canine models with knee joints immobilised by splints or casts for varying periods of time demonstrated cartilage thinning, tissue softening and reduced proteoglycan content (Palmoski, *et al.* 1979; Jurvelin, *et al.* 1986). Only a few *in vitro* cartilage models have been used directly for assessing the static effects. Nevertheless, data from the control group of different studies has revealed that the matrix GAG content of the cartilage decreased and could be continuously detected in the culture media for several days after the bovine cartilage explants were statically cultured (DiMicco, *et al.* 2004; Moo, *et al.* 2011).

1.3.2 Effects of physiological mechanical stimuli

The effect of mechanical stimuli within physiological range have been extensively investigated *in vitro* by applying compression force on cartilage explants or on tissue-engineered constructs, and the outcome assessed using a range of outcome measures, such as gene expression (gene level), extracellular matrix (protein level), and cartilage functionality (tissue level) (Bader, *et al.* 2011). It has been well-established that compressive force on the cartilage explants within moderate physiological level (0.01-5 MPa) and physiological frequency (0.01-1.0 Hz) can stimulate the biosynthesis of collagen, proteoglycan and fibronectin (Sah, *et al.* 1989; Steinmeyer, *et al.* 1997). However, at the gene level, several studies have failed to show consistent up-regulation of the gene expression with similar dynamic compression on tissue engineered constructs (Hunter, *et al.* 2002; Demarteau, *et al.* 2003). The different responses between gene expression and protein synthesis suggest that the effect of this mechanical compression occurs at the post-transcriptional level. It may be an evolutionary adaptation of the chondrocytes to conserve their cell resources and not to be exhausted by the frequently changing mechanical environment during joint movement if the mechanical loads remain within a physiological range (Lee, *et al.* 2006a).

The loading pattern may have different influences on the biosynthesis of the matrix molecules *in vitro*. Dynamic compressive force loaded with a non-continuous manner (1.0 Hz, 45 min on/6 hours off, 4 cycles a day, every other day for 39 days) has positive effects on aggrecan synthesis of the cartilage explants (Kisiday, *et al.* 2004). In contrast, a prolonged loading (1.0Hz, 24 hours for 20 days) led to inferior mechanical and biochemical properties in the chondrocyte-seeded fibrin hydrogels (Hunter, *et al.* 2004).

However, some limitations of the *in vitro* studies should be noted. First, the type of loading force *in vitro* was not the same as those *in vivo*. From the view of an animal joint, physical movement produces several types of mechanical loading, such as hydrostatic pressure, dynamic compression, fluid shear and tissue shear. These forces, which occur concomitantly or sequentially, may have different influences on the cell metabolism (Grad, *et al.* 2011). However, most of the *in vitro* studies use a single type of load for mechanical stimulation in attempts to simplify the experiments. Even though a special bioreactor with a rotating ball was designed to apply multiaxial loads for simulating the loadings given from a complex articular motion (Wimmer, *et al.* 2004), most of the studies cited above were conducted with either compression force or hydrostatic pressure. The secondary major limitation is that the loading conditions *in vitro*, e.g. magnitude and frequency, may not be replicated *in vivo*.

In animal studies, mechanical stimulation is created naturally from the real joint movement. A number of *in vivo* studies with various animal species has demonstrated that daily physiological exercise increased proteoglycan content and cartilage thickness and minimised the development of OA (Kiviranta, *et al.* 1988; Otterness, *et al.* 1998; Galois, *et al.* 2003). Generally, the anabolic effects induced by physiological exercise overrides the catabolic effects, which results in the chondroprotective effects of mechanical loading.

A number of clinical studies have demonstrated that regular activity decreased the incidence of OA in healthy individuals and reduced the pain and disability in the patients with knee OA (Fransen, *et al.* 2002; Jordan, *et al.* 2003; Jansen, *et al.* 2011).

However, the optimal guideline about the exercise prescription, dosage and the length of intervention is still not available (Bennell & Hinman 2011).

1.3.3 Effects of different physical forces of the joint movement

As described before, the joint movement produces several types of forces on the articular cartilage, e.g. hydrostatic pressure, compression and shear force. Each of these has different mechanism on the regulation of cartilage metabolism. In order to differentiate the different effect of each individual force, *in vitro* models are used.

The hydrostatic pressure has been widely applied as the source of mechanical stimulation on the monolayer chondrocytes, the scaffold-embedded chondrocytes and some of the cartilage explants. It has been demonstrated that, in the physiological range, the hydrostatic pressure stimulates the monolayer chondrocytes (Suh, *et al.* 1999), the chondrocytes cultured in agarose gels (Toyoda, *et al.* 2003), and cartilage explants (Hall, *et al.* 1991; Parkkinen, *et al.* 1993) to increase the matrix proteoglycan. However, controversy exists because of non-consistent results in different *in vitro* models even if identical hydrostatic pressure has been applied. For example, it has been shown that 5 MPa load at 0.5 Hz inhibited GAG synthesis in monolayer chondrocytes while stimulating GAG synthesis in cartilage explant culture (Parkkinen, *et al.* 1993). The reason may be related to the interaction between the chondrocytes and the extracellular matrix, which is absent in the monolayer cell culture.

Compression is by far the most commonly used method of applying mechanical load to cartilage explants or tissue-engineered constructs. This uniaxial force, if it is controlled within the physiological range, has been demonstrated to produce beneficial effects on the biosynthesis of the extracellular matrix, which has been discussed in the previous paragraphs (Chapter 1.3.2). However, if the tissue-engineered constructs are used, the ‘bioactivity’ of the scaffold should be carefully evaluated because the transmission of the compression load to the cells may be influenced by the material properties of the scaffold. For example, in studies using

three-dimensional cross-linked poly(ethylene glycol) (PEG) hydrogels as the scaffold, dynamic compression of 15% strain at 1 Hz did not have a major effect on the chondrocyte extracellular matrix gene expression (Nicodemus & Bryant 2008), but, if the hydrogels were augmented with Arg-Gly-Asp (RGD) peptides, which can act as binding sites for the chondrocytes, the upregulation of the matrix gene expression was substantial (Villanueva, *et al.* 2009).

Shear force, produced by sliding motion of an articular joint *in vivo*, is relatively difficult to reproduce *in vitro*. A flow bioreactor has been used to create the flow shear force of 0.001 or 0.1 Pa on the monolayer chondrocyte culture (Gemmiti & Guldberg 2009), and a rotational plate, which can produce 1-3% sinusoidal shear strain, has been designed to evaluate the effect of the pure tissue shear stress on the bovine cartilage explants (Jin, *et al.* 2001). A more complex bioreactor system using the computer-controlled ceramic hip ball can produce variable types of stresses on the *in vitro* tissues to imitate the mechanical stimulation of real joint motion (Wimmer, *et al.* 2004). All of these results demonstrate that shear force is a potent modulator for stimulation of the extracellular matrix synthesis. Further studies using the hip ball system show that the sliding surface motion may have more effects on enhancing both the proteoglycan 4 (PRG4) and cartilage oligomeric matrix protein (COMP) gene expression, whereas the compression may be more associated with the upregulation of collagen type II and aggrecan (Grad, *et al.* 2006a; Grad, *et al.* 2006b).

1.3.4 Mechanical signalling pathways

The mechanical signalling pathways of the chondrocyte are complex and have not been fully elucidated.

It is known that normal mechanical load activates the α5β1 integrin on the cell membrane of the chondrocyte (Salter, *et al.* 2001; Bader, *et al.* 2011). Excessive mechanical load additionally stimulates the stretch-activated ion channels (SACs) and causes a series of intracellular reactions, e.g. disruption of the actin cytoskeletal

network, stimulation of the nuclear factor-kappa B (NFκB) members, activation of the mitogen activated protein kinase (MAPK) family and increase of the intracellular calcium level. There is an increased production of various molecules such as nitric oxide (NO), proteolytic enzymes (MMP-1, 3, 8, and 13), ADAMTS (4 and 5), reactive oxygen species (ROS), cytokines (IL-1, TNFα), and prostaglandins (PGE2) (Fernandes, *et al.* 2002; Henrotin, *et al.* 2003; Martel-Pelletier, *et al.* 2008). All of these mediators are catabolic and result in cartilage destruction and cell apoptosis. In contrast, reduced loading, e.g. stasis and immobilisation, triggers the IL-1 receptor on the cell membrane (Murata, *et al.* 2003). The following intracellular reaction activates the extracellular signal-regulated kinase 1/2 (ERK1/2) and the activating protein-1 (AP-1), which increase the production of MMPs. This leads to the destruction of both matrix proteoglycan and type II collagen (Li, *et al.* 2003).

In contrast, mechanical stimuli within physiological range of intensity, duration and frequency induce a number of anabolic signalling cascades that leads to production of the extracellular matrix components. First, the α5β1 integrins and some stretch-sensitive ion channels on the cell membrane are stimulated by the mechanical load, which subsequently cause the intracellular reactions, e.g. activation of the actin cytoskeleton and the increase of calcium concentration (Salter, *et al.* 2001; Chowdhury, *et al.* 2006). An intact cytoskeleton leads to intracellular interleukin-4 (IL-4) release, and the increase of calcium ions may cause the instability of the inducible nitric oxide synthase (iNOS) mRNA, both of which block the transcription of the pro-inflammatory genes of the chondrocyte (Millward-Sadler, *et al.* 2006; Vincent, *et al.* 2007). Another intracellular pathway involves the ATP release and the subsequent purinoreceptor (P2) or cAMP activation, which leads to the up-regulation of the aggrecan gene expression (Fitzgerald, *et al.* 2004).

1.3.5 Mechanical influence on chondrogenesis.

From the very early embryonic stage to the skeletally mature adult, cartilage development is greatly influenced by mechanical stimulation. Chondrogenesis occurs in 5 sequential stages: (1) migration of the mesenchymal stem cells to limb buds and

condensation of the cells, (2) differentiation into chondrocytes, (3) synthesis of extracellular matrix, (4) maturation of chondrocytes, and (5) chondrocyte hypertrophy and tissue maturation. During these stages, the mechanical stimulus has a crucial effect, which has been extensively studied using both *in vitro* and *in vivo* models (Responte, *et al.* 2012).

In the embryonic stage, compression force has been shown to trigger the chondrogenic gene expression of the mesenchymal cells of the embryonic limb bud, which suggests that mechanical stimulation plays a role in the chondrogenic gene regulation (Takahashi, *et al.* 1998; Elder, *et al.* 2000). I*n vivo* animal studies using chick embryos with chemically paralysed limbs demonstrated that early immobilisation of the limbs resulted in abnormal limb shape and complete failure of synovial joint formation (Roddy, *et al.* 2011), while later limb paralysation decreased the cartilage matrix contents and its mechanical properties (Mikic, *et al.* 2004). In contrast, early joint loading of a rabbit model enhanced the maturation of matrix proteins and improved the integrity of the collagen network (Saamanen, *et al.* 1987; Julkunen, *et al.* 2010).

In the neonatal stage, the regional variation and the heterogeneity of the articular cartilage is believed to be correlated with mechanical stimulation. In an animal study, the cartilage of the weight-bearing joints of newborn horses revealed biological and biomechanical homogeneity. However, after birth, functional adaptation began. Stiffer and thicker cartilage developed in the regions bearing greater loads (Brommer, *et al.* 2005). After skeletal maturation of the horse, which was approximately after 18 months from the birth, no major adaptation occurred. This suggested that the heterogeneity of the articular cartilage in a mature individual might result from different mechanical stimuli on different joints or different cartilage areas of the same joint.

1.4 Cartilage injury and healing

Articular cartilage can be damaged by direct trauma or indirect torsional loading of a joint. The magnitude and rate of the damaging force influence the outcome of the injured cartilage. For example, a slowly applied physiological load only deforms the cartilage in a limited range, because the fluid movement of the extracellular matrix redistributes the load within the cartilage tissue and to the subchondral bone, while a suddenly applied load disrupts the matrix macromolecular framework because the force happens too rapidly for fluid movement and all the stress is carried by a restricted area of cartilage. This causes severe damages to the matrix and/or the chondrocytes (Buckwalter 2002). *In vivo*, some peri-articular structures should also be taken into account. For example, the peri-articular muscles play an important role in determining the outcome of the involved cartilage, because contractions of the muscle groups around the joint absorb much of the energy and stabilise the joint provided the applied load occurs slowly or expectedly (Brandt, *et al.* 2006). Thus, small and unexpected loads may be much more damaging to the joints than large loads that have been anticipated.

1.4.1 Lesion classification and biology

Morphologically, the articular cartilage injury can be considered in 3 categories:
(1) Chondral matrix damage: The injury affects the cartilage matrix but no visible disruption of the articular surface can be detected. This occurs when the magnitude of the impact load is above the physiological level of the cartilage matrix but less than the magnitude for production of cartilage disruption. A previous study revealed that this type of trauma led to the loss of the matrix proteoglycan and to an increase in the water content in the matrix, but no microscopic disruption on the articular surface (Donohue, *et al.* 1983). Nevertheless, the ultramicroscopic structure of the matrix network organisation may alter, e.g. distortions of the collagen fibril network or disruptions of the interaction between collagen fibril and the proteoglycan. However, if the basic matrix structure remains intact and the number of viable chondrocytes remains sufficient, the normal matrix composition can be restored

(Buckwalter 2002). Clinically, this type of injury is asymptomatic.

(2) Cartilage disruption (Chondral fractures): If the articular cartilage suffers from a force that is a little greater than the force described previously, or if the force is applied more rapidly, the cartilage tissue can be disrupted but the subchondral bone can remain intact. Chondral fissures, flaps or tears can be observed arthroscopically. After this injury, proliferation of the remaining chondrocytes and increased synthesis of the matrix macromolecules near the injury site can be observed. However, the newly synthesised matrix and the proliferating cells are not able to fill the chondral defect and the cellular reactions cease after a short period (Buckwalter 1998). Clinically, this type of injury may cause mechanical symptoms, synovitis, pain and joint effusions.

(3) Cartilage and bone disruption (osteochondral fractures): The injury extends into the subchondral bone area because the damaging force exceeds the limit the cartilage can withstand. It causes haemorrhage from the bone marrow, which brings red and white blood cells, platelets and a few stem cells, and forms blood clot (Altman, *et al.* 1992; Shapiro, *et al.* 1993). This blood clot can completely fill a defect if the lesion size is less than 2 mm diameter. Larger lesions may not be completely filled with blood clots, resulting in incomplete healing (Jackson, *et al.* 2001). Inflammatory responses, such as chemotaxis of thrombocytes and neutrophils, are activated to repair the osteochondral defect. These cells, thereafter, release a number of growth factors and cytokines, which stimulate vascular invasion from the subchondral bone (Gunsilius, *et al.* 2000). The neovascularisation facilitates more mesenchymal cells of the bone marrow to migrate to the blood clot. They proliferate within the clot and begin to synthesise a matrix that contains type I and type II collagen and a relatively high concentration of proteoglycans. After six to twelve weeks, the osteochondral defect contains many chondrocyte-like cells and a hyaline-like matrix (Shapiro, *et al.* 1993).

Within the repair tissue, enchondral ossification is initiated after the hyaline-like matrix has formed. This repair tissue ossifies in the portion close to the floor of the defect but not in the uppermost portion, where a mixed type of cartilage tissue that contains both type I and type II collagen fibres is formed (Furukawa, *et al.* 1980).

However, within the repair tissue, neither an arcade-like organisation of the collagen fibre nor a well-defined zonal differentiation of the chondrocytes can be found. In addition, the mechanical properties of the repair tissue are significantly inferior to those of normal articular cartilage (Heath & Magari 1996). Their stiffness is less and permeability is more than the normal articular cartilage. The relationship of the proteoglycan with the collagen network does not follow the pattern seen in normal articular cartilage. Therefore, after one year or less of normal joint use, the repaired chondral tissue begins to show evidence of fragmentation, fibrillation and disintegration from the surrounding tissues (Shapiro, *et al.* 1993). Depletion of matrix proteoglycans, increase of collagen content and loss of the chondrocyte-like cells was also found. Even though a small amount of the repair tissue can histologically stay unchanged or be remodelled to form a functional joint surface, most of the repair tissue, particularly in large osteochondral defects, deteriorates and disintegrates. Complete loss of the repair tissue and exposure of the subchondral bone are the final results (Buckwalter 2002; Hunziker 2009).

1.5 Cartilage repair

1.5.1 Clinical methods of cartilage repair

Treatment strategies for the cartilage injury depend on several factors, e.g. age, lesion size and the activity level of the patient (Cole, *et al.* 2009; Bekkers, *et al.* 2012). Surgery is the predominant treatment of symptomatic chondral and osteochondral defects of articular cartilage (Detterline, *et al.* 2005). Several surgical procedures have been proposed. The indications, advantages and disadvantages of each method are described below.

(1) Debridement and lavage: These procedures are generally performed under arthroscopy. Debridement removes the diseased chondral tissue and/or free bodies from the joint. Meniscectomy and excision of the osteophytes can be performed concurrently. The irrigation/lavage is thought to remove some of the intraarticular active pain-signalling or pain-mediating molecules (Chang, *et al.* 1993). Suitable candidates for this treatment include aged patients with low activity demand, who have chondral lesions under 2 cm^2 diameter. Immediate pain relief and unrestricted post-operative joint activity have been reported to be the major potential advantages of this approach (Owens, *et al.* 2002). However, there is not a strong scientific basis clinically or experimentally for this treatment. In addition, the shaving-induced cell apoptosis and necrosis (Kim, *et al.* 1991; Tew, *et al.* 2000) and the meniscectomy-created skeletal malalignment may exacerbate the long-term osteoarthritic condition (Hunziker 2002). Therefore, debridement and lavage are now considered as a purely palliative treatment option for temporary relief of pain for a patient with osteoarthritis (Matsiko, *et al.* 2013).

(2) Microfracture: Microfracture is considered as a treatment option for chondral lesions of less than 2-3 cm^2 diameter. It involves surgical access to the bone marrow by drilling holes with approximately 0.5-1 mm diameter through the defective articular cartilage tissue into the bone marrow cavity. It has the same biological rationale as abrasion chondroplasty or Pridie drilling, i.e. it relies on the spontaneous repair reaction that occurs as a result of the recruited cells from the bone marrow,

e.g. the blood cells, platelets and the progenitor cells. The repair tissue contains most of the matrix components similar to hyaline cartilage, but significant quantities of fibrous constituents are also present (Furukawa, *et al.* 1980). Clinically, various retrospective investigations have been reported but the success rates vary (Bert 1993; Moseley, *et al.* 1996; Chen, *et al.* 1999). Their outcome depends on multiple factors, such as the age of the patient, activity level, the severity of the arthritic condition and the length of follow-up. A recent systematic analysis shows that microfracture provides effective short-term functional improvement of the knee joint (Mithoefer, *et al.* 2009), especially when continuous passive motion (CPM) is used post-operatively along with restriction of weight bearing (Kon, *et al.* 2009). However, the long-term results of microfracture cannot be defined because of insufficient data, but an increasing number of clinical studies reveal that the initially synthesised hyaline-like cartilage becomes more fibrous and its biomechanical property is inferior to the original hyaline cartilage, which leads to degeneration and the return of symptoms (Mithoefer, *et al.* 2009; Saris, *et al.* 2009). Therefore, this treatment may serve only to delay the eventual requirement of joint replacement (Matsiko, *et al.* 2013).

(3) Osteochondral transplantation: Autograft or allograft transplantation of the articular cartilage with its subchondral bone is known as mosaicplasty. Generally, it is performed as a secondary treatment option for a lesion larger than 2 cm^2 diameter if the patient is intermediate to high activity demand and the microfracture or debridement cannot adequately solve the problem. For autologous transplantation, a number of cartilage plugs are extracted from a non-weight bearing region of the joint and implanted into the defect site (Detterline, *et al.* 2005). Animal studies reveal that the graft persists for a short-term duration but there is a paucity of long-term data available (Wohl, *et al.* 1998; Bodo, *et al.* 2000; Hurtig, *et al.* 2001). The veterinary data has revealed that the cartilaginous portion of the graft survives for approximately 9 months and then histologic evidence of cartilage degeneration appears. There was little or no new repair tissue between the host and donor cartilage and the loss of the sulphated glycosaminoglycan from the transplanted cartilage was remarkable. In contrast, the osseous portion became well integrated and persisted for long periods within the host bony compartment.

Clinically, mosaicplasty was rapidly applied in human patients before it had been thoroughly tested in animal investigations particularly long-term ones (Hunziker 2002). A considerable number of clinical articles reveal that the short-term outcomes of the mosaicplasty are good to excellent (pain relief and improved joint functionality in 60-90% of cases) (Attmanspacher, *et al.* 2000; Hangody, *et al.* 2001; Laprell & Petersen 2001). However, the outcome usually deteriorates after eighteen to twenty-four months (Harris, *et al.* 2010). A recently published article revealed that the long-term (median 9.8 years) outcome of the mosaicplasty decreased to poor with evaluation of the Tegner Lysholm knee scoring scale (Ulstein, *et al.* 2014). The underlying reason may be due to the inherent drawbacks of this method, such as the donor site morbidity, limited cartilage to cartilage integration, or the poor joint congruity due to the uneven surface resulting from the implantation of multiple plugs (Huang, *et al.* 2004).

(4) Autologous chondrocyte implantation (ACI): ACI is an approach for treatment of a contained, symptomatic knee cartilage defect. The aim of this treatment is to enable the regeneration of hyaline or hyaline-like cartilage, thereby restoring normal joint function. ACI comprises a series of procedures. First, the autologous cartilage tissues are harvested arthroscopically from the edge of the affected knee joint. The chondrocytes inside the cartilage are isolated and cultured *in vitro* for a few weeks for expansion of the cell population to a sufficient amount. Then, in a second surgical procedure, the cultured chondrocytes are injected into the defect area of the joint, under a periosteal flap (Brittberg, *et al.* 1994) or more recently under a collagen membrane (Cherubino, *et al.* 2003).

Some complications are associated with the use of periosteum as the cover material, e.g. hypertrophy of the periosteum and, less commonly, calcification and delamination (Micheli, *et al.* 2001; Ueno, *et al.* 2001). The uneven distribution of the chondrocytes suspension within the defect and cell leakage during the initial few hours after injection have also been reported (Sohn, *et al.* 2002).Thus, a modification of this method, called **matrix-induced ACI** (**MACI**), has been developed. In MACI, the extracted autologous chondrocytes are seeded within a biodegradable scaffold (matrix), which is then implanted directly into the base of a prepared chondral defect

with or without fibrin glue augmentation, and no further coverage is needed to secure the graft (Cherubino, *et al.* 2003).

A number of clinical studies have demonstrated that the repair tissue from ACI is more durable and its biomechanical properties are more similar to native hyaline-like cartilage tissue with better long-term outcomes than those from microfracture (Brittberg, *et al.* 1994; Peterson, *et al.* 2010). A recent article has systemically reviewed 13 Level-I and II studies comparing autologous chondrocyte implantation with microfracture and osteochondral transplantation (Harris, *et al.* 2010). It revealed that all surgical techniques improved the preoperative symptoms. When comparing ACI with microfracture, three of seven studies showed ACI had better clinical results after one to three years, whereas another three studies showed no difference after one to five years and the last one, in contrast, showed microfracture had better outcomes than ACI after two years follow-up. When comparing ACI with osteochondral transplantation, two studies both demonstrated equivalent short-term results, even though there was more rapid improvement after osteochondral transplantation. When comparing ACI with MACI, all of four studies showed equivalent results. However, when arthroscopic techniques were used, the complication rates with MACI were reduced.

1.5.2 Tissue engineering for cartilage repair

In the field of tissue engineering of articular cartilage, a triad of three elements is described consisting of – the cell, the scaffold and the signalling factor. There are a variety of cell sources, scaffold compositions and stimulation factors currently under investigation.

(1) Cells: Various cell types can be used for cartilage repair such as chondrocytes or mesenchymal stem cells (MSCs). The chondrocytes are most commonly obtained from the articular cartilage, particularly from the peripheral areas of the affected knee joint, but the rib cartilage can be an alternative source of chondrocytes (Moskalewski & Bator 1985). However, a detached osteochondral fragment, which can be found in

joints such as the knee or ankle in patients suffering from the diseases such as osteochondritis dissecans (OCD), even though it contains viable chondrocytes, has been reported to be a poor cell source for tissue engineering because of the inferior cartilage-forming capacity of these cells (Candrian, *et al.* 2010). Mesenchymal stem cells have been considered as a promising alternative to chondrocytes for cartilage repair. In adults, MSCs can be found in various sites, e.g. bone marrow, adipose tissue, infrapatellar fat pad or synovium (Barry, *et al.* 2001; Dragoo, *et al.* 2003; Guilak, *et al.* 2004; Fan, *et al.* 2009). However, several factors should be considered before using MSCs for cartilage tissue engineering because different donor sites have different cell yield rate, and the MSCs derived from different sites possess heterogeneous characteristics for chondrogenesis. For example, the bone marrow-derived MSCs have been well characterised and applied in a variety of clinical trials, but the harvest procedure – bone marrow aspiration – is extremely painful and the cell yield rates are low (approximately 1 MSC in 1×10^5 marrow cells) (Barry, *et al.* 2001). In contrast, adipose tissue has a high cell yield rate (approximately 5000 stem cells in 1 gm tissue aspirate) and low donor site morbidity but the MSCs population is inhomogeneous and its chondrogenic potential is low (Lin, *et al.* 2008). The synovium-derived MSCs have both advantages of high chondrogenic responses and high yield rate, but the very limited area of the donor site restricts their broad utilisation (Fan, *et al.* 2009).

(2) Scaffolds: The scaffold serves as a three-dimensional template for the initial cell attachment and the subsequent cell migration and proliferation (Coutts, *et al.* 2001; Capito & Spector 2003). The phenotype and the function of the chondrocyte can also be maintained or re-differentiated if the chondrocytes are cultured in a two-dimensional system for cell expansion (Caron, *et al.* 2012). However, the ideal composition and structure of the scaffold for MACI is still under investigation. A perfect scaffold needs to have some specific characteristics, e.g. good biocompatibility to the host tissue and a suitable porosity for the implanted cells (Capito & Spector 2003). The chemical composition and the mechanical property of the scaffold are also influential for cell attachment and chondrogenic differentiation of the implanted cells (Murphy, *et al.* 2012). In detail, the components of the scaffold

can be grouped into two types – synthetic-based and natural-based materials. The synthetic scaffold contains materials of artificial products, e.g. polycaprolactone (PCL) or polyglycolic acid (PGA). They have low immunological reaction and a flexible configuration. They can be made into different forms such as particles, meshes or fibres that facilitates clinical application (Agrawal & Ray 2001). However, the degraded products from the synthetic scaffold contain acidic molecules that can induce an inflammatory reaction, which restricts their use (Hutmacher 2001). The natural-based scaffolds use collagen, gelatine, fibrin or chitosan (Wakitani, *et al.* 1998; van Susante, *et al.* 1999; Ponticiello, *et al.* 2000). They have non-toxic degradation products and similar mechanical properties like the extracellular matrix of natural cartilage. They also possess a number of functional groups along their backbone that allow interactions with other molecules such as polysaccharides or some protein-based growth factors (Getgood, *et al.* 2009). In collagen-based scaffolds, the metabolism and regenerative capacity of the seeded cells can be significantly improved if the glycosaminoglycan molecules are integrated into the scaffolds (Tierney, *et al.* 2009).

(3) Stimulation factors: Physiological stimuli and biochemical factors, e.g. cytokines, hormones or growth factors, play an important role in cell proliferation and induction of the chondrogenic phenotype in the tissue engineering of cartilage repair. Growth factors, e.g. transforming growth factor beta (TGF-β), fibroblast growth factor (FGF) and insulin growth factor (IGF), are broadly used for *in vitro* chondrogenesis of MSCs (Fukumoto, *et al.* 2003; Buckley & Kelly 2012). Bone morphogenetic proteins (BMPs), in particular BMP-4, -6 and -7, have been shown to promote the maintenance of the chondrogenic phenotype and the up-regulation of the cartilage matrix synthesis for adipose-derived MSCs (Diekman, *et al.* 2010). However, a high concentration of growth factor *in vivo* may be associated with oncogenesis and a potential of ectopic tissue formation (Huang & Huang 1985; Kubota, *et al.* 2002). Therefore, techniques such as specific delivery systems, have been invented to address this problem. The scaffold incorporated with growth factors may be an adequate delivery system because the incorporated growth factor can be

slowly released during degradation of the scaffold (Dickhut, *et al.* 2010; Lee, *et al.* 2011a).

The effect of mechanical stimulation on the cartilage has been discussed in Chapter 1.3. For cartilage tissue engineering, the mechanical stimulus remains an important signalling factor for differentiation and proliferation of the seeded cell. It also improves the mechanical properties of the tissue-engineered cartilage (Kock, *et al.* 2012). A number of bioreactors have been developed to apply different types of mechanical loading regimens to cell-seeded constructs (Schulz & Bader 2007). For example, direct dynamic compression applied to chondrocyte-seeded constructs generally increased the production of matrix macromolecules, which usually resulted in an improvement of the compressive property of the engineered tissue (Kelly, *et al.* 2006; Bian, *et al.* 2010). When MSCs-seeded constructs were stimulated with dynamic compression, an increase in the cartilage-like extracellular matrix components and an up-regulation of the chondrogenic genes was observed (Mauck, *et al.* 2007; Kisiday, *et al.* 2009). In addition to the most commonly applied compression force, different loading forces, e.g. hydrostatic pressure or shear stress, have also been investigated. It was noted that chondrogenic differentiation could also be induced in the bone marrow-derived MSCs (Luo & Seedhom 2007), adipose-derived MSCs (Ogawa, *et al.* 2009) or synovium-derived MSCs (Ogawa, *et al.* 2009) if hydrostatic pressure was introduced in these tissue-engineered constructs. However, the optimal combination of mechanical stimuli or the cells in tissue engineered constructs has yet to be determined.

1.6 Experimental models for cartilage research

Cartilage research has been conducted on a wide range of models ranging from isolated chondrocytes (*in vitro* studies), cartilage explants (*in vitro* studies) or live animal models (*in vivo* studies). Each model has its own advantages and disadvantages; for instance isolated chondrocytes are easy to cultivate and proliferate into a considerable amount of cells in a relatively short period of time in the laboratory, but they change from their original chondrocytic phenotype to a 'fibroblast-like' phenotype, as indicated by the cell shape transforming from round to elongated. This has been postulated to be due to the chondrocytes being cultured in 2-D instead of their natural 3-D environment within their extracellular matrix (Caron, *et al.* 2012).

Cartilage explants are harvested pieces of articular cartilage. They contain the full characteristics of cartilage and permit the study of cartilage as a tissue. The chondrocytes sit in their native extracellular environment and maintain their original shape and alignment with each other. Similar variables can be controlled in experiments using cartilage explants as those using isolated chondrocytes. However, the lack of the whole joint structures of cartilage explants limits its representation of the *in vivo* joint environment accurately, especially if the effects of mechanical stimulation from joint movement, which has been demonstrated to be crucial for maintaining the cartilage integrity by regulating tissue remodelling (Ramage, *et al.* 2009). In addition, the procedures to harvest cartilage explants have been demonstrated to induce the 'explantation injury', which activates intracellular inflammatory signalling pathways and induces expression of mRNA for IL-1α and IL-1β (Gruber, *et al.* 2004).

Animal models overcome the drawbacks of cartilage explants in the aspect of providing entire joint structures, and experiments carried out on live animals reflect the closest correlation to human conditions amongst these three models, especially if large animals are used. However, the disadvantages of live animal models include: (1) The host immune response can act as a confounding variable (however the cartilage is considered to be an immune privileged site and for cartilage this may not

be a major downside), (2) the expense of purchase and maintenance of sufficient numbers of experimental animals, (3) the greater time for creating each model and (4) the time required to obtain regulatory approval and the need to demonstrate that the test variables will not contravene animal welfare (Weed & Raber 2005).

1.6.1 Osteoarthritis model

In the *in vivo* animal model, there are 3 categories of methods for creation of animals with osteoarthritis (Bendele 2001). First, the naturally occurring OA models can be found in the transgenic animals such as mice (Helminen, *et al.* 1993; Fassler, *et al.* 1994). They have similar pathology and pathogenesis to human OA but the slow progress of disease considerably elongates the experiment period. Second, the surgically induced OA models are commonly utilized by induction of joint instability, such as partial meniscectomy in rabbits (Colombo, *et al.* 1983) or anterior cruciate ligament transection in rats or dogs (Lindhorst, *et al.* 2000; Galois, *et al.* 2004). It may mimic the traumatic OA in humans with morphological similarity, but the rapid progression of cartilage degeneration with various histological severity in the lesion increases the bias of result evaluation. Third, the chemically induced OA model can be obtained by intra-articular injection of iodoacetate, an inhibitor of anaerobic glycolysis that kills chondrocytes (Guingamp, *et al.* 1997). Depending on the concentration and frequency used, different degrees of killing and thus degeneration can be achieved. However, the predicting efficacy from chemical compounds is still debated since there is no known agent that can induce human OA in a short period of time.

Development of the *in vitro* model to simulate osteoarthritic change could be more difficult than that of the *in vivo* model. The matrix GAG and collagen degradation, chondrocyte death, chondrocyte cluster formation and histological deterioration (by various histological OA scores) have been thought to be the hallmarks of early-stage osteoarthritis. Thus, a variety of methods have been developed to emulate these changes on the cartilage explants of various species, such as compressive overload (Lee, *et al.* 2013), collagenase treatment (Grenier, *et al.* 2014) and inflammatory

cytokines treatment (Gabriel, *et al.* 2010). However, it would be more suitable to name ‘injury model’ for those established in the *in vitro* level rather than ‘OA model’ since the osteoarthritis is a disease of the entire joint involving the cartilage, joint lining, ligaments, and underlying bone (Martin & Buckwalter 2002a).

1.7 Introduction of the thesis

Disorders affecting articular cartilage, such as chondral injuries and osteoarthritis, are amongst the most common problems in orthopaedics. Despite progress in articular cartilage research, the problem is still far from being defeated. Various models have been established for cartilage research, and the *in vivo* animal models reflect the closest correlation to human conditions. However, in keeping with the guiding principal of replacement in '*in vivo*' research, if a research question can be answered without a live animal, then it should be.

Thus, it was considered that it would be useful if a validated *ex vivo* organ culture system for a mammalian synovial joint was created and used to evaluate therapies prior to animal or patient studies.

The initial hypothesis was that it was possible to maintain a whole mammalian synovial joint *ex vivo* for more than one month so that the early response of articular cartilage to media flows and joint movement could be investigated.

The initial research questions were:

1. What was a suitable joint for *ex vivo* organ culture model and how should it be harvested?
2. How could the joint be kept sterile during the harvest processes and during the whole culture period?
3. What assessments were suitable to characterise this model?
4. How could flow of the culture media and motion of the joint be applied in the model?

The results to answer these questions have been presented in Chapter 2 to Chapter 4.

Once the joint model had been demonstrated to survive in the experimental environment for a period of time, the aim was to use it in certain applications, such as the initial cartilage response to heat and external injury and following this to evaluate the early cartilage repair response in the model when tissue engineered constructs were inserted. These results are presented in Chapter 5 to Chapter 7.

The findings in these areas are laid out in the following chapters of the thesis as set out below:

i. **Static model**: The basic joint model, this chapter includes the detailed development and characterisation of the basic model. (Chapter 2)
ii. **Media-stirred model:** The static model cultured in flowing media (Chapter 3).
iii. **Dynamic model**: The whole joint model to which movement has been added. (Chapter 4)
iv. **Heat-treated model**: The joint has been heat treated in order to kill the chondrocytes. (Chapter 5)
v. **Injury model**: A cutting injury has been applied to the joint model cultured in two different culture media. (Chapter 6)
vi. **Chondrocyte implantation model:** Cartilage defects were created in the joint and isolated chondrocytes were inserted into the defects. (Chapter 7).

In each Chapter, the contents are further divided into four main parts, which are ‘chapter outline’, ‘materials and methods’ specific to that chapter, ‘results’ and ‘chapter discussion’.

Chapter 8 is the overall discussion, which discusses the common and different features of the models, their clinical meanings and the comparison with the literature. A hypothesis to explain the GAG results, the limitation of the joint model and the final conclusion are also presented. Chapter 9 suggests possible future directions for the research.

SECTION B – DEVELOPMENT OF BASIC JOINT ORGAN CULTURE MODEL

Including

Chapter 2: Static Model

Chapter 2: Static Model

2.1 Chapter outline

The static model was the first model created from the bovine metatarsophalangeal joint. It was named ‘static’ because the harvested joint was statically placed in the culture media without any interference. It was the fundamental model in this thesis because, by modifying some aspects of the static model, more advanced models were developed in the following chapters.

The purpose of this chapter is comprehensively to describe and characterise this *ex vivo* joint culture model, as well as to validate the assessment methods of cartilage used in the thesis. Information is presented concerning:

1. Technical methods for joint harvest/culture to the cartilage sampling/testing.
2. The outcomes of the cartilage morphology and chondrocytes viability.
3. Proteoglycan and water contents of cartilage matrix.

To create a comprehensive picture of the static model, experiments were carried out for at least 4 weeks to evaluate the long-term changes of the relevant variables, e.g. chondrocyte viability and matrix proteoglycan content. Some other results were also included in this chapter to demonstrate further the unique characteristics of this model, such as the cell viability distribution in different sites of the joint surface and the change in viability in different storage conditions. In addition, the co-existent cells presented in the culture media are also demonstrated to complete the picture about the static model.

All the data are individually presented in detail and analysed thoroughly either within groups or between groups. Suitable statistical analysis methods are chosen to compare the data after the distribution of each data type are tested to identify if they are normally distributed. Discussion is focused on the validation of the joint culture model and the static effects on the cartilage. Some of the challenges during model development are also discussed.

2.2 Materials and methods

2.2.1 Joint harvesting

The bovine metatarsophalangeal joint **(Figure 2.1)** was chosen to be our target joint because its anatomy, a hinge-typed joint, is similar to the human knee joint and its peripheral location is easy to approach. Furthermore, the cartilage surface is large enough to provide multiple sampling sites and the convex shape of the metatarsus facilitates the harvesting of samples.

All bovine feet were provided and collected from a local abattoir (Scotbeef in Stirling) on the morning of the day of the experiment and were processed within six hours of the animals being slaughtered. The age of the cow was around eighteen to twenty-four months old. The breed was a mixture of beef cattle coming from Angus, Charolais and Simmentals cattle. The collected feet included both the hindfeet and forefeet because the slaughter processes in the abattoir mixed up all the dissected bovine feet and it was difficult to differentiate them by external appearance. Only healthy and disease-free feet were selected to be included in the experiments.

Joint harvest procedures were started once the feet were within the laboratory. The first procedure was to clean all the dirt and blood out of its furs by thoroughly rinsing and brushing the skin surface under running water. After the feet were totally cleaned up, two threaded stainless pins of 3.5 mm in diameter were fixed at the proximal end of metatarsus. These pins provided an extension scaffold that could be firmly fixed onto a specially made stand for suspending the feet **(Figure 2.2a)**. With this stand, the feet could be securely suspended on the surface of the bench. This helped to minimise the risk of contamination during processing, because sterility maintenance of the joint was crucial if the joint was to be cultured for a long time.

The feet were then skinned through the loose connective tissue layer between skin and muscle fascia. An inverted T cut was used, which started with an anterior midline incision on the metatarsus and passed distally to the joint line and ended with a transverse circumferential cut around the proximal interphalangeal joint to separate

the skin and hoof **(Figure 2.2b)**. Care was taken not to cut off too many hairs because once the hairs were attached on the soft tissue it was difficult to remove them, and the hairs potentially could have increased the infection rate. After skinning the exposed soft tissue was rinsed thoroughly with large amount of sterile phosphate buffered saline (PBS). The bare suspended foot with the frame was then moved into a standard class two hood for further processing.

In the hood, a sterile operation field was established first by wrapping a few sheets of sterile paper around the foot **(Figure 2.3a)** and only exposing the target joint for the procedure. The metatarsophalangeal joint was then opened by removal of the covering soft tissues and synovium. Great care was taken not to injure the underlying cartilage accidentally. All surrounding soft tissues, e.g. the joint capsule, synovium, ligaments and tendons, were removed completely. Once the joint capsule was opened the cartilage was kept wet by frequent PBS irrigation. The joint was then isolated by transecting the bones with an electric oscillating saw. The sawing lines were approximately one centimetre above and below the articular cartilage margin **(Figure 2.3b)**. Occasionally, defects or signs of arthritis on the cartilage surface were found in a few joints (approximately 5% in all experimental feet), and these specimens were discarded.

For the static model, the intra-articular ligament, which linked metatarsus and phalanges, was further dissected to expose the whole joint surfaces. The metatarsus part was chosen for further culture because taking samples from the convex joint surface of metatarsus was easier than that from the concave surface of phalanges **(Figure 2.4)**. In order to have the same culturing condition over the whole cartilage surface, the joint was placed in the culture container with the cartilage facing up.

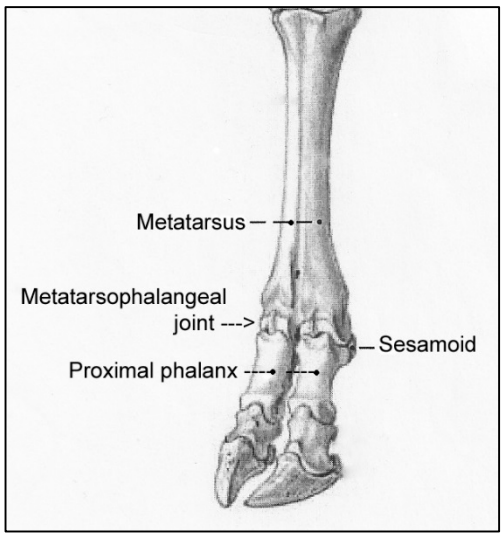

Figure 2.1 Anatomy of bovine extremity

The bovine metatarsophalangeal joint is composed of a fused metatarsus and two separate proximal phalanges. There are also four sesamoid bones posteriorly.

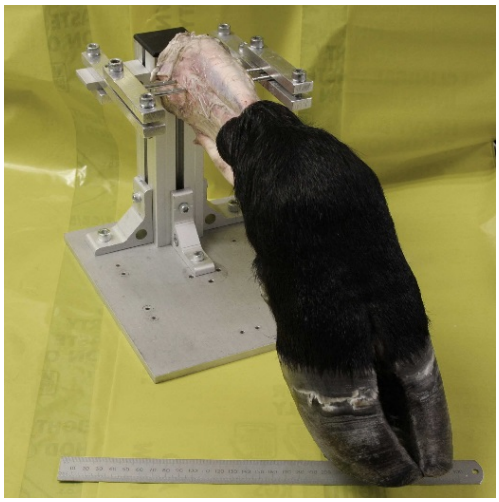
a.

b.

Figure 2.2 Suspension stand and joint approach

a. The bovine foot was suspended in the specially made frame by insertion of 2 metal pins at the proximal metatarsus, and this suspension prevented any contamination from the working surface. **b.** Incision started from the midline of the metatarsus down to the proximal interphalangeal joint with a transverse circumferential cut that removed all of the skin and the hoof without leaving many hairs.


a.

b.

Figure 2.3 Sterile wrapping and bone sawing

a. The skinned foot was wrapped with sterilised paper to establish sterile safety zone. **b.** After removal of all surrounding soft tissues, the metatarsophalangeal joint could be exposed and sawed at a distance of approximately one centimetre above and below the cartilage margin.

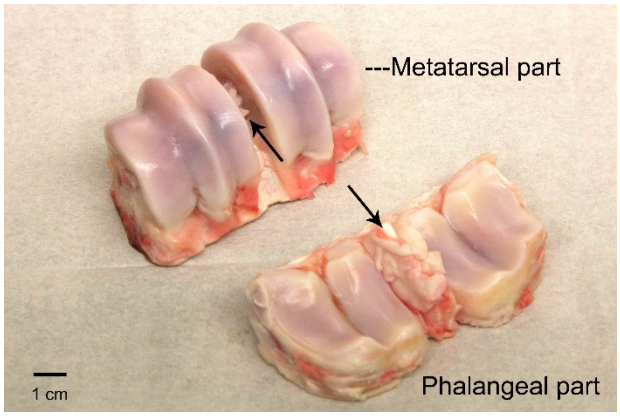

Figure 2.4 Metatarsophalangeal joint separation

The metatarsophalangeal joint was separated into two parts by dissecting the intra-articular ligament (black arrow). The metatarsal part was chosen to present the static joint model because of its convex joint surface that facilitated cartilage biopsy using with scalpels.

2.2.2 Culture environment

One litre glass beakers were sterilised and used as the containers during culture. The culture media were high glucose (4.5 g/L) Dulbecco's Modified Eagle Medium (DMEM) mixed with penicillin (100 U/mL), streptomycin (100 μg/mL) and foetal bovine serum (10%, v/v). Approximately 250 to 300 ml of culture media was sufficient to immerse the entire joint. The opening of the beaker was sealed with double sheets of paraffin membrane, and a ventilation outlet was made around the spout **(Figure 2.5)**. The container was then placed in a humidified incubator with temperature of 37°C and 5% CO_2. The culture media were changed twice a week.

Initially, a wide range of vessels was considered for the task of culturing from the most expensive custom-made glass receivers to the cheapest plastic boxes. The 1L glass beaker was chosen because it was large enough to contain the whole joint model, easy to clean, and readily available in every biologic laboratory.

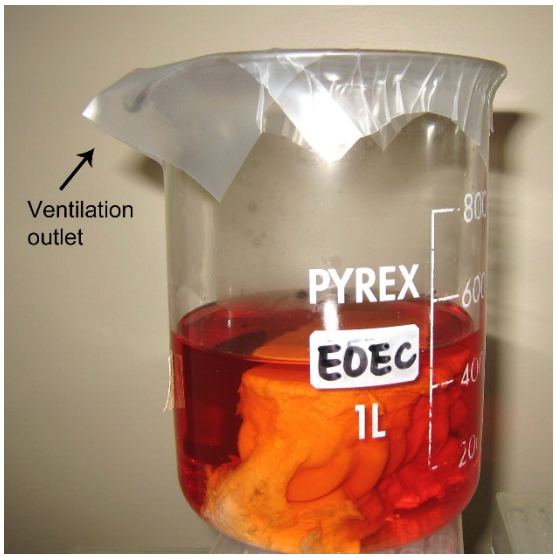

Figure 2.5 Culture container

A one-litre beaker was used as the culture container, which was covered with double sheets of paraffin membrane; a ventilation outlet was preserved around the spout. The joint model was totally immersed in the culture media.

2.2.3 Cartilage sampling

Cartilage samples were taken by using sterile scalpel blades. Blades were changed every 3 cuts because of the concern with the blade sharpness (Amin, *et al.* 2008; Amin, *et al.* 2011). The depth of every cut was controlled manually to reach the level of subchondral bone. There was a learning curve before it was possible to take ideal samples, which would have full thickness of cartilage attaching with a little subchondral bone in the middle of the samples **(Figure 2.6a)**. The sampling site was chosen randomly on the cartilage surface of the joint. Normally, one bovine joint could provide maximal 46 sampling sites among its 8 joint facets **(Figure 2.6b)**. The cartilage samples were kept wet with PBS all the time after being taken from the joint.

For examination of cartilage viability, the sample was further cut through the midline with a new blade to create a new fresh cut surface, in which the coronal plane of chondrocyte viability could be revealed. For matrix glycosaminoglycan (GAG) and water content measurements, the samples were snap-frozen immediately and stored in a -80°C freezer until the date of testing. For histology, the cartilage samples were placed in 10% (v/v) neutral buffered formalin (NBF) for fixation, and then were embedded in paraffin wax for microtome cutting.

The time point of sampling cartilage from the joint model was decided to be every 7 days, from Day 0, Day 7, Day 14… until the end of the experiment. For the static model, the experimental period lasted to Day 42, which was the longest experiment among all models in the thesis. At each time point, six cartilage samples were taken from each joint. Three of them went for viability examination and the others were reserved for GAG, water content and histology tests.

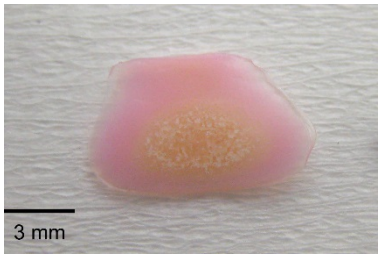

a.

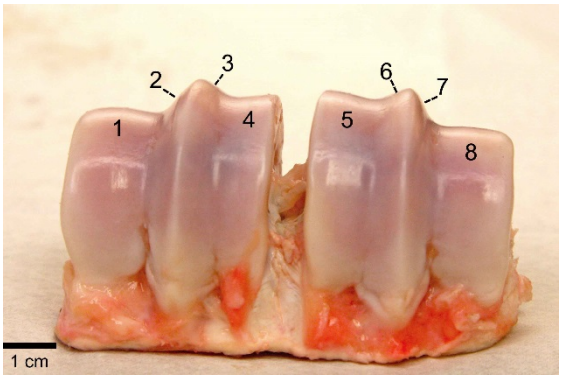

b.

Figure 2.6 An ideal cartilage sample and multiple sampling sites of the joint

a. Samples were taken deep enough to obtain full thickness of articular cartilage, which was indicated by the subchondral bone attached in the centre. **b.** There were 8 articular facets in the metatarsophalangeal joint. The facet-1, 4, 5, 8 are flatter and larger than facet-2, 3, 6, 7 which were located beside the articular ridges. Maximally, facet-1 and 8 each provided 5 sampling sites, and the other 6 facets could have 6 sampling sites in each facet.

2.2.4 Morphology examination

The morphology of cartilage was examined using conventional paraffin embedded and fresh frozen sections. With the conventional paraffin embedded histology, the cartilage samples were immediately fixed by 10% (v/v) Neutral Buffered Formalin (NBF), which contained 10% formalin in PBS solution. After 24 hours fixation, the solution was changed to a decalcifying solution, which contained 5.5% (w/v) EDTA (Ethylene-diamine-tetraacetate) and 10% NBF, in room temperature for 2 weeks in order to decalcify the subchondral bone gently. After complete decalcification, samples were embedded in paraffin with the coronal plane facing up and sectioned with a microtome. The section thickness was set to 4 μm in order to demonstrate the histological structure of cartilage precisely. Haematoxylin and eosin (H&E) stain and Alcian blue stain were used to demonstrate general morphology and the distribution of matrix proteoglycan, respectively.

Some cartilage samples were snap-frozen directly without formalin fixation or decalcification. This was performed by immersing cartilage into Optimum Cutting Temperature (OCT) compound, which is a formulation of water-soluble glycols and resins and is used to embed tissue samples prior to frozen sectioning at temperatures of –20°C or below. OCT compound protected cartilage from distortion during freezing, and also eliminated undesirable background staining because it left no residue on slides after staining procedures. It should be noted that the orientation of cartilage had to be adjusted correctly before it had frozen. The plane of interest should be placed facing up. Therefore, a special fixation chuck was designed to help to keep the correct orientation whilst the cartilage was being frozen in the OCT compound **(Figure 2.7)**. The cryostat was used to section the frozen cartilage samples. The minimal sample thickness for the cryostat was 6 μm, which was thicker than the thickness of paraffin embedded sections. After sectioning, the slides were stained with H&E and Alcian blue.

In order to obtain the best quality of stained images, optimisation of the staining time for both the paraffin embedded and frozen section slides was determined by several trial combinations. The best results were obtained when the cartilage slide was

stained with haematoxylin for 5 minutes, 'blued' with 0.2% ammonia water for 30 seconds and counter stained with eosin for 1 minute. If the Alcian blue was used for staining the GAG of the ECM, the best result was obtained when the Alcian blue stayed on the sample longer than 30 minutes. After staining, subsequent dehydration through 50%, 75%, 90% and 100% alcohol baths was performed, and the sample could then be mounted under a coverslip for permanent preservation.

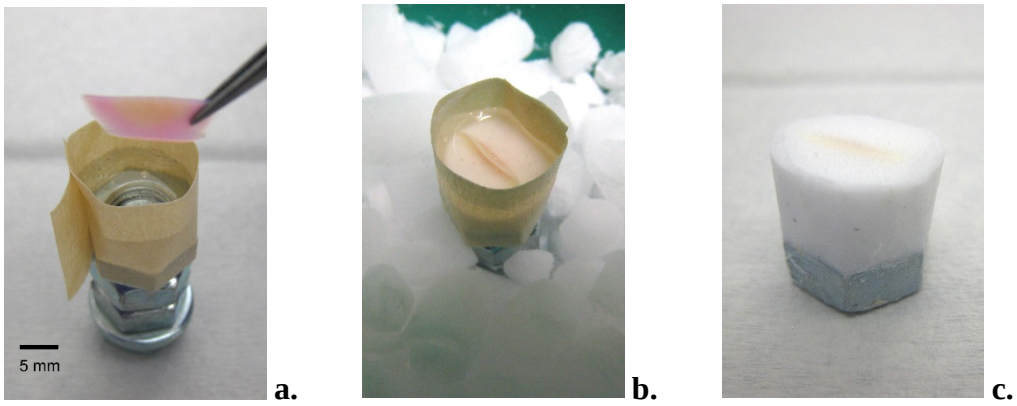

a. **b.** **c.**

Figure 2.7 Fresh sample fixation in OCT compound

a. For frozen section, a chuck made by screws and tapes was used to help keep the correct orientation of the cartilage sample. Approximately 2-3 ml OCT compound was added into the space created by the tapes. The biopsied sample was cut half to reveal the coronal plane of cartilage. **b.** The chuck was placed with dry ice and the cartilage sample was frozen in the OCT compound with the cut surface facing up. **c.** After the OCT compound was totally frozen, the tapes were removed, and the orientation of the cartilage sample was fixed precisely. This chuck was used directly in the cryostat.

2.2.5 Chondrocyte viability examination

Staining principles. Chondrocyte viability was examined by live and dead fluorescent stains (Amin, *et al.* 2008). The live stain, 5-chloromethylfluorescein diacetate (CMFDA), stains the cytoplasm of a live cell green. Initially, CMFDA is colourless and non-fluorescent until its acetate groups are cleaved by cytosolic esterases, which only exist in the cytoplasm of live cells. Hydrolysis of the acetates yields a product, 5-chloromethylfluorescein, which is membrane-impermeant and fluorescent with a spectrum of 492 nm in absorption and 517 nm in emission. This can be detected as green fluorescence with a fluorescent microscope.

The dead stain, propidium iodide (PI), stains the nucleus of a dead cell red. The principle of the stain is that the negative charged PI molecule is membrane impermeant and, therefore, it can be excluded from viable cells. Only dying cells, which have defective cell membranes, allow PI to pass through. After entering into a cell, the molecule of PI intercalates between the bases of DNA in the ratio of one dye per 4-5 base pairs with little or no sequence preference (Suzuki, *et al.* 1997). Its fluorescence is enhanced 20 to 30 fold when the dye is bound to nucleic acids. Its fluorescent spectrum falls on 535 nm in absorption and 617 nm in excitation, which means a red fluorescent colour can be detected with a fluorescent microscope.

Solution making. The solution of CMFDA/PI was made on the day of examination because the fluorescence decays gradually as soon as the dyes are dissolved in the solvents. According to a preliminary result, the reaction activity of these agents disappeared completely after one week storage even when they were stored cold at 4°C.

The concentration of CMFDA was 5 μM, which meant 20 μg of CMFDA powder was first dissolved in 20 μl Dimethyl sulphoxide (DMSO) and further diluted with 15 ml of culture media (DMEM with 1% Pen/Strep, v/v). The concentration of PI was 5 μM as well, which meant 75 μg of PI was added in the 15 ml culture media. The well mixed staining solution was then equally divided and placed into 10 small (15 ml) conical tube (approximately 1.5 ml CMFDA/PI solution in each tube). Aluminium

foil was wrapped around the tube for prevention of the photo decay to these fluorescent dyes.

Staining procedures. As soon as the cartilage samples were harvested from the joint model, they were placed in the staining media and left there for 45 minutes at room temperature in order to let the dyes infiltrate into the cartilage and interact with the chondrocytes. The staining media was then discarded and replaced with 10% neutral buffered formalin (NBF) for sample fixation. These biopsies were kept at a temperature of 4°C for 24 hours to complete the fixation, and the NBF was replaced with PBS. The sample was now ready for microscopic scanning to identify the viability of chondrocytes. All procedures were carried out in a dark environment.

Scanning principles. Confocal laser scanning microscopy (CLSM), (the Zeiss LSM 510 system) was used to acquire the fluorescence images from the cartilage samples. CLSM is a technology that collects high-resolution optical images with depth selectivity, a process known as optical sectioning. The key elements behind CLSM are the single wave-length light source (i.e. a laser) and the pin-hole filter. These features reduce the incorporation of out of focus light or scattered light in the images and enable an extremely narrow area at a defined depth to be studied. Images can be acquired point-by-point and reconstructed with a computer that allows 3-D reconstructions of topologically complex objects. For opaque specimens, this is useful for surface profiling, while for non-opaque specimens, interior structures can be imaged.

The pin-hole filter is the second key element of CLSM because it is designed to screen the out-of-focused light from the fluorescent sample. This produces an all-in-focused image and facilitates the chondrocyte counting to be more precise. Therefore, CLSM overcomes the major problem of fluorescence microscopy (FM) because approximately 90% of the light in the FM image comes from outside the focal plane. Another advantage for using CLSM instead of FM was that the thickness of the cartilage samples harvested from the joint model was much thicker (approximately 1-2 mm) than the conventional microtome-sectioned samples (3-10 μm in the slides). Images of CLSM are obtained from scanning the surface of

cartilage sample layer by layer. If FM had been used to scan the thick sample, the image would have been unreadable because the broad-range mercury illumination of the FM would have excited the fluorescence from entire thickness of the sample and the resulting diffuse fluorescence would have produced an image contaminated by superimposition and interference.

However, FM was evaluated on fresh frozen cryostat-sectioned cartilage samples as a preliminary screening technique before CLSM. However, the freezing and sectioning processes adversely affected the chondrocyte viability. Cells died during these manipulations, and the viability results were far lower than control specimens imaged with CLSM. Therefore, CLSM was chosen as the method of choice for scanning the full-thickness of the cartilage samples, especially when chondrocyte viability was being examined.

CLSM settings. The laser light of CLSM come from Helium–Neon and Argon gas and has an emission wave length of 458, 477, 488, 514 and 543 nm. The pinhole of the filter was set to be 1 Airy unit. The interval of each scanning plane was adjusted to 10 μm, and the scanning region of interest was 921 × 921 μm under the 10× objective. These microscopic parameters meant that the 3-D cartilage sample was optically sectioned layer by layer into multiple 2-D images by CLSM. The area of each image was 921 × 921 μm and the distance between each parallel image was 10 μm. The number of ‘image sections’ obtained from one cartilage sample depended on two factors—the staining depth and the sample position. Due to the penetration ability of the CMFDA/PI dyes to the cartilage, it was found that only a limited depth of the cartilage sample could be stained. Repetitive trials revealed that a depth of only 60 to 80 μm of the cartilage tissue could be penetrated by these dyes. This meant that after staining, the sample consisted of a stained shell-like outside layer with a non-stained inside core. Attempts to increase the staining depth were tried by prolonging the staining time and elevating the temperature to 37°C during the staining period. However, neither time nor temperature increased the staining depth but resulted in more chondrocyte death (which was considered to be attributed to the toxicity of the dyes).

The second factor that influenced the number of 'image sections' was the position of specimen at the moment of scanning. More 'image sections' were needed if the cartilage surface was not placed horizontally on the microscope stage. This was technically challenging because adjusting the sample to be absolutely horizontal by hand in a scale of micrometres was extremely difficult. However, an increase in the number of 'image sections' resulted in an increase of scanning time, which in turn resulted in problematic photo-bleaching on the stained cartilage sample. Therefore, a parallel cutting device was devised in order to create two parallel cuts of the sample. This facilitated horizontal orientation of the scanning surface of the cartilage sample on the microscope stage (**Figure 2.8a**).

Scan processes. During the scan processes, both axial and coronal views were taken from the same cartilage sample. The axial view was taken from cartilage surface upward, which revealed the status of superficial layer of chondrocytes. The coronal view was taken from cartilage surface forward, which was scanned through the cut plane and gave information on superficial, middle and deep zones of cartilage (**Figure 2.8d**). The image volume of the cartilage sample was approximately 921×921×80 μm, which meant the border of the image was 921×921 μm and depth was 80 μm, the deepest distance that stains could penetrate. Ideally if the sample surface was absolutely horizontal, the depth of 80 μm required 9 virtual 'image sections' at 10 μm intervals. The diameter of a single chondrocyte is approximately 10 to 15 μm (Bush & Hall 2003). With the scan interval set to 10 μm, any chondrocyte in the scanning volume would not be missed.

Cell counting. After scanning, all individual 'image sections' were stacked together to form a synthesised 3-D image, and the cells in the image were counted automatically by ImageJ (NIH, Version 1.47). For the axial viability, the region of interest was set to be 500×921 μm – this was to exclude the zone of dead cells at the cut margin (**Figure 2.8e**). For the coronal viability, three regions were set according to the percentage depth from the cartilage surface, and the viability in each zone was counted separately. The regions of superficial, middle and deep zones were set as the most superficial 25%, the middle 50% and the deepest 25% of the cartilage depth

(**Figure 2.8f**). After the region of interest (ROI) of the image was set, the number of live and dead cells in each ROI was automatically calculated by ImageJ. Because there were two different channels recorded from CLSM, which were the green channel representing the CMFDA-stained cells and the red channel for PI-stained cells, the number of live and dead cells could be counted separately. The cells crossing the top and right edge of ROI were included but the cells crossing the left and bottom border were not counted. After calculation, the cell viability was presented as the percentage of live cells of the total cells, i.e. the equation: (live cells)/(live cells + dead cells) ×100.

Cell density calculation. The image volume of ROI in every sample was also recorded, which represented the scanned cartilage volume. The cell density of each ROI was then calculated by the equation: (live cell no. + dead cell no.)/cartilage volume (mm^3).


a.

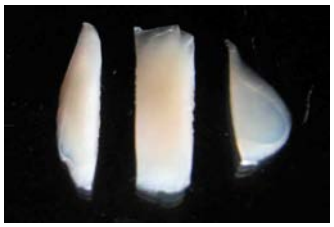
b.

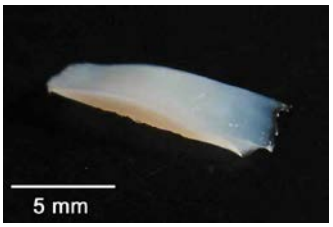

c.


d.

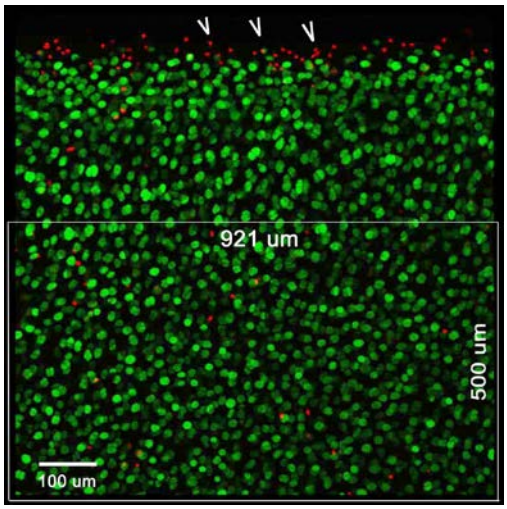

e.

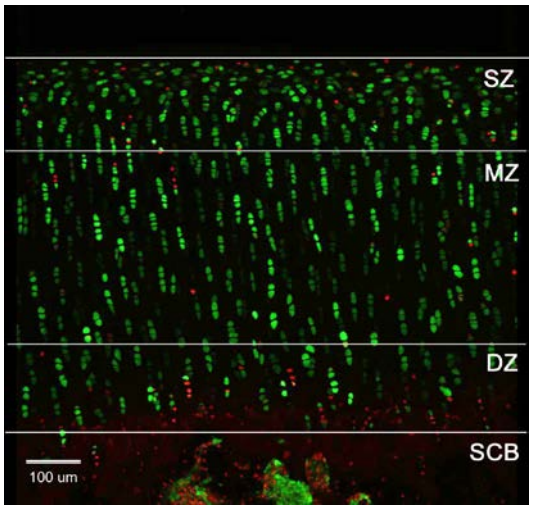

f.

Figure 2.8 Procedures for axial and coronal viability

a. The parallel cutting device was made by two scalpel blades clamping together with a metal plate in the middle. **b.** By using this cutting device, the cartilage explant could be cut into 3 pieces in which the two cut lines were parallel to each other. **c.** The middle part of the cartilage explant was chosen and placed on a small petri dish with cartilage surface facing up for axial view scanning. **d.** After completing the scan of the axial view, the cartilage explant was turned 90° and held within two bits of blue tack for imaging the coronal view. **e.** The region of interests (ROI) in the axial

view was set 921μm × 500μm to get rid of the distortion from the dead cells along the cut edge (arrowed). **f.** The region of interest in the coronal view was set by the cartilage thickness. The first 25% of cartilage was counted as the superficial zone (SZ), and the next 50% and the last 25% were the middle zone (MZ) and the deep zone (DZ), respectively. At the bottom of the image was the subchondral bone (SCB) that contained osteoblasts and osteoclasts with multiple nuclei.

2.2.6 Glycosaminoglycan content assessment – Validation and optimization of Farndale's protocol

The content of sulphated glycosaminoglycan in the extracellular matrix of cartilage was measured by the spectrophotometric microassay method, which was published by Farndale et al. (Farndale, *et al.* 1982). A modified protocol was published later to improve the stability of the reagents (Farndale, *et al.* 1986). This method was wildly accepted for detection of matrix GAG content of the cartilage samples. The following protocol was modified and optimized in some parts of the original one to fit the situations of the experiments in the thesis.

There were three kinds of solution needed for testing the matrix GAG content of the cartilage: (i) 1,9-dimethylmethylene blue (DMMB) solution, (ii) digestion solution and (iii) dilution solution.

(i) The DMMB solution was prepared as follows: 16 mg DMMB was dissolved in one litre distilled water, which contained 3.04g glycine, 2.37g NaCl and 95 ml 0.1 M HCl. The solution was adjusted to pH 3.0. The bottle was wrapped in foil and stored in darkness at room temperature before use. This colour reagent was stable for at least 3 months.

(ii) The digestion solution was a mixture of 1 mM EDTA and 2 mM dithiothreitol in 20 mM sodium phosphate buffer (pH 6.8).

(iii) The dilution solution was a 50 mM Tris/HCl (pH 8.0) solution, which was used to dilute the digested solution to be in the sensitive range of the spectrum in the spectrophotometric microassay.

To validate this method a standard solution was used, which was made by mixing 5 mg chondroitin sulphate (CS) in 50 ml distilled water. The concentration of this standard solution was 0.1μg/μl that meant 10μl of the solution contained 1 μg chondroitin sulphate. Sequential volumes of the standard solutions starting from 10 μl, 20 μl, 30 μl…up to 100 μl were pipetted into micro cuvettes. Distilled water was added until the total volume was 100 μl. One millilitre DMMB solution was then added to the cuvette and the absorbance of the solution was measured immediately

(within 10 seconds after mixture). The illumination wavelength of the spectrophotometer was set at 525 nm, which was the most sensitive wavelength for the GAG-DMMB complex. A chart of CS mass against absorbance was plotted. Absorbance from the test cartilage sample was compared with the standard CS curve to derive the GAG amount in the sample.

The procedures of measuring GAG content in the cartilage consisted of:

(i) The samples were trimmed with a biopsy punch of 2.5 mm diameter to get similar amount of cartilage tissue. The central area of cartilage sample was always chosen for trimming because this area contained the full thickness of cartilage tissue, which was indicated by the subchondral bone attached in the bottom **(Figure 2.9)**. (Histological examination demonstrated that the GAG was not evenly distributed among the cartilage tissue and that most was located in the deep zone. Therefore, an erroneously low value for the GAG content would be obtained if the examined area did not contain tissue from the deep zone.)

(ii) The trimmed sample was weighed to obtain its 'before-digested' wet weight, which included the weight of cartilage and subchondral bone.

(iii) The sample was then placed in a small glass bottle containing 1 ml digestion solution and 300μg papain, and this bottle was then placed in an oven at 60°C. The incubation was continued until the tissue was totally digested.

(iv) After digestion, 10 μl 1M iodoacetic acid solution was added to stop the effect of papain.

(v) The solution was then diluted by adding 4 ml dilution solution (5× diluted). This dilution ensured that the spectrophotometric reading would fall in its sensitive range.

(vi) One hundred microlitres of the solution was taken and placed in a micro cuvette for measuring its absorbance using the same procedure as those used to measure the standard chondroitin sulphate solution.

(vii) The absorbance from the sample was compared with the standard curve to obtain the precise GAG content. This result (mass in micrograms) was then normalized with the total cartilage mass (in milligram) to allow for comparison of any variation in the size of the cartilage specimen. Therefore, the final result of GAG content was presented as the percentage of GAG mass (in μg) per cartilage mass (in mg), which was presented as '%GAG (μg/mg)' in the charts. (The cartilage weight meant the weight of digested cartilage. The subchondral bone of the cartilage sample was not digested by papain. Therefore, the accurate cartilage weight for calculation was the difference between the before-digested wet weight and the subchondral bone weight.) A precision balance was used to measure the weight to be within 0.1 mg in order to increase the accuracy.

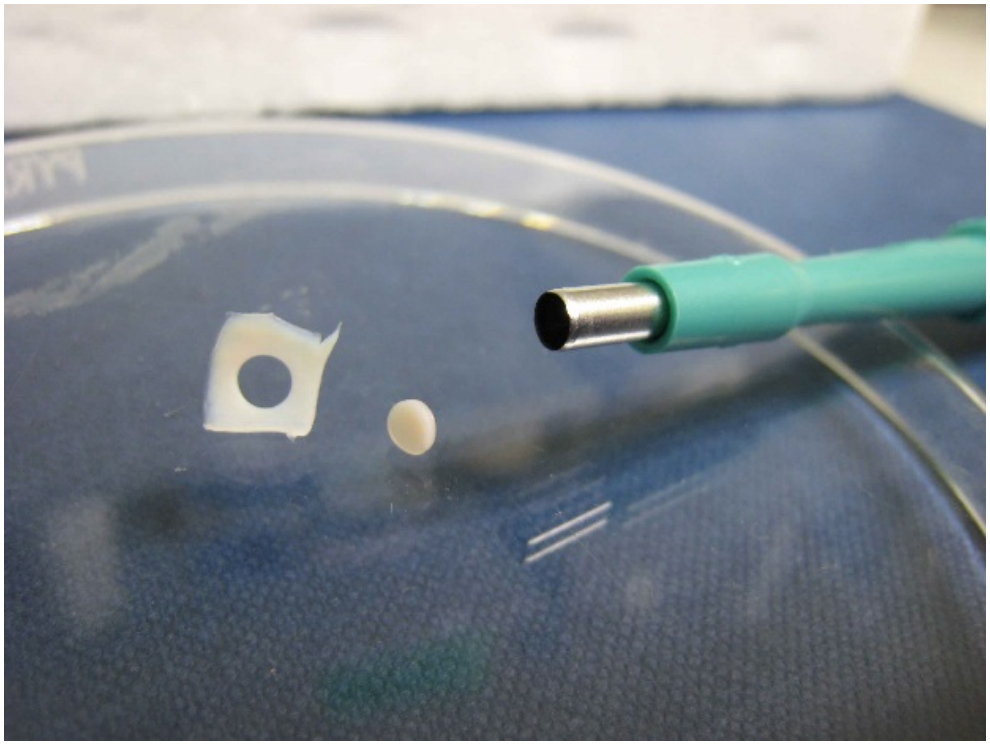

Figure 2.9 Cartilage biopsy

The cartilage sample was trimmed with a biopsy punch of 2.5 mm diameter to obtain the central full-thickness part of the cartilage for matrix GAG assessment

2.2.7 Glycosaminoglycan content assessment – Validation of the DMMB complexation/decomplexation protocol

Before Farndale's protocol was applied, glycosaminoglycan content in the extracellular matrix of cartilage was examined using the method of DMMB complexation/decomplexation (Barbosa, *et al.* 2003). This was a modified protocol, which the authors claimed had better specificity, reproducibility and sensitivity than the previously published GAG assays. However, after a number of careful trials, it was not possible to establish the Barbosa protocol.

The principle of the Barbosa protocol was to generate a precipitate of the GAG-DMMB complex, then to isolate this precipitate and finally to re-dissolve it (decomplexation). The decomplexed solution was then measured by spectrophotometer to quantify the GAG content of the original samples. It was different from the conventional GAG assay in the way it dealt with the GAG-DMMB complex. In the conventional GAG assay as described in the previous section, the GAG-DMMB complex was measured directly and instantly (within 10 seconds after mixing) before precipitation happened. In this modified protocol, the GAG-DMMB complex was induced to precipitate.

Solution preparation

Solutions needed in this modified (Barbosa) protocol included the DMMB solution and the decomplexation solution. In the DMMB solution, 16 mg DMMB were dissolved in 25 ml ethanol and filtered through filter paper. One hundred millilitre of 1 M guanidine hydrochloride (GuHCl), 1 g sodium formate and 1 ml 98% formic acid were added to the DMMB ethanolic solution. Distilled water was added to bring the final volume up to 500 ml. Another 500 ml solution, which contained the same amount of the same constituents except DMMB (i.e. GuHCl, sodium formate and formic acid) was made. These two solutions were mixed together to form the DMMB solution. Barbosa *et al*. claimed that the DMMB solution made this way was more stable than the solution made by the previous method because the twofold dilution of

a double-concentrated solution was a standard strategy for stabilisation of solubility by chemists.

In the decomplexation solution, a 50 mM sodium acetate buffer solution (pH 6.8) containing 10% propan-1-ol was prepared first. Then powdered GuHCl was added to the solution to a final concentration of 4 M (e.g. adding 95.53 g powered GuHCl if the volume of the solution was 250 ml). This decomplexation solution and DMMB solution were stable for at least 4 months at room temperature if they were stored in the darkness.

Cartilage digestion

The procedure of cartilage digestion consisted of:

(i) 50 μg proteinase K in the 1 ml 100 mM K_2HPO_4 (pH 8.0) was used to digest the cartilage sample, which was placed in an oven overnight at 56°C. After complete digestion, the effect of proteinase K was stopped by 10 minutes of heating in a water bath at 90°C.

(ii) The tissue debris was filtered and 100 μl of this filtered solution was taken and placed in an Eppendorf tube.

Measurement of the GAG content

(i) 1 ml DMMB solution was added to the tube, and the mixture was shaken vigorously by a vortex shaker for 30 minutes to promote complete complexation of the GAG with DMMB.

(ii) The insoluble GAG-DMMB complex was then separated from the soluble components by centrifugation at 12000 g for 10 minutes.

(iii) The supernatant was discarded, and 1 ml of decomplexation solution was added to the tube. Once again vigorous shaking for 30 minutes was needed to decomplex the GAG-DMMB complex completely.

(iv) The solution was then placed in the micro cuvette and its absorbance was measured in a spectrophotometer using illumination with a wavelength of 656 nm.

(v) The standard calibration curve was plotted by using chondroitin sulphate solution of different concentrations (from 1 mg/ml to 10 mg/ml).

(vi) The absorbance from the sample was compared with the standard curve to obtain the precise GAG content.

However, the amount of precipitate from the GAG-DMMB complexation was too tiny to be manipulated either in the solution of digested samples or in the standard solution. Thus, the concentration of chondroitin sulphate was increased (from 4 mg/ml to 20 mg/ml). With this manoeuvre the precipitate became large enough to be manipulated, but the result lacked validity because the value of absorbance was reversely proportional to the concentration **(Figure 2.10)**. The acidity of the DMMB solution was considered as a possible cause of this problem and was adjusted: DMMB solutions were made of different acidities (From pH 1.0, pH 2.0… to pH 6.0) and tested with chondroitin sulphate solution. The results showed that the calibration curves varied at the different pHs and the relationship of absorbance to concentration was not consistent. For one pH it was directly proportional, some were inversely proportional, and some were neither **(Figure 2.11)**. The solution of pH 2.0 was the closest to being directly proportional but the linearity and the slope were still not convincing. Barbosa *et al*. had suggested pH 3.0 for the DMMB solution in their paper but, unfortunately, the graph obtained in the current experiments was not proportional. As the results still lacked validation, this method was abandoned.

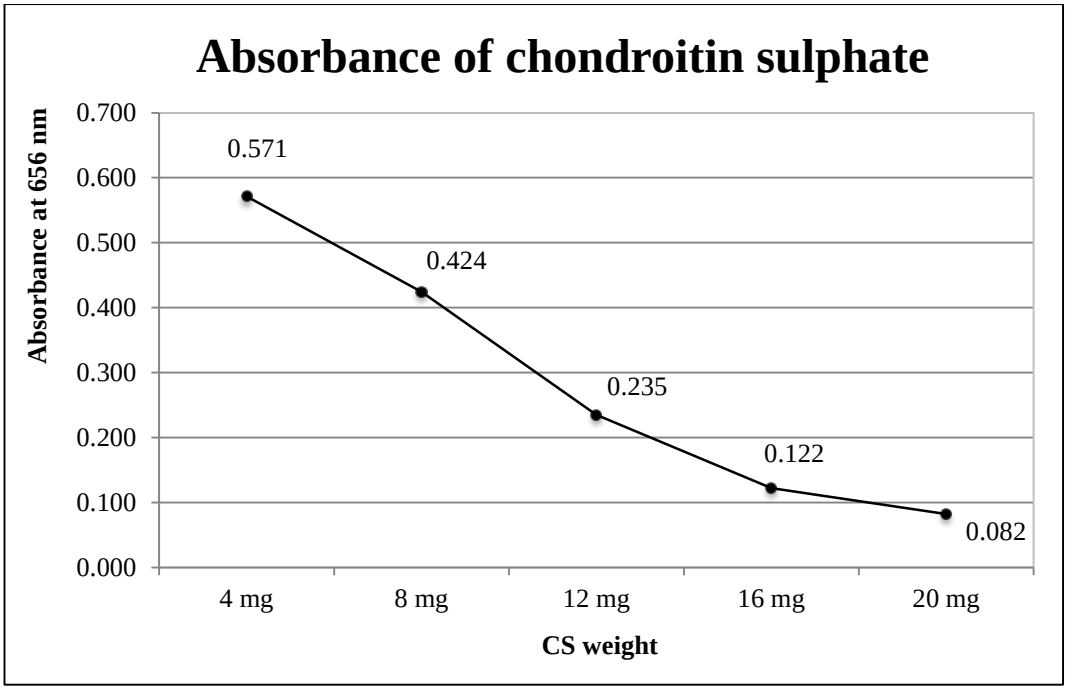

Figure 2.10 Absorbance of chondroitin sulphate in the DMMB complexation/decomplexation assay

The standard curve of chondroitin sulphate by the DMMB complexation/decomplexation assay demonstrated that the absorbance was inversely proportional to the concentration of chondroitin sulphate. This result lacked face validity, i.e. an increase of chondroitin sulphate would not be expected to result in a decrease of DMMB absorbance.

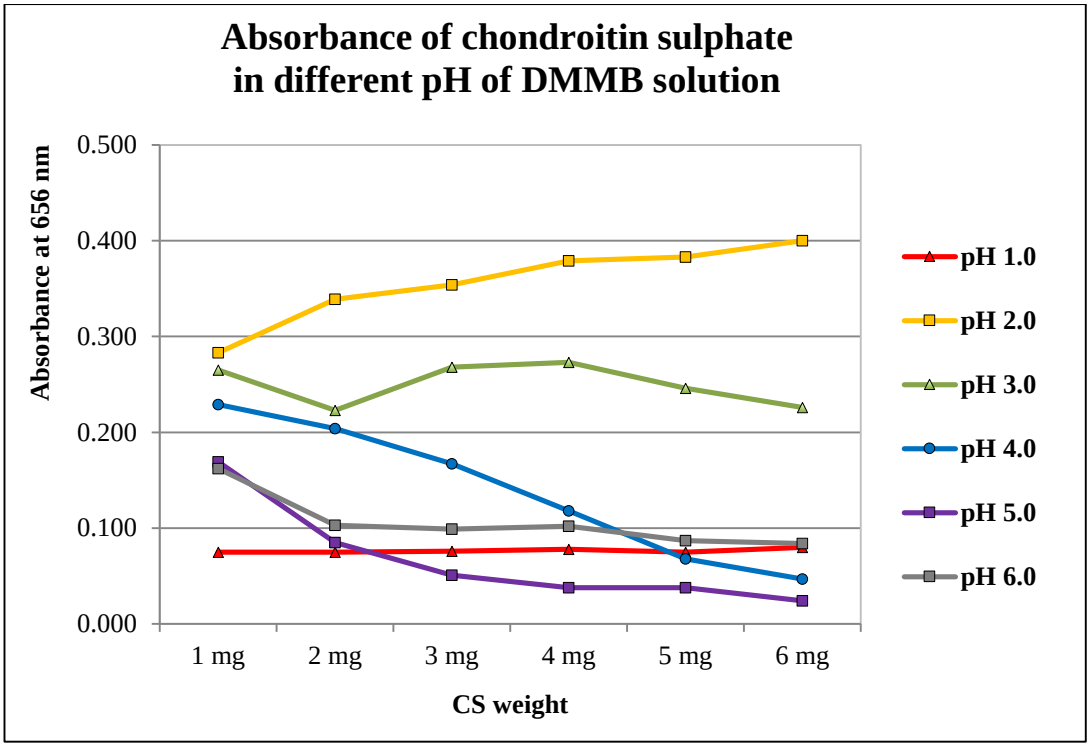

Figure 2.11 Absorbance of chondroitin sulphate in different pH of DMMB solution.

The absorbance of chondroitin sulphate varied with different pHs of the DMMB solution. Even the curve for pH 2.0 showed too narrow a range from 1 mg to 6 mg (absorbance change from 0.283 to 0.400) for it to be discriminative.

2.2.8 Water content assessment

The water content of the cartilage samples was examined by lyophilisation. The conditions for lyophilisation were set at a temperature of -55°C and a pressure of 0.1 atm. The duration of lyophilisation was over 12 hours (overnight). The cartilage sample was weighed before and after treatment to obtain its wet weight and dry weight. The difference represented the water weight in the cartilage. The percentage water content was calculated as the formula:
(water weight)/(wet weight of cartilage) ×100.

2.2.9 Cell isolation from the culture media

The joint culture media was not free of cells and a range of cells were found suspended in the culture media. In order to identify them, the number of the suspended cells was counted by using the haemocytometer, and their morphology was observed under the microscope after culturing the cells in a flask for two weeks.

A haemocytometer was used for cell counting with following procedures:

One hundred millilitres of the culture media was taken from middle layer of the fluid and centrifuged at 400g for 5 minutes. The cell pellet was isolated after discarding the supernatant, and resuspended in 1ml of new culture media. Ten microlitres of cell suspension was stained with 90 μl Trypan blue solution, and mixed well. Twenty microlitres of the mixed solution were pipetted to fill the haemocytometer carefully by capillary action. Under conventional bright field microscope, cells located in the corner of the grid of the haemocytometer were counted. There were 8 corners in two grids within one haemocytometer. The sum of the cells in the 8 corners was divided by 8 to obtain the average cell number in one corner. The average cell number needed to be multiplied by 10 (because the cells had been diluted by a factor of 10 by the Trypan blue stain), and multiplied again by 10,000, (this was determined by the design of the haemocytometer). The final number that was derived was the cell number per millilitre in the test solution.

Some of the isolated cells were cultured in the flask using the same media as was used for the 'whole' joint model. The media was changed twice weekly and the morphology of the cells were observed directly in the flask under the bright light microscope.

2.2.10 Infection control

Infection control is fundamental to the success of developing this joint model. In order to keep the model infection free during the whole culture period, sterile techniques were used and the procedures were standardised. Some of the procedures were developed and modified by experience, and some were derived from the concepts of good surgical practice. The details of the sterile methods are described in this section.

Joint harvest. The joints were obtained from a local abattoir. Infection control started as soon as the joints had been collected. The freshest feet were still felt warm and had just been separated from the animals. The joint harvest began within 6 hours of the animals being slaughtered.

The furs were thoroughly cleaned by rinsing with a large amount of water and brushing off every piece of dirt and blood clot. This step was performed in the laboratory to decrease the possibility of contamination. Establishment of a stable environment where the foot could be manipulated sterilely was the next important procedure. This was achieved by suspending the foot from a specially designed frame. In this, the foot could be safely suspended in the air without contacting the working surface, which helped to minimise the risk of infection. Furthermore, once the foot had been skinned, it was placed in a hood with laminar flow control, a sterile operation area was established by draping with several sheets of sterile paper, in a similar manner to that used in the surgical operating theatre. Any tool or container, which would contact the joint, was autoclaved at 121°C for 15 minutes before use. The gloves for obtaining the sample biopsy or changing the media were also sterile.

Antibiotics. Antibiotics were not the first line for infection control in the experiment. The use of antibiotics was restricted to the minimum. Only penicillin and streptomycin at the lowest concentration (1%, v/v) were added into the culture media. No anti-fungal drugs were added as they are considered to have more side effects on mammalian cells than penicillin or streptomycin (Baginski & Czub 2009).

Container cover. Beakers were used as the culture containers. A paraffin membrane was used to cover the opening of the beaker. It should be noted that the paraffin membrane would crack if it was stretched and placed in the incubator at 37°C for a prolonged period of time. If the membrane lost its integrity, fungi or bacteria from outside the beaker would have the chance to contaminate the culture media. Thus, double layers of paraffin membrane were used for protection of the joint culture in the static model.

2.2.11 Data analysis

Before the experimental data were analysed, the number of variables in each data set and the normality of each variable were determined. Normality of each continuous variables, e.g. cell viability, water content or proteoglycan content, was evaluated by using histograms and the Kolmogorov-Smirnov normality test. Data were categorised as parametric if the possibility (p) value of the Kolmogorov-Smirnov test was above 0.150.

For parametric data, if two sets of data were compared, the paired t-test was used for paired results such as the change in chondrocyte viability in the same joint on different days, while the unpaired t-test was used for two independent groups such as the chondrocytes viability between two different models. If more than two sets of data were together compared, analysis of variance (ANOVA) was used. For non-parametric data, Mann-Whitney U test was used for comparison of two sets of independent results, while the Kruskal-Wallis test was used for three or more sets of non-parametric data.

All statistical calculations were performed using Minitab 16 (Minitab Inc., USA). In the experimental terminology, 'N' refers to the number of different animals used, while 'n' is the number of total sample number. In the tables in this thesis, the chondrocyte viability data for each time point were the means from three cartilage explant samples, and the GAG data were from two samples. Data in the tables were presented as means of these samples, and, in the figures, as (means) ± (standard deviation) for N (different animals). All statistical comparisons were made for N observations, and N in every experiment of the thesis was ≥ 3. The level of significant difference was set at $p<0.05$. If multiple comparisons were performed simultaneously on a single data set, Bonferroni correction was used, which was an adjustment made to *p* values (divide the *p* value by the number of comparisons being made).

2.3 Results

2.3.1 Standard calibration of GAG assay

A standard calibration curve of chondroitin sulphate (CS) was made each time for the DMMB assay before analysing the matrix GAG content of cartilage. The GAG amount in the sample was derived by comparing the spectrophotometric readings of the samples to the readings of the chondroitin sulphate in the standard curve.

Table 2.12 shows the spectrophotometric readings for known amounts of chondroitin sulphate over a period of 3 months. The standard calibration curve was drawn using the average of the absorbance readings and is shown in the following figure. The high repeatability and low standard deviation of the readings demonstrated the reliability of the method for GAG analysis.

CS weight (µg)	1	2	3	4	5	6	7	8	9	10
18/12/2012	0.395	0.429	0.459	0.488	0.516	0.549	0.570	0.594	0.614	0.638
19/12/2012	0.394	0.432	0.462	0.490	0.518	0.543	0.564	0.597	0.617	0.638
09/1/20132	0.394	0.434	0.466	0.490	0.508	0.541	0.576	0.592	0.619	0.642
16/1/2013	0.402	0.420	0.457	0.489	0.518	0.546	0.573	0.598	0.617	0.638
23/1/2013	0.393	0.428	0.461	0.488	0.519	0.547	0.566	0.588	0.613	0.636
30/1/2013	0.394	0.430	0.459	0.485	0.517	0.543	0.570	0.592	0.621	0.639
04/2/2013	0.400	0.432	0.461	0.490	0.521	0.548	0.572	0.596	0.617	0.642
06/2/2013	0.398	0.430	0.462	0.484	0.519	0.541	0.568	0.589	0.616	0.640
13/2/2013	0.397	0.431	0.461	0.494	0.516	0.546	0.573	0.596	0.620	0.641
20/2/2013	0.396	0.430	0.461	0.493	0.518	0.544	0.568	0.592	0.616	0.638
06/3/2013	0.396	0.429	0.464	0.491	0.518	0.543	0.566	0.595	0.616	0.640
13/3/2013	0.395	0.433	0.463	0.490	0.517	0.544	0.568	0.591	0.616	0.633
20/3/2013	0.396	0.431	0.454	0.485	0.516	0.541	0.567	0.594	0.617	0.640
Average	**0.396**	**0.430**	**0.461**	**0.489**	**0.517**	**0.544**	**0.569**	**0.593**	**0.617**	**0.639**
STD	**0.002**	**0.003**	**0.003**	**0.003**	**0.003**	**0.003**	**0.003**	**0.003**	**0.002**	**0.002**

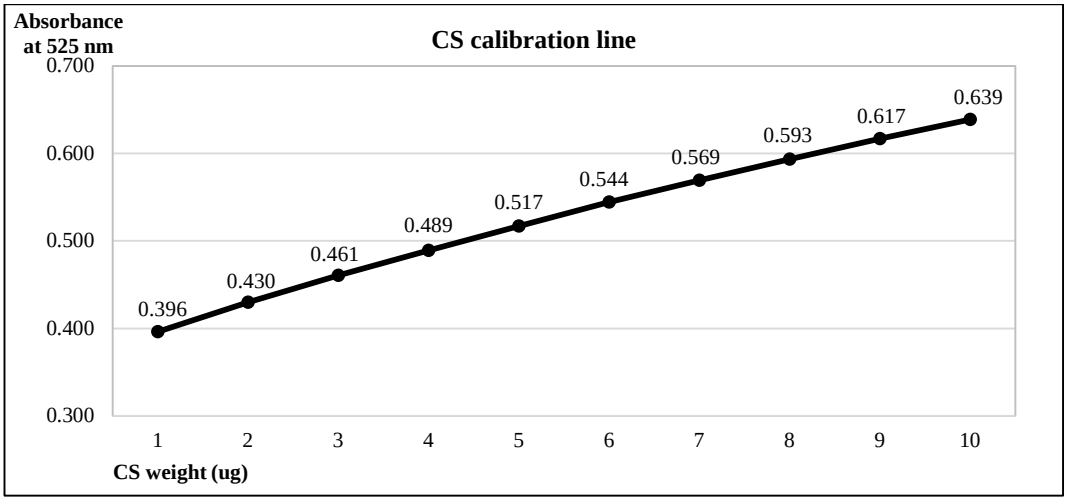

Table and Figure 2.12 Calibration data of chondroitin sulphate obtained over a 3 month period

Different weights of chondroitin sulphate (from 1 µg to 10 µg) were examined using the DMMB assay in the spectrophotometer with a wavelength of 525 nm. The absorbance on different dates was recorded and averaged to compose the standard calibration curve. The standard deviation (STD) of absorbance in each concentration for each date was low (all ≤ 0.003) and the linearity of the calibration curve was high. The regression equation of the calibration curve was: CS weight (µg) = (37.2 × Absorbance) -14. The *p* values for the constant and the average were both <0.001, and the *r* value (correlation coefficient) was 0.998.

2.3.2 Joint mapping

Before the joint model was evaluated in long-term culture, the articular surface of the joint was mapped to see if there was a variation in chondrocyte viability, GAG content and water content in the different areas of the fresh joint surface. The purpose of joint mapping was to determine if there were variations in chondrocyte viability, GAG content and water content that would compromise the validity of sampling different regions of the surface as being representative of the whole surface. In addition, the data from the joint mapping were used to ensure that it was normally distributed and therefore that parametric statistical analysis, e.g. t-test or analysis of variance (ANOVA), could be used.

There were 3 different joints used for each variable, and in each joint 16 cartilage samples were taken from sixteen different sites of a single joint. Cartilage biopsy was obtained from the joint facets numbered-1, 4, 5 and 8 **(Figure 2.6b)** because these facet surfaces were larger and flatter than those of the facets numbered-2, 3, 6 and 7 that facilitated sample biopsy.

The following tables showed the results of chondrocyte viability in 3 zones (**Table 2.13**), GAG content (**Table 2.15**) and water content (**Table 2.16**) with the normality analysis. The cell density of each zone of each joint was also calculated (**Table 2.14**). The pooled data from total 48 sites (3 joints, 16 sites per joint) showed the chondrocyte viability in the superficial, middle and deep zones was 89.4±3.8%, 94.4±2.2% and 77.9±7.8% (Mean±STD), respectively. The difference between these 16 sites was analysed by one-way ANOVA, and the results showed p=0.620, 0.787, and 0.361 in the superficial, middle and deep zone, respectively, supporting the assertion that there was no difference between the sites with respect to chondrocyte viability. The Kolmogorov-Smirnov normality test revealed the *p* value of each zone was above 0.150 indicating that the viability data of each zone was consistent with being normally distributed.

Furthermore, in order to identify if there was difference between each joint, the data were reorganised into **Table 2.17**. The results of chondrocyte viability, GAG content

and water content of each joint came from the average of 16 sites and the *p* value was from one-way ANOVA to compare the difference among the 3 joints.

Chondrocyte viability (%)		site A2	site A3	site A4	site B1	site B2	site B3	site B4	site B5	site C1	site C2	site C3	site C4	site C5	site D2	site D3	site D4	Pooled
Superficial zone	Joint A	94.7	90.6	84.6	82.3	82.1	89.7	89.4	85.7	89.4	88.2	88.8	80.6	91.9	94.4	93.9	86.9	
	Joint B	90.8	89.7	89.3	90.4	89.6	84.0	97.5	84.0	84.0	92.5	92.9	93.5	84.9	92.8	87.6	82.1	
	Joint C	85.4	89.2	90.9	90.7	88.7	91.5	92.9	94.6	91.5	90.9	94.2	89.5	92.5	92.9	88.3	89.5	
	Average	90.3	89.8	88.3	87.8	86.8	88.4	93.3	88.1	88.3	90.5	92.0	87.9	89.8	93.4	89.9	86.2	**89.4**
	STD	3.8	0.5	2.7	3.9	3.4	3.2	3.3	4.6	3.2	1.8	2.3	5.4	3.5	0.7	2.8	3.1	**3.8**
Middle zone	Joint A	91.6	97.1	97.3	91.5	95.8	97.3	93.2	97.7	95.6	95.4	97.2	97.4	90.4	96.5	94.5	95.1	
	Joint B	93.3	93.3	93.9	96.9	95.1	94.4	97.0	93.7	94.0	91.1	96.0	92.0	91.2	93.0	96.4	95.7	
	Joint C	91.1	93.6	90.6	93.8	90.8	94.2	97.1	93.8	92.5	96.6	95.4	95.8	95.6	93.2	93.6	91.1	
	Average	92.0	94.7	93.9	94.1	93.9	95.3	95.8	95.1	94.0	94.3	96.2	95.1	92.4	94.2	94.8	94.0	**94.4**
	STD	0.9	1.7	2.7	2.2	2.2	1.4	1.8	1.9	1.3	2.4	0.7	2.3	2.3	1.6	1.2	2.1	**2.2**
Deep zone	Joint A	78.5	94.5	87.6	84.9	81.0	78.7	80.6	73.9	78.5	85.8	84.0	82.9	72.0	76.0	76.4	78.5	
	Joint B	90.2	74.7	84.9	85.7	91.5	77.3	72.7	64.9	66.4	68.9	86.6	69.6	70.9	78.3	66.2	82.5	
	Joint C	82.8	86.3	66.3	74.6	68.7	73.0	76.7	90.6	69.9	89.6	84.0	65.9	65.7	74.6	76.0	70.6	
	Average	83.9	85.2	79.6	81.7	80.4	76.3	76.7	76.5	71.6	81.4	84.8	72.8	69.6	76.3	72.9	77.2	**77.9**
	STD	4.8	8.1	9.5	5.0	9.3	2.4	3.2	10.7	5.1	9.0	1.2	7.3	2.7	1.5	4.7	4.9	**7.8**

Kolmogorov-Smirnov normality test for viability

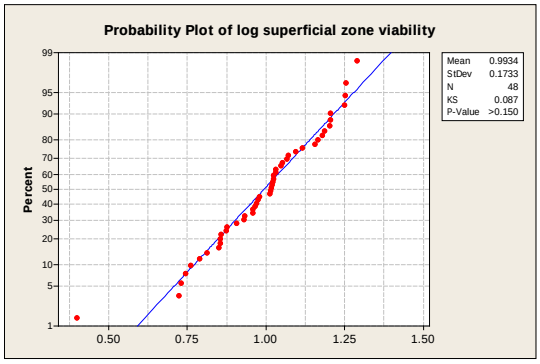

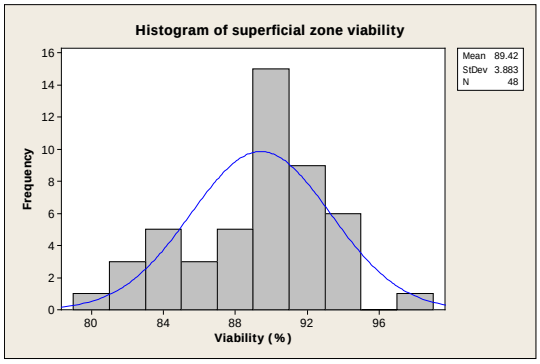

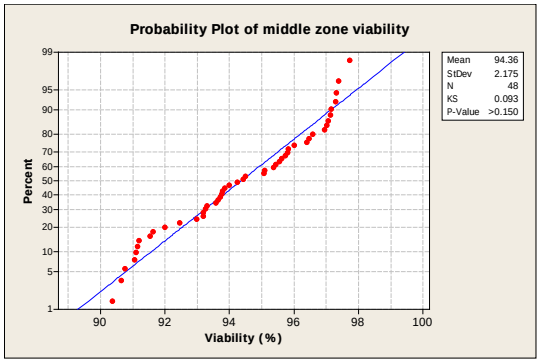

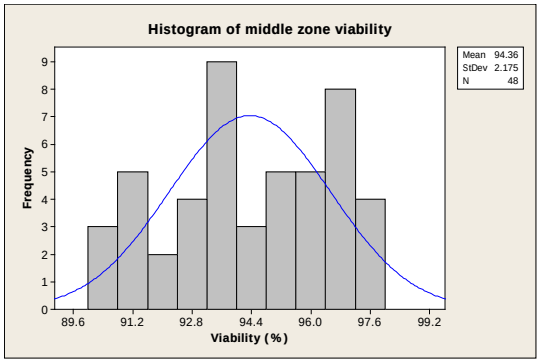

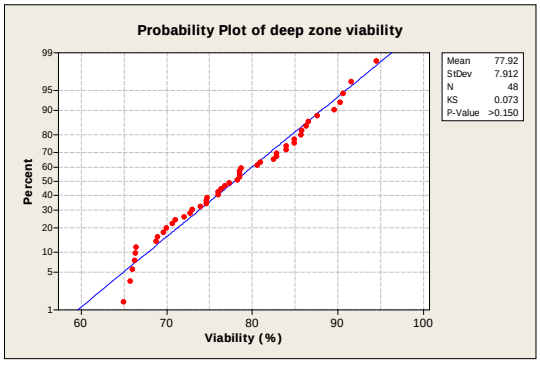

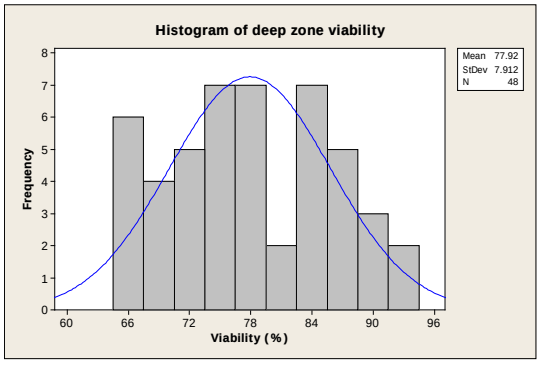

Table 2.13 Chondrocyte viability; mapping of articular surface and testing for normality

There were 3 different joints, and, in each joint, 16 cartilage samples were taken for viability mapping. Sites A2-A4 located on facet 1, and site B1-B5, C1-C5, and D2-D4 located on facet 4, 5, and 8, respectively. The individual viability for each sites, as well as the average and pooled viability are shown in the table with each standard deviation (STD). The Kolmogorov-Smirnov normality test revealed the *p* value of each zone was above 0.150 indicating that the viability data of each zone was normally distributed.

Chondrocyte density: Total cell no. / Cartilage volume (mm^3)				
	Joint A	**Joint B**	**Joint C**	**Pooled**
Superficial zone	43199 ± 4959	44966 ± 7767	48204 ± 7629	45684 ± 7308
Middle zone	31581 ± 5132	32359 ± 6695	30571 ± 5350	31502 ± 5827
Deep zone	32795 ± 4853	29395 ± 4249	31007 ± 4435	31011 ± 4677

Table 2.14 Chondrocyte density in three mapping joints

The chondrocyte density of 16 sites of each zone of each joint is shown in the table (mean ± STD). The pooled data from 48 sites of each zone are also calculated. After statistical analysis, there was no significant difference in each zone between these three joints (p=0.263, 0.699 and 0.267 in the superficial, middle and deep zone; One-way ANOVA).

%GAG (ug/mg)	site A2	site A3	site A4	site B1	site B2	site B3	site B4	site B5	site C1	site C2	site C3	site C4	site C5	site D2	site D3	site D4	Pooled
Joint A	1.34	1.15	1.14	1.19	1.21	1.06	1.20	1.19	1.29	1.16	1.21	1.21	1.36	1.16	1.19	1.23	
Joint B	1.15	1.10	1.25	1.36	1.32	1.18	1.11	1.08	1.27	1.24	1.26	1.16	1.13	1.26	1.11	1.18	
Joint C	1.29	1.18	1.19	1.25	1.30	1.22	1.20	1.08	1.28	1.14	1.42	1.15	1.21	1.12	1.38	1.27	
Average	1.26	1.15	1.19	1.27	1.28	1.15	1.17	1.12	1.28	1.18	1.30	1.18	1.23	1.18	1.23	1.23	**1.21**
STD	0.08	0.03	0.04	0.07	0.05	0.07	0.05	0.05	0.01	0.04	0.09	0.03	0.10	0.06	0.11	0.04	**0.08**

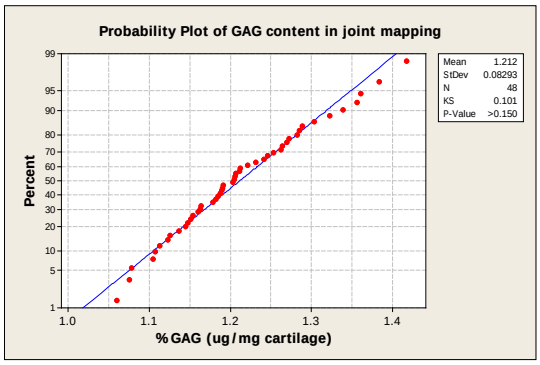

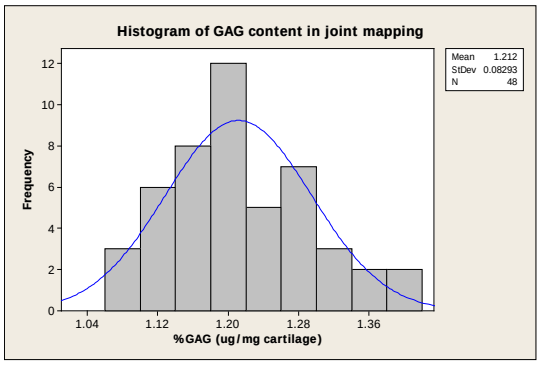

Table 2.15 Matrix GAG content; mapping of articular surface and testing for normality

The GAG content data of the pooled 48 sites (3 joints, 16 sites per joint) ranged from 1.06% to 1.42% with the median value of 1.20% and the average of 1.21±0.08% (Mean±STD). The result of one-way ANOVA to evaluate the difference between each site showed p=0.165 that also reflected there was no statistically significant difference between each site. The Kolmogorov-Smirnov normality test confirmed the GAG content data of the joint model was normally distributed.

Water content (%)	site A2	site A3	site A4	site B1	site B2	site B3	site B4	site B5	site C1	site C2	site C3	site C4	site C5	site D2	site D3	site D4	Pooled
Joint A	69.75	72.54	75.97	73.30	73.68	72.68	72.30	72.06	70.57	71.57	72.50	72.76	74.23	73.30	74.11	74.84	
Joint B	70.87	71.84	74.26	76.84	74.05	72.99	71.66	73.26	74.65	71.00	73.03	72.13	71.90	70.48	72.24	71.43	
Joint C	70.18	70.82	71.46	71.06	70.10	71.81	74.44	70.45	71.94	72.57	71.70	73.78	72.10	72.73	71.46	71.56	
Average	70.27	71.73	73.90	73.73	72.61	72.49	72.80	71.92	72.39	71.71	72.41	72.89	72.74	72.17	72.60	72.61	**72.44**
STD	0.46	0.71	1.86	2.38	1.78	0.50	1.19	1.15	1.70	0.65	0.55	0.68	1.06	1.22	1.11	1.58	**1.52**

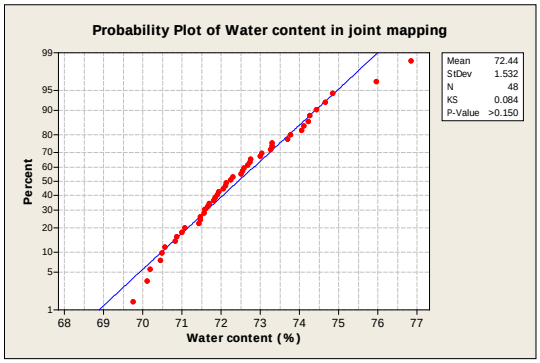

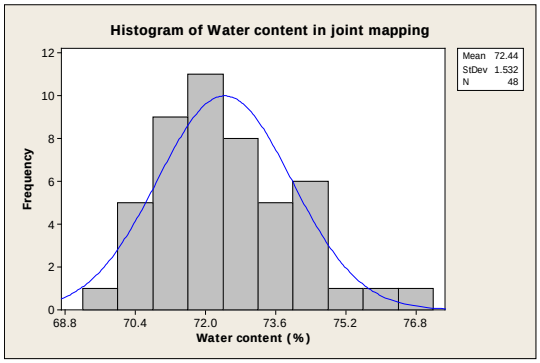

Table 2.16 Water content; mapping of articular surface and testing for normality

The water content data of pooled 48 sites (3 joints, 16 sites per joint) ranged from 69.8% to 76.8% with the median value of 72.2% and the average of 72.4±1.5% (Mean±STD). The *p* value of one-way ANOVA between the 16 sites was 0.628 indicating that there was no statistically significant difference between each site. Kolmogorov-Smirnov normality test confirmed the water content data of the joint model was normally distributed.

	Chondrocyte viability (%)			GAG content (%)	Water content (%)
	Superficial zone	Middle zone	Deep zone		
Joint A	88.3 ± 4.26	95.2 ± 2.29	80.8 ± 5.46	1.21 ± 0.07	72.9 ± 1.50
Joint B	89.1 ± 4.19	94.2 ± 1.84	77.0 ± 8.67	1.20 ± 0.08	72.7 ± 1.61
Joint C	90.8 ± 2.30	93.7 ± 2.00	76.0 ± 8.09	1.23 ± 0.09	71.8 ± 1.16
p value	0.175	0.122	0.184	0.494	0.087

Table 2.17 The average of pooled data of 3 joints in the 3 different measuring variables

The original data from the 16 sites of each joint were used for analysis by one-way ANOVA. The probability value (*p*) showed there was no statistically significant difference between each joint in the chondrocyte viability, GAG content and water content evaluation.

2.3.3 Effect of Storage on Chondrocyte viability

The changes of the chondrocyte viability and the matrix GAG content were considered after the animal was slaughtered. Storage conditions were considered to have an influence on these changes. The following results examine the most suitable times for processing the joints, and how to store the feet if the processing procedures were delayed.

Six fresh feet were collected from the abattoir. Instead of being processed immediately on the collecting day, two of the feet were placed in the laboratory at room temperature of 22°C and the remaining four feet were stored in the cold room with temperature of 4°C. After 24 hours, the chondrocyte viability from 10 different sites of the room temperature-stored joints was examined. The results revealed that the average of chondrocyte viability was 79.0±15.2%, 82.7±9.9% and 40.3±12.3% in the superficial, middle and deep zone, respectively (**Table 2.18**). Compared to the data of fresh joints (from the average data of joint mapping), there were significant differences in all three zones (p=0.008, p<0.001 and p<0.001 in the superficial, middle and deep zone, respectively; unpaired t-test). These indicated that the chondrocyte viability decreased in all three zones with the increase of variability of each site if the joints were placed in the room temperature for only one day.

However, if the feet were stored in the cold room with temperature of 4°C, the chondrocyte viability was 87.3±1.6%, 94.1±2.3% and 81.3±1.6% in the superficial, middle and deep zone, respectively, after one week (**Table 2.19**). Compared to fresh joint data, the p values of unpaired t-test were p=0.151, p=0.866 and p=0.145 in the superficial, middle and deep zone, respectively. These results meant that the chondrocyte viability of three zones was not significantly different between the fresh joints and those stored at 4°C for one week. It indicated that storing the bovine feet in the temperature of 4°C was a suitable method to preserve the cell viability of the joint.

Joint A overnight mapping		site A2	site A3	site B2	site B3	site B4	site C2	site C3	site C4	site D2	site D3	**Mean**	**STD**
Superficial zone	Viability %	91.0	67.7	35.4	85.5	84.5	93.4	88.8	58.8	96.5	92.2	**79.4**	**18.5**
Middle zone	Viability %	88.5	68.4	66.6	87.6	94.5	71.2	88.4	72.0	91.0	89.4	**81.8**	**10.2**
Deep zone	Viability %	36.0	27.0	37.2	37.2	39.5	11.5	48.2	63.5	36.4	42.2	**37.9**	**12.7**

Joint B overnight mapping		site A2	site A3	site B2	site B3	site B4	site C2	site C3	site C4	site D2	site D3	**Mean**	**STD**
Superficial zone	Viability %	88.0	68.5	88.0	71.1	56.0	70.7	92.8	83.5	82.1	85.4	**78.6**	**10.9**
Middle zone	Viability %	90.3	82.1	87.3	61.6	77.3	74.5	92.6	89.4	92.0	88.8	**83.6**	**9.4**
Deep zone	Viability %	50.7	46.4	38.0	39.7	43.4	14.6	61.9	38.8	47.4	46.3	**42.7**	**11.5**

Table 2.18 Chondrocyte viability mapping of the joints stored at room temperature for 24 hours

There were two joints placed in the laboratory at room temperature of 22°C. After 24 hours, the chondrocyte viability from 10 sampling sites of each joint was examined. The sampling sites were similar to those previous described except that one sample less was obtained from the peripheral facets (facet 1,8) and two samples less were obtained from the central facets (facet 4,5).

Viability (%)	Joint A	Joint B	Joint C	Joint D	**Mean**	**STD**
Superficial zone	88.0	85.7	89.6	86.1	**87.3**	**1.58**
Middle zone	96.1	90.5	93.8	96.0	**94.1**	**2.29**
Deep zone	83.5	79.0	81.4	81.5	**81.3**	**1.59**

Figure 2.19 Chondrocyte viability of 4 joints after one week storage at 4°C

There were four joints stored in the cold room immediately after delivery. After one week storage, three random biopsies of each joint were taken and the chondrocyte viability of three zones were examined.

2.3.4 Cartilage morphology, chondrocyte viability and matrix content of GAG and water in long-term culture of the static model

The static joint model was the first model developed for long-term culture. As there were no previous data available for this novel experiment, it was hard to decide how long the culture should continue. Therefore, a time course experiment was performed to determine when the chondrocyte viability of any zone (in the coronal view) came down to zero percent.

Cartilage morphology was demonstrated with conventional histology using H&E and Alcian blue staining **(Figure 2.20)** and with confocal laser scanning microscopy using CMFDA and PI stain **(Figure 2.21, 2.23)**. Two scanning planes (axial and coronal planes) were obtained in each cartilage sample with the confocal microscopy. Quantification of the viability of the 3 zones was done automatically by ImageJ software (the data are shown in **Figure 2.22** and **Figure 2.24**). GAG and water change in the static model is reported in **Figure 2.26** and **Figure 2.27**, respectively.

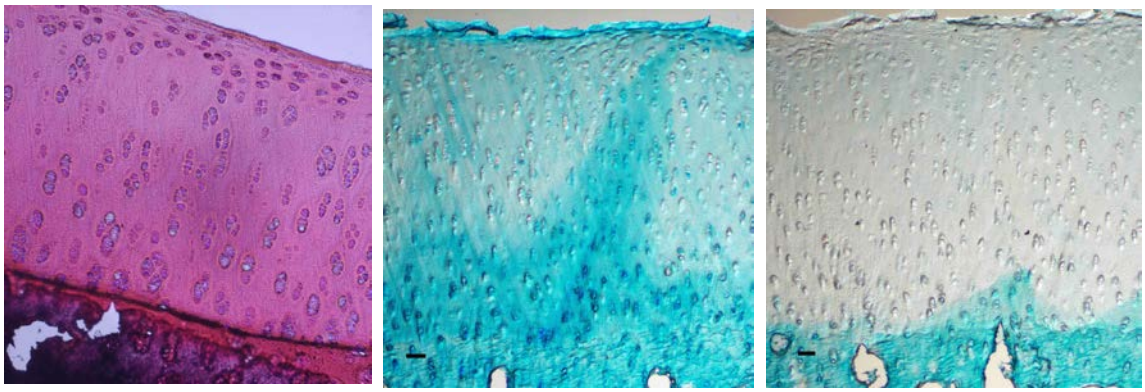

a. (Day 28, H&E) **b. (Day 0, Alcian blue)** **c. (Day 28, Alcian blue)**

Figure 2.20 Cartilage morphology in coronal section of the static model

a. Photomicrographs show the histological heterogeneity of chondrocytes and of the extracellular matrix: Superficial zone chondrocytes are oval, flat and parallel to the articular surface, whereas those in the middle and deep zones are rounder, larger and clustered in columns with perpendicular orientation to the articular surface. **b.** The GAG distribution examined using Alcian blue varied in the different zones and changed after culture. In the Day 0 sections, there was a greater amount of GAG staining in the middle and deep zones compared to the superficial zone. **c.** However, after 4 weeks of culture, most of the GAG staining had been lost and only a small amount of GAG was left in the deep zone. (Frozen section, ×100, black bar = 50 μm).

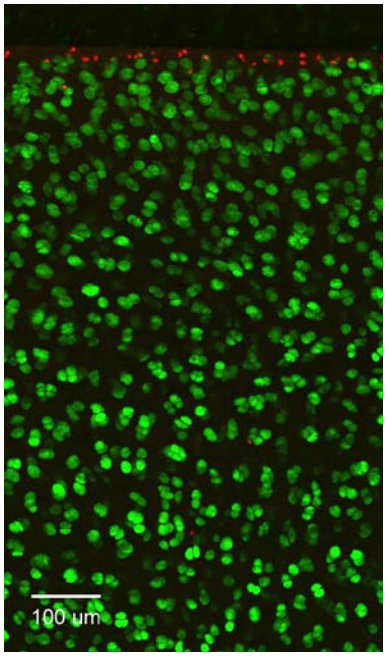

a. (Day 0)

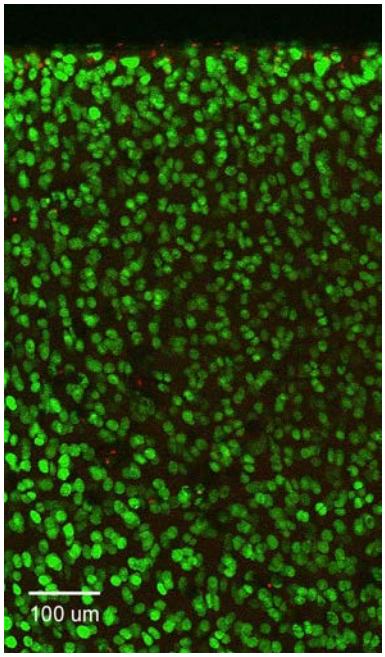

b. (Day 14)

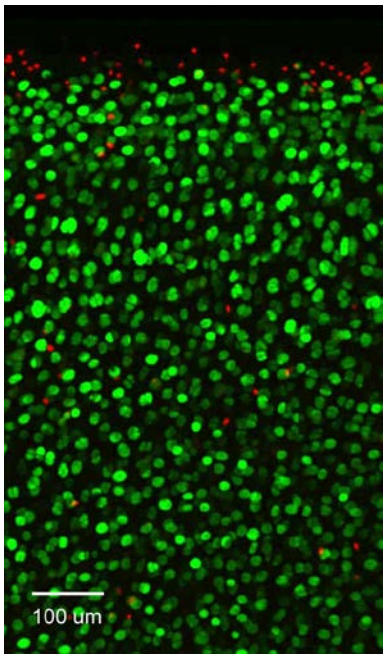

c. (Day 28)

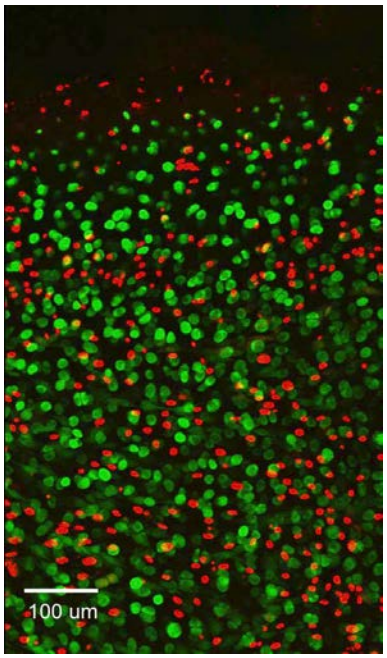

d. (Day 42)

Figure 2.21 Cartilage axial morphology change with time in the static model (staining with CMFDA and PI).

The axial view of cartilage sample revealed the shape and the status of chondrocytes in the superficial zone. Most of the chondrocytes had a round cell shape and demonstrated a tendency to couple together. It could be noted that the percentage of dead cells increased from Day 0 to Day 42. The top margin of each image was the cut edge; this demonstrated a band of dead cells resulting from the cutting process as

previously reported (Amin, *et al.* 2008). In order to exclude the confounding effect of cell death secondary to the cutting process, dead cells along this margin were not included in the analysis. Thus the lower part of the image was used for cell counting, and the results are shown in the following figure.

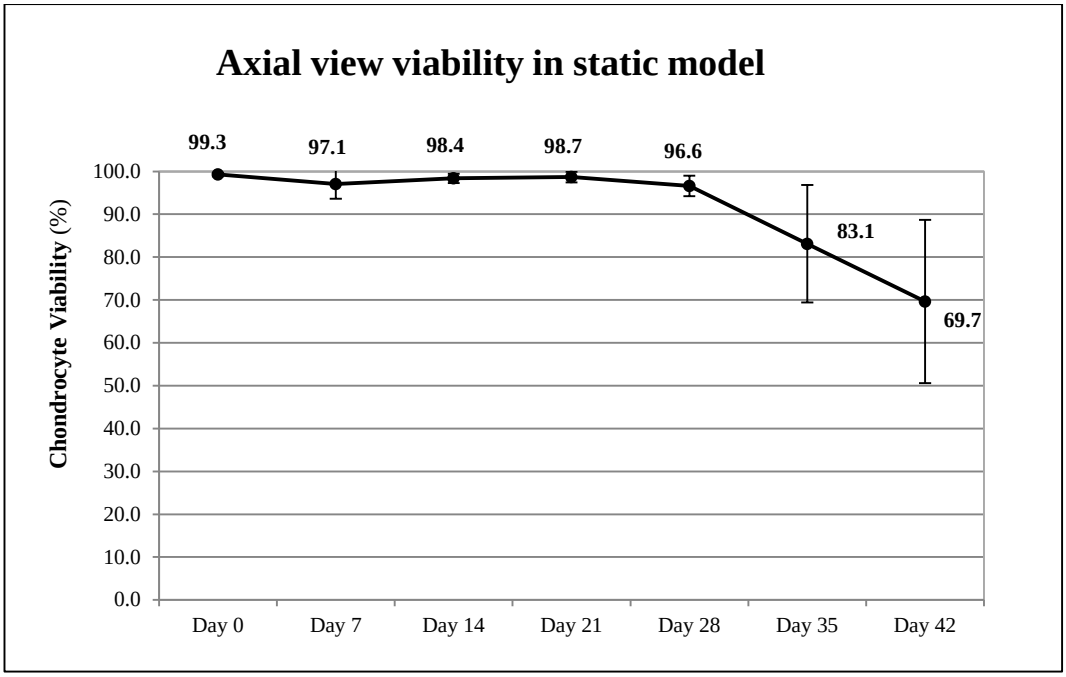

Figure 2.22 Change in chondrocyte viability in the axial views of 6 joints from the static model

There were eighteen samples examined at each time point (3 biopsies in each joint, and 6 different joints). The sampling sites from each joint were chosen randomly by using a randomisation table. The results revealed the chondrocyte viability in the axial view of cartilage sample could be maintained very well until the 3rd week of culture. After the 4th week, the superficial zone chondrocytes began to wither and the viability curve started to turn down but approximately 70% of the cells were still alive at the end of the 6th week. Statistical evaluation of these data by one-way ANOVA revealed there was significant difference after Day 35, (p=0.001).

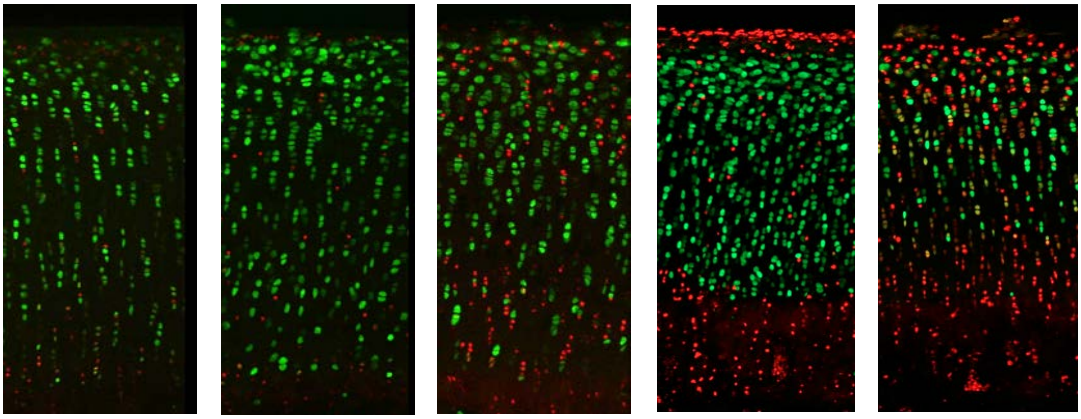

Figure 2.23 Cartilage coronal morphology change with time in the static model (staining with CMFDA and PI).

In the coronal view of the cartilage sample, the chondrocyte viability of three zones could be assessed. The zonal differentiation of the cartilage could also be recognised because the CMFDA stained the total cytoplasm of live chondrocytes green that revealed their different cell shapes in the different zones. Comparing the images from Day 0 to Day 42, most of the PI-stained dead cells started to appear at the Day 28, especially in the superficial and deep zones, and then these ‘dead zones’ expanded to the middle area at the end of the time period.

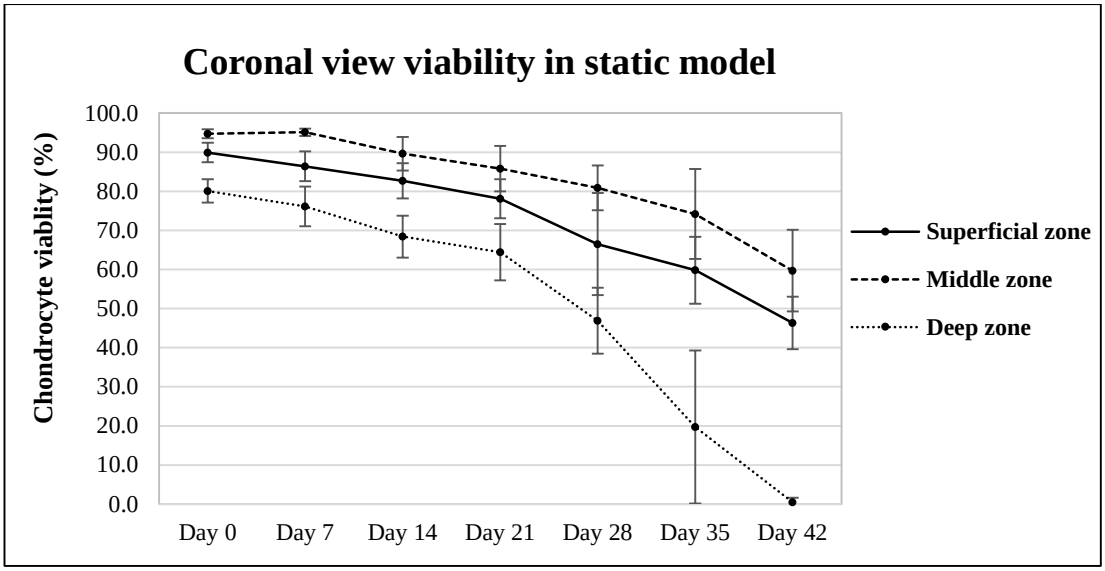

Figure 2.24 Change in chondrocyte viability in the coronal views of 6 joints from the static model

Zonal chondrocyte viability plot of 6 joints of the static model showed the viability in the middle zone remained the highest at all time-points. Deep zone viability was the first to drop to zero percent, which it did at the end of the 6th week. Statistical comparison between all time-points of the same zone showed that there was significant difference in each zone (p<0.001 in all 3 zones, one-way ANOVA). Further evaluation by post-hoc Tukey's test revealed that the superficial and deep zone viability after Day 21 and the middle zone viability after Day 14 had statistically significant difference to Day 0.

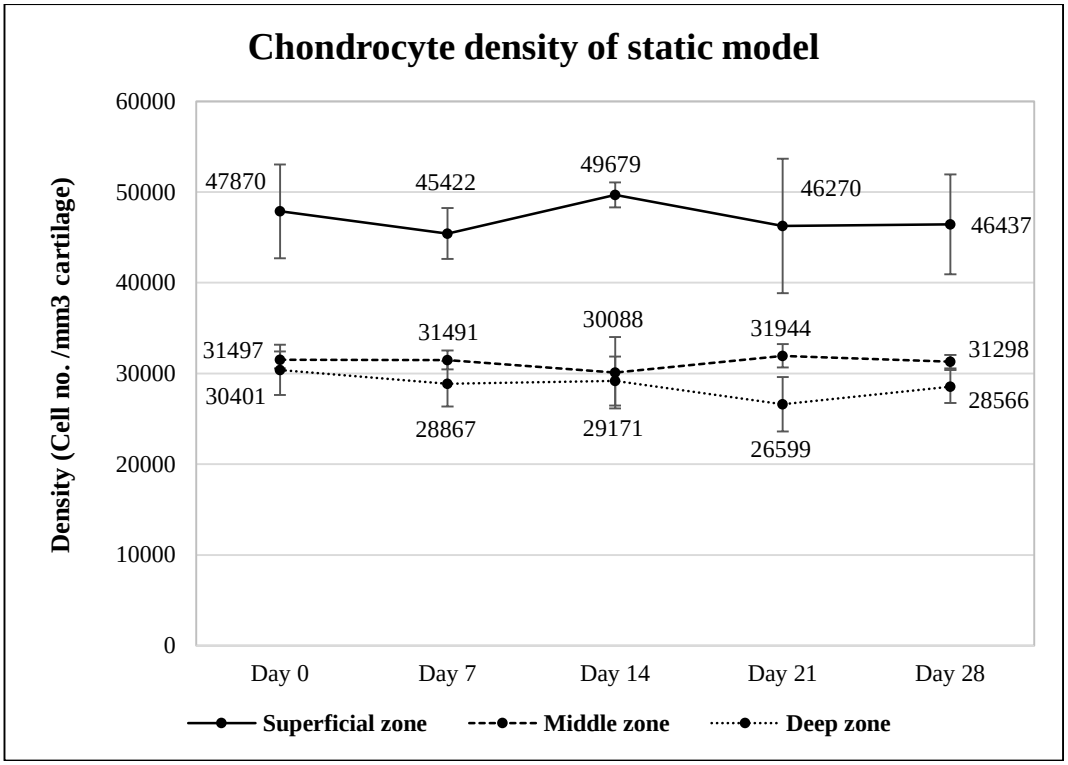

Figure 2.25 Chondrocyte density in the static model

The superficial zone had the highest cell density amongst all three zones while the deep zone was the lowest density area. The cell density of the static model did not have statistically significant change during the culture period (p=0.684, 0.652 and 0.262 in the superficial, middle and deep zone, respectively; One-way ANOVA).

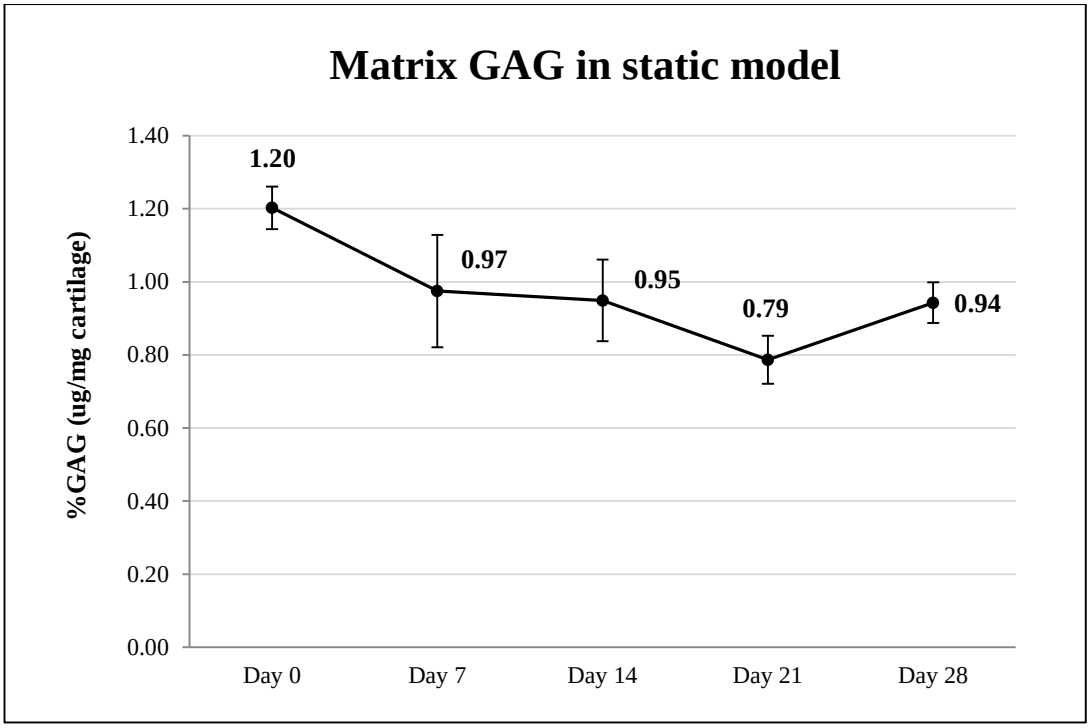

Figure 2.26 Change of the matrix GAG content in 5 joints from static model

The matrix GAG content in 5 joints of the static model showed the average GAG amount in Day 0 was 1.20%. The GAG amount decreased with culture and reached the lowest value of 0.79% at Day 21. However, it returned to 0.94% at the end of Day 28. Statistically, there was significant change of GAG amount during the 4 weeks culture, and it occurred after Day 7 ($p<0.001$, one-way ANOVA and its post-hoc Tukey's test).

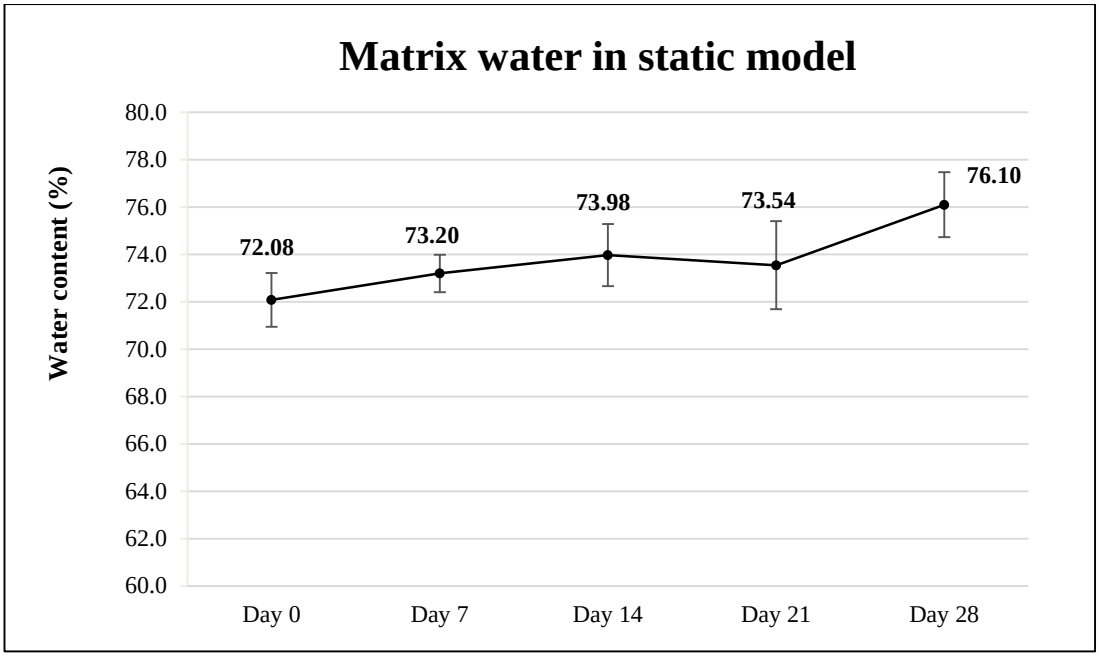

Figure 2.27 Change of matrix water content in 5 joints from static model

The marix water content increased slowly and gradually after culturing. It gained 4.02% more water over the 4 weeks of culture. Statistical analysis showed that there was significant differences over these culture period, and, compared to Day 0, the data after Day 14 were significantly different (p=0.007, one-way ANOVA and its post-hoc Tukey's test).

2.3.5 Cells in the culture media

Cells were observed floating in the culture media and attached on the surface of the cartilage during the culture period. The cells in the culture media were found to be of two cell types after they were isolated by centrifugation from the culture media: the majority were the cells with small round disc-like shape and the minority were the large nucleated cells (**Figure 2.28a**). These cells were cultured for 14 days, and a number of polygonal elongated cells were observed proliferating in the culture flask (**Figure 2.28b to 2.28d**). The morphology and behaviour of the nucleated cells indicated that they were most likely to be fibroblasts. The small round disc-like cells were believed to be red blood cells because of the lack of nuclei in the cells. Even though the culture media were changed twice a week, these cells still could be found in the culture media after 2 weeks (**Table 2.30**).

The cells on the joint surface were noted occasionally at the time of evaluating the chondrocyte viability of the cartilage samples. The morphology of these cells were clearly different from the chondrocytes because they were with polygonal or spindle cell shapes (**Figure 2.29a & 2.29b**). These cells had the propensity for proliferation on the surface of cartilage, and eventually could cover the entire joint surface and block penetration of the CMFDA/PI dyes. If this occurred, an accurate number of chondrocytes in the axial view could not be obtained. Fortunately this was only a problem with prolonged culture (most commonly after 4 weeks of culture), and it affected the axial view only. In the coronal view, the dyes could penetrate into the cartilage without any blockage because the coronal plane was a new plane which had been cut just before staining (**Figure 2.29c**). This layer of cells were further examined by scratching them from the joint surface, and culturing them in a flask. It revealed that the cells were polygonal or spindle-shaped and easy to proliferate in the flask that resembled the large nucleated cells seen in the culture media (**Figure 2.29d**).

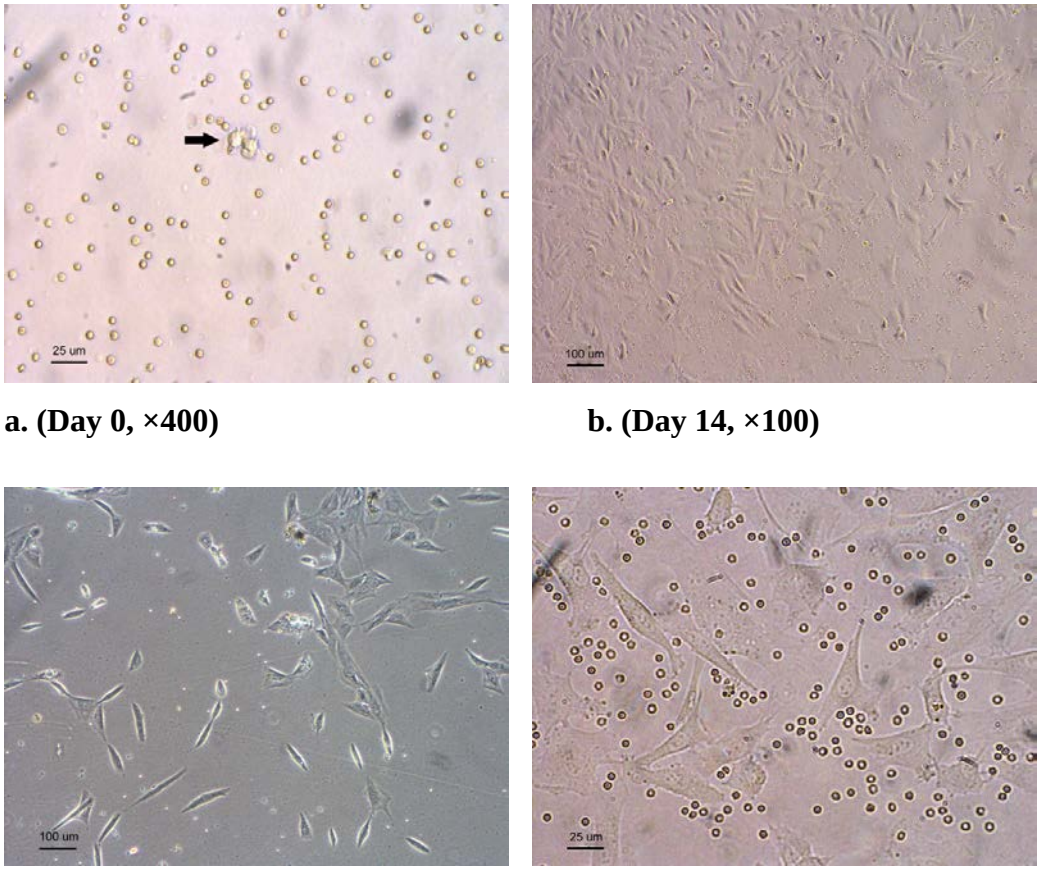

a. (Day 0, ×400) **b. (Day 14, ×100)**

c. (Day 14, ×100) **d. (Day 14, ×400)**

Figure 2.28 Cells floating in the culture media

a. Numbers of small round disc-like cells and a few large nucleated cells (arrowed) were found in the culture media after centrifugation of culture media. **b&c.** After culturing in the flask for 14 days, a number of polygonal elongated cells proliferated. **d.** At 400× magnification, these polygonal cells were seen to be heterogeneous with a diverse appearance. The cytoplasm looked coarse and branched, and the nucleus had more than one nucleolus.

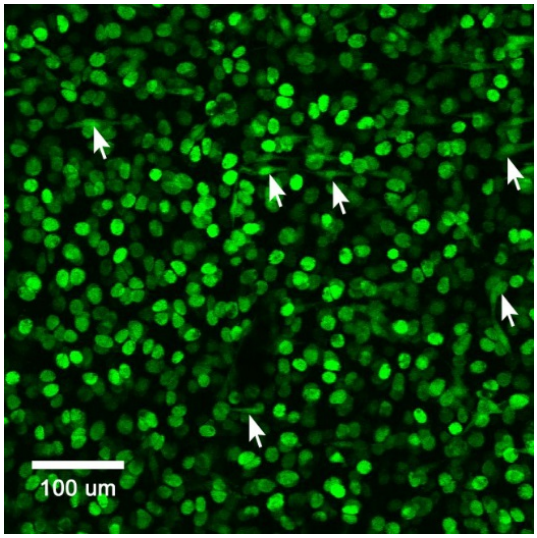

a. (Day 28, axial view)

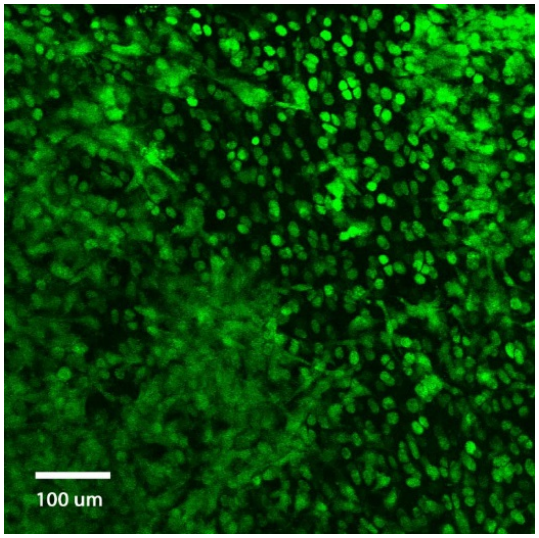

b. (Day 35, axial view)

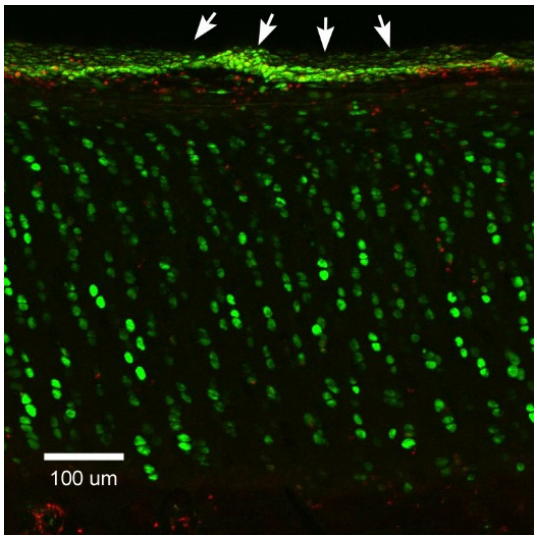

c. (Day 28, coronal view)

d. (×400, cell culture)

Figure 2.29 Cells attached on the surface of the joint model

a. Polygonal or spindle-shaped cells (white arrows) were occasionally found on the surface of the joint model. They were clearly different in shape compared to the chondrocytes. **b.** These cells could cover the joint surface and block penetration of the dyes that blurred the image. **c.** In the coronal view, these cells formed a membrane-like layer that coated the joint surface (white arrows). However, the chondrocytes of the different zones could be identified clearly. **d.** These coated cells were scratched and cultured in a flask. The shape of these cells was spindle or polygonal that resembled the cells seen in the culture media.

Cell amount in 50 ml culture media				
	Day 3	**Day 7**	**Day 10**	**Day 14**
Joint A	750,000	425,000	578,750	75,000
Joint B	10,350,000	462,500	258,750	65,000
Joint C	1,268,750	350,000	253,750	85,000
Average	**4,122,917**	**412,500**	**363,750**	**75,000**

Table 2.30 Total cell amount in the culture media of 3 joint models

50 ml of the culture media was taken from the middle part of the culture vessel for cell counting when the culture media was changed (This was carried out twice per week). All cell types were counted together and the cell number is shown. The amount of cells decreased with time but still could be identified in the culture media after 2 weeks.

2.4 Discussion

2.4.1 Challenges of the model development

There were several challenges during the development of this joint model. Resolving these problems were crucial to the success of the model. Three of the difficult tasks are discussed below.

The culture vessel, the bioreactor, was the first challenge that needed to be resolved. Previous organ culture studies have used variable vessels, e.g. the flexible sterile polypropylene bag (Nugent-Derfus, *et al.* 2007), large petri dishes (Lee, *et al.* 2006b; Korecki, *et al.* 2007; Jim, *et al.* 2011), or custom-made plastic boxes (Lovett, *et al.* 2010). All of these vessels were carefully considered for their suitability for the bovine joint, but all were too small. However, no matter how the bioreactors was designed, the principles were to supply the organ with oxygen and nutrients, and to remove the metabolites. Thus, a common large 1L glass beaker was chosen as the container of the joint organ culture because of several advantages (namely availability, sustainability and the ability to be autoclaved for sterility). Furthermore, by using several of the beaker, a number of joint experiments could be performed at the same time that shortened the total experiment period.

If the beaker was used as the culture vessel, the culture media were changed twice per week in keeping with routine cell culture experiments. The oxygen was supplied by natural dissolving from the atmosphere to culture media. As the joint was immersed several times deeper in the culture media than the cells in cell culture, the oxygen concentration around the cartilage may have been lower than in cell culture experiments, however, the chondrocytes have been reported to be well-adapted to a hypoxic environment (Rajpurohit, *et al.* 1996) and were seen to survive well in the joint model.

The second challenge came from the maintenance of the sterility of the joint model during a long-term culture period, which would be exacerbated by weekly harvesting of cartilage biopsies. The main steps taken to prevent infection relied on strict adherence to the sterile techniques that are described in detail in Chapter 2.2.10. If an

infection was discovered, the potential sources and the possible routes that allowed microbes into the culture media were identified and completely rectified in order to prevent further infections (Lincoln & Gabridge 1998). During the entire period of experiment of the joint model, there were a small number of infections that resulted from bacteria and fungi. The overall infection rate was approximately 10%. However, if rigorous sterile principles were applied, the culture period of the joint model could be longer than 10 months without any sign of contamination in the culture media.

The third challenge was related to the sampling technique of the joint cartilage. In addition to the sterility issues, the hardness of the subchondral bone made the biopsy from the model extremely difficult, if at the same time chondrocyte viability was to be maintained. Previous studies used chisels (Amin, *et al.* 2008), scalpels (Smith, *et al.* 2013), cork borers (Brighton, *et al.* 2013), or saws (Moo, *et al.* 2011) to remove the cartilage explants out of the bone tissue. In the thesis, gouges, plug cutters and trephines were also tested in the preliminary experiments for cartilage sampling. After evaluation of the advantage and disadvantage of each tool, the scalpel was considered the most ideal among these tools for the reasons that it not only caused the least damage to the articular congruency of the joint model but also preserved the maximal amount of live chondrocytes in the biopsied explants, which was due to the least amount of pressure on the cells by its thinnest profile and the sharpest edge compared to other tools. However, the sampling technique needed a period of learning to achieve a reliable and reproducible level.

2.4.2 Organ culture model for cartilage research

This joint organ culture model was developed to lie between *in vitro* cartilage explants and *in vivo* animal models for experimental cartilage studies. No ‘organ’ level long-term organ culture systems of mammalian synovial joints have been created before. The closest similarity was made by Nugent-Derfus et al. (Nugent-Derfus, *et al.* 2007). They introduced a bovine stifle joint model, which was cultured in a complicated bioreactor for 24 hours. A flexible sterile polypropylene bag was

used as the culture vessel, and 4 openings of the bag were made for connection of 2 bone clamps at both joint ends and 2 Tygon tubes that provided culture media circulation. A continuous passive motion (CPM) machine was linked to the bone clamps for moving the joint at a rate of 0.025 Hz and with movement arc of 36°. Their experimental purpose was to determine the effect of CPM on chondrocyte metabolism by measuring the proteoglycan 4 (PRG4) within chondrocytes and in the culture media. Their results indicated that joint motion might contribute to increase PRG4 expression and to maintain the joint health. Nevertheless, the complexity of the culture system might limit its reproducibility because the sterility, especially in the aspect of setting the joint in a soft bag with connection to a moving device, would be very difficult to maintain for a long time.

Other published cartilage-related organ culture models have not been for articular cartilage but for intervertebral disc cartilage (Lee, *et al.* 2006b; Korecki, *et al.* 2007; Jim, *et al.* 2011). Although the anatomy of the intervertebral disc and the components inside are totally different from the articular joint, the processes and methods of validating a new organ culture model are relevant. As demonstrated in these articles, the cell viability is a major factor in determining if the developed organ culture model is successful. Since there is only one cell type – the chondrocyte – in the articular cartilage and the extracellular matrix is composed of macromolecules from chondrocytes, the viability of chondrocytes is crucial for the success of the joint organ culture model. The components of extracellular matrix, such as the GAG content, may indicate if there has been a functional change of the chondrocytes. Thus, the assessments of both the chondrocyte viability and the matrix GAG content were the two major methods in the thesis.

2.4.3 Reliability of chondrocyte viability assessment

The viability data in the thesis were the ‘examined viability’ which might not be exactly the same as the ‘real viability’, because it was examined by the method of sectioning that caused an artificially cell death. Therefore, possible differences between the ‘examined viability’ and ‘real viability’ were explored.

However, there was no direct way to detect cell viability without affecting the natural status of the chondrocytes. Therefore, the data obtained could always differ from the real situation. For example, the viability of chondrocytes from a fresh joint of a healthy animal would be expected to be close to 100% viability. However, even though the viability data from the axial view of the static model at Day 0 was 99.3% (**Figure 2.22**) that matched the expectation, the coronal view viability data were not able to reach this ideal level from either the fresh joint mapping set of experiments (maximum 94.4% viability in the middle zone, **Table 2.13**) or the static model at Day 0 (maximum 94.7% viability in the middle zone, **Figure 2.24**).

The difference of the 'examined viability' between the axial view and the coronal view was considered to be due to the methodology used to examine the axial view was less invasive than that used for the coronal view. For axial viewing, apart from the application of dyes and laser beams, the cells were undisturbed before scanning that maintained their viability. In contrast, for the coronal viewing, the chondrocytes had to be scanned through a newly cut plane. The cutting brought pressures on the cut plane that adversely affected the viability of chondrocytes. Therefore, the 'examined viability' data of static model coronal view at Day 0 revealed only 89.9%, 94.7% and 80.1% in the superficial, middle and deep zones, respectively (**Figure 2.24**). However, the viability assessment of coronal view was still being used because it revealed more information about the zonal differences of articular cartilage than the axial view.

The cutting effect decreased the coronal view viability and this was unavoidable. However, if the effect stayed consistent in every testing sample, the coronal results remained comparable. According to the coronal viability data from the joint mapping model and static model at Day 0, the viability of superficial, middle and deep zones was 89.4±3.8%, 94.4±2.2% and 77.9±7.8% (Mean±STD), respectively for the joint mapping data, and 89.9±2.5%, 94.7±1.1% and 80.1±3.0%, in the static model Day 0 data. The viability of the joints after one week storage at 4°C was 87.3±1.6%, 94.1±2.3% and 81.3±1.6%. After statistical evaluation, there were no significant differences among these three sets of data if the viability of the same zone was compared (p=0.240, p=0.856 and p=0.307 in the superficial, middle and deep zone,

respectively; one-way ANOVA). From the cell density data (**Figure 2.14 and 2.25**), the chondrocyte density did not significantly change in different sites of the mapping model or in the static model during the 4 weeks culture. All of the results indicated that the cutting effect stayed consistent in every sample during the culture period.

With the methodology used in this thesis, which used a sharp cut with a new scalpel for the coronal views, it could be inferred that the scalpel produced similar cutting effect in every sample. In previous related experiments, the reproducibility of sharp injury has been reported if new scalpel blades were used every time for cutting (Redman, *et al.* 2004; Amin, *et al.* 2008). Thus, in the coronal viability examination in this thesis, standard methods that used new blades to take cartilage samples from joints, and the parallel cutting of cartilage samples by two number-22 new scalpel blades with 'rocker motion' were established.

The chondrocyte density of bovine cartilage was clearly identified in the previous literature (Wong, *et al.* 1996). Wong *et al* described that if confocal microscopy was used for evaluation of the chondrocytes of mature bovine articular cartilage, the cell density could be precisely calculated. There were 8 equally divided sites from the cartilage surface to the junction of subchondral bone in their coronal view image of cartilage. If the site 1 and site 2 in their study, which consisted of the upper 25% thickness from the cartilage surface, was combined together, it could be the same ROI as the superficial zone in the thesis. The site 3 to site 6 (the middle 50% thickness) and the site 7 and site 8 (the lower 25% thickness) in the literature could also be combined for comparison of the middle and deep zone, respectively, to the thesis. The re-calculated cell density of the superficial, middle and deep zone in the literature was approximately 46000, 31000 and 30000 cells/mm^3 cartilage, respectively. It was quite similar to the cell density of the static model (Day 0), which was 47870±5161, 31497±926 and 30401±2778 cells/mm^3 in the superficial, middle and deep zone, respectively, or to the joint mapping model with 45684±7308, 31502±5827 and 31011±4677 cells/mm^3 in the same corresponding zone. Although it was impossible to obtain the original data from the literature for statistical confirmation, the similarity of the cell density outcomes could at least increase the reliability of the method of the chondrocyte viability assessment in the thesis because

of the similar chondrocyte number of bovine cartilage being detected. The consistent maintenance of the chondrocyte density in the static model for at least 4 weeks could additionally increase the reliability of applying this method in the long-term culture model.

In addition, the articular cartilage is traditionally divided into 4 zones, which are superficial, middle, deep and calcified zones. However, the border of each zone is difficult to identify, particularly in the images of confocal microscope. Therefore, with ease of calculation and reproducibility, the zonal regions in this thesis were divided by percentage of cartilage thickness. From the articular surface to the subchondral bone, the first quartile of cartilage was defined as the superficial zone, followed by the middle zone as the middle 50% of the thickness, and the deep zone as the last quartile. The calcified zone was included in the deep zone in this thesis because of the elusive border between these two under the CMFDA/PI stains. The percentage of zonal definition in the thesis was similar to the previously published articles (Mow & Lai 1974; Buckwalter, *et al.* 1994; Ulrich-Vinther, *et al.* 2003).

2.4.4 Validation of the bovine metatarsophalangeal joint organ culture model

The validity of the joint model could be assessed by some factors, such as the reliability of the joint model, the appropriateness of the model in the cartilage research field and the sense of content. Evaluation of the appropriateness and the content validity of this joint model tended to be subjective because no similar model was developed previously. However, the reliability of this joint model could be internally confirmed by the results of the initial three studies - the joint mapping study, the storage experiment at 4°C and the Day 0 data of the static model - because similar results were produced when the joint model was used in different experiments.

The purpose of joint mapping study was to confirm the distribution of the chondrocyte viability, the GAG content and the water content among the entire surface of the joint. It was hypothesised that there was no difference in chondrocyte

viability, GAG and water content across the whole joint surface of bovine metatarsus. However, there were no previous studies reporting on these variables.

The results (**Table 2.13, 2.15, 2.16**) showed that there was no statistically significant difference between the 16 sampling sites with respect to the chondrocyte viability, the matrix GAG content and water content, supporting the above. Additionally, these data established the fundamental characteristics of the basic fresh (Day 0) model, which could be used for comparison with the advanced models, e.g. long-term cultured static or dynamic models. Furthermore, because there were 3 different joints included in the mapping studies, the data were reorganized based on individual joints to determine if there was difference among each joint. The results (**Table 2.17**) still showed no statistical difference of these three variables among these three different joints, which might indicate that the similarity of the cartilage properties existed not only on the same joint surface but also among individuals of the bovine species.

If the fresh bovine feet have been collected from an abattoir, there may be a delay before they can be used in the laboratory. In the stored joints experiments, the difference of the chondrocyte viability between the specimens that had been at room temperature for 24 hours and those that had been in a cold room for 7 days demonstrated the importance of the storage conditions for this joint model. Comparing the results of joint mapping study to the results from the feet stored in room temperature for 24 hours (**Table 2.18**) revealed a drop in chondrocyte viability in all three zones combined with an increase of the standard deviation between the 10 biopsy sites of each joint (79.0±15.2%, 82.7±9.9% and 40.3±12.3% in the superficial, middle and deep zones, respectively), suggesting that some, but not all, of the chondrocytes died if the feet were kept at room temperature for 24 hours. In contrast, if the feet were stored in the cold room with the temperature of 4°C for 7 days, the chondrocytes viability remained high 87.34±1.6%, 94.1±2.3% and 81.3±1.6% in the superficial, middle and deep zones, respectively, with no statistically significant difference to the fresh joints (joint mapping study). Thus, it could be inferred that 4°C was a suitable temperature for storage of the bovine feet and that at this temperature the chondrocyte viability could be maintained for at least 7 days. These findings concur with the results of Drobnic *et al*., Kim *et al*. and

Pallante *et al*. who also found the storage temperature to be critical. (Kim, *et al.* 1996; Drobnic, *et al.* 2005; Pallante, *et al.* 2009).

Although the chondrocytes in the joint model were found to have the surprising ability to keep their viability for a period of time at 4°C, it was still considered preferable to standardise the procedure using fresh feet and therefore the following experiments were carried out using fresh feet, with an ischemic time of less than 6 hours. This also helped to allay concerns about bacteria growth in the furs of the feet that could potentially contaminate the joint model during harvesting procedures.

2.4.5 Static effects on the cartilage

Once the metatarsophalangeal joint model had been validated, it was of vital importance to know how long the chondrocytes of the joint model could stay alive in the controlled experimental environment, and whether there was any change in the component of the extracellular matrix. The first long-term culture model, namely the static model, was developed by keeping the joint static in the culture media. The hypothesis of the static model was that it was possible to maintain a mammalian articular synovial joint *ex vivo* for a prolonged period of time. The experimental aim was to evaluate how long the chondrocytes could survive in the model, and what changes occurred with respect to the GAG and water content of the cartilage matrix.

Chondrocyte viability. The viability of the chondrocyte of the static model was evaluated by the CMFDA/PI stains with confocal laser scanning microscopy. Both the axial and coronal views of the biopsied cartilage explants were examined. On the axial view, the chondrocytes were observed to maintain 98.7% viability until the 3rd week of the culture. At this time point, the viability curve began to bend downward (**Figure 2.22**). This result indicated that almost all of the chondrocytes of the superficial zone, in which the cells were detected by the axial view scan, remained alive for 3 weeks in the static model.

The coronal view viability of the static model (**Figure 2.24**) demonstrated that all of the three zonal viability curves turned downward gradually week by week. The

viability of middle zone was always the highest of the three zones at every time point, while the viability of superficial zone was in the middle. The lowest viability was the deep zone, which dropped to zero percent at the end of the 6th week. The greater drop in deep zone viability could be explained by the difficulty of the chondrocytes in the deep zone obtaining nutrients from the culture media. However, the heterogeneous sensitivity of chondrocytes of different zones to the scalpel injury might be another factor to affect the 'examined' chondrocyte viability of coronal view. This phenomenon could be further recognised in **Figure 2.23** where it can be seen that the viability change started at the surface and the bottom of the cartilage. The band of dead cells (in red colour) extended from both sides into the middle portion of the cartilage from Day 0 to Day 42. Although this heterogeneity of chondrocyte viability to injury has not been thoroughly evaluated in the previous literature, similar results could also be observed in a series of studies by Amin *et al*. (Amin, *et al.* 2008; Amin, *et al.* 2009a; Amin, *et al.* 2009b; Amin, *et al.* 2011).

Other tissues in this joint model such as the ligaments and bones may have different survival ability compared to the chondrocytes. The viability of these tissues was not the primary aim of this work, but the osteoblasts in the subchondral area of the cartilage explant were sometimes scanned concurrently in the same images as the cartilage. Viable osteoblasts were not observed beyond one week of culture. However, the death of the surrounding tissues did not seem to have an adverse effect upon the chondrocytes. During the early phase, the subchondral bone might have positive influence on the survival of the chondrocytes as Amin *et al*. have demonstrated that cartilage co-cultured with the sub-chondral bone had improved viability (Amin, *et al.* 2009b).

GAG content. The result of GAG content change in the cartilage extracellular matrix revealed that, in the static joint model, 19.2% GAG loss happened within one week of culture. After this, it remained at a constant level from Day 7 to Day 14, before dropping again by 15.0% at Day 21 to its lowest value of 0.79 μg/mg. At the end of 4th week, it returned back to the similar level as Day 14. Compared to a related article using bovine cartilage explants for culture to a total of 17 days, the GAG content in their cartilage explant dropped approximately 40% within 2 days

and then kept almost the same level until the end of their experiment (Moo, *et al.* 2011). In another paper using discs of bovine articular cartilage, the discs were split into superficial and deeper layers and received compression force before culture. The GAG contents in the cartilage and in the culture medium were assessed using the same DMMB assay. The matrix GAG loss of 17.8% in the superficial layer and 2.8% in the deeper layer were found after 48 hours culture (Rolauffs, *et al.* 2010).

Several i*n vivo* studies have revealed that the immobilization of the articular joint—the similar situation as the static joint model in this thesis—reduced the rate of synthesis of proteoglycan (Vanwanseele, *et al.* 2002). The GAG concentration was found significantly decreased 20-23% after 11 weeks of rigid external fixation of the canine knee joints (Haapala, *et al.* 1999). In addition, the ability of chondrocytes to synthesise proteoglycan decreased 41-48% (Palmoski, *et al.* 1980; Behrens, *et al.* 1989). The neutral metalloprotease (MMP-2) has been reported to be elevated in adult mongrel dogs after 4 weeks of limb fixation indicating that there is an association between proteolytic events and joint immobilization (Grumbles, *et al.* 1995).

According to these results, even though the models and experimental conditions in the published articles were different from the static joint model, the matrix GAG loss, in particular within a few days from the beginning of experiment, seemed to be ubiquitously reported. It has been described that the amount of proteoglycan in the cartilage matrix is in a dynamic balance between proteoglycan production and its loss (Urban 1994). The rate of proteoglycan production depended on the balance of anabolic or catabolic effects of the chondrocytes, while the rate of the proteoglycan loss was not only related to the chondrocytes but the porosity of the matrix surface, which has also been reported to influence the release of the matrix proteoglycan to the surrounding environment (Torzilli & Grigiene 1998). The matrix proteoglycans released into the medium were found to have a smaller hydrodynamic size than those in the cartilage matrix, and they were unable to aggregate with hyaluronate. Campbell *et al*. reported that these released proteoglycan molecules were some small segments from proteolytic cleavage at various sites along the proteoglycan core protein (Campbell, *et al.* 1989). This probably was the result of the elevation of some

catabolic enzymes in the cartilage that were trying to remodel their surrounding extracellular matrix in response to an unloaded environment (Vanwanseele, *et al.* 2002). Thus, the loss of matrix GAG in the static model might be the final outcome resulting from the reduction of GAG synthesis from the chondrocyte, acceleration of proteolysis in the extracellular matrix and the increase of collagen porosity on the surface of the joint.

Water content. The result of water content revealed that the fresh bovine cartilage contained 72.08% (w/w) of water. After culture for 28 days, the water content in the cartilage increased to 76.1% with approximately 1 % rise of water every week (**Figure 2.27**). In the cartilage explant culture in a related article, the total increase of water was approximately 10% over the culture period of 17 days (Moo, *et al.* 2011), while in another organ culture experiments using intervertebral disc, which contained fibrocartilage instead of hyaline cartilage, the water content increased approximately 20% after 30 hours if the disc was with endplate and exaggeratedly to 70% if no endplate was attached (Jim, *et al.* 2011). An *in vivo* study using a canine with a rigid external fixator to limit the joint movement revealed that the water content of the knee joint increased 7% after 6 weeks (Behrens, *et al.* 1989). Thus, the percentage of water gain of the joint model was similar to the *in vivo* animal model.

It is known that water is passively drawn into the cartilage by the osmotic difference between the cartilage matrix and the culture media in the experimental environment. The negatively charged proteoglycan molecules in the cartilage matrix are responsible for the majority of water attraction, and the integrity of the collagen network restricts the expansion of cartilage (Lindahl & Hook 1978; Buckwalter & Mankin 1998). Therefore, after culturing for a period of time, it could be inferred that the change of water content might, at least partially, represent the integrity of the cartilage matrix in the model. As the joint organ culture model kept the structure intact, there was only minimal and gradual change of water content after culturing, despite the previously noted fall in matrix GAG within the first week. In addition, as the weekly percentage change in water was similar to that observed in the *in vivo* canine study (Behrens, *et al.* 1989), it suggests that the matrix integrity of the *ex vivo* static model described here and the *in vivo* animal model was almost identical.

Cartilage morphology. The histological appearance of the cartilage when stained with H&E did not change greatly during the culture period (**Figure 2.20a**). However, if the cartilage was stained with Alcian blue, a marked change could be seen over the time period because the GAG content dropped by approximately 20% by the end of the 4th week (**Figure 2.20b**&**c**). At day 28, most of the remaining proteoglycan was in the deeper layer of the cartilage suggesting that the GAG was lost from the cartilage surface. Macroscopically, there was no recognisable change of the joins during the culture period. Thus, the cartilage morphology provided another evidence for the structural stability of the joint model.

SECTION C – DEVELOPMENT OF ADVANCED JOINT ORGAN CULTURE MODEL

Including

Chapter 3: Media-Stirred Model

Chapter 4: Dynamic Model

Chapter 3: Media-Stirred Model

3.1 Chapter outline

The media-stirred model was developed from the static model. The purpose of this model was to evaluate the effect of flow of the culture media on the chondrocyte viability and the matrix GAG content. The hypothesis to be tested with this model was that both the chondrocyte viability and the matrix GAG content of the joint would be maintained for a longer period of time than those of the static model because the flow of the culture media would facilitate nutrient and waste exchange between the media and the chondrocytes.

The bovine joint for this model was created and cultured in the same way as that used in the static model. The only different part between these two models, which was the test variable in this model, was the status of the culture media. In the previous static model, the culture media, like most other *in vitro* experiments, was placed steadily around the joint, whereas in the media-stirred model, the culture media was stirred by a magnetic stirrer for creation of the media flow around the joint. The duration of applying the stirring flow was set in an intermittent pattern, which was related to animal activity and was designed to be the same duration as that used in the dynamic model. The speed of the flow was also adjusted to be as similar to the dynamic model for further comparison.

There were 3 different joints from 3 different animals included in this experiment. Each joint was cultured for 4 weeks. The chondrocyte viability of both axial and coronal view and the GAG content of the cartilage matrix were assessed every week. These results were compared with the data of the static model to identify if the media flow affected the chondrocyte viability or the matrix GAG change.

3.2 Materials and Methods

The media-stirred model used the same methods to harvest and culture the bovine metatarsophalangeal joint. The timing and technique of harvesting the cartilage biopsies were also the same as those in the static model. There were 3 fresh bovine feet studied in the media-stirred model. The culture media were high glucose (4.5 g/L) Dulbecco's Modified Eagle Medium (DMEM) well mixed with penicillin (100 U/mL), streptomycin (100 μg/mL) and foetal bovine serum (10%, v/v). The culture vessel was the 1L glass beaker. One joint culture was continued for 4 weeks, and a total of 3 months was needed to complete the entire 3 experiments. Every week, five cartilage samples at randomly chosen sites of the articular surface were biopsied. Three of them were stained immediately with the CMFDA/PI dyes for detection of the live and dead chondrocytes by using the confocal laser scanning microscopy (Amin, *et al.* 2008). The other two samples were snap-frozen in the -80°C freezer for assessment of the matrix GAG content by using the spectrophotometric DMMB assay (Farndale, *et al.* 1986). Specific equipment and the settings are described below.

Instrumentation. The magnetic stirring machine was bought from Fisher Scientific (Fisher Scientific™ Basic Magnetic Stirrers). The magnetic stirrer was 30 mm in length and 6.4 mm in diameter and autoclaved sterilisation was needed before use. All instruments could be placed into a standard incubator, where the standard cell culture environment of 37°C, 5% CO_2 and 95% humidity was provided (**Figure 3.1**).

Stirring speed and duration setting. The stirring speed was determined by a preliminary experiment, in which the speed of the media flow was observed by adding small Styrofoam balls into the culture vessel. The speed of 400 rpm on the stirring machine was found to create a similar flow speed of the media to that observed with joint movement in the dynamic model, which was 20 rpm (0.33Hz). The daily operation of the stirring machine was set to have a pulsatile pattern with the same timing schedule as that in the dynamic model. The stirrer was switched on for 30 minutes and off for 30 minutes for 12 hours, then off for the whole other 12 hours of the day.

Figure 3.1 Media-stirred model

The joint model was placed in the glass beaker with a magnetic stirrer, and the top of the culture vessel was sealed with double-layered paraffin membranes. All instruments were placed in the incubator.

3.3 Results

3.3.1 Viability change of chondrocytes

The change of chondrocyte viability during 4 weeks of culture in 3 joints of the media-stirred models are shown in **Figure 3.2**. After 4 weeks of culture, the chondrocyte viability dropped 3.5% (from 95.9% to 92.4%), 10.4% (from 91.0% to 80.6%) and 15.4% (from 85.8% to 70.4%) in the middle, superficial and deep zones, respectively.

Only the coronal view viability was shown. The axial view viability was not possible to be obtained because the penetration of the CMFDA/PI dyes was blocked by the growth of the fibroblast-like cells on the cartilage surface after Day 14.

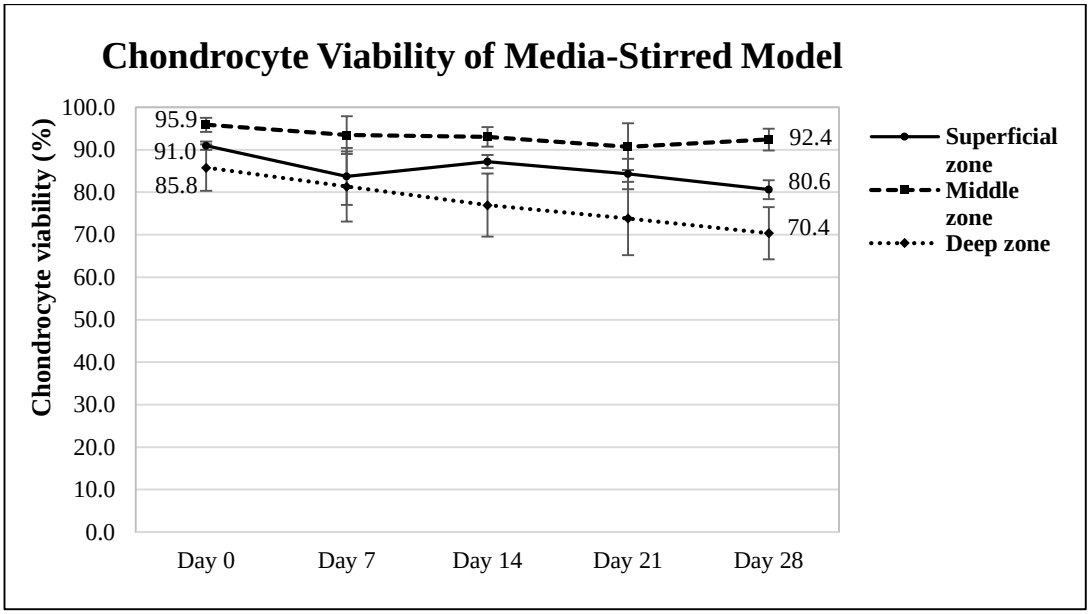

Figure 3.2 Chondrocyte viability change of the media-stirred model

The middle zone kept the highest viability during entire culture period, and the superficial zone and deep zone followed in sequence. After 4 weeks of culture, the chondrocyte viability of each zone dropped. However, statistical analysis revealed that there was no significant difference of the change of viability during the culture period (p=0.051, p=0.548 and p=0.333 in the superficial, middle and deep zones, respectively; one-way ANOVA).

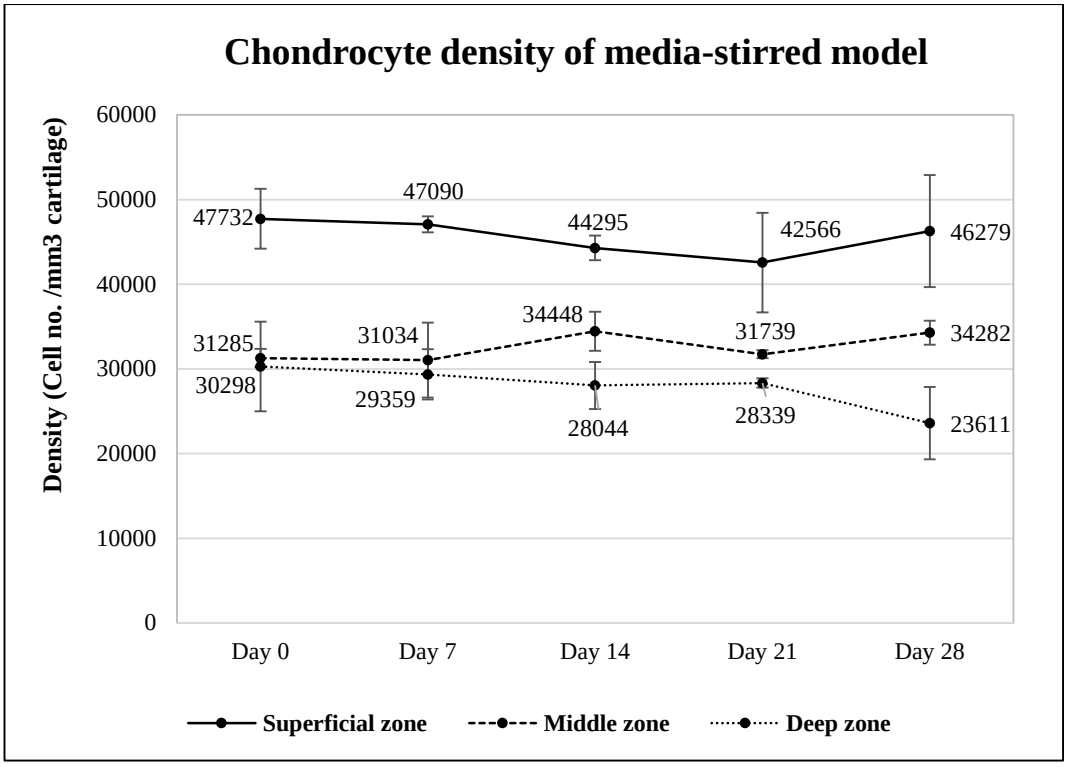

Figure 3.3 Chondrocyte density in the media-stirred model

The superficial zone had the highest cell density amongst all three zones while the deep zone was the lowest density area. The zonal cell density of the media-stirred model did not have statistically significant change during the culture period (p=0.749, 0.458 and 0.430 in the superficial, middle and deep zone, respectively; One-way ANOVA).

3.3.2 GAG change of cartilage matrix

The extracellular matrix GAG content change in the media-stirred model was shown in **Figure 3.4**. The matrix GAG content was initially at 1.22% and decreased to 0.90% after the first week. It continued to drop at the second week, at which time it reached its lowest value, 0.81%. After the 14 day time point, the GAG content increased to 0.92% and remained close to this level to the end of the culture.

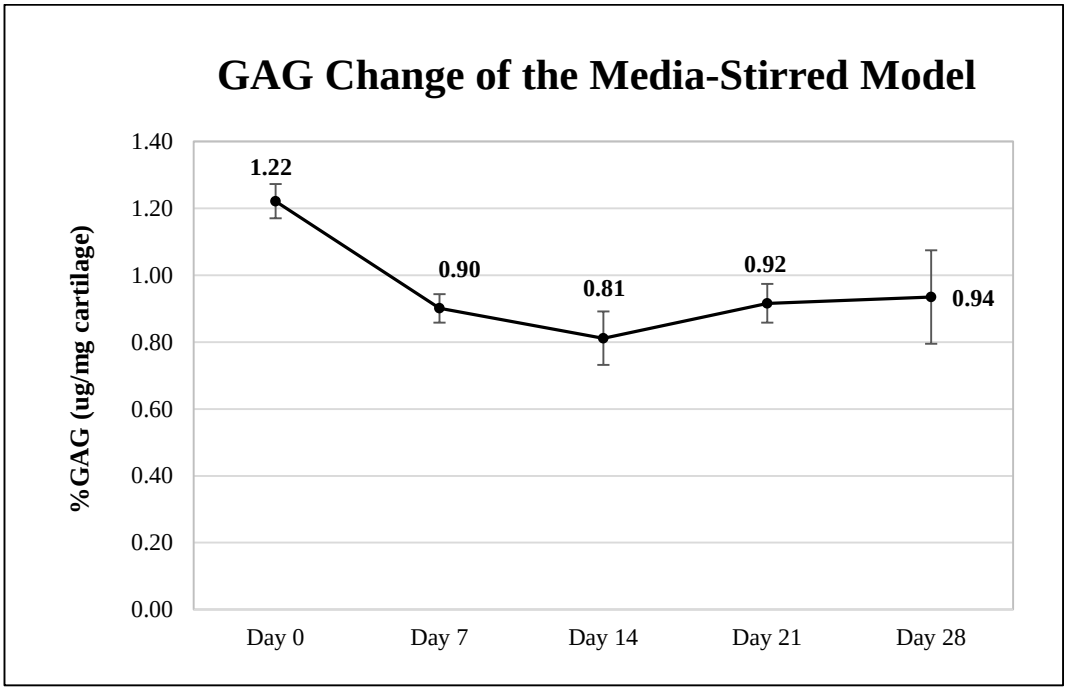

Figure 3.4 GAG change in 3 different joints of media-stirred model

There were 6 cartilage samples in each time point (2 samples of each joint) obtained for evaluation of the matrix GAG content of the media-stirred model. Statistically, there was a significant change in the matrix GAG content during the culture period, which occurred during the difference from the first week (p=0.005; one-way ANOVA and post-hoc Tukey's test).

3.3.3 Zonal viability comparison between static and media-stirred model

The chondrocyte viability between the static model and the media-stirred model was compared to determine the effect of the media flow on the cell viability of the joint. Different zones were compared and plotted separately for clear demonstration in **Figure 3.5**.

The chondrocyte viability of the static model fell relative to the media-stirred model during the culture period. Statistical analysis revealed that there were significant differences in the middle and deep zone but not in the superficial zone (p=0.012, p=0.001 and p<0.001 in the superficial, middle and deep zone, respectively; two-way ANOVA; significance level set at p<0.010 by Bonferroni correction for multiple comparison).

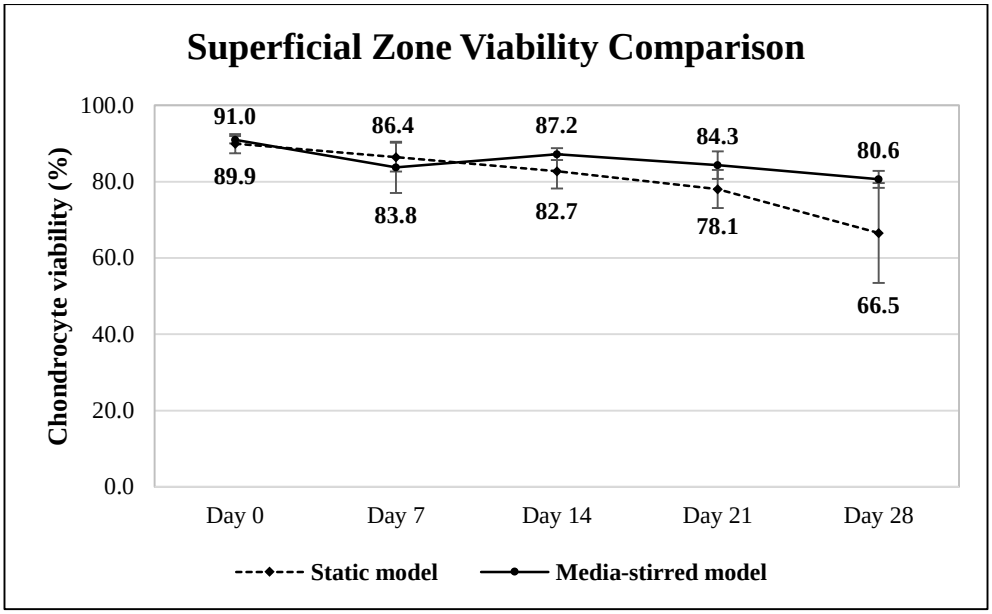
Superficial Zone Viability Comparison
Chondrocyte viability (%)
100.0
80.0
60.0
40.0
20.0
0.0
91.0
86.4
87.2
84.3
80.6
89.9
83.8
82.7
78.1
66.5
Day 0
Day 7
Day 14
Day 21
Day 28
Static model
Media-stirred model

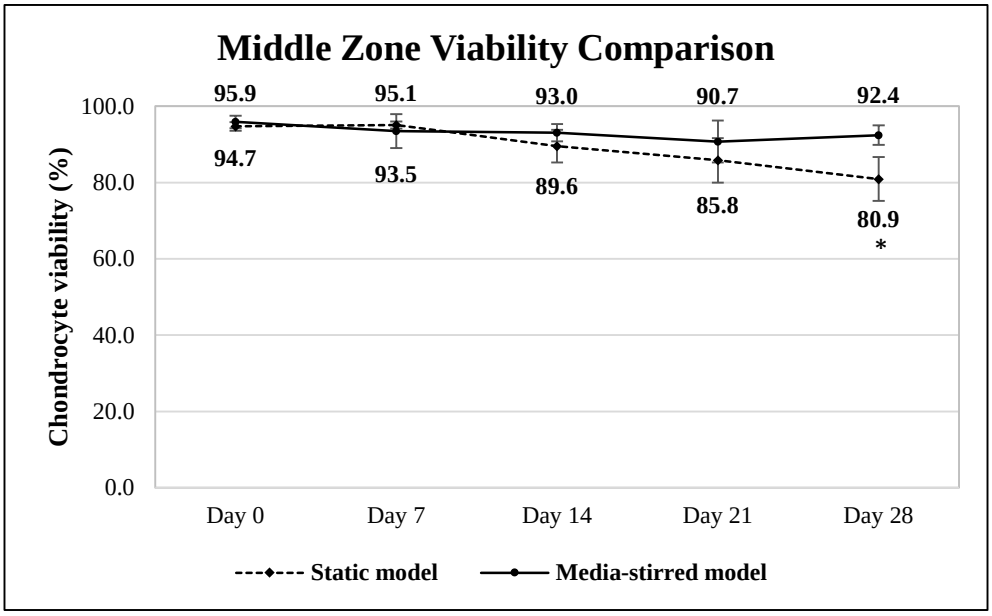
Middle Zone Viability Comparison
Chondrocyte viability (%)
100.0
80.0
60.0
40.0
20.0
0.0
95.9
95.1
93.0
90.7
92.4
94.7
93.5
89.6
85.8
80.9
*
Day 0
Day 7
Day 14
Day 21
Day 28
Static model
Media-stirred model

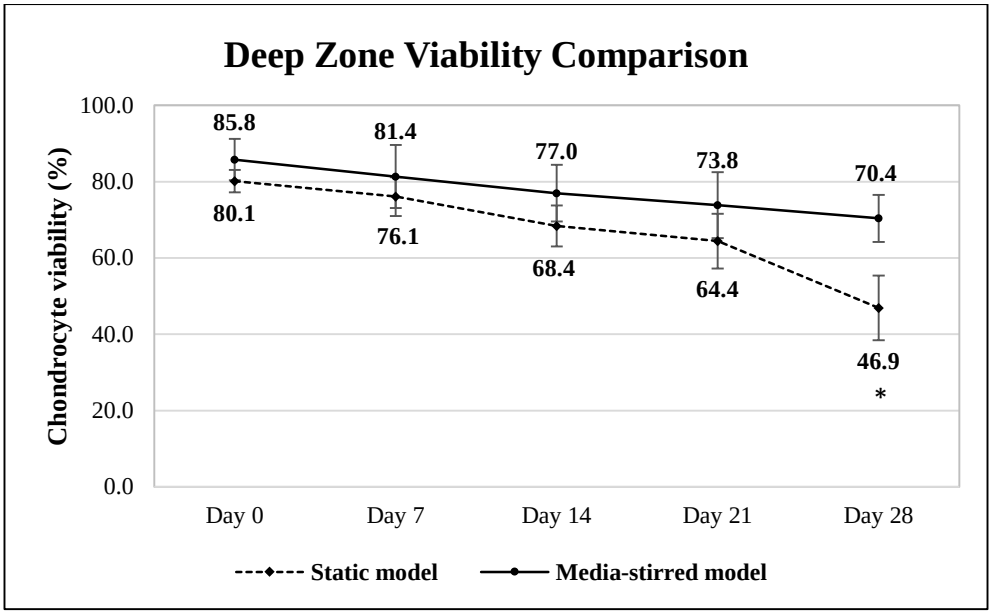

Figure 3.5 Chondrocyte viability comparison between the static model and the media-stirred model

The comparison of the chondrocyte viability change between the static model and the media-stirred model revealed that, in the middle and deep zone of the media-stirred model, the chondrocyte viability was maintained better than those in the static model. The difference gradually enlarged and became statistically significant at Day 28. The chondrocyte viability in the superficial zone of the static model also fell relative to the media-stirred model at Day 28 but this change did not reach statistical significance.

3.3.4 Matrix GAG comparison between static and media-stirred model

The matrix GAG content between the static and the media-stirred model was compared to reveal the effect of the media flow on the amount of matrix GAG. The result revealed that the matrix GAG of both models started at similar levels (1.20% for static model and 1.22% for media-stirred model). The matrix GAG of the static model dropped to its lowest level (0.79%) at Day 21, while the lowest point of the media-stirred model occurred at Day 14 (0.81%). At the end of the culture, the matrix GAG content of both models returned to the same level (0.94%). However, after statistical analysis there was no significant difference between each other (p=0.599; two-way ANOVA).

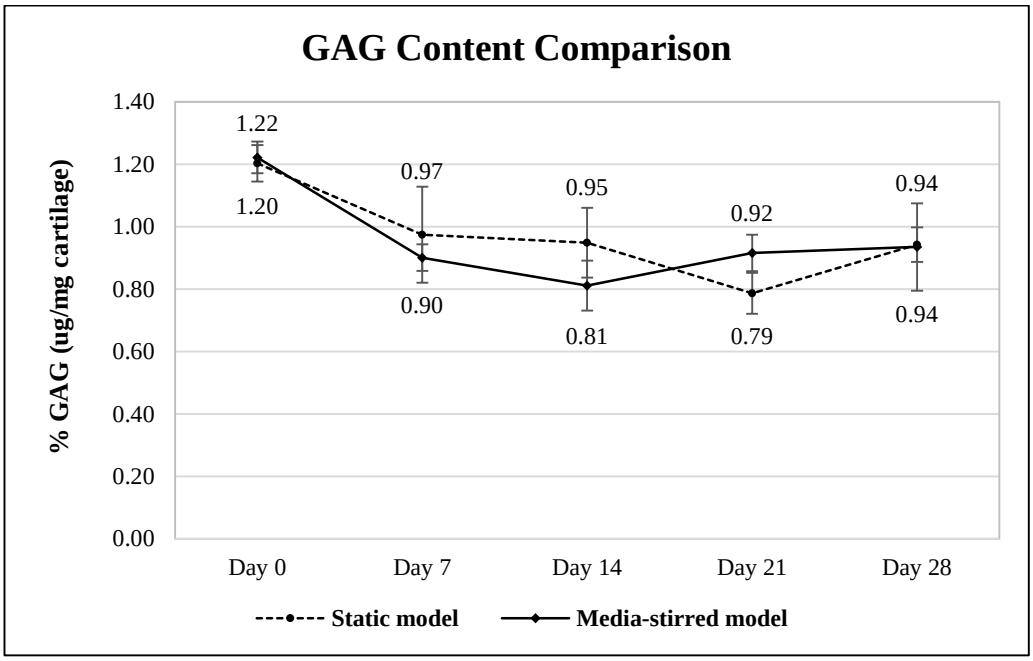

Figure 3.6 The GAG content comparison between the static model and the media-stirred model

The trend of GAG content change between the static model and the media-stirred model was similar. The matrix GAG of static model decreased continuously until Day 21 and returned to a higher level at Day 28, whereas the matrix GAG of media-stirred model dropped to its lowest level at Day 14 and returned to the same level at the end of culture.

3.4 Discussion

The comparison of the media-stirred model and the static model suggested the assertion that the flow of the culture media had a positive effect on the maintenance of the chondrocyte viability but no effect on preservation of the proteoglycan content of the cartilage matrix (**Figure 3.4 & 3.6**). From the assessment of the chondrocyte viability, it could also be observed that the improvement of the chondrocyte viability was not apparent before Week 3 and became significant at the end of the 4th week (**Figure 3.5**). The reliability of chondrocyte viability measurement could be recognised by the consistency of the chondrocyte density during the 4 weeks of culture period (**Figure 3.3**). From the assessment of the matrix GAG content, even though the stirred media had no measured effect on the preservation of the matrix proteoglycan, it might have accelerated the matrix GAG loss into the culture media. This could be observed by the fact that the matrix GAG content of the media-stirred model at Day 7 was lower than that of the static model, and the lowest point of the GAG content of the media-stirred model occurred one week earlier than the static model, which was Day 14 in the media-stirred model and Day 21 in the static model.

Previous investigators have demonstrated that fluid flow over chondrocytes in monolayer culture increased the synthesis of GAG (Smith, *et al.* 1995) and induced the cell proliferation (Malaviya & Nerem 2002). The viability and the function of the cells cultured in a three-dimensional (3D) collagen sponges was enhanced by the flow (Glowacki, *et al.* 1998). Bujia *et al*. also showed that the media flow could promote the production of the type II collagen by human chondrocytes cultured in agarose (Bujia, *et al.* 1994), and Davisson *et al*. showed that there was an increase in the production of GAG in ovine articular chondrocytes in polyglycolic acid (PGA) scaffolds if the cells were subjected to media perfusion at velocities of up to 170 μm/s (Davisson, *et al.* 2002). However, one must be careful when comparing these *in vitro* results with the results from the media-stirred model because these *in vitro* studies used cells in monolayer culture or cells in a scaffold, while the chondrocytes of the *ex vivo* joint model were embedded in a dense extracellular matrix. The shear stress generated by the media flow was more likely to affect the cells in monolayer culture or in the scaffold than the chondrocytes in the joint model. Even though the

articular cartilage has been demonstrated permeable to a number of molecules with the infiltration speed of 0.2-2 μm/s (depended on their charge density and molecular sizes) (Maroudas & Bullough 1968; Mow, *et al.* 1992; Garcia, *et al.* 1996; Garcia, *et al.* 1998), for the media-stirred model, the direct effect of the fluid flow was believed to be only on the cartilage surface and there was no flow-induced stress on the deeper chondrocytes. Thus, only the improvement of chondrocyte viability of the media-stirred model was observed.

For the method of this experiment, the flow of the culture media was created by a magnetic stirrer, which was similar to that with the spinner flask used by Lee *et al*. in a series of experiments on chondrocyte aggregates (Lee, *et al.* 2011b). Certain other systems would create flow for the culture, such as the rotating-wall culture vessel (Takebe, *et al.* 2012), or the pump-driven perfusion bioreactor system (Davisson, *et al.* 2002; Forsey, *et al.* 2012). However, considering the size of the model and the ease of operation, the magnetic stirring system was a practical choice.

This stirring system generated fluid movement around the joint model. The increase of the nutrient transport and the waste removal of the cartilage tissue was considered to be a possible reason for the improvement of the chondrocyte viability in the media-stirred model. The fluid movement might also have an influence on the chondrocyte function. However, the method of DMMB assay was only to test the matrix GAG content but not to examine the ability of matrix synthesise of the chondrocyte. If there was an effect from the fluid movement to chondrocytes, this was small as no response was observed; in particular there was no significant increase of the matrix GAG content in the media-stirred model compared to the static model.

In addition, after a period of culture, a layer of fibroblast-like cells overgrew the joint surface. This was observed as early as at the second week of culture in the media-stirred model. It caused difficulty with the assessment of the chondrocyte viability with the axial view, but otherwise did not to have any perceptible adverse effect. The source of those fibroblast-like cells were considered to be from the bone marrow or the surrounding soft tissues. It was postulated that these fibroblast-like cells were

agitated by the fluid movement and floated into the media. Once in the media, they could precipitate and proliferate on the cartilage surface during the static periods of the intermittent stirring protocol.

Chapter 4: Dynamic Model

4.1 Chapter outline

The dynamic model was a further development from the static model. The purpose of this experiment was to create a suitable machine to move the joint model automatically, and allow the effects of the joint movement to be evaluated. The hypothesis of the dynamic model was that both the chondrocyte viability and the matrix GAG content could be maintained for a longer period of time than the static model because the joint movement would give the cartilage mechanical stimulation as well as moving the culture media, both of which benefit the maintenance of the homeostasis of the articular cartilage.

The bovine joint for this model was harvested and cultured by the same methods as the static model. In order to move the joint automatically, a custom-made driving machine was built and applied to the joint model. The machine was further modified to allow 3 joints to move at a time rather than one. This considerably shortened the total experimental period. The movement duration and the motion speed was set in an intermittent pattern to imitate the real life situation of human as well as obtaining the maximal movement effect.

There were 5 different joints from 5 different animals included in the dynamic experiment. Each joint was cultured for 4 weeks. At each time point, the cartilage samples were obtained from two different areas of the joint surface. One from the cartilage within the moving arc and one from the ‘off-moving-arc’ area. The chondrocyte viability and the matrix GAG content were assessed every week. Comparison with the static model and the media-stirred model was made to identify the effect of dynamic joint movement.

In addition, for further extension of the experimental capacity and to test the effect of diminished movement time, a manually moved dynamic model was designed. The methods and the results of this hand-moved model are also presented in this chapter for comparison.

4.2 Materials and Methods

4.2.1 Construction of mechanical motion instrument

The motion instruments were designed and built for this model to provide the driving power for moving the harvested joint. Construction of the mechanical instruments is illustrated according to its three major parts—the driving motor, the connecting bar and the fixation peg. These 3 parts were constructed by using and modifying some existing materials.

To build the driving motor, an old laboratory tube rotator was used and remodelled. The original rotator plate of the tube rotator was removed and replaced with a custom-made circular plastic plate (**Figure 4.1**). On the plastic plate, several holes, which had different distances to the centre, were pre-drilled and threaded for linkage with the connecting bar. An ‘adjustable telescopic strut’ taken from an Ilizarov external fixator apparatus was refashioned as the connecting bar. A suitable screw was added on its proximal end for connection with the plastic plate by screwing into one of the pre-drilled holes. The third part, the peg, was modified by cutting an external fixation pin (3.5 mm in diameter) short for connection of the joint model, and its cut end was threaded for linkage with the distal segment of the telescopic strut (**Figure 4.1**).

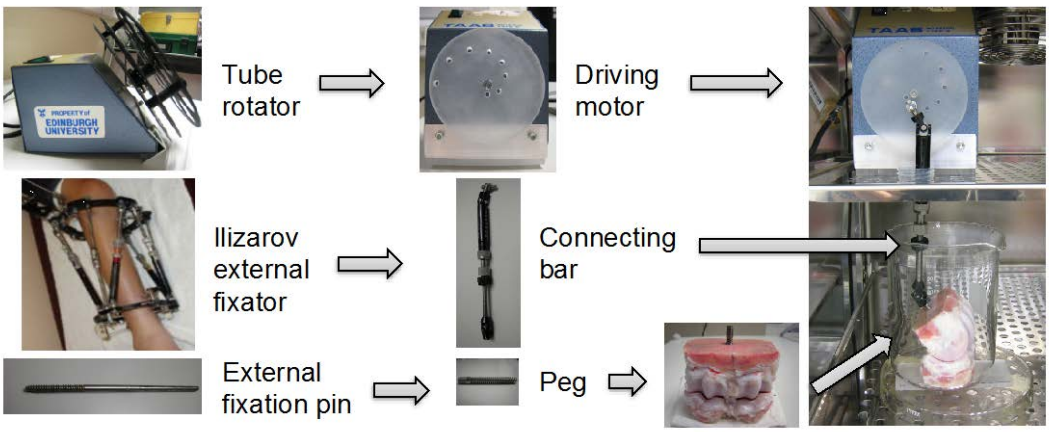

Figure 4.1 Construction of the motion machine for dynamic model

The motion machine was built by modifying materials that already existed. The tube rotator was converted into a driving motor by replacing the rotator plate with a custom-made plastic plate, in which a series of holes at different distances from the plate centre were drilled. The adjustable telescopic strut of the Ilizarov external fixator was used to connect the tube rotator with the joint. The external fixation pin was cut short to fix into the top of the transected metatarsal bone of this joint model. When the motor rotated, the strut moved upward and downward. The joint model was moved by this oscillating motion. All instruments were designed to be placed in a standard incubator for joint culture.

4.2.2 Creation of sterile environment

Compared to the static model, the maintenance of culture sterility was much more difficult in the dynamic model because there was a connecting bar passing through the paraffin membrane, which was an important barrier on the top of the culture vessel. As soon as the connecting bar moved, the integrity of the paraffin membrane was broken and the joint culture was at risk of being contaminated by environmental microbes.

After several trials, additional coverage of the chamber with a sterile plastic bag over the paraffin membrane was found to be a suitable solution to this crucial technical problem because the flexibility of the plastic bag allowed the connecting bar to move within its range. The sterile environment could then be maintained with its well-sealed margins around the beaker and the connecting bar (**Figure 4.2**).


a.

b.

Figure 4.2 Sterile environment creation of the dynamic model

a. A sterile plastic bag was trimmed to form a mantle-like shape and was placed on the top of the culture vessel. **b.** The top of the plastic bag was pierced through by the connecting bar inside-out, and the margin of the bag was well sealed around the bar and the culture vessel. A few ventilation cuts were made around the margin top of the bag for gas exchange (not shown in the picture).

4.2.3 Construction of the dynamic model

For harvesting the bovine metatarsophalangeal joint, the same methods as those described in the static model were used. Subsequently, additional procedures were performed to convert the static model into the dynamic model.

On the transected surface of the metatarsus, a central drill hole was made by using a sterile drill bit (Ø 3.0 mm). Care was taken to ensure the depth of the drill hole was only within the cancellous bone of the metatarsus and that it did not penetrate into the joint space. The custom-made peg was screwed into the drill hole directly and the connecting bar was linked onto the peg. During these procedures, the cartilage was kept wet with frequent PBS rinse. Afterward the joint was then placed into the culture vessel and immersed within the same culture media used before, which was DMEM with 10% FBS and 1% pen/strep.

The culture vessel was first covered with two layers of the paraffin membranes, in which central splits were pre-cut to let the connecting bar pass through. The sterile plastic bag was the second layer placed over the paraffin membranes. The margins of the bag were secured with sticky tape around both the beaker and the connection bar (**Figure 4.2**). Several small ventilation holes were cut around the peripheral margin of the plastic bag for gas exchange. With these double protection layers, the sterile environment of the joint culture could be maintained without affecting the movement of the connecting bar, and the possibility of microbe contamination from direct transmission through ventilation holes was minimised.

After the joint culture system was sealed properly, it was placed in the incubator with a standard environment of 37°C, 5% CO_2 and 95% humidity. The connecting bar was then linked onto the driving motor for joint movement. Some adjustments were necessary to make the motion smooth. (These are described in the following paragraph.)

4.2.4 Movement setting

The movement arc of the joint model, which meant the angle during the joint motion, should be adjusted when the model was connected to the machine. This purpose was to maximise the moving range of the joint model. According to the mechanics of the dynamic machine, the joint moving arc was determined by the moving range of the connecting bar, and the moving range of the bar was partially controlled by the distance between the chosen holes to the centre of the plastic rotator plate (**Figure 4.3**). Holes of various distances to the plate centre were chosen along with various distances from the culture vessel and the machine in order that a suitable combination of these distances could be obtained for the smoothest joint motion.

However, the entire surface of the joint model could not be fully used during the joint motion, which was one of the limitations of the dynamic machine. Therefore, part of the cartilage surface was defined as the contacted i.e. the ‘under-moving-arc’ area, as opposed to the ‘off-moving-arc’ area for the cartilage surface which was not articulating. The ‘under-moving-arc’ area was made as large as possible to provide sufficient test cartilage for assessment. Cartilage samples were taken from these two areas.

The movement speed was set at 20 rpm (0.33 Hz) on the driving motor to mimic a slow walking speed of a human. The movement duration was designed as an intermittent pattern, with 12 hours moving and 12 hours silence. In the moving period, 30 minutes continuous movement followed by 30 minutes stasis was used. This duration setting was in accordance with the physiology of the mammalian animal and the activity level of human (Campbell & Tobler 1984). Operation of the movement duration was controlled precisely by an electric timer that switched the machine power on and off according to the scheduled programme.

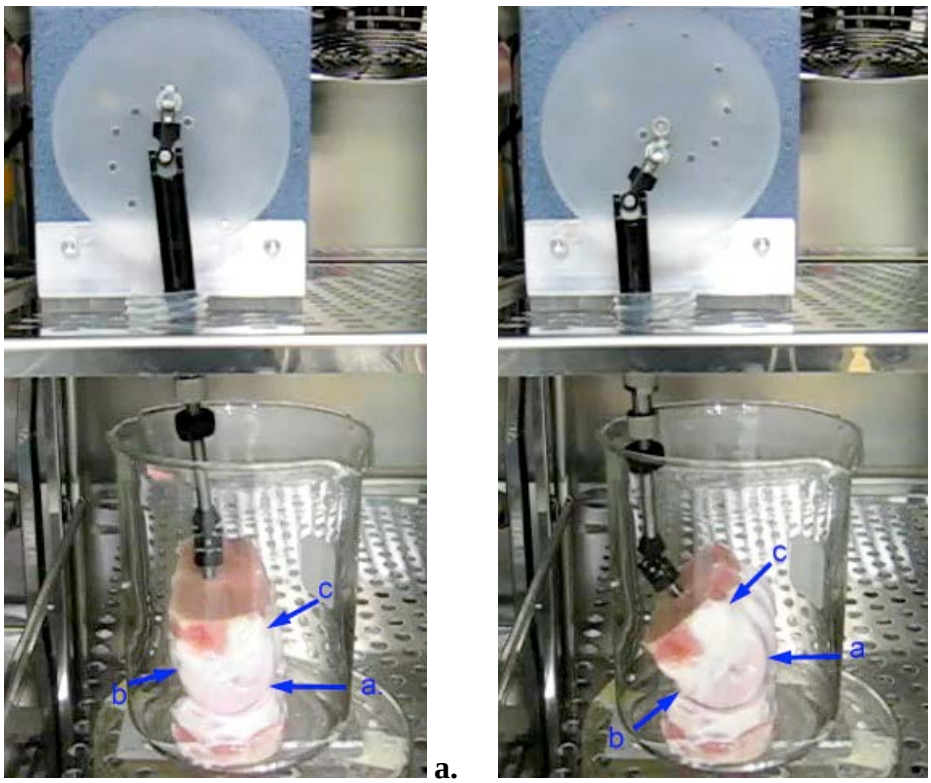

a. **b.**

Figure 4.3 Joint moving arc of the dynamic model

The joint was placed naturally on the bottom of the culture vessel without any fixation. Only the metatarsal part of the joint was moved by the connecting bar. The phalangeal part and the beaker were not moved accordingly. When the connecting bar moved to the highest point, the joint was lifted up and its anterior articular surface moved to point ‘a’; when the connecting bar continuously moved to the lowest point, the joint rotated backward and its posterior articular surface moved to point ‘b’. The arc from point ‘a’ to point ‘b’ consisted of the moving arc of this joint. The articular cartilage under the moving arc contacted each other during the joint movement, while the cartilage of metatarsus between point ‘a’ and point ‘c’ had no chance to contact the bottom cartilage of phalanges, which consisted of the ‘off-moving-arc’ area. In addition, according to the configuration of each individual joint, the culture vessel needed to be placed a little eccentrically and to be elevated by placing a spacer underneath the beaker to make the joint movement smooth. (Please noted that there was no culture media and top covers in the pictures for demonstration of the joint position clearly.)

4.2.5 Second generation motion instrumentation

The limitation of the dynamic machine was realised after a few trials. Two major drawbacks of the machine were the speed of the driving motor, which could not be easily adjusted, and the capacity of this machine, which allowed only one joint to be tested at a time. As each test lasted for one month and 5 joints were planned for this part of the research, it was necessary to evolve the apparatus so that multiple joints could be tested simultaneously. Thus, the second generation of the dynamic machine was designed.

In the new system, the connecting capacity was extended by remodelling the connecting bar to be able to link three joints at a time. The driving motor was replaced by a peristaltic pump, which could provide more power than the previous motor and the motor speed was adjustable (**Figure 4.4**).

Figure 4.4 The second generation dynamic machine

Structure of the connecting bar was redesigned for extension of its connecting capacity from one joint to three joints. The driving motor was replaced with a speed-adjustable peristaltic pump, which could provide greater power to drive three joints simultaneously.

4.2.6 Manually moved dynamic model

The manually moved dynamic model was built for applying the joint movement by hand directly. It was not possible for the movement time to be as long as the machine-moved dynamic model. Therefore, 10 minutes movement a day was applied for a total of 2 weeks. The motion speed was the same as the machine-moved dynamic model, which was 20 rpm (0.33 Hz).

For the manually moved dynamic model, the same procedures as the machine moved dynamic model were used to harvest the bovine joint, but no mechanical instrument was needed after the joint isolation. During the culture period, the joint was moved 10 minutes every day by hand. Sterile gloves were worn and the upper margin of the metatarsal bone of the joint model was held by thumb and index finger for applying the motion. No compression pressure but smooth and steady movement was given through fingers. The moving arc in the manually moved dynamic model was able to reach its maximal range, in which every surface of the articular cartilage could contact each other during joint motion (**Figure 4.5**). Thus, there was no ‘off-moving-arc’ area in this model.


a.

b.

Figure 4.5 Manually moved dynamic model

For infection control, the joint model needed to be placed in a biological hood for the manipulation. Sterile gloves were worn to give the joint motion by hand. Due to the narrow opening of the biological hood, the wrist of the examiner needed to be flexed in an unnatural position to move the joint model. During the movement, the whole articular surface could be tracked by the hand-controlled movement.

4.3 Results

Both the machine-moved and the hand-moved dynamic model included 5 different joints from 5 different animals. The cartilage biopsy was taken every week for 4 weeks in the machine-moved dynamic model and for 2 weeks in the hand-moved dynamic model. For the machine-moved joints, the biopsy sites were discriminated into two areas according to whether the cartilage was under the moving arc or not under the moving arc. The chondrocyte viability and the matrix GAG content were assessed by the same methods as described before. For the hand-moved dynamic model, all samples represented the ‘under-moving-arc’ area, and only the matrix GAG content was assessed.

4.3.1 Change of chondrocyte viability under the moving arc

The viability change of chondrocytes under the 'moving-arc' is shown in **Figure 4.6** and **Figure 4.7**. The curve of each zone did not change greatly during the entire culture period. Statistical comparison of the viability of each zone revealed that there was no significant difference (p=0.760 in the superficial zone, p=0.334 in the middle zone and p=0.416 in the deep zone; one-way ANOVA).

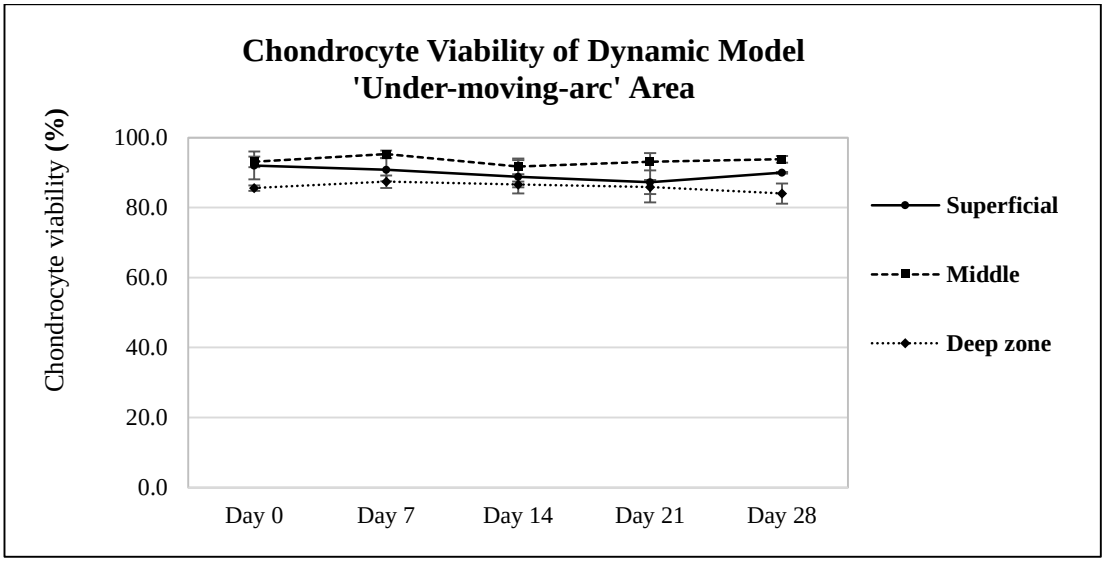

Figure 4.6 Change of chondrocyte viability of the dynamic model in the 'under-moving-arc' area

The chondrocyte viability of the cartilage under the moving arc of the machine-moved dynamic model is shown. The highest viability was found in the middle zone, and then, in sequence, the superficial zone and the deep zone. The slope of each curve was horizontal during these 4 weeks of culture, and the viability remained all over 80%.

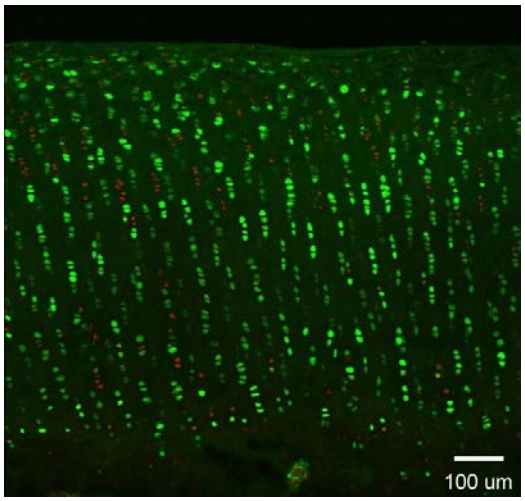

a. (Day 0, coronal view)

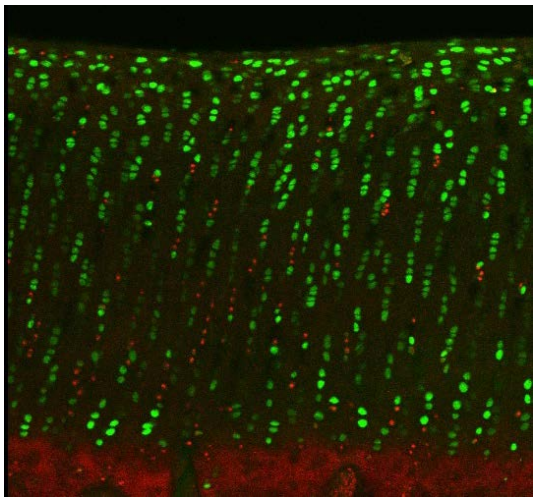

b. (Day 28, coronal view)

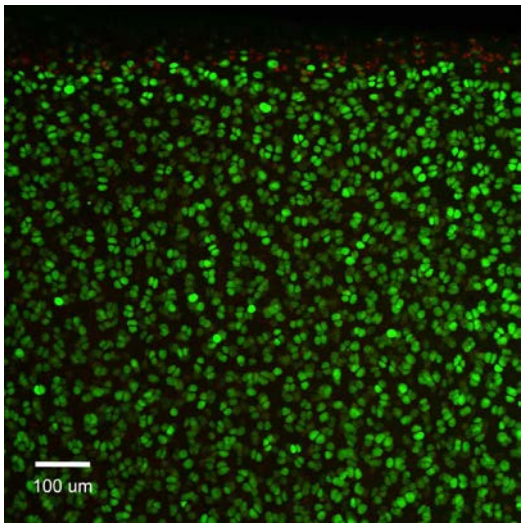

c. (Day 0, axial view)

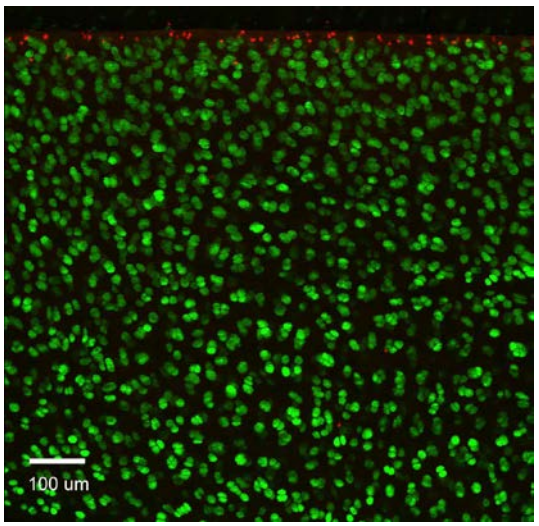

d. (Day 28, axial view)

Figure 4.7 CMFDA/PI stained confocal microscopy images of the under-moving-arc cartilage of the dynamic model

Confocal images of the cartilage samples in the 'under-moving-arc' area of machine-moved dynamic model revealed that the percentage of chondrocyte viability did not change greatly from Day 0 to Day 28. Either in the coronal view or axial view viability image, similar percentage of viable cells was found at Day 0 compared to Day 28. Coincidentally, a live multiple nucleated osteoblast was observed at Day 0, while at Day 28 there were no live cells in the subchondral area.

4.3.2 Change of chondrocyte viability in the ‘off-moving-arc’ area

The chondrocyte viability in the area that was not directly in contact with the opposing surface during joint movement is shown in **Figure 4.8**. The viability curve of each zone dropped a small amount during the culture period. However, only the deep zone had a statistically significant decrease (p=0.001, one-way ANOVA). No significant fell occurred in the superficial zone (p=0.044, one-way ANOVA) or the middle zone (p=0.587, one-way ANOVA).

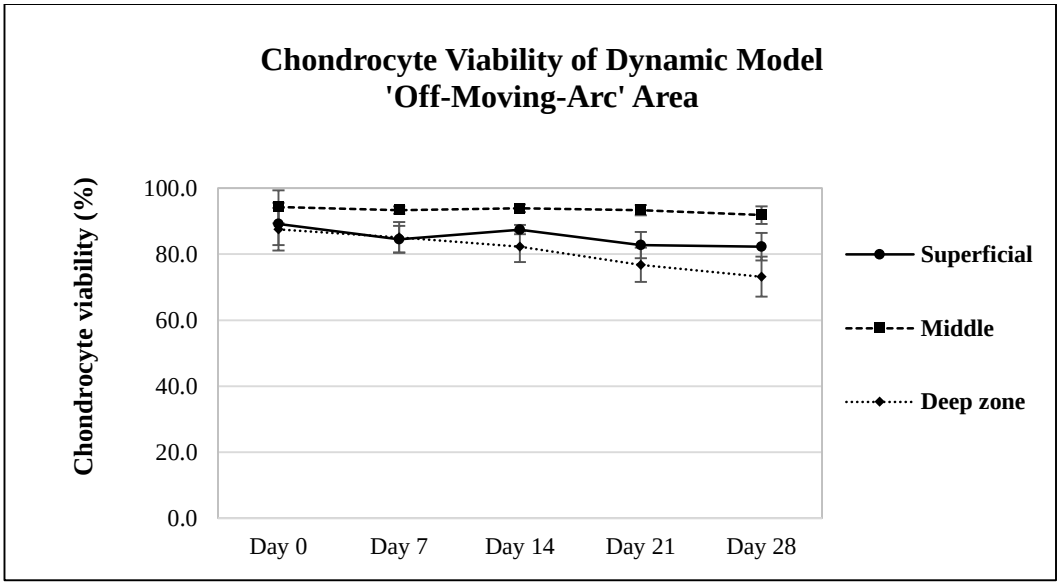

Figure 4.8 Change of chondrocyte viability of the dynamic model in the ‘off-moving-arc’ area

The chondrocyte viability change in the noncontact ‘off-moving-arc’ area of the dynamic model is shown. Viewed vertically, it demonstrates similar zonal viability sequence as those in the ‘under-moving-arc’ area, where the middle zone kept the highest viability and the superficial and deep zone viability decreased in sequence. Viewed horizontally, the slope of the deep zone seemed steeper than the other two zones. At Day 21 and Day 28, the viability of deep zone was below the 80% line.

4.3.3 Zonal viability of the ‘under-moving-arc’ area and the ‘off-moving-arc’ area of the dynamic model

Chondrocyte viability in each zone of the ‘under-moving-arc’ area and the ‘off-moving-arc’ area of the machine-moved dynamic model was compared to identify the effects of joint movement on the chondrocyte viability in the same joints.

Statistical analysis revealed that there were significant differences in the superficial zone and the deep zone between its articulating and non-articulating areas ($p<0.001$ for both the superficial and deep zones, $p=0.906$ in middle zones; two-way ANOVA) (**Figure 4.9**). Further analysis revealed that the difference occurred in the superficial zone at Day 28, the deep zone at Day 21 and Day 28.

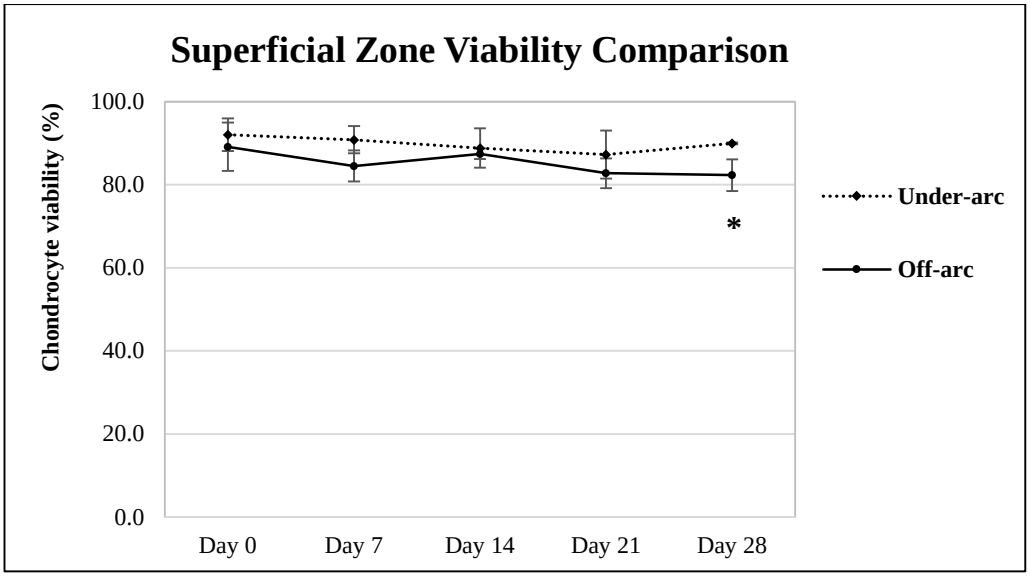
Superficial Zone Viability Comparison
Chondrocyte viability (%)
100.0
80.0
60.0
40.0
20.0
0.0
Day 0
Day 7
Day 14
Day 21
Day 28
*
Under-arc
Off-arc

a.

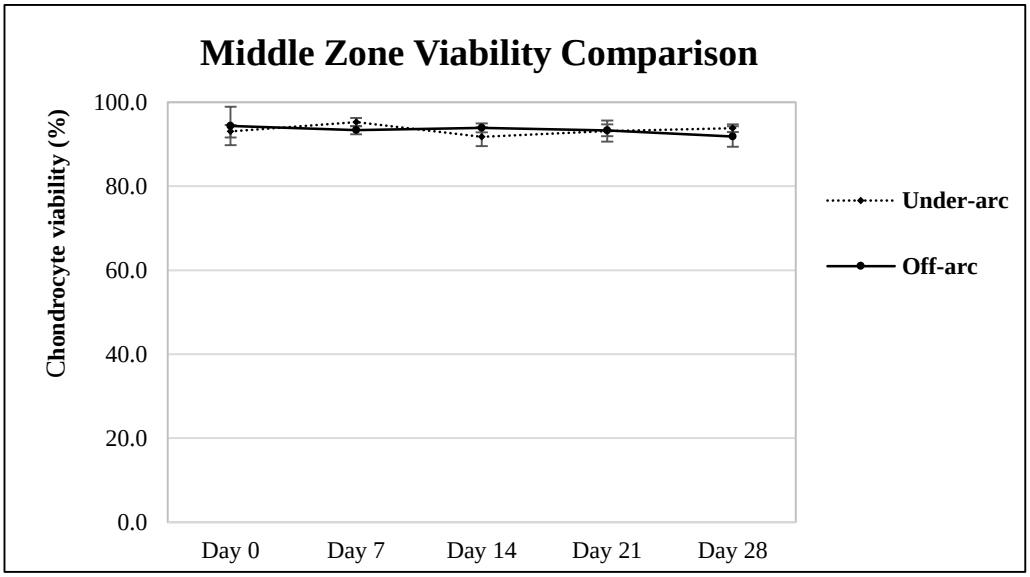
Middle Zone Viability Comparison
Chondrocyte viability (%)
100.0
80.0
60.0
40.0
20.0
0.0
Day 0
Day 7
Day 14
Day 21
Day 28
Under-arc
Off-arc

b.

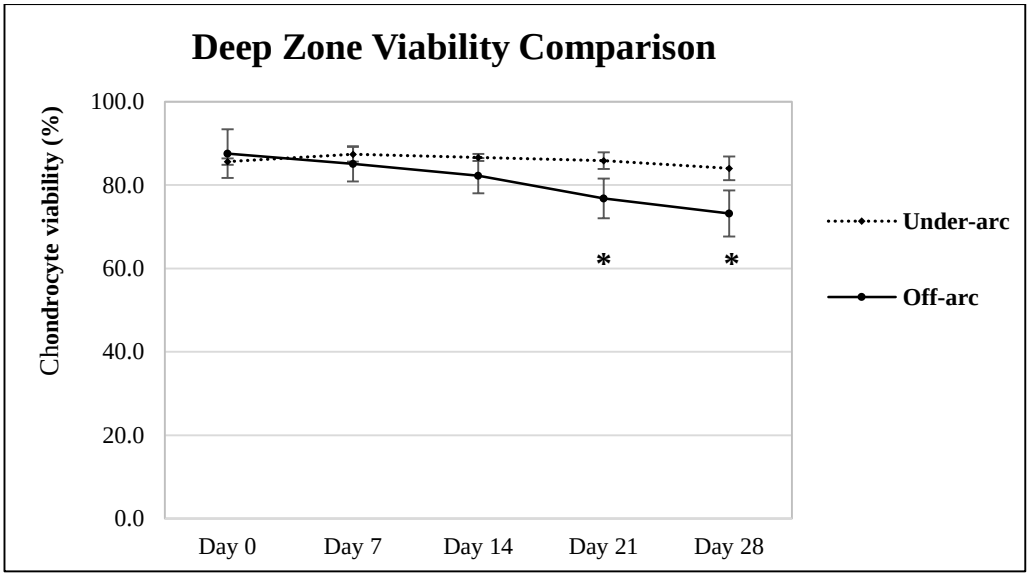

c.

Figure 4.9 Zonal viability comparison between the 'under-moving-arc' and the 'off-moving-arc' area of the dynamic model

The chondrocyte viability of the 'under-moving-arc' area and the 'off-moving-arc' area of the dynamic model was compared in the separate zones. **a.** In the superficial zone, the chondrocyte viability of both areas decreased slightly during the culture period. **b.** In the middle zone, both the viability curves were horizontally oriented and difficult to differentiate. **c.** In the deep zone, the two curves could be identified clearly because the slope of the 'off-moving-arc' curve was steeper than the slope of the 'under-moving-arc' curve.

4.3.4 GAG content of the 'under-moving-arc' area and the 'off-moving arc' area of the dynamic model

The matrix GAG content change in both the 'under-moving-arc' area and the 'off-moving-arc' area of the machine-moved dynamic model is shown together in **Figure 4.10** for comparison.

The GAG content in the 'under-moving-arc' area maintained a nearly constant level during the entire culture period along the 1.20% line. In contrast, the curve of the GAG content in the 'off-moving-arc' area dropped from 1.18% to 0.99% in the first week and then stayed at approximately 1.00% during the second and third week before dropping again slightly at the end of the culture period. After statistical analysis, there was significant difference between these two curves ($p<0.001$, two-way ANOVA).

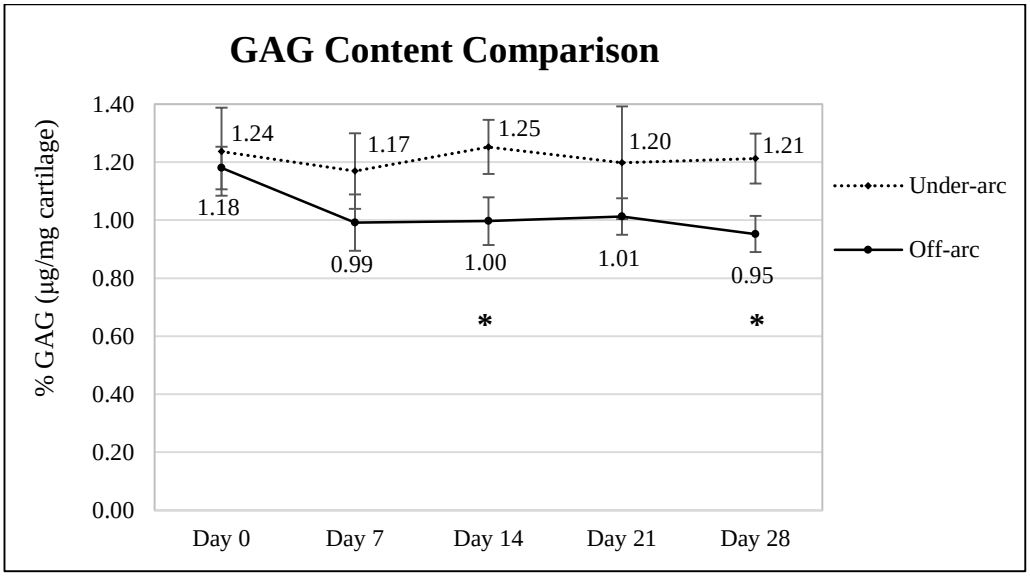

Figure 4.10 The GAG content change in the under-moving-arc area and the off-moving-arc area of the dynamic model

The curve of the GAG content of the 'off-moving-arc' area decreased at the first week and kept this similar lower level to the end of the 4th week. In contrast, the curve of the 'under-moving-arc' area did not change significantly at Day 7 and maintained a consistent level during the entire culture period. Statistically, Day 14 and Day 28 were significantly different ($p<0.001$, paired t-test).

4.3.5 Change of the matrix GAG of the manually moved dynamic model

The matrix GAG content of the manually moved dynamic model kept a quite consistent level during the two weeks of culture (**Figure 4.11**). It started at a level of 1.23%, which was similar to that of the dynamic model (1.24%; 'under-moving-arc' area). This level was maintained during the first week but dropped a non-significant amount (to 1.20%) at Day 14. No significant difference between each time point was found (p=0.949, one-way ANOVA). In addition, there was also no significant difference between the GAG content of the 'under-moving-arc' area of the machine-moved dynamic model and the manually moved dynamic model (p=0.972, two-way ANOVA).

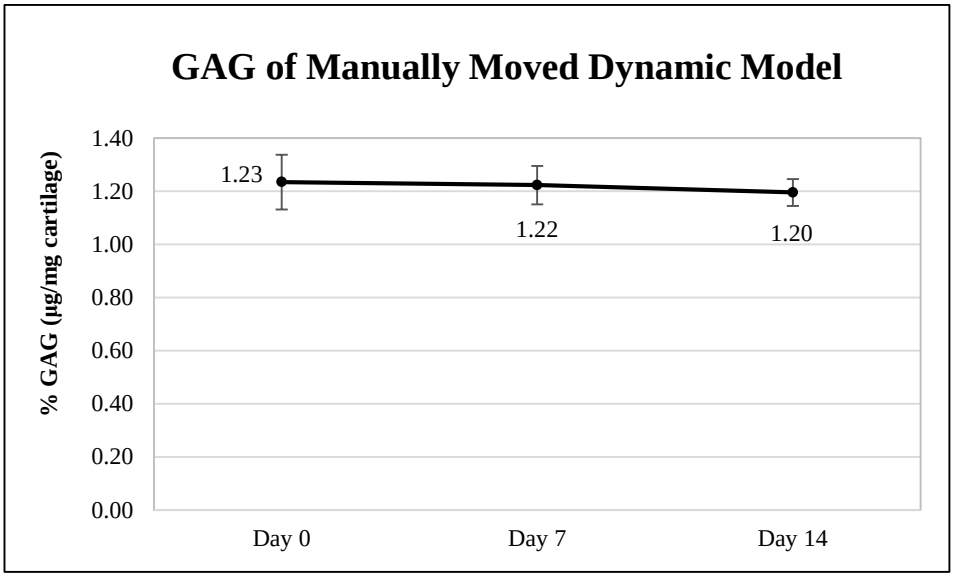

Figure 4.11 Matrix GAG content change of 5 manually moved dynamic joints
There were 10 samples from 5 different joints obtained in each time point. During the two weeks of culture, the matrix GAG content kept a quite consistent level and only a non-significant decrease was found.

4.3.6 GAG content comparison between the dynamic model and the static model

The GAG content of the dynamic model 'under-moving-arc' area was compared with the GAG content of the static model (**Figure 4.12**). The GAG content of the dynamic model 'under-moving-arc' area was maintained at a relatively consistent level along the line of 1.20%. However, the GAG content of the static model decreased at the first week to 0.97% and dropped further at the 3th week to 0.79%, which made significant difference between each other. Even though the GAG value of static model returned a little at the 4th week (to 0.94%), the difference remained.

The GAG content of the static model was also compared with the GAG content of the dynamic model 'off-moving-arc' area (**Figure 4.13)**. These two curves seemed well-overlapped except at the point of Day 21, where the matrix GAG of the static model was 0.79% and the dynamic 'off-moving-arc' area was 1.01%. However, after statistical analysis, there was no significant difference between these two curves (p=0.056, two-way ANOVA).

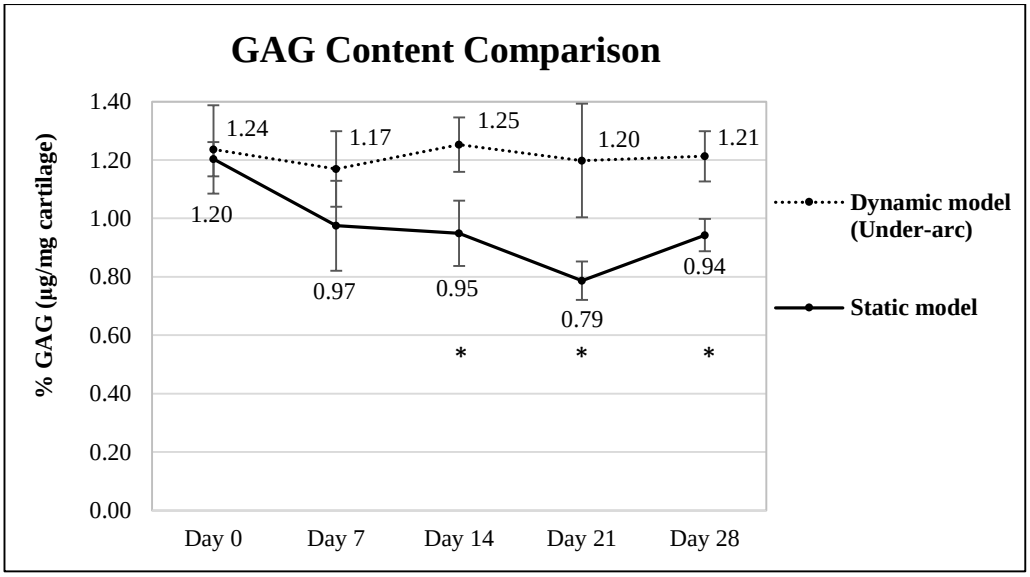

Figure 4.12 GAG content comparison between the dynamic model 'under-moving-arc' area and the static model

There was a clear difference in the matrix GAG content of these 2 models with the dynamic model retaining its GAG better than the static model, and the difference became significant after Day14 (p<0.001; two-way ANOVA).

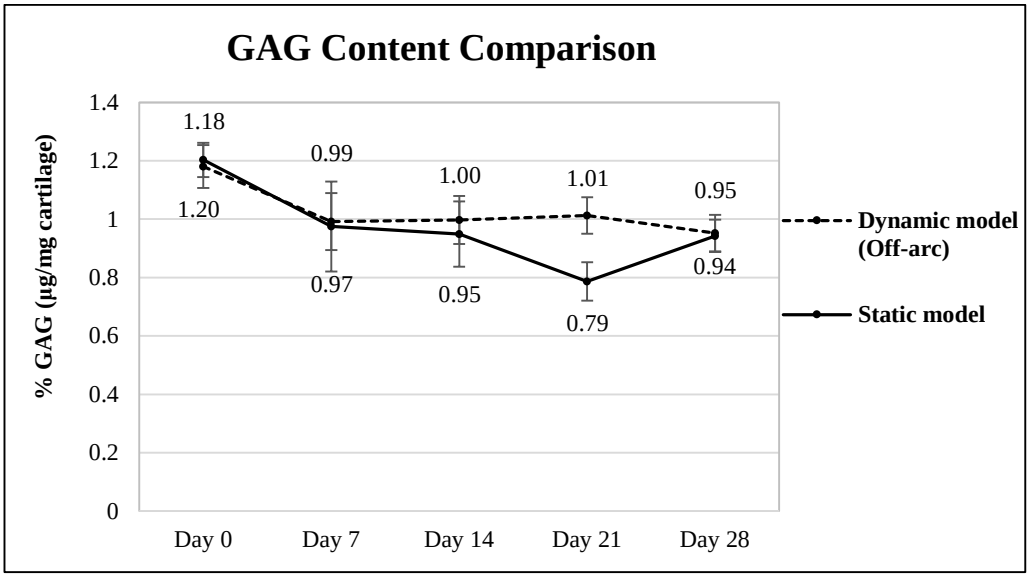

Figure 4.13 GAG content comparison between the dynamic model 'off-moving-arc' area and the static model

Throughout the timeline, the GAG content moved in similar way in both models except at Day 21. However, no statistically significant difference was obtained between these two curves (p=0.056, two-way ANOVA).

4.3.7 GAG content comparison between and the dynamic model the media-stirred model

The matrix GAG content of the dynamic model 'under-moving-arc' area was compared with the matrix GAG content of the media-stirred model (**Figure 4.14**). In the dynamic model 'under-moving-arc' area, the GAG content was maintained at a relatively consistent level approximately along the line of 1.20%, while the GAG content of the media-stirred model decreased at the first week to 0.90% and dropped further at the 2nd week to 0.81%. Even though the GAG amount of the media-stirred model returned a little at Day 21 (0.92%) and Day 28 (0.94%), there was still statistically significant difference between these two models after the first week of culture (p<0.001; two-way ANOVA) .

The GAG content of the media-stirred model was also compared with the GAG content of the dynamic model 'off-moving-arc' area (**Figure 4.15**). In both models, the GAG content decreased in the first week of culture (from 1.22% to 0.90% in the media-stirred model; from 1.18% to 0.99% in the dynamic model). The matrix GAG continued to drop to 0.81% in the media-stirred model but not in the dynamic model that maintained its matrix GAG at 1.00% level during the second week. It returned to a similar level at the end of the 4th week in both models. However, there was no significant difference between these two curves (p=0.027, two-way ANOVA; significance level set at p<0.010 by Bonferroni correction for multiple comparison).

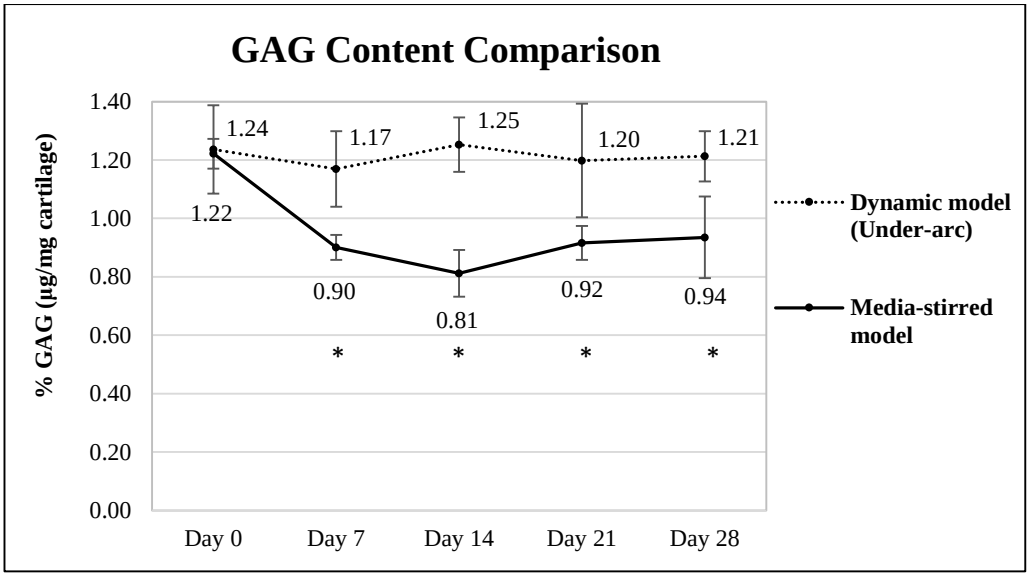

Figure 4.14 GAG content comparison between the dynamic model under-moving-arc area and the media-stirred model

The matrix GAG content between these two models was significantly different (p<0.001; two-way ANOVA). Further evaluation revealed the difference occurred after the first week of culture (p<0.05 after Day 7, unpaired t-test).

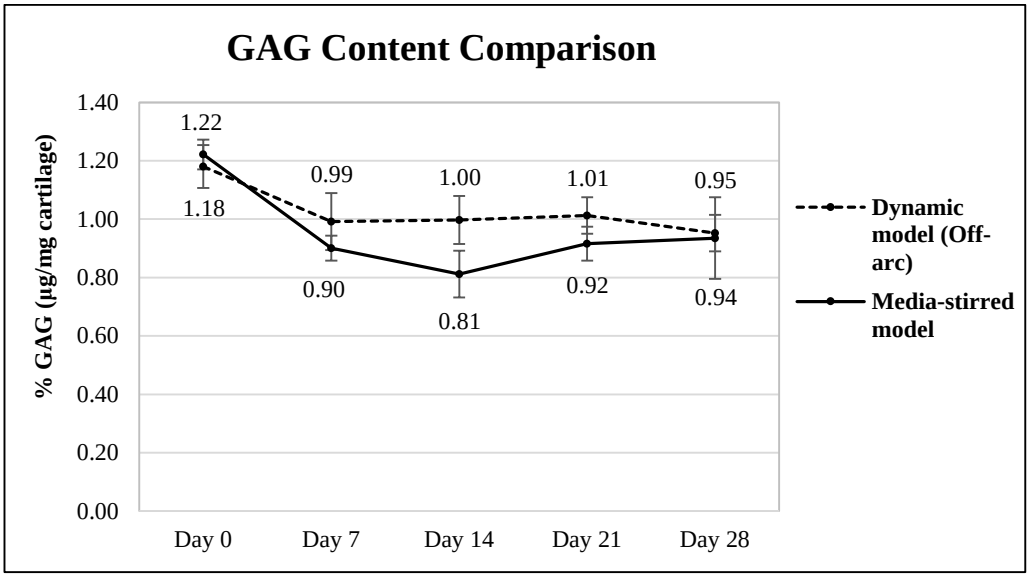

Figure 4.15 GAG content comparison between the dynamic model off-moving-arc area and the media-stirred model

The pattern of matrix GAG loss was similar in these 2 models. Although the values of the media-stirred model were lower than those of the dynamic model after Day 7, there was no significant difference between them (p=0.027, two-way ANOVA).

4.3.8 Zonal viability comparison between the dynamic model and the static model

The zonal chondrocyte viability of the static model was compared to the dynamic model 'off-moving-arc' area to examine whether factors such as fluid flow caused by the joint movement affected the chondrocyte viability (**Figure 4.16**).

The difference of the viability curves in every zone between these two models could be identified clearly in the comparison plots. In the superficial zone (**Figure 4.16a**), the chondrocyte viability of both models decreased slightly during the culture period. In the middle zone (**Figure 4.16b**), the viability curve of the dynamic model was more horizontally orientated, whereas the viability curve of the static model decreased after Day 14. In the deep zone (**Figure 4.16c**), the viability decreased in both models during the culture period, but the slope of the static model was steeper than the slope of the dynamic model.

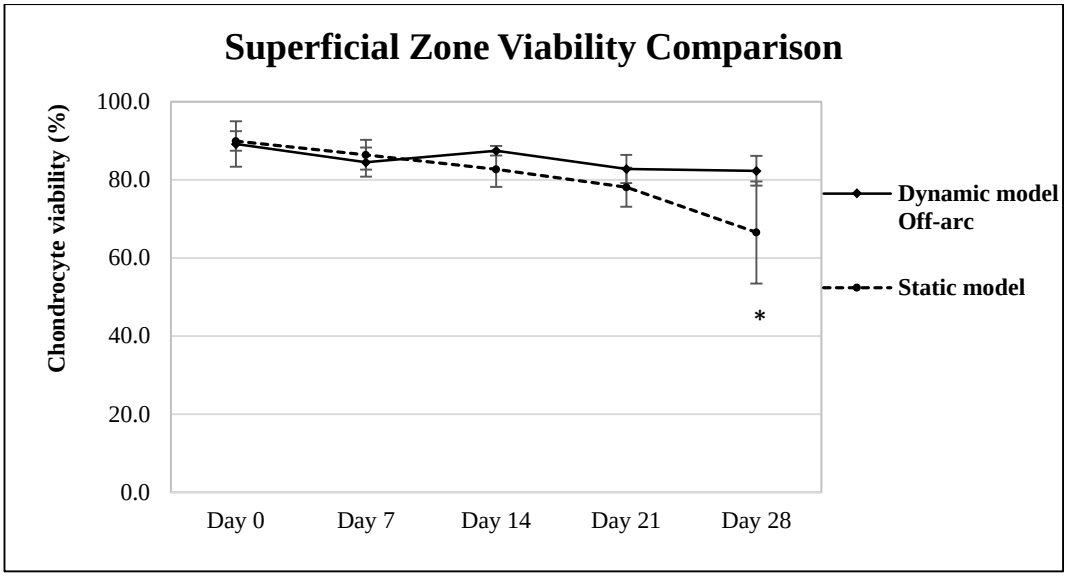
Superficial Zone Viability Comparison
Chondrocyte viability (%)
100.0
80.0
60.0
40.0
20.0
0.0
Day 0
Day 7
Day 14
Day 21
Day 28
*
Dynamic model Off-arc
Static model

a.

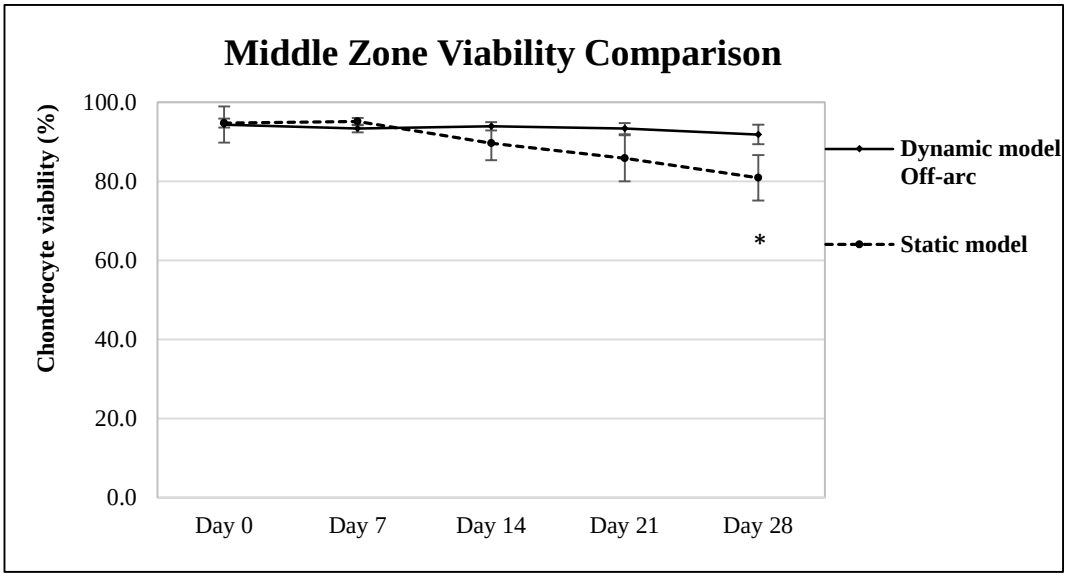
Middle Zone Viability Comparison
Chondrocyte viability (%)
100.0
80.0
60.0
40.0
20.0
0.0
Day 0
Day 7
Day 14
Day 21
Day 28
*
Dynamic model Off-arc
Static model

b.

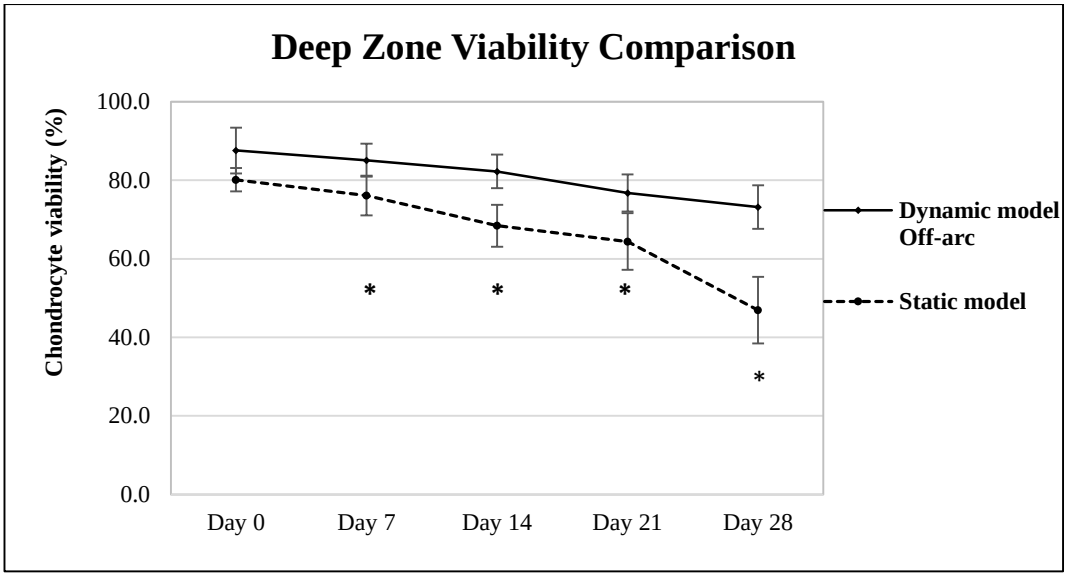

c.

Figure 4.16 Zonal viability comparison between the 'off-moving-arc' area of the dynamic model and the static model

The chondrocyte viability difference of different zones between these two models could be identified clearly after statistical analysis. The results revealed that there were significant difference in all three zones (p=0.007 for the superficial zone comparisons and p<0.001 in both the middle zone and the deep zone comparisons; two-way ANOVA). Further analysis revealed that the difference occurred in the superficial zone at Day 28, the middle zone at Day 28 and the deep zone from Day 7 to Day 28 (p<0.05, unpaired t-test).

4.3.9 Zonal viability comparison between the dynamic model and the media-stirred model

Chondrocyte viability comparison between the 'off-moving-arc' area of the dynamic model and the media-stirred model was done to identify if any viability difference occurred between these two models (**Figure 4.17**). In both of these models, the cartilage was subjected to flow either from the joint movement or from the magnetic stirrer.

The comparison plots revealed that the similarity of the chondrocyte viability in the 'off-moving-arc' area of the dynamic model and the media-stirred model was strong. In the superficial zone (**Figure 4.17a**) and the middle zone (**Figure 4.17b**), the viability curves overlapped to a great extent making it very difficult to differentiate each curve. In the deep zone (**Figure 4.17c**), the slope of these two curves was also remarkably similar even though the viability values of the media-stirred model were slightly lower than those of the dynamic model.

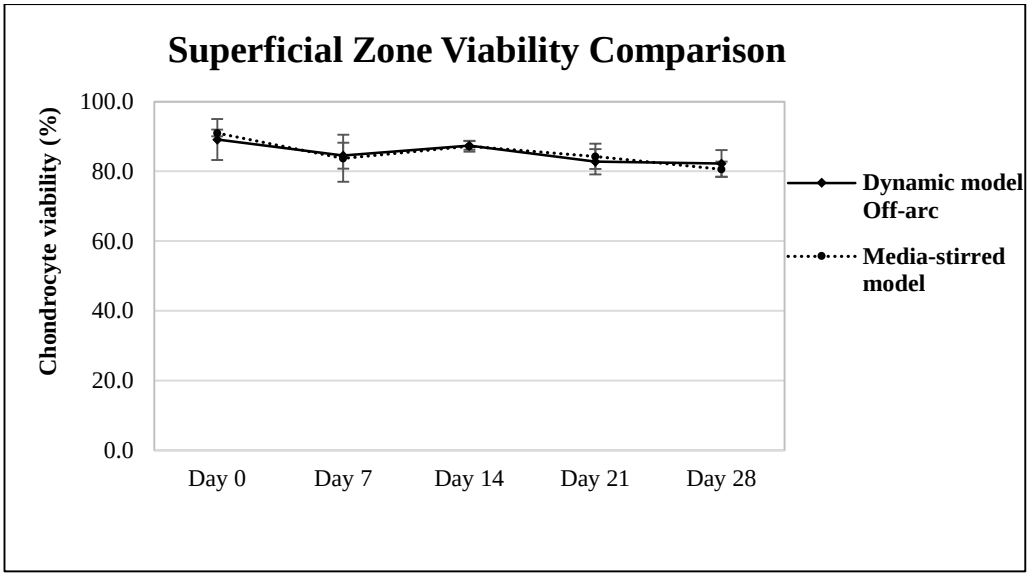
Superficial Zone Viability Comparison
Chondrocyte viability (%)
100.0
80.0
60.0
40.0
20.0
0.0
Day 0
Day 7
Day 14
Day 21
Day 28
Dynamic model Off-arc
Media-stirred model

a.

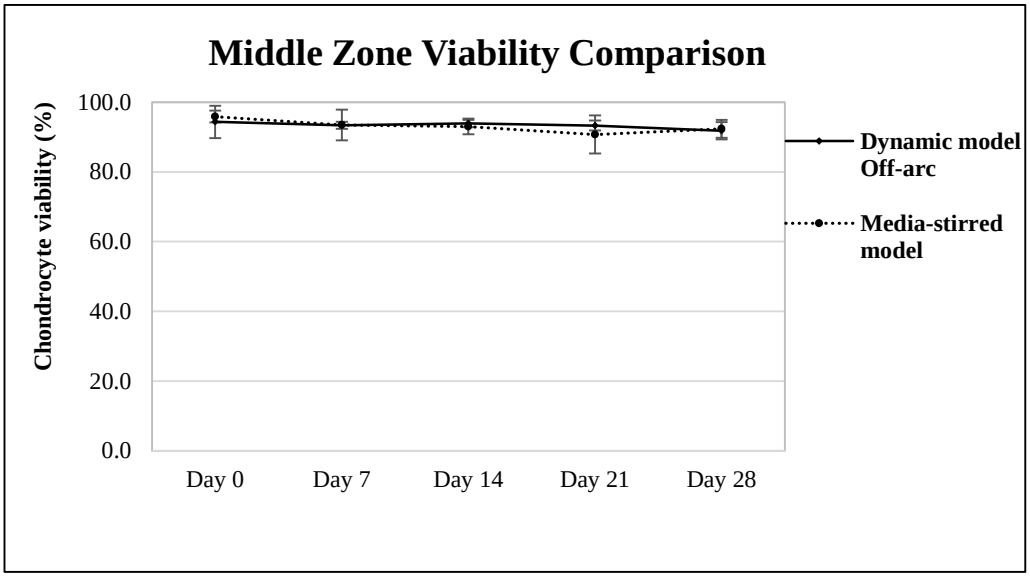
Middle Zone Viability Comparison
Chondrocyte viability (%)
100.0
80.0
60.0
40.0
20.0
0.0
Day 0
Day 7
Day 14
Day 21
Day 28
Dynamic model Off-arc
Media-stirred model

b.

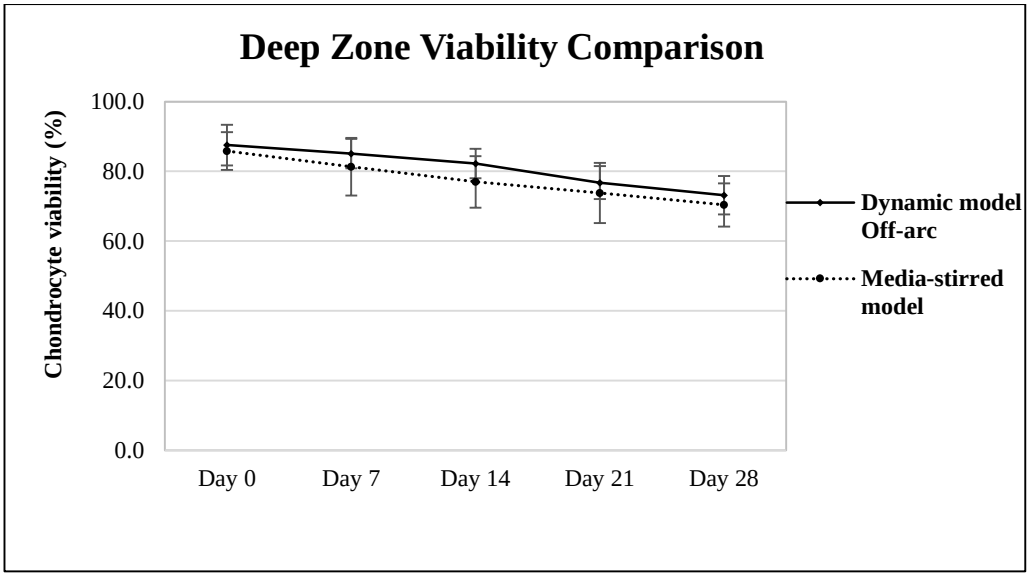

c.

Figure 4.17 Zonal viability comparison between the 'off-moving-arc' area of the dynamic model and the media-stirred model

From these figures, the similarity of the chondrocyte viability change between the 'off-moving-arc' area of the dynamic model and the media-stirred model could be identified. Statistical analysis revealed that there were no significant difference of the chondrocyte viability between these two models in any of the zones (p=0.863, p=0.714 and p=0.294 in the comparison of the superficial zone, the middle zone and the deep zone, respectively; two-way ANOVA).

4.3.10 Chondrocyte density of the dynamic model

In the ‘under-moving-arc’ area of the dynamic model, the cartilage was subjected to media flow and the moving force, but in the ‘off-moving-arc’ area, the cartilage received only the media flow from the joint movement. Chondrocyte density in both areas was calculated to identify if any cell density change occurred between these two areas or in the same area during the culture period.

The plots revealed that the similarity of the chondrocyte density between these two areas (**Figure 4.18 and 4.19**). Statistical calculation further confirmed that there was no difference in between (p=0.377, 0.073 and 0.919 in the superficial, middle and deep zone, respectively; two-way ANOVA), and, in each area, there was also no difference during the culture period.

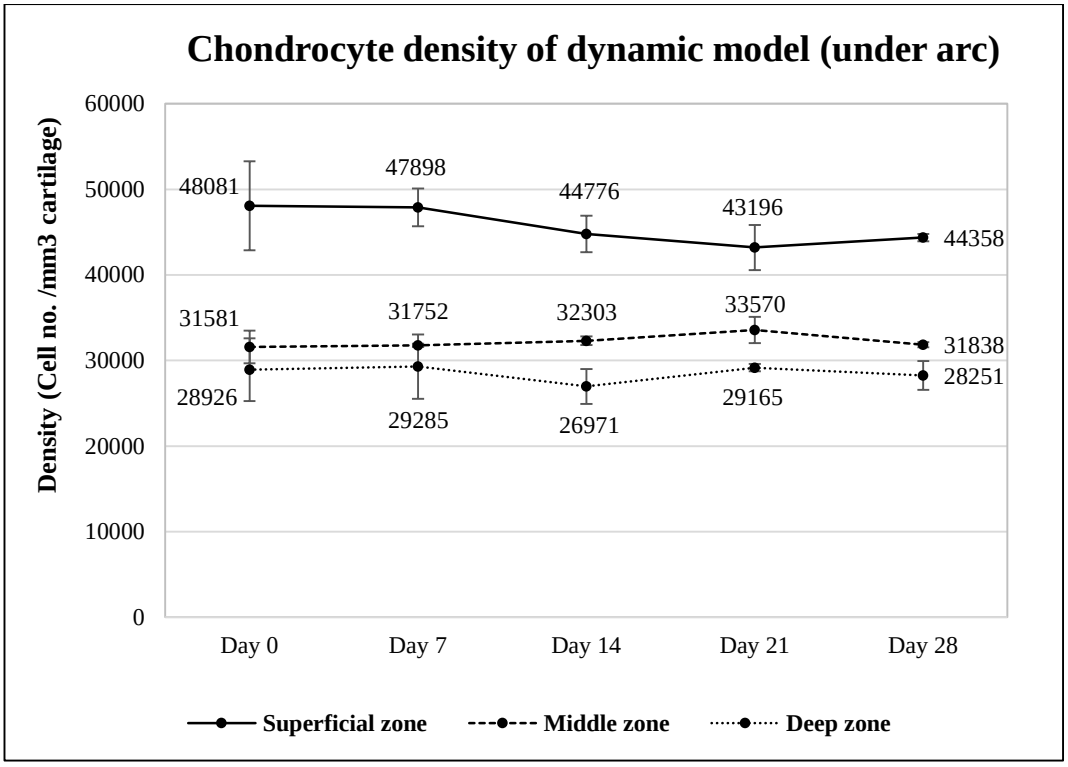

Figure 4.18 Chondrocyte density of dynamic model in the 'under-moving-arc' area

Chondrocyte density in the 'under-moving-arc' area revealed that the superficial zone had the highest cell density than the middle and deep zone at all time point. Even though the density values of superficial zone slightly decreased from Day 0 to Day 28, statistical analysis revealed that there was no significant change during the culture period (p=0.402, 0.439 and 0.891 in the superficial, middle and deep zone, respectively; one-way ANOVA).

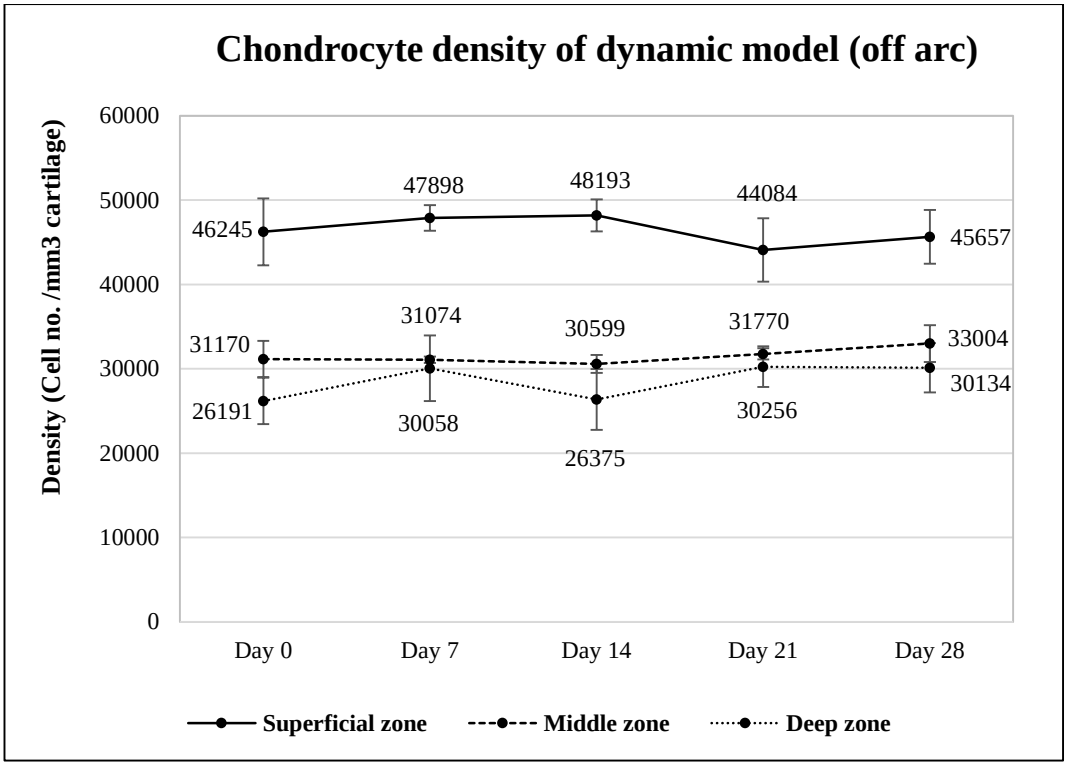

Figure 4.19 Chondrocyte density of dynamic model in the 'off-moving-arc' area
Cell density change of the 'off-moving-arc' area looked similar to that of the 'under-moving-arc' area. There was still no statistically significant difference from Day 0 to Day 28 of each zone (p=0.218, 0.138 and 0.093 in the superficial, middle and deep zone, respectively; one-way ANOVA).

4.4 Discussion

4.4.1 Dynamic effects on the articular cartilage

The dynamic model was developed to evaluate the mechanical effects of joint movement on the articular cartilage. The results supported the hypothesis that both the chondrocyte viability and the matrix GAG content were maintained as the initial levels for a longer period of time than the static model.

Chondrocyte viability. The chondrocyte viability of the dynamic model was significantly improved compared to the static model (**Figure 4.16**). This effect was more marked with prolonged culture. The best maintenance of the cell viability occurred in the 'under-moving-arc' area of the dynamic model, where the chondrocyte viability in the superficial zone at Day 28 and the deep zone at Day 21 and Day 28 was greater compared to the second best area, the 'off-moving-arc' area of the dynamic model (**Figure 4.9**). After 28 days of culture, the viability in the 'under-moving-arc' area of dynamic model was maintained nearly at the initial level without the significant drop. It was considered that this was due to two factors – the direct effect from the joint movement and the indirect effect from the fluid flow created by the joint movement. As the direct effect, the maintenance of the chondrocyte viability might be related to the mechanical stimulation on the chondrocytes decreasing apoptosis as described by Bader *et al*. and Galois *et al*. (Galois, *et al.* 2003; Bader, *et al.* 2011), or, as the indirect effect, it might be related to the increase of exchange of nutrients and waste products caused by the joint compression movement on the cartilage (Strangeways 1920) combined with the media flow.

The 'off-moving-arc' area of the dynamic model and the media-stirred model were both considered to have the second best chondrocyte viability because their viability changes were remarkably similar without statistically significant differences during the culture period (**Figure 4.17**). The indirect effect of the media flow in both models was considered to be the positive factor that maintained the chondrocyte viability better than that of the static model. As the result shown in **Figure 4.16**, this effect

caused statistically significant differences in the superficial zone of Day 28, the middle zone of Day 28 and the deep zone after Day 7 between the 'off-moving-arc' area of the dynamic model and the static model. The effect of fluid movement on the cartilage metabolism has been thoroughly discussed in Chapter 3.4.

Matrix proteoglycan content. Both the 'under-moving-arc' area of the machine-moved dynamic model and the manually moved dynamic model were considered to have the best maintenance of the matrix GAG amongst all models of the thesis. Their GAG content could be maintained as the initial level throughout the culture period (**Figure 4.10 & 4.11**). Other models such as the static and the media-stirred model or the 'off-moving-arc' area of the dynamic model could not maintain their initial GAG and lost it during the first week of culture (**Figure 4.10, 4.12 & 4.14**).

The cartilage of both the 'under-moving-arc' area of the dynamic model and the manually moved dynamic model received the compression force and the shear stress from the joint movement, which were considered positive factors for maintenance of the matrix proteoglycan because the forces stretched the collagen network and altered the hydrostatic pressure of the cartilage matrix. As suggested by Bader *et al*., these biomechanical changes would stimulate the mechanoreceptors on the surface of the chondrocytes, which, in turn, would trigger the intracellular anabolic pathway to synthesise matrix protein or they would inhibit the production of degenerative enzymes (Bader, *et al.* 2011). From the result demonstrating the consistently maintained GAG content, it could be inferred that, in these two models, the balance of the anabolic and catabolic metabolism inside the chondrocytes, or between the chondrocyte and the matrix, did not change.

The cross comparison of the matrix GAG content amongst these models revealed some interesting findings. First, on reviewing the weekly samples, the result at Day 7 appeared to be the 'watershed'. The GAG values after Day 7 could be divided into two levels: (1) the high level, where the GAG values returned to a similar level to the starting Day 0 level (approximately 1.20%). This was observed in the 'under-moving-arc' area of the dynamic model and the manually moved dynamic model. (2) The low level, where the GAG level fell to a new lower level, was in a range

between 0.80% and 1.00%, approximately. This was seen with the static model, the media-stirred model and the 'off-moving-arc' area of the dynamic model. It was noted that only the loaded cartilage followed the higher level indicating the joint movement played an important role for the maintenance of the matrix GAG. Without the joint movement, the matrix GAG would decrease to the low level soon after the joint was cultured.

Second, there was a significant difference between the media-stirred model and the 'under-moving-arc' area of the dynamic model occurred as early as Day 7 (**Figure 4.14**), whereas the difference between the static model and the dynamic model at Day 7 was not significant (**Figure 4.12**). It could be explained by the matrix GAG in the media-stirred model being lost more quickly than that in the static model because of the fluid movement in the media-stirred model.

Finally, the GAG level did not drop below 0.80%. This might indicate that there is a critical level and when the GAG content drops below this level, synthesis of the matrix protein is triggered by the chondrocytes. However, further experiments are required to explore this hypothesis.

Chondrocyte density. The results of chondrocyte density of the dynamic model demonstrated that even though the cartilage in the 'under-moving-arc' area additionally received forces from joint movement, the cell number in the area could be kept in a statistically consistent amount during the 4 weeks culture, and with no significant difference from the 'off-moving-arc' area (**Figure 4.18 and 4.19**). This subsided the concern that the chondrocyte could be scraped away by friction when the joint was moved, especially for the cells of superficial zone.

4.4.2 Effects of joint movement

The maintenance of the cell viability and the matrix GAG content of the dynamic model and the manually moved model was considered to be from the joint movement. However, articular cartilage *in vivo* is subjected to the complex mechanical loads of joint movement, which consist of a combination of both

compressive and shearing force under normal physiological conditions (Mankin, *et al.* 1994). These forces have been evaluated in different models. Compression force is the most commonly used force for mechanical stimulation in the *in vitro* studies. It has been broadly demonstrated to have positive effects on the matrix molecular synthesis if the force is within the physiological range (Sah, *et al.* 1989; Steinmeyer, *et al.* 1997). In contrast, pure tissue shear stress has not been so commonly studied. It has been evaluated in one study, which used a rotational plate to produce 1–3% sinusoidal shear strain amplitudes over a wide range of frequencies (0.01–1.0 Hz) (Jin, *et al.* 2001). Their results revealed that even though the tissue shear force caused less volumetric deformation than the compression force, its stimulatory effect remained effective as the synthesis of protein was increased by up to 50% and the proteoglycans by up to 25% at frequencies between 0.01 and 1.0 Hz. The increase of the matrix protein synthesis from the stimulation of the shear stress was also shown in a series of studies by Grad *et al*. (Grad, *et al.* 2006a; Grad, *et al.* 2006b). Their results suggested that the signal transduction pathways of the compression force and the shear stress might be different inside the cartilage tissue. Waldman *et al*. further indicated that these two forces might have a synergistic effect, which enhanced the synthesis of matrix proteins (Waldman, *et al.* 2007). Thus, compression with rolling movement was suggested to be a more appropriate method to conduct the loading process on the articular cartilage (Heath & Magari 1996; Grad, *et al.* 2011).

However, only a few *in vitro* experimental systems could exert both forces onto the cartilage being tested. For instance the bioreactor systems developed by Grad *et al*. and Wimmer *et al*., in which the ball of a ceramic hip was used to produce variable types of stresses on the cartilage explants (Wimmer, *et al.* 2004; Grad, *et al.* 2006a; Grad, *et al.* 2006b). Therefore, this *ex vivo* dynamic joint model, which has more natural ‘cartilage-on-cartilage’ joint movement, provides another suitable platform for studying the mechanical effects on cartilage because both the compression and shear stress can be produced. The frequency and pattern of the joint movement in the dynamic model presented here could be adjusted to be similar to a live animal, but the range of the joint movement and the magnitude of the compression force were

less than that in the live animal. However, despite this, there was still a clear effect of the dynamic motion on the cartilage.

4.4.3 Characteristics of the dynamic model

Two specific characteristics of the dynamic model could be observed:

Topographical heterogeneity. The topographical heterogeneity of the dynamic model could be observed clearly from the difference of GAG content between the 'under-moving-arc' and the 'off-moving-arc' area. It concurred with the findings of Nugent-Derfus *et al*., which used a rehabilitation machine, a continuous passive motion (CPM) device, to move a bovine knee joint (Nugent-Derfus, *et al.* 2007). Their study reported that there were different levels of proteoglycan 4 (PRG4) biosynthesis in the contact and non-contact areas of the articular surface. In the human, the cartilage of weight-bearing areas has been reported to have a significantly higher concentration of GAG when compared with non-weight-bearing areas (Rogers, *et al.* 2006). Therefore, the difference of the matrix GAG content in the 'under-moving-arc' and the 'off-moving-arc' area of the dynamic model additionally supports the concept of a topographical heterogeneity in an articular joint. However, it could also be inferred that the heterogeneity of the cartilage matrix could be easily diminished by giving only a few minutes of movement per day, which was demonstrated in the manually moved dynamic model.

Threshold of the duration of mechanical stimulation. This duration threshold could be observed by comparison of the matrix GAG content between the 'under-moving-arc' area of the machine-moved dynamic model and the manually moved dynamic model. In the machine-moved dynamic model, a total of 6 hours movement in one day was set but, in the manually moved dynamic mode, only 10 minutes joint movement by hand was performed. However, the GAG content of the extracellular matrix was well maintained at the initial high level during the culture period in both models. This indicated that the duration of the joint movement could be in a wide range, e.g. from 6 hours to 10 minutes per day, and yet the effect of the mechanical stimulation on the cartilage still remained.

The minimal duration of joint movement that maintains cartilage health is not well defined in the literature. However, different durations of an intermittent compression load (from 8 sec, 72 sec, 12 min to 1 hour per day, 0.5 Hz, in physiological strain) have been applied on the ulnar bone of an *in vivo* avian model for 42 days (Rubin & Lanyon 1984). Their results showed the mineral content of the ulnar bone increased in the groups of 72 sec, 12 min, and 1 hour. Instead of being proportional to the increase of the stimulation duration, the corresponding mineral amount reached to a similar high level in these 3 groups, which was approximately 140% increased from the control. Even though the model and the force were not comparable, the results of both the avian and the dynamic joint study suggest that the duration of the mechanical stimulation could have a 'threshold'. Any stimulation over this threshold resulted in the same outcome, i.e. the increase in the matrix was not proportional to the increase in duration of the mechanical stimulation.

This concept of a 'threshold' for the response to the mechanical stimulation has not been described in the *in vitro* cartilage studies. Although it has been reported that, in cartilage explants and tissue-engineered chondrocyte constructs, an increase of the frequency or the magnitude of the compression force within the physiological range resulted in an upregulation of the matrix gene expression or an increase in the matrix protein synthesis (Sah, *et al.* 1989; Guilak, *et al.* 1994), the duration of the mechanical stimulation had still not been tested. This might be because if the effect of the duration of mechanical stimulation is attempted to be studied, a longer experimental period is needed, and, in most of the *in vitro* studies, the duration was less than 24 hours that was not enough for the expression of this effect. Thus, as this *ex vivo* joint model was characterised for 4 weeks of culture, it might have a sufficient period to test the duration effect of mechanical stimulation.

SECTION D – MODEL APPLICATION

Including

Chapter 5: Heat-treated Model

Chapter 6: Injury Model

Chapter 7: Chondrocyte Implantation Model

Chapter 5: Heat-Treated Model

5.1 Chapter outline

The relationship between the chondrocyte and the extracellular matrix of the cartilage tissue is extremely close. This is not only because the matrix is formed from components secreted by the chondrocytes, but also because the signals that stimulate the chondrocyte to secrete are transmitted via the matrix. It is known that chondrocyte death occurs through necrosis or apoptosis in impact-damaged articular cartilage explants (Chen, *et al.* 2001; Borrelli, *et al.* 2003) or 'chondroptosis' in the *in vivo* studies (Roach, *et al.* 2004). Chondrocyte-derived apoptotic bodies may contain enzymatic activity that has been demonstrated to be involved in the calcium deposition of the extracellular matrix (Lotz, *et al.* 1999). However, the direct effect of chondrocyte death on the matrix components is not well established.

The heat-treated model was a preliminary experiment designed to start to evaluate the effect of chondrocyte death to extracellular matrix. All of the chondrocytes of this model were killed by heat and the change of matrix GAG and water content was evaluated for 4 weeks. The hypothesis was: "The GAG content of the extracellular matrix of cartilage was affected if the chondrocytes were dead." It was assumed that the cytoplasm of chondrocyte contained proteolytic substances, which were released if the chondrocytes were dead.

There were 6 different joints used in this study. They were harvested in the same way as in the static model. A hot water bath of 95°C was used as the heat source and the joints were immersed in it for 5 minutes. After this sacrificial procedure, the joints were cultured in the same culture media as those used in the previous models for 4 weeks. The cartilage samples were taken every week for the morphology, water content and the GAG content assessment.

5.2 Materials and Methods

The heat-treated model used the same material and methods to harvest and culture the bovine metatarsophalangeal joint as those in the static model, and the method for assessment of the morphology of cartilage, water content and the GAG content were the same as well. The specific equipment and procedures are described below.

A hot water bath. A sterile 1L glass beaker containing 500 ml phosphate-buffered saline (PBS) was heated to the temperature of 95°C by a heating plate. The harvested bovine joint was placed in the hot PBS solution for 5 minutes (**Figure 5.1**). Then the joint was removed out of the hot solution by a clamp and cooled down by rinsing with room temperature PBS. After this treatment, the joint was placed in a culture vessel and the same culture media were added. The culture environment was 37°C and 5% CO_2 in a standard incubator.

Cartilage biopsy. The cartilage samples were taken before and after the joint was heated to confirm the cell death and to assess the immediate effect on the GAG content of the cartilage. Regular biopsies, once per week, were done during the culture period to evaluate the change in matrix GAG content.

a.

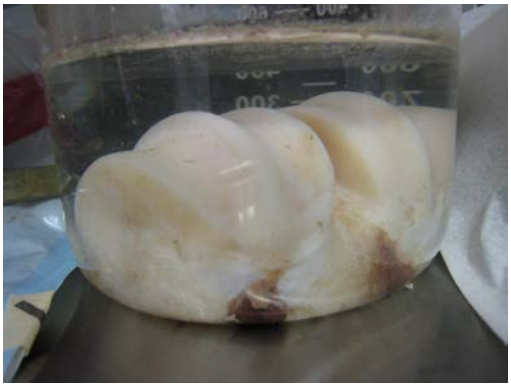

b.

Figure 5.1 Hot water bath

a. A 1L glass beaker containing 500 ml PBS was placed on a heating plate and the solution was heated to 95°C. The harvested joint was then immersed in the hot solution for 5 minutes to kill the chondrocytes. **b.** The surface lustre of the articular cartilage turned a cloudy white, and blood that had leaked from the bottom of the joint coagulated after heat treatment.

5.3 Results

After heat treatment, the assessment of the live/dead cells by CMFDA/PI stains showed that all the cells of the articular cartilage died, but the heterogeneity of the cell arrangement of the articular cartilage remained as that seen in the static model (**Figure 5.2**). The originally measured GAG content of the matrix showed that the matrix GAG content of the fresh joints started at the level of 1.20%, which was similar to the level from the earlier experiments, but the value immediately increased to 1.72 % after heat treatment (**Figure 5.3**). Then it dropped to 1.34 % at Day 7 and was maintained at this same level from Day 7 to Day 21. It then decreased to 1.18% at the end of the 4^{th} week.

The water content of the heat-treated cartilage samples was measured and compared with the water content of the static model (**Figure 5.4**). The water content of the heat-treated model was lower than that of the static model. In the heat-treated model, it decreased to 50.9% immediately after heat treatment and gradually increased after culture. It finally reached a level of 69.2% at Day 28, which was still lower than the level of the static model. In comparison between these two models throughout the culture period, the largest difference occurred at the start, but the gap gradually narrowed after culture.

It was found that the ratio of GAG content change (from 1.72% to 1.20%) in the samples of Day 0 before and after heat treatment was similar to the ratio of water content change (from 72.1% to 50.9%) of the Day 0 samples between the static model and the heat-treated model. Thus, the immediate increase of the GAG content was reasonably inferred to be due to the instant loss of the water content of the cartilage matrix as soon as the joint was heated. Thus, the ratio of the difference of water content between the heat-treated model and the static model was used to adjust for the cartilage wet weight of the heat-treated model at every time point.

The matrix GAG content of the heat-treated model was then re-calculated by normalising with the ‘adjusted wet weight’ instead of the ‘measured wet weight’. The adjusted wet weight was an estimated weight that the same percentage of lost

water was added back. The result of the adjusted GAG content are shown in the **Figure 5.5**.

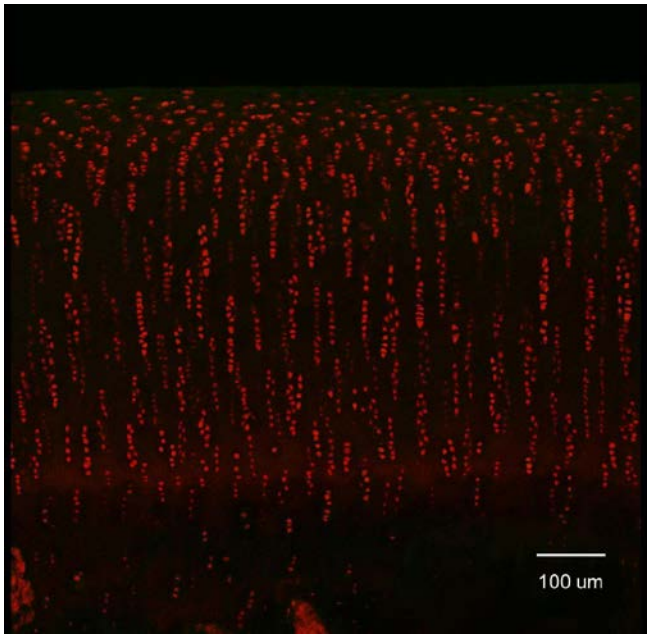

Figure 5.2 Cartilage morphology after heat treatment

After the joint was treated by hot water, all the chondrocytes and the osteoblasts were confirmed dead because there were only PI-stained red cells but no CMFDA-stained green cells in the image.

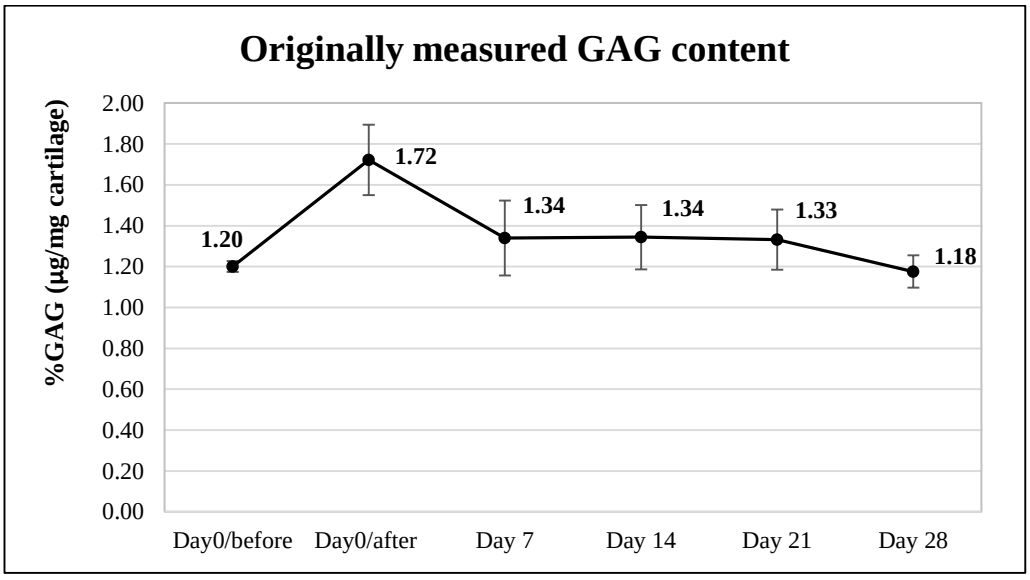

Figure 5.3 Originally measured GAG content in 5 heat-treated joints

The measured matrix GAG content increased immediately after heat treatment at Day 0 and then decreased and maintained a quite consistent level afterward. 'Day0/before' and 'Day0/after' in the figure mean 'before heat treatment' and 'after heat treatment' at Day 0, respectively.

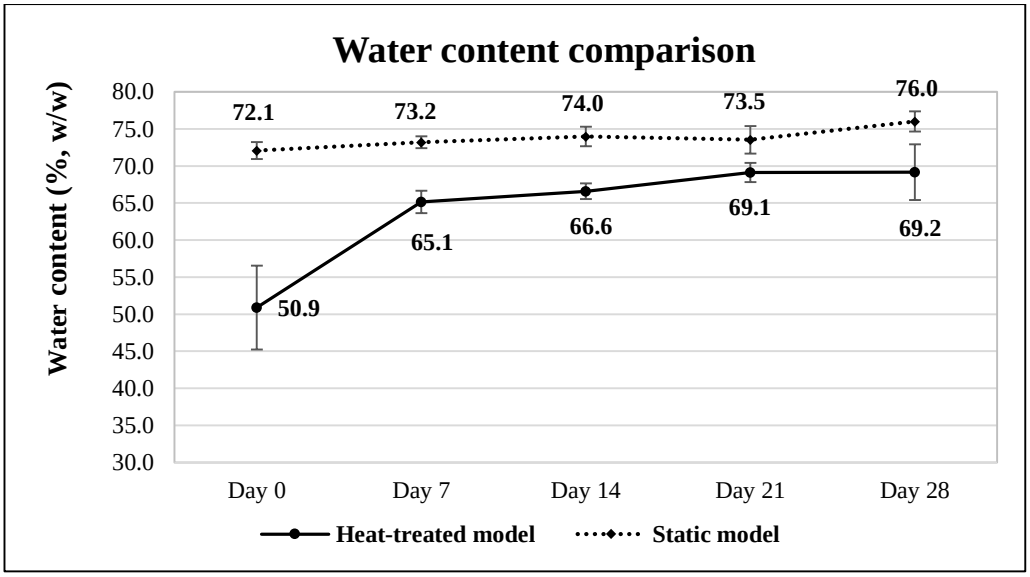

Figure 5.4 Water content comparison between the heat-treated and static model

The water content of the heat-treated model was lower than that of the static model at every time point. However, the difference between these two models decreased gradually after culture.

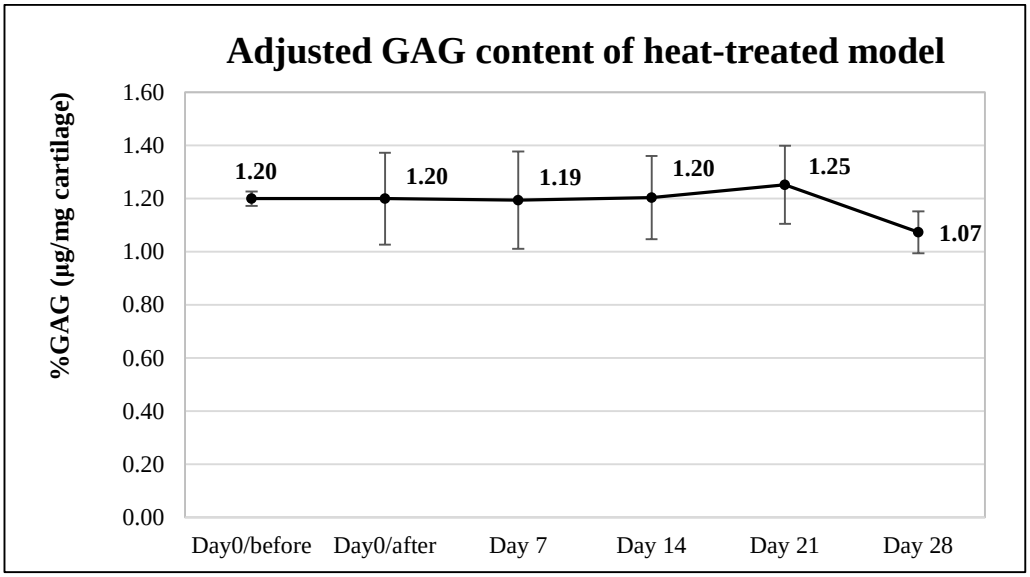

Figure 5.5 Adjusted GAG content of the heat-treated model

After adjusting for the water loss following heat treatment, the matrix GAG content of the heat-treated model was observed not to change greatly from the beginning to Day 21. A small non-significant drop occurred at Day 28.

5.4 Discussion

The purpose of this model was to evaluate if there were effects of the dead chondrocytes on the matrix GAG contents. However, from the originally measured data (**Figure 5.3**), the matrix GAG increased immediately after heat treatment and maintained this higher level during the first three weeks. From the result of the adjusted GAG content of the heat-treated model, no matrix GAG loss from the cartilage was found (**Figure 5.5**).

The reason of obtaining this result was considered to be related to the method used to kill the chondrocytes was heat.

It was observed that the lustre of the cartilage changed immediately after heating, and the texture of the treated cartilage became harder than fresh cartilage, which made the cartilage biopsy more difficult (**Figure 5.1b**). The water content of the heated cartilage also decreased immediately after heating (**Figure 5.4**). The method in the thesis to calculate the matrix GAG content was the GAG weight (μg) normalised with the cartilage wet weight (mg). Therefore, the most reasonable explanation of the immediate increase of the matrix GAG content of the heat-treated model was due to the instant loss of the matrix water as soon as the joint was heated. The similarity of the ratio of the GAG content change to the water content change in the samples before and after heat treatment could support this inference. Therefore, it would be more appropriate to use the adjusted cartilage wet weight, instead of the directly measured cartilage wet weight, for calculation of the matrix GAG content in the heat-treated model when comparing the results of this experiment with the previous models.

Using heat to kill the chondrocytes may not have been the most appropriate method for evaluation of the hypothesis as the extracellular matrix is mostly composed of proteins. It is known that the secondary and tertiary structure of a protein is maintained by hydrogen bonds. When heated, these weak bonds disrupt that results in permanent denaturation of the protein configuration and destruction of the protein's biological functions. Therefore, after the joint was immersed in the hot solution for a period of time, no biologically active substances could be expected left

in the cartilage, which meant the dead chondrocytes in this model were not able to influence the extracellular matrix. Therefore, the method in this preliminary experiment was not appropriate to study the research hypothesis.

Another method, such as using the cytotoxic toxins or liquid nitrogen, might be more suitable to address the kill of chondrocytes without too much disturbing the properties of the intracellular substances.

However, the results still revealed an important observation: i.e. there was no change in the matrix GAG content of the heat-treated cartilage for 3 weeks. Compared to the static model or the injury model (the next chapter), it was found that the matrix GAG content was easily decreased in the beginning of culture (a few hours to days), in particular when the integrity of the cartilage was damaged. However, in the heat-treated model, the matrix GAG seemed to be 'locked' in the cartilage tissue for at least 3 weeks, and the ratio of the matrix water to total tissue mass was not recovered until 4 weeks of immersion of the joint in the culture media. These indicated that there was no GAG loss from the denatured cartilage matrix and the matrix expansion was also restricted.

It is known that the main components of the extracellular matrix of cartilage are the collagen fibril and proteoglycan (Huber, *et al.* 2000). The negatively charged proteoglycan molecules attract water that makes the tissue swell but the collagen network restricts its expansion (Lindahl & Hook 1978). However, once the collagen was heated to a temperature over 70°C, contracture of the collagen fibrils occurred (Hayashi, *et al.* 1997; Lin, *et al.* 2005). This suggests that the collagen network of the cartilage shrank. This in turn could restrict the leakage of the matrix proteoglycan to the culture media. Moreover, the matrix proteoglycan molecules would also be denatured by the heat and this would change their structure (Jamieson, *et al.* 1987). This deformation might further restrict their passage through the collagen network. Therefore, no matrix GAG could be released outside the cartilage once the joint was treated by heat. The observation of the proteoglycan restriction in the heat-treated model could provide another evidence for explanation of the matrix GAG turnover, and this will be described in detail in Chapter 8.

Additionally, in **Figure 5.2**, in order to confirm the death of chondrocytes after heat treatment, the cartilage explants were stained by CMFDA/PI dyes, which were the same stains as those in the previous experiments. Results showed that all the chondrocytes and the osteoblasts were stained red by PI because all of them were killed by heat. However, the lack of control of the stains was another defect of the method design in this model because no green (live) cells in the image could internally confirm the effect of CMFDA. Thus, an external control should be given to confirm both the effect of CMFDA and PI dyes if this experiment is repeated in the future.

Chapter 6: Injury Model

6.1 Chapter outline

An injury to articular cartilage has particularly profound consequences as the ability for repair is very limited. Clinically, the articular cartilage can be damaged by accidents or sport injuries. Some inflammatory or infectious diseases, e.g. rheumatoid arthritis or pyoarthritis can also destroy the articular cartilage. Iatrogenic cartilage injury may occur during surgery. Nevertheless, trauma is the most common cause of osteochondral lesions (Falah, *et al.* 2010). Experimental methods to create chondral trauma included applying compression force to introduce blunt trauma (Jeffrey, *et al.* 1995; Loening, *et al.* 2000; Seol, *et al.* 2012) or using a scalpel cut to create sharp trauma on the cartilage (Redman, *et al.* 2004; Amin, *et al.* 2008).

This experiment was designed to evaluate the response of the chondrocytes in the *ex vivo* joint to sharp trauma. Thus, scalpel cuts were used to create the injury. Two different types of culture media were used; one with foetal bovine serum and one without foetal bovine serum. This allowed the effect of serum on the viability of the damaged chondrocytes and on the change in matrix to be evaluated. For the chondrocyte viability, it was hypothesised that, with a sharp scalpel cut, the viability of the chondrocyte was affected in a limited range of the joint surface and, after a period of culture, the amount of the dead cells along the cut line increased. For the extracellular matrix, it was hypothesised that the matrix GAG content would decrease at the beginning in a similar pattern as that in the static model. In addition, it was postulated that the GAG level would be restored by increase production from the chondrocytes, if the culture media was supplemented with serum.

6.2 Materials and methods

Ten fresh bovine feet were studied in the injury model. The same methods as those in the static model were used to harvest the bovine metatarsophalangeal joints. After the joint was isolated from the bovine foot, the metatarsus was separated and the cartilage was wounded with a new scalpel (No.22). Six longitudinal cuts were made on articular facets-1, 3, 4, 5, 6 and 8 (**Figure 6.1**). When performing the cut, the scalpel blade was kept perpendicular to the articular surface and slid smoothly along the cartilage. No extra compression but only the weights of the scalpel and the handle was applied on the cartilage for creation of a sharply injured full-thickness cut. During this procedure, the cartilage surface was always kept wet by frequent rinsing with PBS.

The culture media was a high glucose (4.5 g/L) Dulbecco's Modified Eagle Medium (DMEM) mixed with penicillin (100 U/mL) and streptomycin (100 μg/mL). Five joints were cultured with the media to which foetal bovine serum (10%, v/v) had been added, while the other 5 joints were cultured without serum added. The culture media stayed static without flow and was changed twice a week. Each joint culture lasted for 4 weeks for assessment of the chondrocyte viability and the matrix GAG content. Every week, six cartilage biopsies were harvested from the joint. Four of them were taken from the injured facets, where a segment of the cut line was included in the middle of the sample, and the other two were taken from the non-injured facets for comparison.

After biopsy, two injury site samples were further cut into halves with another new scalpel and immediately stained with the CMFDA/PI dyes in order to obtain the coronal and axial views of the chondrocyte viability with confocal scanning microscopy as described before (Chapter 2.2.5). The rest of the samples were snap-frozen and stored in the -80°C freezer for assessment of the matrix GAG content by using the spectrophotometric DMMB assay (Farndale, *et al.* 1986). For assessment of the GAG content in the injury site, a skin biopsy punch (Ø 2.5mm) was used to take cartilage pieces along the cutting line (**Figure 6.2**).

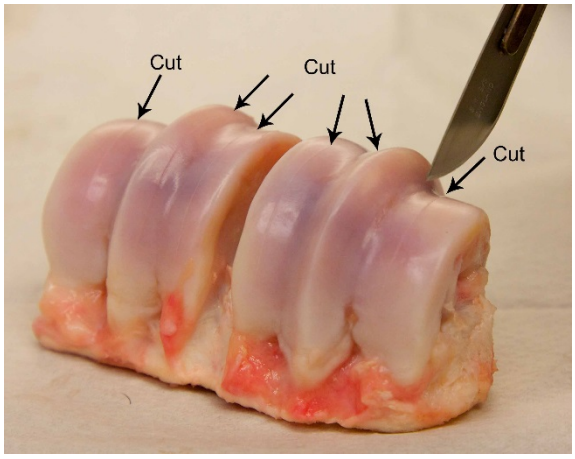

Figure 6.1 Scalpel cutting on the joint model

A new scalpel was used to wound the cartilage. The cuts in the articular facets were made in a sagittal plane. Six cut were made. Samples of the injury site were taken from these facets, which included a segment of the cut line. The other 2 facets, where no cuts had been performed, provided the control samples for non-injured cartilage.

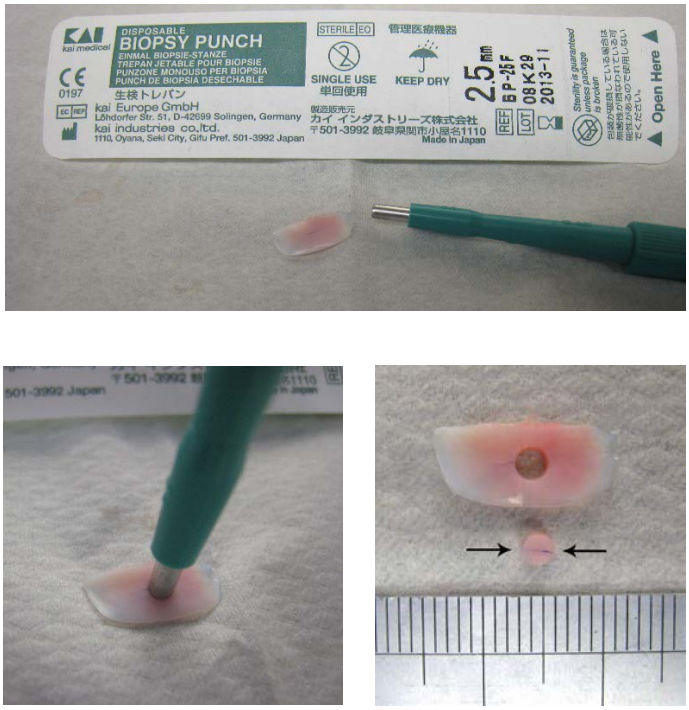

Figure 6.2 Injury site cartilage sampling

A skin biopsy punch of 2.5 mm in diameter was used to take the middle portion of the biopsied cartilage explant. The punch region included a segment of the cut line. This cut line is stained blue (between arrows) in the picture for demonstration.

6.3 Results

6.3.1 Viability change of chondrocyte

The region of interest (ROI) of the axial view of the injury site cartilage explant was focussed at the cross point of two cuts, which were the original injured cut performed at Day 0 and a new cut performed on the biopsy day. The axial view of the cartilage explant revealed the chondrocyte viability in the surface layer of the cartilage sample, in particular the viability along the injured cut line (**Figure 6.3** and **Figure 6.4**). Through the new cut plane, the coronal view could be demonstrated, which revealed the cell viability distribution from superficial to deep zone of the injury cut (**Figure 6.5** and **Figure 6.6**).

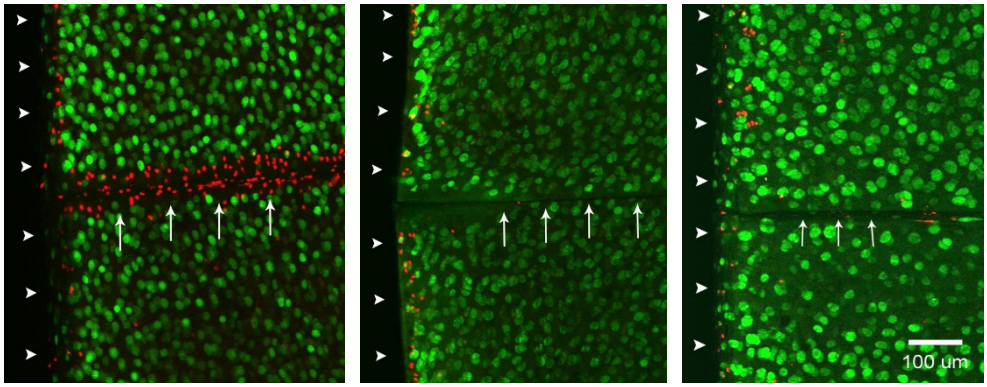

a. Day 0 **b. Day 7** **c. Day 28**

Figure 6.3 Axial view of the chondrocyte viability change of the injury model cultured with serum-supplied media

The horizontal cut line (arrows) is the original injured cut line performed at Day 0. The vertical margin of the cartilage explant (arrow heads) is created by a new cut on the biopsy day. In the injury model cultured with the media added with foetal bovine serum, the PI-stained red cells at Day 0 can be found on both the vertical cut margin and the horizontal cut line, while, at Day 7 and Day 28, there are few PI-stained cells on the horizontal cut line but red cells on the vertical cut line can still be observed.

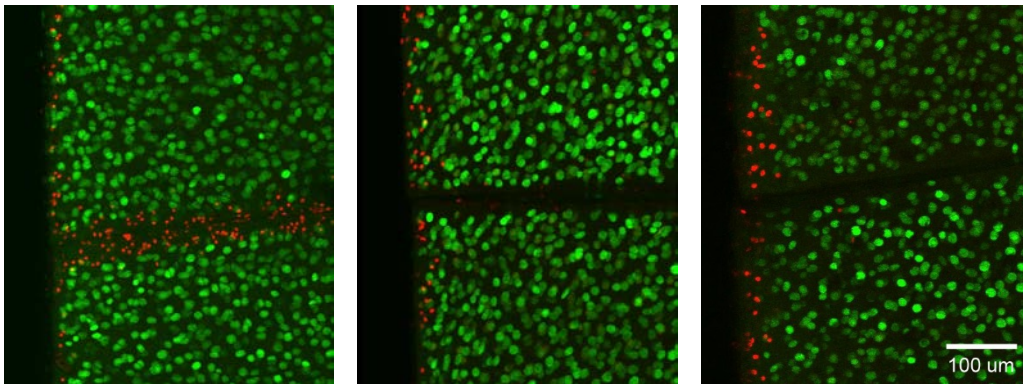

a. Day 0 **b. Day 7** **c. Day 28**

Figure 6.4 Axial view of the chondrocyte viability change of the injury model cultured without serum-supplied media

In the injury model cultured in the media without the foetal bovine serum supplied, the viability images looks similar to the above pictures. The PI stained red cells at Day 0 are visible on both the vertical cut margin and the horizontal cut line, while, at Day 7 and Day 28, a large amount of red cells can be found on the vertical cut margin but only a few on the horizontal cut line.

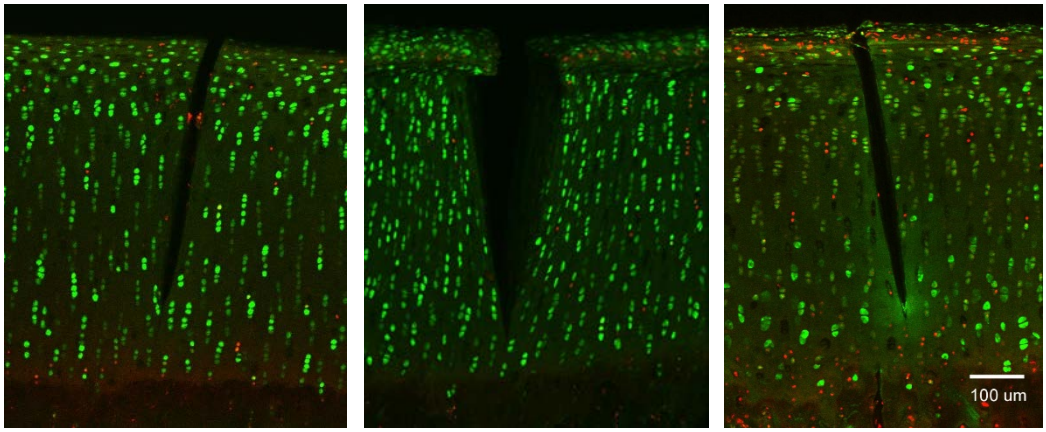

a. Day 0 **b. Day 7** **c. Day 28**

Figure 6.5 Coronal view of the chondrocyte viability change of the injury model cultured with serum-supplied media

The coronal viability image reveals that the depth of the original injured cut reaches to the deep zone of the cartilage but does not penetrate into the subchondral area. The cartilage matrix is split by the cut, but the chondrocytes on the margin of the cut seem not to be affected as there are still viable chondrocytes located just adjacent to the split.

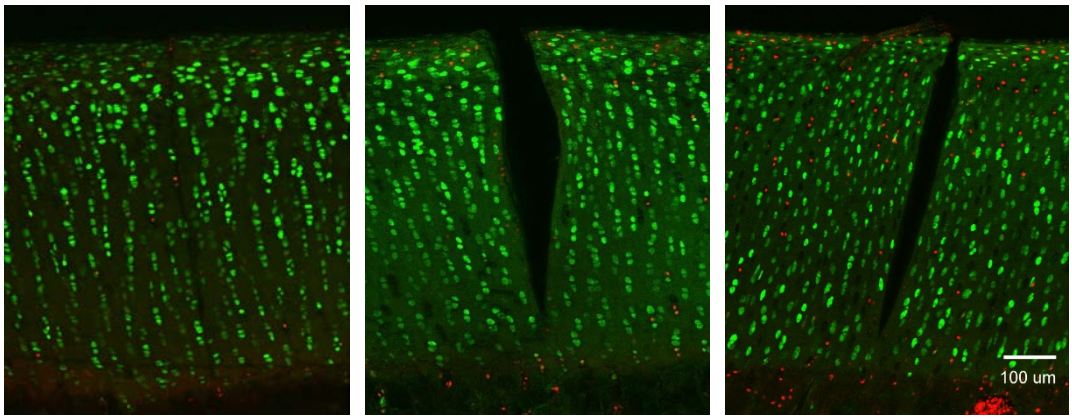

a. Day 0 **b. Day 7** **c. Day 28**

Figure 6.6 Coronal view of the chondrocyte viability change of the injury model cultured without serum-supplied media

In the injury model cultured without foetal bovine serum supply, the coronal viability images were still similar to the images of the serum-supplied model, and there were still live chondrocytes located very close to the split.

6.3.2 Matrix GAG content

In the site along the injury cut (injury site), the Day 0 matrix GAG started at 1.07% and 1.08% in the model cultured with serum-supplied media and without serum-supplied media, respectively (**Figure 6.7**). After culture, the injury site GAG content of serum-supplied model gradually increased to 1.17% at Day 28, while the model without serum supply decreased day by day and finally declined to 0.70% at Day 28.

In the non-injury site, the matrix GAG content of both models started at the same level (1.20%) (**Figure 6.8**). After culture, the values of these two models decreased to a similar level at Day 7, i.e. 1.00% and 1.01% in the serum-supplied model and non-serum-supplied model, respectively. Subsequently, in the serum-supplied model, the non-injury site matrix GAG returned to 1.15% at Day 21 and maintained a similar level to the end. However, in the non-serum-supplied model, the non-injury site GAG content continued decreasing to 0.83% at Day 21 and maintained this level to Day 28.

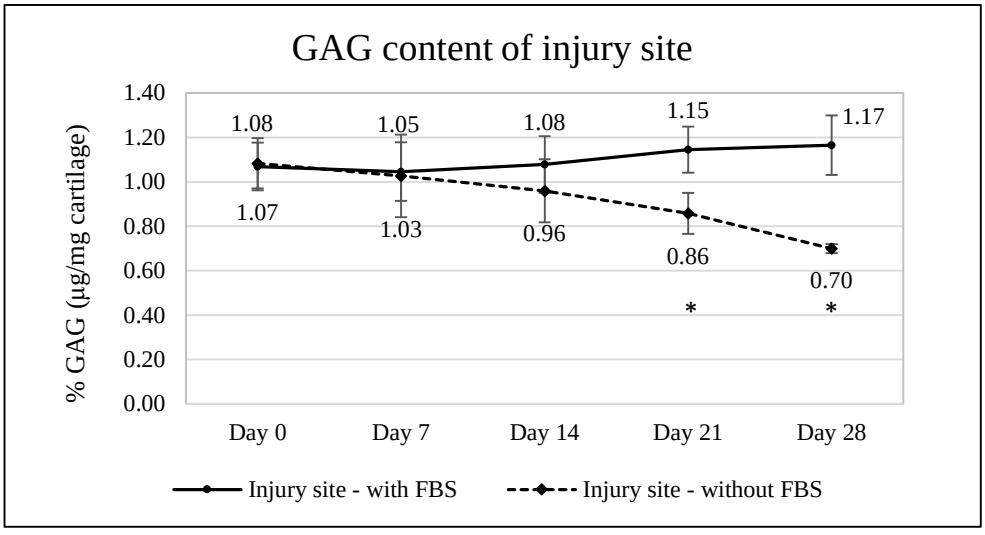

Figure 6.7 Matrix GAG content change of the injury site in the injury model
The injury site GAG content in the serum-supplied model increased week by week, while that of the non-serum-supplied model decreased at each time point. There was a significant difference between the two curves ($p<0.001$; two-way ANOVA).

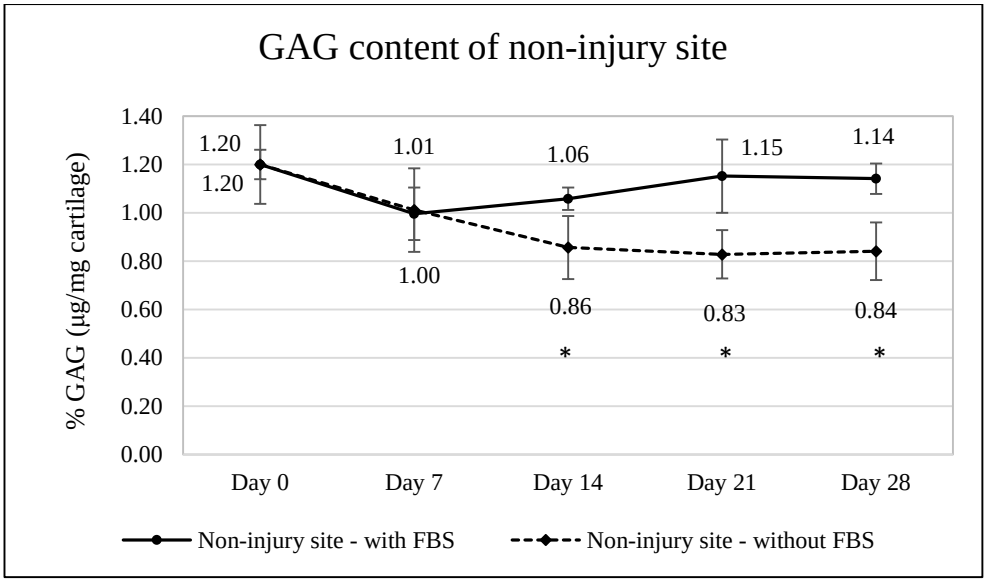

Figure 6.8 Matrix GAG content change of the non-injury site cartilage in the injury model

In the non-injury site, the values of the matrix GAG content in both models were similar at Day 0 and Day 7, but subsequently separated. From Day 14 to Day 21, the values increased in the serum-supplied model but decreased in the non-serum-supplied one. From Day 21 to Day 28, the matrix GAG content of both models did not change further. There was a significant difference between these two models (p<0.001; two-way ANOVA).

6.3.3 Fibroblast-like cells on the joint surface

Occasionally, the fibroblast-like cells were found again on one of the 10 joints of the injury model (**Figure 6.9**). This affected joint was in the serum-supplied group, and the time to find these cells was at Day 28. Confocal images revealed that their cell shape was polygonal or spindle, which was similar to the previous findings in the static model (**Figure 2.29**).

These cells coated on the joint surface that blocked the dyes penetration into the cartilage in the axial view examination and some were found to cross the gap of the injury cut (**Figure 6.9b & 6.9c**).

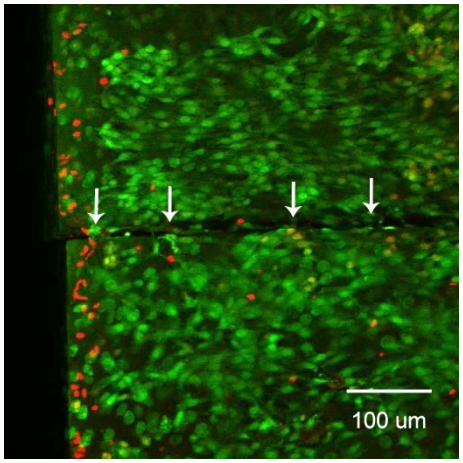

a. Axial view, Day 28

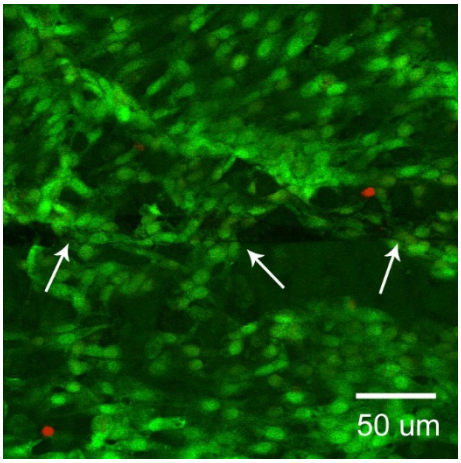

b. Axial view, Day 28

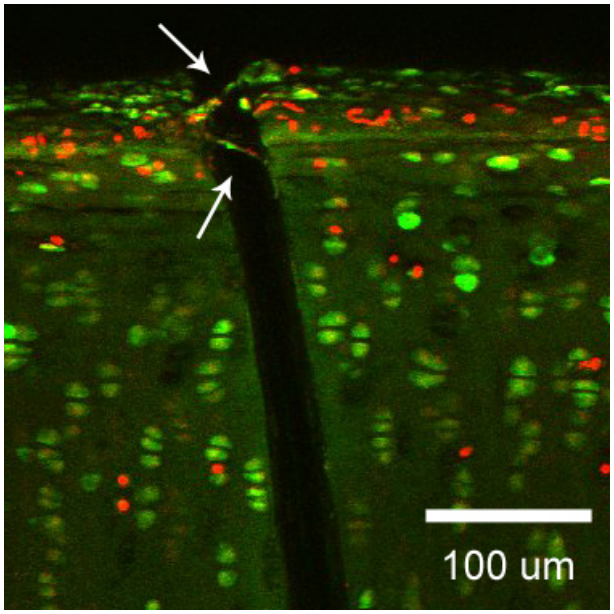

c. Coronal view, Day 28

Figure 6.9 Fibroblast-like cells on the joint surface of injury model

The polygonal or spindle-shaped cells (arrows) were incidentally found on both the axial view and coronal view of one of the injury model cultured in the serum-supplied media. The cells coated over the joint surface, and even crossed the 'cut' gap, which was approximately 10-20 μm in width.

6.4 Discussion

The results supported the hypothesis concerning the effect of serum on the chondrocytes for matrix GAG production because the matrix GAG content increased if the culture media was supplied with foetal bovine serum. However, the results did not fully support the hypothesis concerning the chondrocyte viability to sharp injury, because, even though the sharply injured cells could be detected at Day 0, they were not found after Day 7 either in the serum-supplied or non-serum-supplied model.

6.4.1 Chondrocyte viability

From the results of the confocal microscopy images, the sharp scalpel cut killed the chondrocytes at the superficial layer, where a red band of the PI-labelled cells along the cut line could be seen in the axial view of the scan (**Figure 6.3** & **Figure 6.4**). However, this sharp injury did not seem to affect the viability of the chondrocytes in the deeper layers, because many viable chondrocytes could be found closely adjacent to the cut edge in the coronal view of the scan (**Figure 6.5** & **Figure 6.6**). For coronal view viability, a published article demonstrated similar results, where the cartilage explant was wounded by a scalpel and many viable chondrocytes were found near the wounded margin on the coronal section (Redman, *et al.* 2004). Nevertheless, they did not investigate the viability in the axial view because the axial image of the cartilage surface was difficult to obtain with conventional fluorescent microscopy. By using the confocal scanning microscope, the axial view viability could be easily scanned, which was one of the advantages of the confocal scanning microscopy system that has been thoroughly discussed in Chapter 2.2.5.

Possible explanations for the different viability on the axial and coronal views include: heterogeneous sensitivity of the chondrocytes in the different zones to mechanical pressure produced by scalpel cuts and secondly the variable orientation of the collagen fibres inside the cartilage. It is known that articular cartilage is not a homogenous tissue and the size and function of the chondrocytes and the amount of extracellular matrix differs from layer to layer (Brower & Hsu 1969; Darling, *et al.* 2004). Therefore, it was considered that the mechanical sensitivity of the

chondrocytes in different layers might not be the same. From the viability result, the chondrocytes of the superficial layer appeared to be more sensitive to the mechanical stress than those in the deeper layers.

In addition, it is known that the collagen fibres run parallel to the surface in the superficial layer and become radially oriented in the deep layer. The density of the collagen has been reported to be higher in the superficial layer than that in the deep layer (Jeffery, *et al.* 1991; Gelse, *et al.* 2003). Thus, more pressure could be produced by the scalpel cut on the superficial layer compared to the deep layer. This higher pressure could damage the superficially located chondrocytes along the injury cut. Furthermore, because of the densely parallel-orientated collagen fibres in the superficial layer, this pressure would be expected to spread a small distance from the cut, which resulted in the observed dead cell band along the injury cut line in the axial view scan (**Figure 6.3a & 6.4a**).

After culture for one week, an unexpected result was observed i.e. that almost all red PI-stained cells vanished on the injury cut line. The same result was both obtained for the joints cultured in the media supplied with serum and for the joints cultured without serum, which demonstrated that the components of the foetal bovine serum were not responsible for the disappearance of the PI-stained cells.

One of the alternative explanations was that the injury cut damaged the integrity of the cell membrane, following which the chondrocytes would swell and then rupture their cell membranes. It was postulated that the cell nuclei of the injured chondrocytes were lost into the media after a period of culture. Thus, at Day 7 or later, the PI stain could not find its binding target – the DNA bases of the nucleus – and therefore no PI-stained red cells could be detected along the injury cut. Another possible reason might be that some of the damaged chondrocytes had ability to recover after a period of time. The initially damaged cell membrane might be repaired and the entrance of the PI stain would then be prevented after one week of culture. However, more experiments, e.g. clarification of the morphological and biological changes of the injured chondrocytes, would be needed to verify these hypotheses.

Furthermore, this viability result indicated a possible observation bias if the dead cells were not immediately stained and detected. If there was a delay between injury and measurement, the amount of the dead cells might be under-estimated. The results of this section also demonstrated the very limited damage to the adjacent chondrocytes in the deep layer of the cartilage if a sharp instrument was used to create the lesion edge, which could be important in facilitating the integration of an implanted tissue-engineered construct for the cartilage repair (Tew, *et al.* 2000; Redman, *et al.* 2005).

6.4.2 Matrix GAG content

The matrix GAG content in the injury model at Day 0 at the injury site was 1.07% and 1.08% in the serum-added and non-serum-added groups, respectively. These results were slightly lower than that of the non-injury site (1.20% in both groups). There was a significant difference (p=0.035; unpaired t-test; for comparison of the pooled Day 0 data) between the injury site and non-injury site. This result provided further evidence to support the phenomenon that damaged or degenerated articular cartilage would lose its matrix proteoglycan (Martin & Buckwalter 2001); however, the rate that the matrix content would be lost is seldom discussed.

During the creation of the injury, the cartilage was kept wet by rinsing frequently with PBS. Therefore, if the cartilage was wounded with a scalpel, the GAG could be lost from the damaged matrix network by the frequent PBS rinses. In a previous article, a related result has been illustrated, in which bovine cartilage explants were injured by mechanical compression (20 MPa) and the release of matrix GAG to the culture media was measured by the same DMMB assay (DiMicco, *et al.* 2004). They found that the highest rate of the GAG release from the injured cartilage was within the first 4 hours after injury. The GAG content in the media remained higher than the uninjured controls during the first 24 hours, and became similar to the controls from 24 to 72 hours. They also found that this matrix GAG release could not be inhibited by the inhibitors of degradative enzymes, and most (>99%) of the released GAG was not newly synthesised but previously produced and stored in the cartilage matrix.

Combining their results with the outcomes of the current injury model, it could be inferred that once the cartilage was damaged, the pre-existing matrix GAG would be lost very quickly after the injury.

After a few weeks of culture, if foetal bovine serum was added into the culture media, the matrix GAG content of the injury site increased week by week and nearly reached as high as the initial level at the end of the 4th week. In contrast, if no serum was added in the culture media, the matrix GAG content of the injury site decreased gradually and finally dropped to the value of 0.70%, which was the lowest value observed in any of the models in this thesis (**Figure 6.7**). This result indicated that the foetal bovine serum might have an anabolic influence on the chondrocytes in the injury model. It is known that animal serum is a complex mixture, which includes a large number of serum proteins, hormones, growth factors, lipids, carbohydrates, vitamins and trace elements (Brunner, *et al.* 2010). It provides the essential components for maintenance of the normal cell metabolism *in vitro*. Therefore, without these important factors of serum, the chondrocytes of the injury model could not normally respond to the injury cut. The matrix GAG loss of the injured cartilage could not be compensated by the chondrocyte, and, thus, continuous GAG loss of the extracellular matrix was observed. In contrast, if the serum was supplied in the culture media, the chondrocytes could respond to the injury cut and increase the synthesis of matrix proteoglycan to correct for GAG lost from the injured matrix.

In the uninjured area, the matrix GAG content of the serum-supplied group dropped from 1.20% to 1.00% during the first week, but started to rise during the second week to 1.15% at Day 21 (**Figure 6.8**). A similar level was maintained at Day 28 (1.14%). This result suggested that even distant chondrocytes could be stimulated by the signals released from the injury site and they could respond with a rise in matrix GAG synthesis. However, if serum was not added to the culture media, the chondrocytes from an uninjured area were not able to respond to the ‘cut’ stimulus and a decrease of the matrix GAG occurred (approximately 0.83% of baseline level at Day 21 and Day 28). However, the drop in GAG content at the injury site was still greater (0.70%).

6.4.3 Cartilage injury mechanism

The increase of the matrix GAG content in the injury model raised the question as to whether the sharp injury had a catabolic or an anabolic effect on the cartilage.

Redman *et al*. reported that chondrocyte proliferation and new matrix synthesis occurred at the wound margin within 10 days (Redman, *et al.* 2004). Their observation supported the findings of the matrix GAG increase at the injury site in this model. From a number of articles, several molecules on the cell membrane of the chondrocyte have been demonstrated to be involved in the transmission of the extracellular signals to the chondrocyte, such as the integrins, cell-surface ion channels, purinergic receptors, and the primary cilium (Ramage, *et al.* 2009; Garcia & Knight 2010; Mobasheri, *et al.* 2010; Leong, *et al.* 2011; Wann, *et al.* 2012). Therefore, once the cartilage was damaged with the cut injury, the stretch of the collagen fibres or the osmotic change of the matrix tissue stimulated the chondrocytes through these signalling molecules. Both anabolic and catabolic effects could occur depending on factors such as the intensity of the injury (Ramage, *et al.* 2009). Thus, it may be possible to induce an anabolic effect directly on the chondrocyte by the sharp injury especially as the cut pressure on the cartilage tissue was very low.

An extracellular mechanism could be involved in the anabolic effect on the chondrocytes located near or far from the cut; for instance through the release of fibroblast growth factor 2 (FGF-2) (Chong, *et al.* 2013). It has been reported that FGF-2 was stored in the pericellular matrix of cartilage attached to the heparan sulphate proteoglycan and was liberated upon mechanical stimulation (Vincent & Saklatvala 2006; Vincent, *et al.* 2007). *In vitro,* FGF-2 was able to inhibit induction of aggrecanase ADAMTS-5, and it was able to induce a number of genes with anticatabolic and repairing activities, e.g. tissue inhibitor of metalloproteinases 1 (TIMP-1) and activin A (Vincent, *et al.* 2002; Alexander, *et al.* 2007; Sawaji, *et al.*

2008). *In vivo*, FGF-2 has been demonstrated to have chondro-protective effects because osteoarthritis developed spontaneously and rapidly with the mice deficient in FGF-2 and, in contrast, it was delayed by injection of FGF-2 into destabilised murine joints (Chia, *et al.* 2009; Li, *et al.* 2012b).

Therefore, a possible explanation for the increase of the matrix GAG in the injury model, could be the release from the damaged matrix into the culture media of a growth factor stored in the matrix such as FGF-2. The chondrocytes at a distant site as well as those near the injury site could be influenced. However, more investigation is needed to determine if FGF-2 or another factor was the mediator in the injury model.

Chapter 7: Chondrocyte Implantation Model

7.1 Chapter outline

Cell-based tissue engineering cartilage repair provides the hope for regeneration of damaged cartilage (Hunziker 2002). However, at present the newly formed tissue lacks structural integration to the recipient cartilage and has inferior mechanical properties and as such is prone to failure (Hunziker 2009). The results from the injury model reported in the previous section indicated that a sharp cutting instrument was able to create a margin where most of the cells below the surface could be maintained alive. Therefore, in this chondrocyte implantation model, a sharp skin biopsy punch was used to create the recipient hole for cell implantation. Different passages of the isolated chondrocytes were aggregated to form cell pellets as a form of 3-D culture, which would preserve the chondrocytic phenotype (Caron, *et al*. 2012). They were implanted into the created hole for evaluation of the interaction between the cell pellet and the recipient cartilage.

The hypothesis of the chondrocyte implantation model was that using a sharp instrument to create a recipient hole on the joint for cell implantation could preserve the chondrocyte viability at the margin of the hole as well as that seen in the injury model. Thus, the better-preserved cell viability around the margin of the hole might enhance the cell integration or the increase of matrix proteoglycan production of the recipient cartilage. Two different passages of aggregated chondrocytes were tested for comparison.

7.2 Materials and methods

7.2.1 Chondrocyte isolation and pellet culture

Cartilage tissue was excised from the metatarsophalangeal joint of bovine feet and was placed in a 150 ml glass beaker, which contained 50 ml phosphate buffered saline (PBS). The excised cartilage tissue was washed 3 times with PBS to get rid of the blood and synovial fluid and then diced into small pieces under sterile conditions. 30 ml of digestion media, which contained DMEM, Penicillin (100 U/ml), Streptomycin (100 μg/ml), FBS (10%, v/v) and Collagenase type Ia (1mg/ml), was used for 16 hours (overnight) to digest the diced cartilage at 37°C.

The digested fluid was filtered through a sterile 70μm Nylon Mesh (Fishbrand®) to remove the undigested debris. The filtrate was collected in a 50 ml conical tube and was centrifuged at 1500 rpm for 6 min for sedimentation of the cells. The supernatant was discarded and the sediment cells were resuspended with DMEM. This procedure was repeated 3 times to wash the isolated chondrocytes. Then, the cell number was counted by using the Trypan blue stain and the haemocytometer. Cell suspensions containing approximately 5×10^5 cells were separated and placed into Falcon tubes (15 ml), which contained 2 ml of the mixture of DMEM, penicillin/streptomycin (1%) and FBS (10%) for cell culture. This tube was centrifuged again to form the cell pellet of the initial passage (P0 group) (**Figure 7.1**). The cap of the tube was loosened for gas exchange, and the tube was placed in a standard incubator with 37℃, 95% humidity and 5% CO_2. The culture media of the tube was changed every two days by gently replacing 80% of the culture media of the tube. After 5 days of culture, the cell pellets were consolidated sufficiently for direct handling.

The cell suspension of half of the tubes was not centrifuged to form a cell pellet but was cultured in the T75 tissue culture flask for cell expansion until their fifth passage (P5). The P5 chondrocytes were aggregated into cell pellets with the same method and cultured for 5 days in the tube for pellet consolidation.

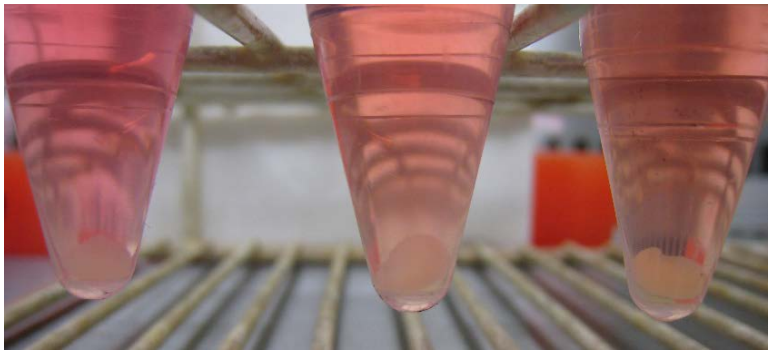
a.

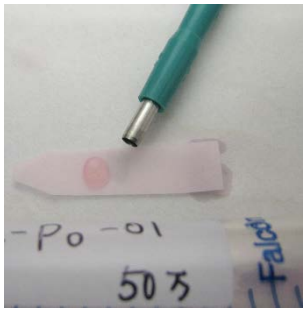

b.

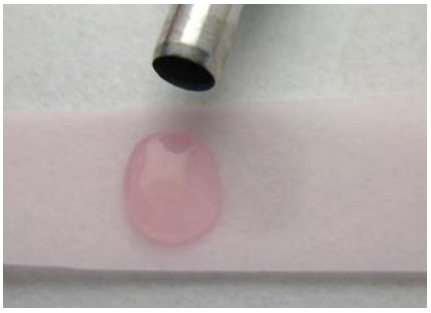
c.

Figure 7.1 Chondrocyte pellet culture

a. The chondrocyte suspension was centrifuged to form the cell pellet in the tip of the conical tube. They consolidated after a few days of culture. **b & c.** The cell pellet was removed from the tube and placed on a piece of filter paper so that most of the culture fluid was absorbed. This fragile cell mass was transferred easily on the filter paper. The diameter of the biopsy punch in the picture is 2.5 mm, which was equal to the diameter of the implantation hole of the joint.

7.2.2 Cell implantation model preparation

There were 10 bovine feet studied in the cell implantation model. Five of them were used in the P0 group and the other five feet were for P5 group. The same methods as those in the static model were used to harvest the bovine metatarsophalangeal joint. After the joint was isolated from the bovine foot, the metatarsal part was separated. On the flat articular facets of the joint (facet-1, 4, 5 and 8), fourteen circular holes in the arrangement of 3-4-4-3 on the facets were created for cell implantation (**Figure 7.2**). A sterile drill bit of 2.0 mm in diameter was used first to make a pilot hole on the cartilage. The drill depth was controlled to be just reach to the subchondral area in order to obtain full thickness holes. A new 2.5 mm biopsy punch was then used to enlarge the hole for creation of a sharply-cut margin. During these procedures, the cartilage was always kept wet by frequent rinsing with PBS.

Cell pellets of allogeneic chondrocytes including both the P0 pellets and the P5 pellets were implanted in the holes (**Figure 7.3**). Six cell pellets were implanted into six individual holes of one joint and the other eight holes were left empty as controls. Five joints were implanted with P0 pellets and the other 5 joints with P5 pellets. The implanted hole was not covered to allow free nutrient exchange between the cell pellet and the culture media. The joint was placed into the culture vessel and the culture media was filled with care to avoid the pellet being lost from the hole.

The culture media were the same high glucose (4.5 g/L) Dulbecco's Modified Eagle Medium (DMEM) well mixed with penicillin (100 U/mL), streptomycin (100 μg/mL) and foetal bovine serum (10%, v/v). The culture media was kept static without flow and was changed twice a week. Every joint was cultured for 2 weeks for assessment of the pellet morphology and the matrix GAG content around the implantation holes. Every week, seven cartilage samples were biopsied from the joint. Three of them were taken from the holes together with the implanted pellets, two of them were from the control empty holes and the other two were taken from the normal surface of the joint. For sample biopsy, a new scalpel was used to obtain the full thickness cartilage tissue, on the bottom of which a small amount of

subchondral bone was attached. The entire cell pellet was harvested inside the cartilage sample.

One of the samples containing the cell pellets was immediately stained with CMFDA/PI dyes for observation of the cell viability and morphology. The coronal and axial view images were taken with the confocal laser scanning microscopy (Amin, *et al.* 2008). The rest of the samples were snap-frozen and stored in the -80°C freezer for another assessment of the matrix GAG content by using the spectrophotometric DMMB assay (Farndale, *et al.* 1986). For assessment of the GAG content in the surrounding tissue adjacent to the hole, a larger skin biopsy punch (Ø 3.0 mm) was used to take the cartilage precisely from the margin of the hole (**Figure 7.4**).

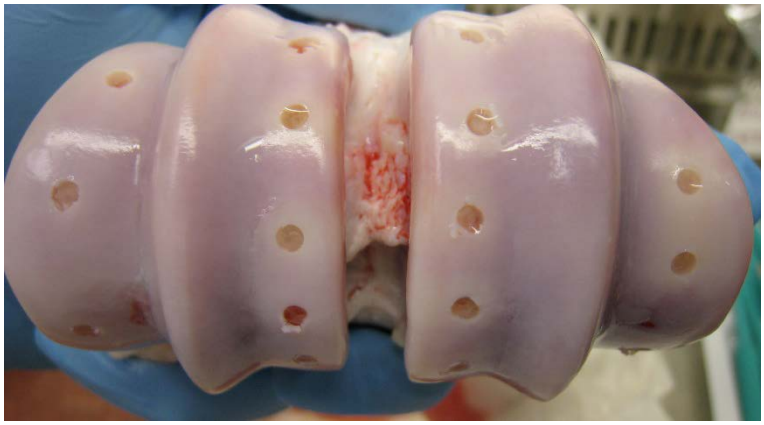

Figure 7.2 Creation of the implantation holes of the model

Several circular holes of 2.5 mm diameter were created on the relatively flat facets (facet 1, 4, 5 & 8) of the isolated metatarsus. These implantation holes were made by drilling a pilot hole with a 2.0 mm drill bit and then completed with a new 2.5 mm biopsy punch. The depth of these holes was just into the subchondral region without penetrating the bone marrow.

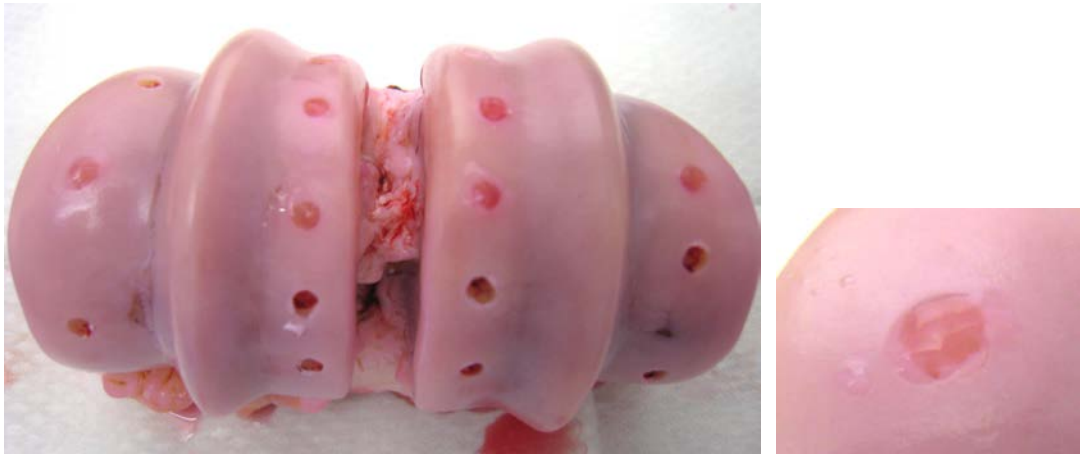

Figure 7.3 Implantation of the cell pellets into the joint

Six cell pellets were implanted into the holes that were located on the top of the joint. There was no coverage over the holes to allow free exchange of the nutrients and metabolites. The cell pellets stayed in the holes without fixing agents. The volume of the cell pellet just filled the hole.

7.3 Results

7.3.1 Chondrocyte viability around the implantation hole

From the axial view of the implantation hole, the death of the chondrocytes was limited. Most of the dead cells were located just adjacent to the margin of the hole, which formed a thin red band of less than 20 μm width from the cut edge (**Figure 7.4**). From the coronal view, which showed the status of the wall of the implantation hole, the chondrocyte viability could also be maintained well in some but not whole region. A number of dead cells were observed in the deep layers of a region (**Figure 7.5**).

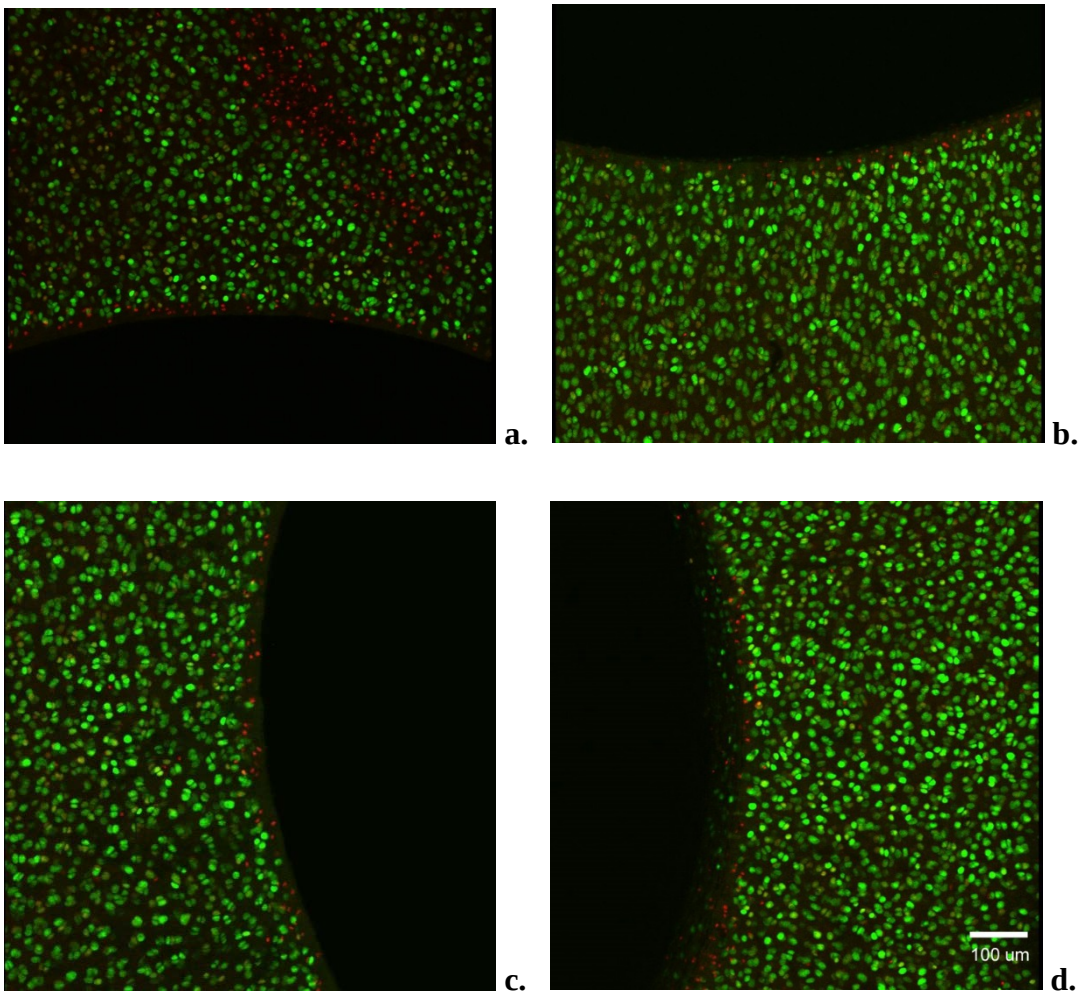

Figure 7.4 Chondrocyte viability around the implantation hole (axial view)
These pictures show the chondrocyte viability at four symmetrical of a single implantation hole. A narrow red band of dead cells around the cut edge was found. However, there were still viable cells just adjacent to the cut edge. An area of dead cells was seen in the first picture (**a**), which may have been due to an accidental injury when the hole was created. Except for this red band, almost all of the surface chondrocytes were alive.

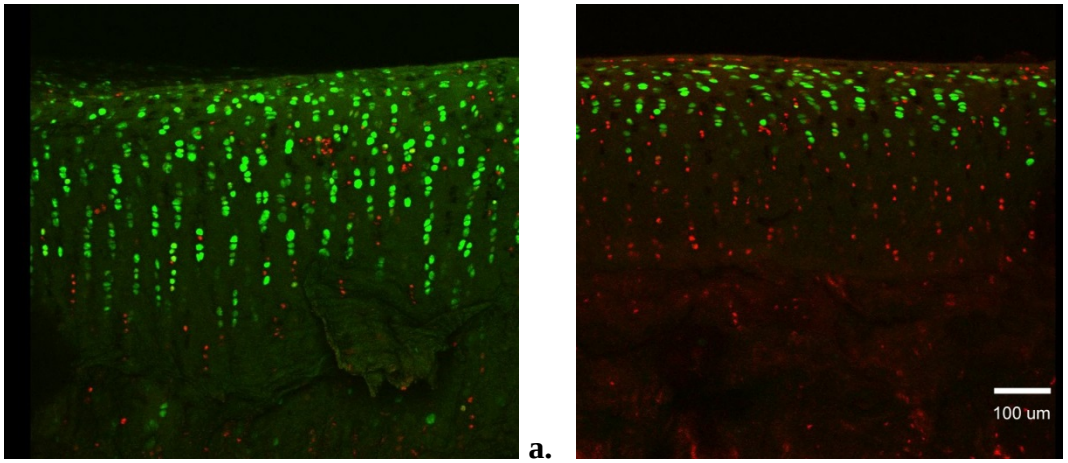

a. **b.**

Figure 7.5 Chondrocyte viability around the implantation hole (coronal view)
The chondrocyte viability of the coronal view was not as consistent as that of the axial view because some regions maintained higher viability than other areas. **a.** In the regions of good viability, most of the chondrocytes were viable from the superficial zone to the deep zone. **b.** In the worst viability regions, many dead cells were found in the middle and deep zones.

7.3.2 Morphology of the implanted chondrocyte pellet

After implantation of the cell pellet into the recipient hole and culturing for one week, some of the aggregated P0 chondrocytes at the margin of the pellet began to transform their cell shape from spherical into spindle or polygonal (**Figure 7.6a**). Migration of these cells from the pellet onto the adjacent cartilage surface could also be noted in the axial view images. After one more week of culture, more amount of the ectopic cells could be found on the surface of the recipient cartilage (**Figure 7.6b**).

Compared to the P0 pellet, chondrocyte cell shape in the P5 pellet was more elongated and polygonal, and the junction between the cell pellet and the recipient cartilage was not able to be clearly identified at Day 7 (**Figure 7.6c**). At Day 14, a number of the P5 cells covered the surface of the recipient cartilage that prevented the CMFDA/PI dyes penetrating into the native cartilage tissue (**Figure 7.6d**). In the coronal view image, only the cells in the superficial layer of the pellet appeared to spread onto the adjacent cartilage surface (**Figure 7.7**).

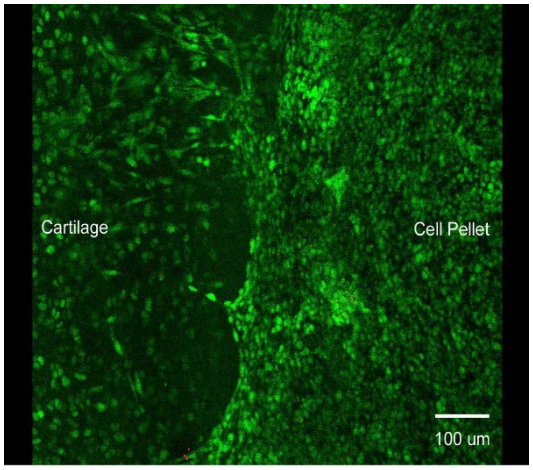

a. P0 cell pellet, Day 7

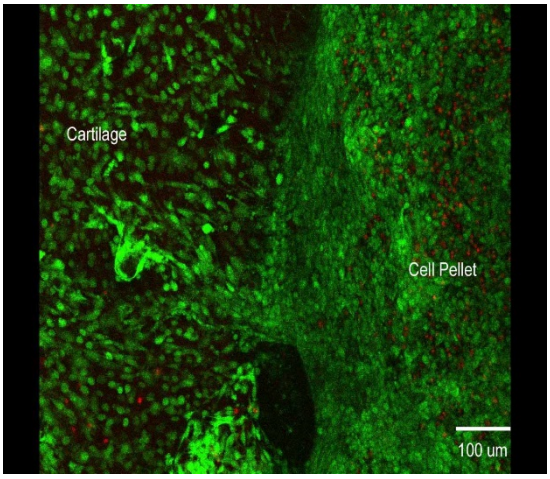

b. P0 cell pellet, Day 14

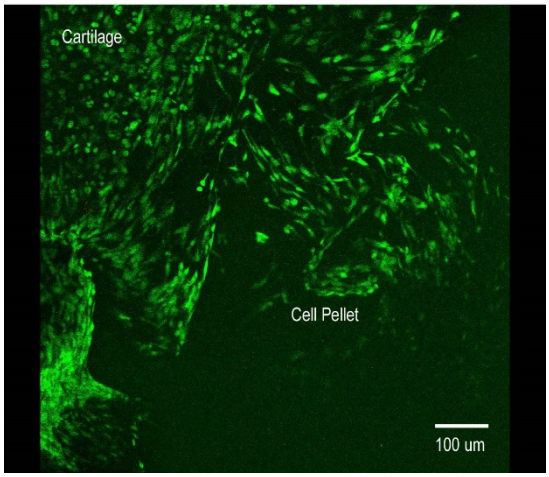

c. P5 cell pellet, Day 7

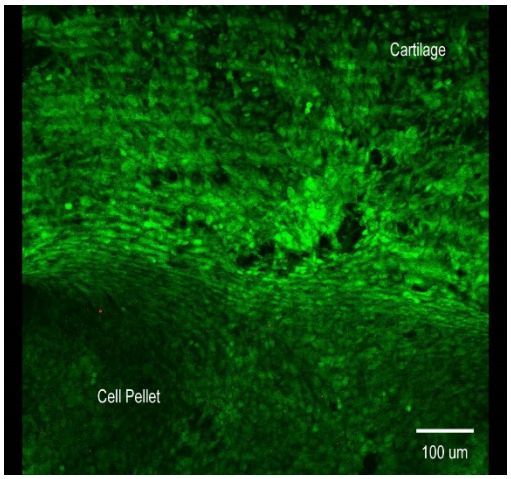

d. P5 cell pellet, Day 14

Figure 7.6 Morphology of the implanted chondrocyte pellet at the cartilage-pellet junction (axial view)

The shape of P0 cells inside the cell pellet was spherical but they became spindle or polygonal when they started to migrate onto the adjacent cartilage surface. The shape of P5 cells inside the cell pellet was more elongated. The junction of the P5 pellet and the joint cartilage could not be identified clearly. At Day 14, a number of P5 cells had migrated to the adjacent tissue and they covered most of the surface of the recipient cartilage around the hole.

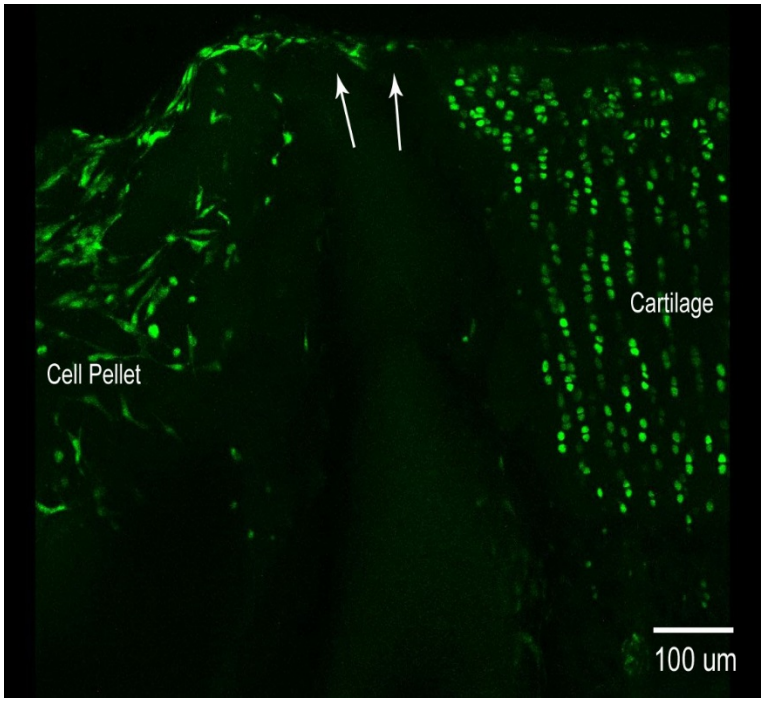

Figure 7.7 Morphology of the implanted chondrocyte pellet at the cartilage-pellet junction (coronal view)

The coronal view at the junction of the P5 cell pellet and the recipient cartilage after 14 days culture revealed that only the cells in the superficial layer (arrows) migrated. The cells in deeper layer of the pellet were not able to spread, which resulted in a big gap between the pellet and the margin of the hole.

7.3.3 Matrix GAG content around the implantation hole

The GAG content around the edge of a hole implanted with a cell pellet (cell hole) and a hole without a cell pellet (empty hole) was compared for evaluation of their interaction. In the P0 pellet group, the GAG content around the edge of the empty hole started at 1.06% at Day 0, and came down to 0.83% and 0.88% at Day 7 and Day 14, respectively. If the P0 pellet was implanted, the marginal GAG content of the cell hole was 0.93% at Day 7 and 0.82% at Day 14 (**Figure 7.8**). In the P5 pellet group, the GAG content of the empty hole started at 1.00% at Day 0, and decreased to 0.90% and 0.91% at Day 7 and Day 14, respectively. If the P5 pellet was implanted, the marginal GAG content of the cell hole was 0.94% at Day 7 and 0.97% at Day 14 (**Figure 7.9**). The GAG content of the normal site of both groups is also demonstrated in **Figure 7.10** for comparison.

P0 group

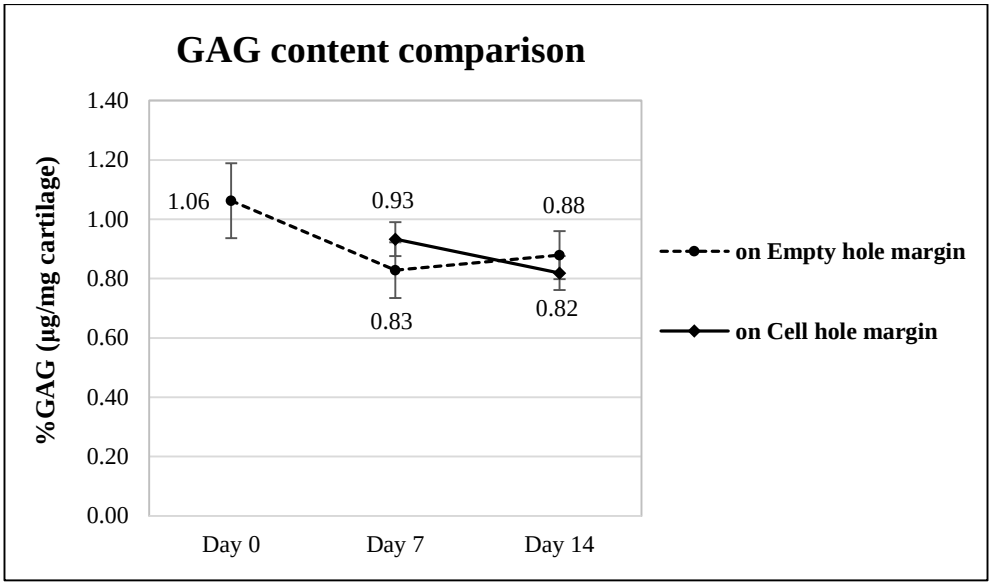

Figure 7.8 Matrix GAG content around the implantation hole of P0 pellet group

In P0 group, from Day 7 to Day 14, the values of the matrix GAG content between the empty hole and the cell hole overlap to a substantial extent, which result in no significant difference between each other (p=0.533; two-way ANOVA).

P5 group

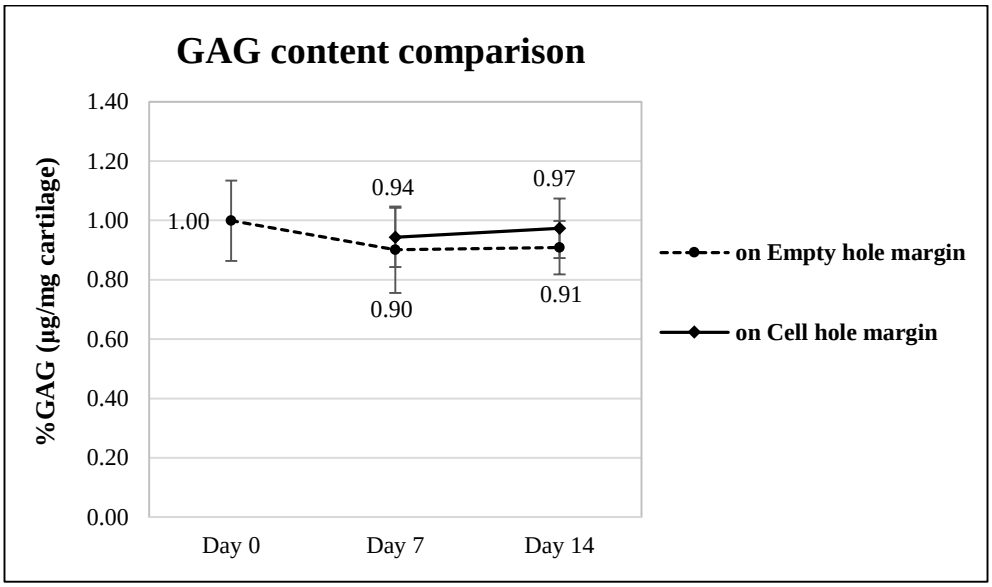

Figure 7.9 Matrix GAG content around the implantation hole of P5 pellet group

In the P5 group, the error bars for the matrix GAG content between the empty hole and the hole implanted with cells were also substantially overlapped and there was no statistical significant difference (p=0.743; two-way ANOVA).

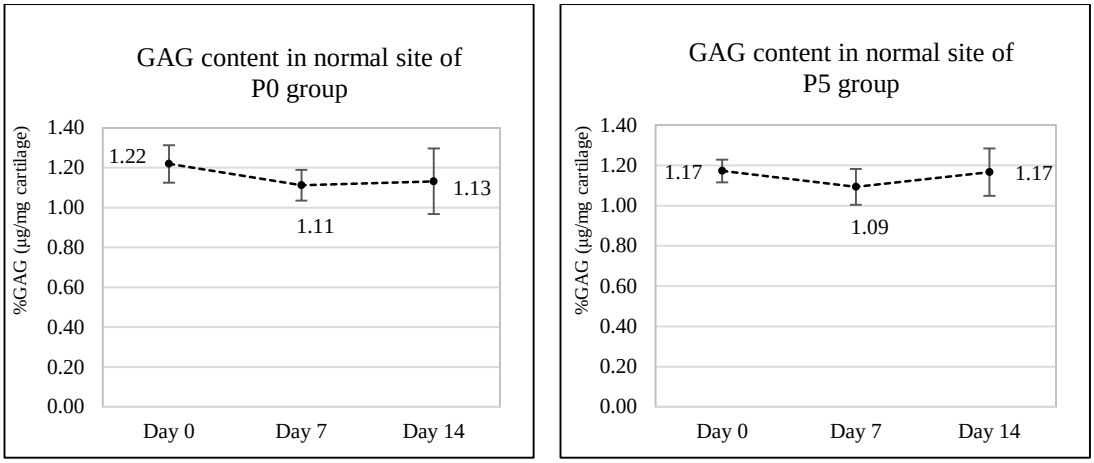

Figure 7.10 Matrix GAG content of normal site of both groups

The matrix GAG content of the normal site of the joint revealed a similar trend in both groups. They decreased a little at Day 7 but then reversed to rise up at Day 14. There was no statistically significant difference between these two datasets (p=0.419; two-way ANOVA).

7.4 Discussion

The results from the assessment of the chondrocyte viability around the implantation hole supported the hypothesis because the cell viability could be preserved well if a sharp cutting instrument, the biopsy punch, was used for creation of the recipient hole. However, there were no results that supported the hypothesis related to the interaction of the implanted cells and the host cartilage because cell migration was observed only to occur in the superficial layer of the cell pellet, and there was no detectable increase of the matrix GAG around the margin of the recipient cartilage holes.

7.4.1 Chondrocyte viability of the model

The results in Chapter 6 revealed that the chondrocyte death of the injury model was controlled within a narrow range along the cut margin if a scalpel was used for wounding the cartilage. In this cell implantation model, the death of the chondrocytes along the cut margin remained in a limited range if a sharp skin biopsy punch was used (**Figure 7.4**). It has been reported that blunt injury, such as that caused by a blunt drill or trephine, produced more cell death than the sharp injury (Redman, *et al.* 2004; Huntley, *et al.* 2005). Thus, for the creation of the implantation holes, a drill bit with a smaller diameter was used first to create a pilot hole, which aimed to remove most of the cartilage tissue out of the implantation hole but would have induced much cell death (Farhan-Alanie & Hall 2014). The sharp biopsy punch was then used to 'clean' the hole margin in order to create an implantation hole surrounded with a maximal number of viable cells. The pilot hole made the following punch procedure easier because if no cartilage tissue was removed first, direct creation of the implantation hole with the biopsy punch would be very difficult, and more surrounding cell death might be produced by bending or twisting the biopsy punch, which was necessary to remove the punched tissue out of the joint.

The chondrocyte viability of the axial view presented the expected positive results of the sharp cut, but the chondrocyte viability on the coronal view was not as well maintained in some areas. In one area of the implantation hole, except for the

chondrocytes in the superficial zone, almost all the cells located in the middle and deep zone died; this deterioration in viability was thought to be due to an unavoidable slight levering action on this site during creation of the hole. In contrast, in the other area of the implantation hole, the cell viability of whole three layers was maintained (**Figure 7.5**). Even though most of the cartilage tissue in the centre had been eradicated by the pilot drill, a minor bending of the biopsy punch was still needed to completely remove the punched tissue, which may produce excess pressure on the wall of the deeper layer. Therefore, an improvement of the cutting procedure for removal of the articular cartilage was still necessary to reduce the cell death around the implantation hole.

Additionally, on the coronal view, the chondrocyte viability in the deep zone could not be fully recognised (**Figure 7.5**). Tissues in the deeper layer were not well stained with CMFDA/PI dyes. It was postulated that this was due to the uneven exposure of the dyes to the tissue that was close to the bottom of the hole. The access of the stain would be restricted at that area.

The inner wall of the implantation hole was not flat but curved, and the curved surface made it extremely difficult to take clear images with a conventional fluorescent microscope. By using the confocal microscope, images of different focal planes were scanned individually and then stacked together in the computer to reconstruct a clear in-focus picture. Thus, this confocal system makes scanning the curved surface of samples possible, such as the inner wall of the implantation hole or the convex surface of the cell pellet.

For cartilage repair, integration of the transplanted tissue with the recipient tissue was one the important aspects for assessment of its success. However, in several clinical studies, poor integration of the implanted tissue with native cartilage has been recognised (Ahsan, *et al.* 1999; Hunziker 2001). Discontinuity of the extracellular matrix and the absence of the chondrocytes in the region of the cartilage-cartilage interface made cartilage repair incomplete, which could proceed with degeneration in both sides (Hunziker 2002). Therefore, various measures were developed to promote the integration by establishing good contact between implants

and native cartilage, e.g. the use of collagen cross-linkers (Ahsan, *et al.* 1999), biological glues (Jurgensen, *et al.* 1997), or brief enzymatic degradation of the proteoglycans along defect surfaces (Hunziker & Kapfinger 1998). However, maintenance of the chondrocyte viability at the defect edge might be another fundamental factor to enhance the integration, but it has only been discussed by a few authors (Hunziker 2002; Huntley, *et al.* 2005). In clinical practice, the cell viability at the edge of the cartilage defect is usually compromised by the surgical intervention, e.g. debridement or shaving, which iatrogenically damaged the cells of the wound edge (Hunziker & Quinn 2003). As a result, the integration of the repair tissue with the recipient cartilage was severely affected. Thus, from the method of this model, a promising result could be achieved if two-stage procedures, such as using conventional instruments to debride the wound base followed by using sharp instruments to clean the wound margin, were performed.

7.4.2 Morphological change of the implanted chondrocyte pellet

The cell shape has been reported to be closely associated with the phenotypic expression of the chondrocytes (Glowacki, *et al.* 1983; Stokes, *et al.* 2002). The cells that maintained a round shape displayed a chondrocytic phenotype, while the cells with flattened and elongated shapes were more fibroblast-like. When the chondrocytes were isolated from the articular cartilage and cultured in monolayer at low cell density, they eventually lost their chondrocytic phenotype after 3 or 4 passages (von der Mark, *et al.* 1977). In approximate one month of culture in the 2-D environment, the chondrocytes synthesised the type I collagen instead of cartilage-specific type II collagen (Mayne, *et al.* 1976). In contrast, if the isolated chondrocytes were cultured in a 3-D environment, e.g. being seeded in a scaffold (Yates, *et al.* 2005) or being centrifuged into cell pellets (Schulze-Tanzil, *et al.* 2002), most of the chondrocytic characteristics, e.g. chondrogenic gene expression or the synthesis of the cartilage matrix molecules, was maintained. Additionally, the dedifferentiated chondrocytes, which were the result when the chondrocytes were cultured in the 2-D environment for cell expansion, might re-differentiate if they

were transferred to a 3-D culture environment (Caron, *et al.* 2012). Thus, the chondrocytes in the P0 cell pellet were considered that they still kept their originally chondrocytic phenotypes because they were directly aggregated into cell pellets after they were isolated from cartilage, whereas the P5 cell pellet was considered to be composed of the dedifferentiated chondrocytes because the isolated chondrocytes were cultured in the 2-D environment for more than one month before they were aggregated into the cell pellets.

From the confocal images of the implanted cell pellets (**Figure 7.6**), the shape of most cells inside the P0 pellet remained spherical, which suggested that they had retained a chondrocytic phenotype, while the shape of the cells in the P5 pellet looked more elongated, which indicated that the cells might be dedifferentiated into more fibroblast-like cells during the expansion procedures. Their phenotype was still not converted to a chondrocytic type despite them being aggregated into cell pellets. At the junction of the implanted pellets and the recipient cartilage, some P0 cells were observed to transform their shapes to become more elongated and begin to migrate onto the adjacent cartilage surface. However, the P5 cells had already transformed their cell shape during the culture period and their migration could be occurred directly after implantation. Thus, more migrated cells were noted in the margin of P5 pellet than the P0 pellet if the same day images were compared.

In the coronal image of the P5 pellet after 14 days culture (**Figure 7.7**), only the cells in the superficial layer of the pellet migrated and contacted the adjacent cartilage of the joint model. The cells in the deeper layer of the pellet seemed not to have any interaction with the recipient tissue. This result might indicate that only the surface cells of the pellet were able to migrate or only the surface of the cartilage provided adhesive ligands that might be necessary for cell migration. Morales *et al*. reported that cell-matrix adhesion was essential for cell migration and tissue integrity, which involved a number of molecules and mechanisms (Morales 2007). Many pioneering studies have shown that isolated chondrocytes were able to migrate under the stimulation of various chemoattractants, e.g. bone morphogenetic factors (Frenkel, *et al.* 1996) or transforming growth factor-β (Chang, *et al.* 2003), both on and within various matrices, e.g. 3-D collagen I gel (Frenkel, *et al.* 1996) or polymer scaffolds

(Gosiewska, *et al.* 2001). The extracellular matrix can also provide motility signals for chondrocytes to migrate, through the interaction between the adhesion receptors of the cell membrane and the components of the matrix (Morales 2007). The best-studied adhesion receptors were type I transmembrane proteins that comprised the integrin family. It is known that integrins are finely regulated receptors with many combinations of α and β subunits. These heterodimers interact with specific components of the extracellular matrix (Hynes 2002; Humphries, *et al.* 2006). For example, four combination of the β1 subunits (α1 β1, α2 β1, α10 β1 and α11 β1) had the potential to bind collagen fibrils of the matrix, while another three β1 integrins (α3 β1, α6 β1 and α7 β1) were highly selective for laminin receptors (Humphries, *et al.* 2006). Therefore, the migration of the chondrocytes to the adjacent cartilage surface might be associated with these different interactions but not to the created wall of the implantation hole. However, further investigation is necessary to investigate the hypothesis that the cartilage surface ligands are different to the exposed matrix ligands in their ability to attract chondrocytes.

7.4.3 Matrix GAG content of the implantation hole

The initial purpose of assessing the matrix GAG content around the implantation hole was to determine if the function of the chondrocytes of the recipient cartilage were influenced by the implanted cells. The results showed that whatever the culture passage of chondrocyte was implanted, the peripheral matrix GAG content of the implantation hole decreased to a similar level as that of the non-implantation hole (**Figure 7.8 & 7.9**). This indicated that the implanted cells had no major influence on the recipient cartilage tissue in the maintenance of their matrix GAG content. However, it should be noted that this result concerning the peripheral matrix GAG content of the implantation hole did not address whether the implanted chondrocytes had an effect on the recipient chondrocytes. To assess the cellular response an alternative technique, such as ^{35}S-incorporation or analysis of matrix-mRNA expression of the chondrocyte, might be more suitable.

Furthermore, when comparing the Day 0 matrix GAG content of the normal site of the joint and the peripheral site of the implantation hole, the acute matrix GAG loss could be observed and the lost amount was similar to that of the injury model. If the data of all normal sites and the data of all empty holes was compared, there was a statistically significant difference (p=0.001, unpaired t-test). This result provided further evidence for the loss of matrix GAG occurring as soon as the cartilage tissue was disrupted at the time of creation of the implantation holes.

In addition, it was noted that there was no significant decrease of matrix GAG content of the uninjured area at Day 7 or Day 14 (**Figure 7.10**). It was postulated that this was due to the same effect as in the injury model i.e. that matrix-stored growth factors released from the disputed matrix of the implantation hole stimulated the distant chondrocytes, however an influence from the implanted cells could not be ruled out.

7.4.4 Improvement and limitations of the chondrocyte implantation model

This chondrocyte implantation model was a preliminary study to apply this newly created *ex vivo* joint in the field of tissue engineering cartilage repair. The early effect of the implanted construct and the recipient cartilage could be evaluated with this model. However, some aspects of this model could be improved. For example, the implanted cell pellets could be replaced with the tissue engineered construct to simulate the real condition of the autologous chondrocyte implantation (ACI). Furthermore, the joint movement, a particular advantage of this *ex vivo* joint model, could be applied for evaluation of the additional effect from mechanical stimulation. However, some inherent limitations should also be noted if the joint model was used to examine cartilage repair, such as the relative short culture period (2-4 weeks), which might not be long enough to reveal the whole picture of the repair process, or the co-existent fibroblast-like cells mentioned in Chapter 2 and 6, which might have an influence on the result.

SECTION E – DISCUSSION AND FUTURE DIRECTION

Including

Chapter 8: Discussion

Chapter 9: Future Direction

Chapter 8: Discussion

8.1 Model characterisation

This is a novel model developed at the *ex vivo* organ culture level. It provides a new platform for articular cartilage research in addition to commonly used *in vivo* animal models and *in vitro* models such as isolated chondrocytes and cartilage explants. Because no previously similar model could be compared, the validity of this model could only be assessed internally by evaluating its reliability in the biochemical features, e.g. histology, cell viability or cell density, which has been discussed in Chapter 2.4.4. However, after the successfully internal validation of this novel joint model in the thesis, further validation, e.g. temporal validity (over time and geography) and external validity (e.g. to cartilage repair), would be needed to make this model being widely accepted in the cartilage research society.

The advantage of this model mainly relates to its completeness of articular structure, which provides: (1) the original joint movement that produces complex mechanical loads such as compression and shear that occur *in vivo* (Mankin, *et al.* 1994), (2) a large volume of cartilage tissue that gives sufficient sampling areas for multiple assessment in the same joint, and (3) a natural extracellular environment for chondrocytes. Cartilage explant models can also provide a similar extracellular environment for chondrocytes. However, the procedures to harvest cartilage explants from a joint cause injuries that might induce the inflammatory signals such as interleukin-1 (IL-1) (Gruber, *et al.* 2004; Watt, *et al.* 2013), and the matrix GAG could also be released quickly from the cut edges (**Figure 6.7, 7.8 and 7.9**). In the joint model presented here, the direct harvesting injury to cartilage is prevented because the articular cartilage is harvested as a whole and thus, the cartilage is not damaged inadvertently, but only by intention (such as the injury model).

However, disadvantages remain in this joint model. First, there are a number of particular steps in the harvesting process that need to be undertaken carefully, there is therefore a significant learning curve that has to be mastered for the successful use

of this model. Second, it is difficult but essential to maintain sterility of the model. However, with increased experience with the model this is achievable purely with careful technique. Third, compared to cartilage explants or isolated chondrocyte systems, the large size of the whole joint, requires a considerable volume of culture media every week and this increases the expense of experiments. Finally, the total experimental period may be prolonged as only one or two joints can be set up each day and it may take a number of days to establish the required number of whole joint models. However, the time taken is still likely to be less than the time it would take to carry out the experimental procedures *in vivo*.

8.2 Fresh (Day 0) joint models

Characterisation of the chondrocyte viability and the matrix proteoglycan content in a fresh (Day 0) joint is important because it provides the baseline values for comparison with the values obtained from different experimental conditions. Knowing the variability of these values in different sites of the same joint is also important because it could reduce the sampling bias if some areas with outlying values could be avoided in advance. However, there is no such data available in the current literature even though the cartilage explants of animal joints have been used extensively for many years. The data from the joint mapping study and the results of all Day 0 samples of different models in the thesis help to rectify this deficiency.

The joint mapping results for the chondrocyte viability and the GAG content (**Table 2.13 & 2.15**), demonstrated that there were no significant differences between the biopsy sites, which indicated that the cartilage samples could be taken from anywhere on the joint surface at least for chondrocyte viability and GAG content, but potentially for other factors as well. However, the variability of the readings was least for site B3 and site C3, both of which were located in the middle of the articular surface, which may indicate that these sites could be more suitable than others if only one or two cartilage samples are required from each bovine joint.

From the results of the joint mapping and the Day 0 samples of different models (a total of 52 different joints), the chondrocyte viability (as measured from the axial view) was above 98% in all of the samples and the coronal view viability was within the range of 89-91%, 94-96% and 78-88% in the superficial, middle and deep zones, respectively. The average GAG content of these samples was 1.206% (from 1.17% to 1.24%). The data provide useful baseline values for this joint model.

However, it is difficult to compare these data to published figures because there are no prior e*x vivo* joint models to provide equivalent data from. In addition, different methods for testing the chondrocyte viability result in different outcomes. Amin *et al*. reported the coronal view chondrocyte viability with 86.4%, 91.9% and 82.2% in the superficial, middle and deep zone, respectively, from the cartilage explants of human knee joints (Amin, *et al.* 2011). In addition, Pun *et al*. studied cartilage explants of human knee joints (Pun, *et al.* 2006). They demonstrated the chondrocyte viability on day 0 of the 3 zones was 80.5%, 80.0% and 83.0% for the superficial, middle and deep zones respectively. The viability values from the papers are not as high as the results reported in this thesis. This may be because the samples of the other studies were from surgical specimens of osteoarthritic patients. The chondrocyte viability in these surgical specimens may be reduced because of the disease itself or as a result of the surgical manipulation and shaping of the cartilage explant. Thus, the experimental data from explants of parts of the joint surface may not be directly comparable to the results reported here.

For the GAG content of the extracellular matrix, if the same magnification of dilution was applied, Hoemann *et al*. has reported that the fresh cartilage explants from bovine shoulder joint contained 0.98% to 1.16% GAG (Hoemann, *et al.* 2002). Lewis *et al*. has demonstrated that the matrix GAG content in the cartilage explants of bovine carpo-metacarpal joint was 0.80% after 48 hours of explant culture (Lewis, *et al.* 1998). These data closely match the results from the static model, even though different bovine joints were used.

8.3 Long-term cultured joint models

Every model in the thesis was cultured for at least 2 weeks (2-6 weeks) for evaluation of their long-term outcomes. The improvement in chondrocyte viability and the maintenance of the matrix GAG level in the 'under-moving-arc' area of the dynamic model was confirmed and has been discussed in Chapter 4.4.2 and Chapter 4.4.3. These outcomes were considered to be related to both the direct mechanical stimulation of the joint movement and the indirect media flow caused by the joint movement (Strangeways 1920; Galois, *et al.* 2003; Bader, *et al.* 2011). However, the clinical relevance of these results has not been discussed before and is considered below:

(1) First, the maintenance of the cell viability and the matrix content in the dynamic model provides additional experimental evidence for the chondro-protective effect of joint movement. Previously, it has been illustrated in an *in vivo* rat model that both slight (30 cm/s for 15 min per day) and moderate (30 cm/s for 30 min per day) exercise programmes had a beneficial influence on chondral lesions (Galois, *et al.* 2004); in this study, the severity of OA lesions were graded on a scale adapted from Mankin's score by two independent observers. The histological severity decreased after a 14 day exercise programme. In addition to this '*in vivo*' study, a clinical randomised controlled study demonstrated that exercise increased both intraarticular and peri-synovial concentrations of interleukin-10 (IL-10) in a group of females with knee OA (Helmark, *et al.* 2010). IL-10 has been reported to be a chondroprotective anti-inflammatory cytokine (Schulze-Tanzil, *et al.* 2009), and its increase indicates the positive effect of exercise. Therefore, in recent systematic reviews, rehabilitation exercise has been considered effective as a first-line treatment for osteoarthritic patients (Roos & Juhl 2012; Davis & MacKay 2013).

(2) Second, when the results of the manually moved and the machine-moved dynamic model were compared, it was evident that the chondroprotective effect was obtained with only a few minutes of joint movement combined with slight contact pressure on the articular surface. It was also observed that this effect only existed in the articulated region of the joint surface, i.e. in the 'under-moving-arc' area and not

in the ‘off-moving-arc’ area of the dynamic model. The clinical implication of this is that, it may be more beneficial for patients to have rehabilitation programmes that concentrate on the range of motion rather than the duration or the loading of the joint.

8.4 Injury model and repair model.

Having developed the whole joint model, the next step was to create a reproducible injury on cartilage and then to investigate its repair, including tissue engineering approaches for cartilage regeneration.

The type of injury is crucial because it influences the subsequent repair processes, which has been thoroughly discussed in Chapter 1.4.1. The cartilage injury in the injury model was created by using a sharp scalpel applied with reproducible pressure as reported by Amin *et al*. (Amin, *et al.* 2008) and Chapter 2.4.2. Using the scalpel in this way split only the cartilage tissue and did not penetrate into the subchondral area (**Figure 6.5**). To a degree, it was considered to represent the ‘chondral fracture’ described in Chapter 1.4.1. The results showed that there was no morphological repair observed after one month of culture (**Figure 6.5 & 6.6**), even though the GAG content of the surrounding tissue along the cut line increased week by week in the serum-supplied model (**Figure 6.7**). This indicated that the cartilage tissue reacted to the cut injury with an increase in the matrix proteoglycan production, but with no visible repair processes. Even when a 3-D tissue engineered construct in the form of a chondrocyte pellet was inserted to the defect, there was still no morphological evidence of repair (cell integration) at the end of the second week (**Figure 7.7**).

In previous studies, Enders *et al*. demonstrated an *in vitro* model for studying cartilage repair, which was a human cartilage explant with a smaller diameter hole created in the centre (Enders, *et al.* 2010). Aggregated chondrocytes were added in the central hole and cultured for 4 weeks. Their results revealed that proteoglycans and type II collagen were synthesised in the cell pellet but only minimal integration occurred between the aggregated chondrocytes and the cartilage explant. Another *in*

vitro study using the co-culture system of chick cartilage explants with isolated chondrocytes still had no the evidence of cell integration at the interface between chondrocyte pellet and explant after 2 weeks culture (Zhang, *et al.* 2005). However, by electron microscopy, they revealed a tight attachment of chondrocytes on smooth surfaces of the explant, in contrast to a loose attachment of chondrocytes on rougher surfaces of the explant side wall. This finding was similar to one of the results of chondrocyte implantation model shown in **Figure 7.7**, and the possible reason has been thoroughly discussed in Chapter 7.4.2.

8.5 Cells in the culture media

It was found that two cell types were isolated from the culture media of the joint model. The main type of cells were small and disc-like in shape. The other type of cells, which were difficult to be seen under the microscope because of their low number, were the large spindle-shaped cells (**Figure 2.28**). The small disc-like cells were considered to be red blood cells on the basis of their characteristic discoid shaped morphology and their lack of nuclei. They were thought to have leaked out of the bone marrow or the blood vessels of the joint model. Their numbers reduced after every change of culture media, but still could be identified after 14 days (**Table 2.30**).

The large elongated spindle-shaped cells were considered to be fibroblast because of their cell configuration and their ease of proliferation in the culture flask. These cells could also have come from the bone marrow or alternatively from the residual soft tissues of the joint. These cells could adhere to the cartilage surface and proliferate to produce a considerable number of cells. These cells had ability to grow over each other and thus form a layer with 2-3 cell thickness over the cartilage (**Figure 2.29c**). This layer obstructed the penetration of the CMFDA/PI stains and resulted in blurred images (**Figure 2.29b**). This effect was more apparent in the axial view compared to the coronal view because the scan of the coronal view was through a newly cut plane and the CMFDA/PI stains could reach the chondrocytes directly without interference. In contrast, in the axial views, the stains needed to pass through this layer to reach

the chondrocytes. Most of the stains were absorbed by the cells of this layer, and few underlying chondrocytes were stained. This caused difficulty with chondrocyte counting and could lead to an inaccurate determination of the axial view viability of the joint model, if this 'fibroblast' cell layer was present.

It was observed that this layer occurred more frequently and at an earlier stage when the joint was static but the media was flowing (i.e. the media-stirred model). This obstacle layer could be found as early as Day 14 in the media-stirred model. In the static model, it usually did not occur until after Day 28 of culture. At Day 35 of the static model, approximately half of the samples had been covered with this layer, and at Day 42, almost all of the samples could not be scanned using axial views. However, if the joint was passively-moved (i.e. the dynamic model), the layer was not found on the cartilage surface at any time point. In addition, the adhesion of the cells onto the cartilage surface may be related to the existence of foetal bovine serum in the culture media because, if no serum was added, no adhesion cells could be found in the axial view viability assessment during the 4 weeks culture (i.e. the injury model without serum-supplied group).

These findings could be explained by the flowing culture media helping to transport the fibroblast-like cells from the bone marrow or the soft tissue to the cartilage surface. If the joint was not moving, the cells were able to adhere to the cartilage surface and proliferate, but, in contrast, if the joint was dynamically moved, the motion between two contacting surfaces prevented the cells from adhering and proliferating. The difference between the serum-supplied and non-serum-supplied group of injury model also indicated that the adhesion of the fibroblast-like cells was related to the existence of foetal bovine serum in the culture media. It was inferred that some membrane molecules, such as the integrins (Morales 2007), could be induced in the serum-supplied media that helped the cell adhesion on the cartilage surface.

The existence and influence of these fibroblast-like cells should be taken into account if the joint model is being considered for any cartilage repair studies. For example, in the injury model of the serum-supplied group, these cells were found to

cross the gap of the injury cut at Day 28 (**Figure 6.9**), and they were easily to be misunderstood as the cells with attempts to repair the defect.

8.6 Comparisons of findings common to all the models

Repetitive use of the same assessment methods throughout the models, e.g. CMFDA/PI stains for chondrocyte viability and the DMMB assay for matrix proteoglycan, made all the results comparable in the thesis.

The matrix GAG analysis in the thesis, demonstrated that when the cartilage surface was intact in the static and media-stirred model, the matrix GAG content decreased within a few days (**Figure 3.6**). If the integrity of the cartilage surface was disrupted, as with the injury model or the tissue around the implantation hole of the cell implantation model, the loss of the matrix GAG, occurred within a few minutes (**Figure 6.7, 7.8 & 7.9**). In contrast, if dynamic movement was applied to the intact cartilage surface, the matrix GAG content of the contact area was maintained at a consistent level (**Figure 4.10**). If the cartilage was heat treated, the matrix GAG appeared to be 'locked' inside the cartilage tissue and no loss was evident for several weeks (**Figure 5.5**). All of these observations suggest that there is a profound mechanism for regulating the matrix proteoglycan turnover of articular cartilage, which has yet to be fully elucidated.

8.7 Control of proteoglycan turnover in the articular cartilage

Existing evidence. For the biosynthesis of the proteoglycan molecule of the articular cartilage, it has been reported that the carbohydrate chains were directly synthesised on the protein core within the chondrocyte to form a proteoglycan monomer (Hardingham & Fosang 1995). The time required for preparation and synthesis of the proteoglycan was approximately 20 to 30 minutes. Then, the intracellularly synthesised proteoglycan monomers are secreted into the extracellular matrix, and

several monomers non-covalently bound with the hyaluronic acid chain with the help of the link protein to form aggrecan. The link protein and the hyaluronic acid chain have been described as being synthesised and secreted separately by the chondrocyte (Buckwalter, *et al.* 1984). Once the aggrecans have been formed, they are immediately trapped within the collagen network of the cartilage matrix. However, some non-aggregated proteoglycan monomers can be found in the cartilage matrix (Vasan & Lash 1979). The existence of these loose molecules has been postulated to be due to their unstable hyaluronic acid binding region of the core protein or the inferior function of the link protein (Vasan & Lash 1977).

As well as these newly synthesised matrix molecules, smaller molecular weight proteoglycans could also be derived from larger proteoglycan molecules cleaved by the catalytic enzymes such as aggrecanase (ADAM-TS4/ADAM-TS5) or matrix metalloproteinase (MMP). Also present within the cartilage matrix, are small quantities of the smaller-sized proteoglycans such as decorin, biglycan and fibromodulin, which have different biological functions (Hildebrand, *et al.* 1994). Thus, the proteoglycan molecules found inside the extracellular matrix of the articular cartilage had a variety of molecular weights. In contrast, studies using bovine cartilage explant cultures revealed that the majority of the proteoglycans released into the culture media were of smaller hydrodynamic size and were unable to form aggregates with hyaluronate. This provides further support for the concept of the existence of these smaller-sized proteoglycans in the cartilage matrix (Campbell & Handley 1987; Campbell, *et al.* 1989). In a normal human joint, the synovial fluid contains a number of proteoglycan molecules. Some of these have been synthesised and secreted by synovial cells: Hyaluronic acid was the most common proteoglycan to come from the synovial cells (Balazs, *et al.* 1967). However, the majority of the synovial proteoglycans was not hyaluronic acid but chondroitin sulphate that seemed to be transferred directly from the articular cartilage without major alteration in the apparent size of the proteoglycan core protein (Heimer, *et al.* 1992).

Postulate

Both from already published data and from the results of this thesis, a control system for the turnover of proteoglycan in articular cartilage could be postulated. It was supposed that the large aggregated proteoglycan molecules of the cartilage matrix would not be released or not able to pass through the collagen network of the cartilage surface freely. Only the non-aggregated monomers or the smaller-sized proteoglycans could be released or pass through the pores of the cartilage matrix into the environment outside the cartilage, which would be the synovial fluid *in vivo* and the culture media *ex vivo*. Diffusion might be the major force for the proteoglycan movement. In a healthy *in vivo* joint, the total content of the matrix proteoglycan might be maintained at a consistent level because the synovial fluid contained a large amount of proteoglycan. High concentration of proteoglycan molecules in the synovial fluid prevented the movement of proteoglycan from the cartilage matrix to the synovial fluid that maintained the amount of the matrix proteoglycan of cartilage. However, if the joint was harvested and cultured in an artificial media, which did not contain any proteoglycan molecules, the transmissible smaller-sized proteoglycans could be diffused into the environment along the concentration gradient that decreased the proteoglycan content of the cartilage matrix if no new proteoglycans were synthesised. In contrast, if the collagen fibre or the proteoglycan was denatured by heat, the porosity of the collagen network might decrease and the denatured proteoglycan might incarcerate within the matrix tissue, which would interfere the diffusion of matrix proteoglycan that would lead to a fixed level of the matrix GAG for a few weeks.

This postulate was able to explain all the observed results of the matrix GAG change in the thesis. The DMMB assay measured the total GAG content in the cartilage matrix, and this result represented the balance of the matrix GAG production and loss. Two specific components of the articular cartilage, the chondrocytes and the extracellular matrix, should be considered together because they individually or cooperatively influence this balance. The observed decrease of matrix GAG content might be due to a decrease in GAG production by the chondrocytes, an increase in GAG loss from the matrix into the media, or both. This decrease could be observed in the static model, media-stirred model, the non-contact area of the dynamic model

and the injury model, but each of them needs further discussion to clarify what the most likely underlying mechanism is.

The results from the non-injury site of the serum free injury model (**Figure 6.8**) showed that the matrix GAG content decreased to a baseline at Day 14 without any further decrease. This curve represented the GAG loss from the existing matrix GAG without the confounding factor of newly produced GAG from the chondrocytes (because of non-serum supplement). The drop in GAG up to day 14 can be explained by the smaller-sized matrix proteoglycans being lost into the culture media over the first two weeks. The baseline GAG level would then be explained by the large aggregated proteoglycans not being released but being retained in the cartilage matrix.

However, if the culture media contained serum, the chondrocytes were able to produce matrix proteoglycans (if they were stimulated), and the outcome was more difficult to account for. In this thesis, there were several types of stimulation. In the static and media-stirred model, the low GAG matrix itself could possibly be one of the stimulation factors that caused the chondrocytes to produce the matrix proteoglycan molecules, as suggested by the partial rebound after the matrix GAG content had decreased to the baseline level (**Figure 2.26 & 3.4**).

The second stimulation was from joint movement. The mechanical joint motion in the dynamic model (**Figure 4.10 & 4.11**) appeared to be a consistent stimulus for the chondrocytes to synthesise matrix proteoglycans. The observed result could be accounted for by the matrix GAG content being maintained at the initial level by the newly synthesised proteoglycans balancing the proteoglycans lost into the media. Alternatively, the maintenance of the matrix GAG in the dynamic model could be accounted for by a change in the porosity of the collagen network as a change in the configuration of the collagen fibres on the cartilage surface has been reported in response to compression forces (Wada & Akizuki 1987). In Wada & Akizuki's study, the compression forces caused a reduction in the porosity of the collagen network, which might prevent the movement of some of the larger proteoglycan molecules. Thus, an increase in GAG production from the chondrocytes or a

decrease in GAG loss from the matrix could both contribute to the maintenance of the matrix proteoglycans in the dynamic model.

The third stimulatory factor of this thesis was the injury cut (**Figure 6.7 & 6.8**). The possible mechanism of injury cut has been thoroughly discussed in Chapter 6.4.3. This factor was considered to be less effective than mechanical stimulation because the amount of matrix GAG did not reach the initial level at the end of the experiment, which indicated the recovery was not complete.

On the other hand, some factors could increase the rate or amount of the GAG loss from the cartilage matrix in addition to the hypothesised normal loss. The first factor observed was the fluid flow demonstrated in the media-stirred model. The exchange of the molecules between the cartilage tissue and the culture media would be facilitated if the media flowed. For nutrients and metabolites, increasing their exchange speed was beneficial because the chondrocytes viability was maintained. However, for the matrix proteoglycans, this flow increased the loss speed of the small proteoglycans from the matrix to the media, which was supported by the lowest GAG value occurring at Day 14 in the media-stirred model i.e. at an earlier time point than in the static model (**Figure 3.4**).

The second factor to increase the rate and amount of the GAG loss from the matrix was the injury cut performed in the injury model. The observed phenomenon of the acute GAG loss from the injury cut line in Day 0 (**Figure 6.7**) could be explained by the cut creating more openings for the proteoglycans to be released easily from the cartilage matrix, in particular for the proteoglycans in the deeper layer of the cartilage. The GAG loss from the cut site was so serious that the matrix GAG content continued to decrease during the whole culture period, and when the loss was not offset by new GAG production as in the serum free experiments, eventually reached the lowest GAG value measured in this thesis.

Finally, for the heat-treated model, the situation was quite different from all other models. The consistent maintenance of the matrix GAG was not due to replenishment by the chondrocytes but due to the inability to release the components

of the cartilage matrix. The proteins in both the proteoglycans and the collagen fibres would be denatured by heat that prevent the release of matrix GAG into the culture media.

8.8 Research limitations

The limitations of each individual model have already been discussed in the relevant chapters. Some of the limitations applicable to the overall research are discussed below.

Sample number. Using a sample to represent the whole population is always a limitation for scientific research. If more joints had been included in the experiments, the reliability and the reproducibility of the data could have been improved. However, increasing the joint number meant the overall cost of the experiment would increase. Therefore, a reasonable compromise was made to balance the expenses and the result reliability. The preliminary experiments demonstrated that the outcome measures (specifically, confocal microscopy and the DMMB assay) had good reliability and repeatability and therefore, the number of repeat experiments could be kept within a reasonable range, which was generally 5 or 6 joints.

Culture environment. The joint culture environment was not exactly the same as that *in vivo*. The components of the culture media were different from the synovial fluid of the joint, which might influence the cell behaviour of the joint model and the matrix GAG release between the cartilage and the environment. However, it was not possible to culture the joint in the real synovial fluid, and to reproduce components of the real synovial fluid might be very difficult in the experiment.

Livestock condition. It is known that the individual difference always exists even in the same species. However, some imposed factors, e.g. the joint damage when the animal was transported or slaughtered, additionally increased the range of the difference. Even though the joints used in the experiment were carefully selected to rule out the macroscopically abnormal ones, some invisible minor damage of the articular cartilage might have been missed by the naked eye (such as the chondral

matrix damage described in Chapter 1.4.1), which could have influenced the cell function. In addition, although all the bovine feet in the experiment were provided from the same slaughter house, the joints of each model were likely to have come from different farms. Further, over the experimental period of more than two years, it was possible that a seasonal variation or a species variation between farms might have influenced the results.

8.9 Conclusion

The metatarsophalangeal joint of bovine was successfully isolated and established as an *ex vivo* organ culture model for over 4 weeks. Chondrocyte viability could be assessed precisely using CMFDA/PI stains under the confocal laser scanning microscope. The results revealed that the overall cell viability of the cartilage was still maintained at approximately 70% at the end of the 4th week in static culture. If the joint was subjected to the flowing culture media produced by either the stirring machine or the joint motion, the chondrocyte viability could be significantly increased to approximately 90%.

By using the DMMB assay, the proteoglycan content of the cartilage extracellular matrix could be assessed accurately. It was observed that the proteoglycan content of the cartilage decreased to a baseline level if the joint model was cultured in the environment without stimulations. In contrast, if the cartilage was subjected to some form of stimulation, e.g. the joint movement or cut injury, and the joint was cultured in the serum-supplied media, the proteoglycan content of the cartilage could be maintained at a level similar to the initial level without decrease, or, alternatively, the initial decrease in proteoglycan level could be returned up to but not beyond the initial level. A coexistent fibroblast-like cell type could sometimes be found on the joint surface. Application of this model to the study of cartilage repair was promising because if a sharp instrument was used, the chondrocyte viability was also maintained around the surface defect where a tissue-engineered construct could be implanted. This model provides another experimental platform for articular cartilage research.

Chapter 9: Future Direction

Four research directions can be considered in the future. First, some additional studies could be conducted for reinforcement and completeness of the experiments of this thesis. Second, further new models could be created based on this exciting model for better simulation of real joint movement. Third, some experiments could be considered to test the postulate discussed in Chapter 8. Fourth, the model has a great potential for application in numerous research fields related to the articular cartilage.

9.1 Studies extended from previous models

In the manually moved dynamic model, it is known that the movement period can be shortened to only 10 minutes per day and the maintenance of the initial matrix GAG is not changed compared to the long-time machine-moved dynamic model (**Figure 4.11**). However, the minimal threshold of the joint movement to maintain the matrix content is still not defined. Thus, another manually moved dynamic model with shorter movement time, e.g. 5 minutes, 2 minutes, 1 minutes and 30 seconds per day, can be performed in the future to find the minimal movement time that the matrix proteoglycan can still be maintained.

Using the results of the above manually moved model, the recovery experiment can further be considered. In an *in vivo* canine model, immobilisation of the knee joint for 11 weeks induced 20% to 23% reduction of the cartilage GAG (Haapala, *et al.* 1999). Remobilisation for the following 50 weeks partially recovered the initially loss but it was still 9% to 17% less than that in controls. However, it is still unknown that if the period of immobilisation has effects on the recovery of the chondrocyte activity, and the intensity of the remobilised joint movement may influence this. Thus, by controlling both the period of immobilisation and the remobilisation, a series of recovery experiments can be designed with this joint model.

9.2 Creation of a new model

In the *in vivo* situation, the joint bears the whole weight of the host body. During some intense exercises, the compression load may increase to several times of body weight (Wilk, *et al.* 1996).The loaded dynamic model, which means applying controlled compression on the joint during its movement, could provide a better simulation of the *in vivo* joint.

This idea has been considered in the beginning of designing the dynamic model. It was thought that providing the load through this simple dynamic machine would be complex. Alternatively, applying the load by using two springs fixed on each side of the joint might be an effective way of providing the compression force. However, due to the narrow space in the culture vessel, only small springs could be used. The force of small springs was too limited to represent the forces within an animal. Therefore, a special compression device, has been designed to provide a controllable force on the joint. However, assembly of this device would prolong the time of joint harvesting and the maintenance of the sterility during culture period may be more difficult.

However, once the dynamic model has been verified, the loaded dynamic model may be worth developing further. Because the compression load is an important variable for the joint, it would be of great value if the load can be evaluated *ex vivo*. In particular, the chondrocyte may have a different bioactivity under different joint compression loads.

9.3 Studies on the postulate concerning proteoglycan turnover

In order to verify the postulate put forward in Chapter 8, two directions of experiments could be considered. First, the released proteoglycans in the culture media should be quantified, and their morphology and molecular sizes should be assessed. The quantity of the matrix proteoglycans lost from the joint cartilage should be similar to the amount in the culture media, and these released proteoglycans should have a smaller molecular size compared to the proteoglycans in the cartilage matrix (Campbell, *et al.* 1989).

Second, these released proteoglycan molecules should be demonstrated to be able to pass through the collagen network of the cartilage surface. This can be done by labelling the proteoglycans that are already inside the cartilage, and collecting the released molecules after the joint is cultured in the media. The labelled proteoglycan molecules should be found outside the cartilage to establish their connections. It would be preferable if the labelling agents had an ability to label the large and small molecular weight proteoglycans differently.

In addition, the relationship of the three-dimensional configuration of the collagen network and the proteoglycans would be another interesting topic. It has been found that there are structural interactions between type I collagen fibres and proteoglycans in the bovine cornea by using the three-dimensional electron tomography (Lewis, *et al.* 2010). The ultrastructural interaction in the type II collagen fibres of the articular cartilage is still unknown. According to the results of the dynamic model, the joint movement is supposed to have effects on this structure that prevents the initial loss of the matrix proteoglycan. This can be further studied if this technique can be applied in this model.

9.4 Applications of this model

This organ culture system for a whole joint can be applied in a number of fields of the cartilage research. It will enable the critical first month of results to be examined. The tissue engineering cartilage repair can be conducted in this model mentioned in Chapter 7. Other interesting applications are described below.

9.4.1 Pharmacological agents

A number of pharmacological agents are developed at present for chondroprotection of articular cartilage or disease modification of osteoarthritis. The effects of the chondroprotective agents, e.g. the high osmolar solution (Amin, *et al.* 2008) or the IL-1 receptor antagonist (Caron, *et al.* 1996), can be evaluated in this model combined with the naturally protective effects from the joint movement to see if synergistic result occurs. The disease-modifying osteoarthritis drugs (DMOADs), e.g. strontium ranelate (Reginster, *et al.* 2013), calcitonin (Karsdal, *et al.* 2010) or bone morphogenetic protein 7 (BMP-7) (Jelic, *et al.* 2001), can also be studied by using this model in the preclinical stage.

9.4.2 Cartilage tribology

The progression of local cartilage surface damage to early stage osteoarthritis is likely to depend on the severity of the damage and its impact on the local lubrication. However, there is little understanding of the interactions between lubrication, stress and damage (Bonnevie, *et al.* 2011). Traditionally, the studies of cartilage tribology have used cartilage explants sliding over a lubricated surface. Most of the results from these studies have demonstrated that the friction was initially extremely low but increased with time (Krishnan, *et al.* 2004; Caligaris & Ateshian 2008). However, one of the studies revealed that if cartilage was moved against cartilage, sustainable low friction could be observed (Bell, *et al.* 2006). Moreover, another study found that this sustained low friction condition could also be achieved if a spherical glass slider against a cartilage surface was used (Caligaris & Ateshian 2008), and this might be

explained by a previous hypothesis that fluid pressurisation could be maintained during rolling movement (Ateshian & Wang 1995). Thus, with the complete and natural articulation, this joint model can be a suitable experimental model for studying the cartilage tribology.

9.4.3 *Ex vivo* bioreactor

This concept comes from the *in vivo* bioreactor of bone for organ engineering (Stevens, *et al.* 2005). The authors injected the alginate gel or hyaluronic acid-based gel into a deliberatively created space (bioreactor) between the periosteum and the tibia in New Zealand White rabbits. After 6 weeks, the newly formed tissue at this space was biomechanically identical to native bone and had a great integration ability if it was transplanted into the contralateral tibial defects. They also found that if angiogenesis was inhibited and a hypoxic environment was created within this space, cartilage formation could be exclusively promoted. However, inhibition of angiogenesis and hypoxia could not be tolerated by a living animal. Thus, using the joint model as an *ex vivo* bioreactor under certain chondrogenic culturing conditions (e.g. applying the mechanical stimulation by the joint movement) for generation of the hyaline cartilage from the tissue engineered constructs may be an another potential opportunity for this joint model.

REFERENCES

1. Agrawal, C.M. & Ray, R.B. (2001) Biodegradable polymeric scaffolds for musculoskeletal tissue engineering. *J Biomed Mater Res* **55**, 141-150.

2. Ahsan, T., Lottman, L.M., Harwood, F., Amiel, D. & Sah, R.L. (1999) Integrative cartilage repair: inhibition by beta-aminopropionitrile. *J Orthop Res* **17**, 850-857.

3. Alexander, S., Watt, F., Sawaji, Y., Hermansson, M. & Saklatvala, J. (2007) Activin A is an anticatabolic autocrine cytokine in articular cartilage whose production is controlled by fibroblast growth factor 2 and NF-kappaB. *Arthritis Rheum* **56**, 3715-3725.

4. Altman, R.D., Kates, J., Chun, L.E., Dean, D.D. & Eyre, D. (1992) Preliminary observations of chondral abrasion in a canine model. *Ann Rheum Dis* **51**, 1056-1062.

5. Amin, A.K., Huntley, J.S., Bush, P.G., Simpson, A.H. & Hall, A.C. (2008) Osmolarity influences chondrocyte death in wounded articular cartilage. *J Bone Joint Surg Am* **90**, 1531-1542.

6. Amin, A.K., Huntley, J.S., Bush, P.G., Simpson, A.H. & Hall, A.C. (2009a) Chondrocyte death in mechanically injured articular cartilage--the influence of extracellular calcium. *J Orthop Res* **27**, 778-784.

7. Amin, A.K., Huntley, J.S., Patton, J.T., Brenkel, I.J., Simpson, A.H.R.W. & Hall, A.C. (2011) Hyperosmolarity protects chondrocytes from mechanical injury in human articular cartilage. *J Bone Joint Surg Br* **93-B**, 277-284.

8. Amin, A.K., Huntley, J.S., Simpson, A.H. & Hall, A.C. (2009b) Chondrocyte survival in articular cartilage: the influence of subchondral bone in a bovine model. *J Bone Joint Surg Br* **91**, 691-699.

9. Archer, C.W. & Francis-West, P. (2003) The chondrocyte. *Int J Biochem Cell Biol* **35**, 401-404.

10. Arden, N. & Nevitt, M.C. (2006) Osteoarthritis: epidemiology. *Best Pract Res Clin Rheumatol* **20**, 3-25.

11. Arkill, K.P. & Winlove, C.P. (2008) Solute transport in the deep and calcified zones of articular cartilage. *Osteoarthritis Cartilage* **16**, 708-714.

12. Arokoski, J., Kiviranta, I., Jurvelin, J., Tammi, M. & Helminen, H.J. (1993) Long-distance running causes site-dependent decrease of cartilage

glycosaminoglycan content in the knee joints of beagle dogs. *Arthritis Rheum* **36**, 1451-1459.

13. Ateshian, G.A. & Wang, H. (1995) A theoretical solution for the frictionless rolling contact of cylindrical biphasic articular cartilage layers. *J Biomech* **28**, 1341-1355.

14. Attmanspacher, W., Dittrich, V. & Stedtfeld, H.W. (2000) [Experiences with arthroscopic therapy of chondral and osteochondral defects of the knee joint with OATS (Osteochondral Autograft Transfer System)]. *Zentralbl Chir* **125**, 494-499.

15. Bader, D.L., Salter, D.M. & Chowdhury, T.T. (2011) Biomechanical influence of cartilage homeostasis in health and disease. *Arthritis* **2011**, 979032.

16. Baginski, M. & Czub, J. (2009) Amphotericin B and its new derivatives - mode of action. *Curr Drug Metab* **10**, 459-469.

17. Balazs, E.A., Watson, D., Duff, I.F. & Roseman, S. (1967) Hyaluronic acid in synovial fluid. I. Molecular parameters of hyaluronic acid in normal and arthritis human fluids. *Arthritis Rheum* **10**, 357-376.

18. Barbosa, I., Garcia, S., Barbier-Chassefiere, V., Caruelle, J.P., Martelly, I. & Papy-Garcia, D. (2003) Improved and simple micro assay for sulfated glycosaminoglycans quantification in biological extracts and its use in skin and muscle tissue studies. *Glycobiology* **13**, 647-653.

19. Barry, F., Boynton, R.E., Liu, B. & Murphy, J.M. (2001) Chondrogenic differentiation of mesenchymal stem cells from bone marrow: differentiation-dependent gene expression of matrix components. *Exp Cell Res* **268**, 189-200.

20. Behrens, F., Kraft, E.L. & Oegema, T.R., Jr. (1989) Biochemical changes in articular cartilage after joint immobilization by casting or external fixation. *J Orthop Res* **7**, 335-343.

21. Bekkers, J.E.J., de Windt, T.S., Brittberg, M. & Saris, D.B.F. (2012) Cartilage repair in football (soccer) athletes: What evidence leads to which treatment? A critical review of the literature. *Cartilage* **3**, 43S-49S.

22. Bell, C.J., Ingham, E. & Fisher, J. (2006) Influence of hyaluronic acid on the time-dependent friction response of articular cartilage under different conditions. *Proc Inst Mech Eng H* **220**, 23-31.

23. Bendele, A.M. (2001) Animal models of osteoarthritis. *J Musculoskelet Neuronal Interact* **1**, 363-376.

24. Bennell, K.L. & Hinman, R.S. (2011) A review of the clinical evidence for exercise in osteoarthritis of the hip and knee. *J Sci Med Sport* **14**, 4-9.

25. Bert, J.M. (1993) Role of abrasion arthroplasty and debridement in the management of osteoarthritis of the knee. *Rheum Dis Clin North Am* **19**, 725-739.

26. Bian, L., Fong, J.V., Lima, E.G., Stoker, A.M., Ateshian, G.A., Cook, J.L. & Hung, C.T. (2010) Dynamic mechanical loading enhances functional properties of tissue-engineered cartilage using mature canine chondrocytes. *Tissue Eng Part A* **16**, 1781-1790.

27. Bloebaum, R.D. & Radley, K.M. (1995) Three-dimensional surface analysis of young adult human articular cartilage. *J Anat* **187 (Pt 2)**, 293-301.

28. Bodo, G., Hangody, L., Szabo, Z., Peham, C., Schinzel, M., Girtler, D. & Sotonyi, P. (2000) Arthroscopic autologous osteochondral mosaicplasty for the treatment of subchondral cystic lesion in the medial femoral condyle in a horse. *Acta Vet Hung* **48**, 343-354.

29. Bonnevie, E.D., Baro, V., Wang, L. & Burris, D.L. (2011) In-situ studies of cartilage microtribology: roles of speed and contact area. *Tribol Lett* **41**, 83-95.

30. Borrelli, J., Jr., Tinsley, K., Ricci, W.M., Burns, M., Karl, I.E. & Hotchkiss, R. (2003) Induction of chondrocyte apoptosis following impact load. *J Orthop Trauma* **17**, 635-641.

31. Brandt, K.D., Radin, E.L., Dieppe, P.A. & van de Putte, L. (2006) Yet more evidence that osteoarthritis is not a cartilage disease. *Ann Rheum Dis* **65**, 1261-1264.

32. Brighton, C.T., Wang, W., Clark, C.C. & Praestgaard, A. (2013) A Spectrophotometric Analysis of Human Osteoarthritic Cartilage Explants Subjected to Specific Capacitively Coupled Electric Fields. *Open Journal of Biophysics* **3**, 158-164.

33. Brittberg, M., Lindahl, A., Nilsson, A., Ohlsson, C., Isaksson, O. & Peterson, L. (1994) Treatment of deep cartilage defects in the knee with autologous chondrocyte transplantation. *N Engl J Med* **331**, 889-895.

34. Brommer, H., Brama, P.A., Laasanen, M.S., Helminen, H.J., van Weeren, P.R. & Jurvelin, J.S. (2005) Functional adaptation of articular cartilage from birth to maturity under the influence of loading: a biomechanical analysis. *Equine Vet J* **37**, 148-154.

35. Broom, N.D. & Myers, D.B. (1980) A study of the structural response of wet hyaline cartilage to various loading situations. *Connect Tissue Res* **7**, 227-237.

36. Brower, T.D., Akahoshi, Y. & Orlic, P. (1962) The Diffusion of Dyes Through Articular Cartilage in Vivo. *J Bone Joint Surg Am* **44**, 456-463.

37. Brower, T.D. & Hsu, W.Y. (1969) Normal articular cartilage. *Clin Orthop Relat Res* **64**, 9-17.

38. Brunner, D., Frank, J., Appl, H., Schoffl, H., Pfaller, W. & Gstraunthaler, G. (2010) Serum-free cell culture: the serum-free media interactive online database. *Altex* **27**, 53-62.

39. Buckley, C.T. & Kelly, D.J. (2012) Expansion in the presence of FGF-2 enhances the functional development of cartilaginous tissues engineered using infrapatellar fat pad derived MSCs. *J Mech Behav Biomed Mater* **11**, 102-111.

40. Buckwalter, J.A. (1998) Articular cartilage: injuries and potential for healing. *J Orthop Sports Phys Ther* **28**, 192-202.

41. Buckwalter, J.A. (2002) Articular cartilage injuries. *Clin Orthop Relat Res*, 21-37.

42. Buckwalter, J.A. & Lane, N.E. (1997) Athletics and osteoarthritis. *Am J Sports Med* **25**, 873-881.

43. Buckwalter, J.A. & Mankin, H.J. (1998) Articular cartilage: tissue design and chondrocyte-matrix interactions. *Instr Course Lect* **47**, 477-486.

44. Buckwalter, J.A., Martin, J. & H.J., M. (2000) Synovial joint degeneration and the syndrome of osteoarthritis. *Instr Course Lect.* **49**, 481-489.

45. Buckwalter, J.A., Mow, V.C. & Ratcliffe, A. (1994) Restoration of Injured or Degenerated Articular Cartilage. *J Am Acad Orthop Surg* **2**, 192-201.

46. Buckwalter, J.A., Rosenberg, L.C. & Tang, L.H. (1984) The effect of link protein on proteoglycan aggregate structure. An electron microscopic study of the molecular architecture and dimensions of proteoglycan aggregates reassembled from the proteoglycan monomers and link proteins of bovine fetal epiphyseal cartilage. *J Biol Chem* **259**, 5361-5363.

47. Bujia, J., Sittinger, M., Hammer, C. & Burmester, G. (1994) [Culture of human cartilage tissue using a perfusion chamber]. *Laryngorhinootologie* **73**, 577-580.

48. Bush, P.G. & Hall, A.C. (2003) The volume and morphology of chondrocytes within non-degenerate and degenerate human articular cartilage. *Osteoarthritis Cartilage* **11**, 242-251.

49. Caligaris, M. & Ateshian, G.A. (2008) Effects of sustained interstitial fluid pressurization under migrating contact area, and boundary lubrication by synovial fluid, on cartilage friction. *Osteoarthritis Cartilage* **16**, 1220-1227.

50. Campbell, M.A. & Handley, C.J. (1987) The effect of retinoic acid on proteoglycan turnover in bovine articular cartilage cultures. *Arch Biochem Biophys* **258**, 143-155.

51. Campbell, M.A., Handley, C.J. & D'Souza, S.E. (1989) Turnover of proteoglycans in articular-cartilage cultures. Characterization of proteoglycans released into the medium. *Biochem J* **259**, 21-25.

52. Campbell, S.S. & Tobler, I. (1984) Animal sleep: a review of sleep duration across phylogeny. *Neurosci Biobehav Rev* **8**, 269-300.

53. Candrian, C., Miot, S., Wolf, F., Bonacina, E., Dickinson, S., Wirz, D., Jakob, M., Valderrabano, V., Barbero, A. & Martin, I. (2010) Are ankle chondrocytes from damaged fragments a suitable cell source for cartilage repair? *Osteoarthritis Cartilage* **18**, 1067-1076.

54. Capito, R.M. & Spector, M. (2003) Scaffold-based articular cartilage repair. *IEEE Eng Med Biol Mag* **22**, 42-50.

55. Caron, J.P., Fernandes, J.C., Martel-Pelletier, J., Tardif, G., Mineau, F., Geng, C. & Pelletier, J.P. (1996) Chondroprotective effect of intraarticular injections of interleukin-1 receptor antagonist in experimental osteoarthritis. Suppression of collagenase-1 expression. *Arthritis Rheum* **39**, 1535-1544.

56. Caron, M.M., Emans, P.J., Coolsen, M.M., Voss, L., Surtel, D.A., Cremers, A., van Rhijn, L.W. & Welting, T.J. (2012) Redifferentiation of dedifferentiated human articular chondrocytes: comparison of 2D and 3D cultures. *Osteoarthritis Cartilage* **20**, 1170-1178.

57. Chang, C., Lauffenburger, D.A. & Morales, T.I. (2003) Motile chondrocytes from newborn calf: migration properties and synthesis of collagen II. *Osteoarthritis Cartilage* **11**, 603-612.

58. Chang, R.W., Falconer, J., Stulberg, S.D., Arnold, W.J., Manheim, L.M. & Dyer, A.R. (1993) A randomized, controlled trial of arthroscopic surgery versus closed-needle joint lavage for patients with osteoarthritis of the knee. *Arthritis Rheum* **36**, 289-296.

59. Chen, C.T., Burton-Wurster, N., Borden, C., Hueffer, K., Bloom, S.E. & Lust, G. (2001) Chondrocyte necrosis and apoptosis in impact damaged articular cartilage. *J Orthop Res* **19**, 703-711.

60. Chen, F.S., Frenkel, S.R. & Di Cesare, P.E. (1999) Repair of articular cartilage defects: part II. Treatment options. *Am J Orthop (Belle Mead NJ)* **28**, 88-96.

61. Cherubino, P., Grassi, F.A., Bulgheroni, P. & Ronga, M. (2003) Autologous chondrocyte implantation using a bilayer collagen membrane: a preliminary report. *J Orthop Surg (Hong Kong)* **11**, 10-15.

62. Chia, S.L., Sawaji, Y., Burleigh, A., McLean, C., Inglis, J., Saklatvala, J. & Vincent, T. (2009) Fibroblast growth factor 2 is an intrinsic chondroprotective agent that suppresses ADAMTS-5 and delays cartilage degradation in murine osteoarthritis. *Arthritis Rheum* **60**, 2019-2027.

63. Chikanza, I. & Fernandes, L. (2000) Novel strategies for the treatment of osteoarthritis. *Expert Opin Investig Drugs* **9**, 1499-1510.

64. Chong, K.W., Chanalaris, A., Burleigh, A., Jin, H., Watt, F.E., Saklatvala, J. & Vincent, T.L. (2013) Fibroblast growth factor 2 drives changes in gene expression following injury to murine cartilage in vitro and in vivo. *Arthritis Rheum* **65**, 2346-2355.

65. Chowdhury, T.T., Appleby, R.N., Salter, D.M., Bader, D.A. & Lee, D.A. (2006) Integrin-mediated mechanotransduction in IL-1 beta stimulated chondrocytes. *Biomech Model Mechanobiol* **5**, 192-201.

66. Cole, B.J., Pascual-Garrido, C. & Grumet, R.C. (2009) Surgical management of articular cartilage defects in the knee. *J Bone Joint Surg Am* **91**, 1778-1790.

67. Colombo, C., Butler, M., O'Byrne, E., Hickman, L., Swartzendruber, D., Selwyn, M. & Steinetz, B. (1983) A new model of osteoarthritis in rabbits. I. Development of knee joint pathology following lateral meniscectomy and section of the fibular collateral and sesamoid ligaments. *Arthritis Rheum* **26**, 875-886.

68. Coutts, R.D., Healey, R.M., Ostrander, R., Sah, R.L., Goomer, R. & Amiel, D. (2001) Matrices for cartilage repair. *Clin Orthop Relat Res*, S271-279.

69. Darling, E.M., Hu, J.C. & Athanasiou, K.A. (2004) Zonal and topographical differences in articular cartilage gene expression. *J Orthop Res* **22**, 1182-1187.

70. Davis, A.M. & MacKay, C. (2013) Osteoarthritis year in review: outcome of rehabilitation. *Osteoarthritis Cartilage* **21**, 1414-1424.

71. Davisson, T., Sah, R.L. & Ratcliffe, A. (2002) Perfusion increases cell content and matrix synthesis in chondrocyte three-dimensional cultures. *Tissue Eng* **8**, 807-816.

72. Demarteau, O., Wendt, D., Braccini, A., Jakob, M., Schafer, D., Heberer, M. & Martin, I. (2003) Dynamic compression of cartilage constructs engineered from expanded human articular chondrocytes. *Biochem Biophys Res Commun* **310**, 580-588.

73. Detterline, A.J., Goldberg, S., Bach, B.R., Jr. & Cole, B.J. (2005) Treatment options for articular cartilage defects of the knee. *Orthop Nurs* **24**, 361-366; quiz 367-368.

74. Dickhut, A., Dexheimer, V., Martin, K., Lauinger, R., Heisel, C. & Richter, W. (2010) Chondrogenesis of human mesenchymal stem cells by local transforming growth factor-beta delivery in a biphasic resorbable carrier. *Tissue Eng Part A* **16**, 453-464.

75. Diekman, B.O., Estes, B.T. & Guilak, F. (2010) The effects of BMP6 overexpression on adipose stem cell chondrogenesis: Interactions with dexamethasone and exogenous growth factors. *J Biomed Mater Res A* **93**, 994-1003.

76. DiMicco, M.A., Patwari, P., Siparsky, P.N., Kumar, S., Pratta, M.A., Lark, M.W., Kim, Y.J. & Grodzinsky, A.J. (2004) Mechanisms and kinetics of glycosaminoglycan release following in vitro cartilage injury. *Arthritis Rheum* **50**, 840-848.

77. Donohue, J.M., Buss, D., Oegema, T.R., Jr. & Thompson, R.C., Jr. (1983) The effects of indirect blunt trauma on adult canine articular cartilage. *J Bone Joint Surg Am* **65**, 948-957.

78. Dragoo, J.L., Samimi, B., Zhu, M., Hame, S.L., Thomas, B.J., Lieberman, J.R., Hedrick, M.H. & Benhaim, P. (2003) Tissue-engineered cartilage and bone using stem cells from human infrapatellar fat pads. *J Bone Joint Surg Br* **85**, 740-747.

79. Drobnic, M., Mars, T., Alibegovic, A., Bole, V., Balazic, J., Grubic, Z. & Brecelj, J. (2005) Viability of human chondrocytes in an ex vivo model in relation to temperature and cartilage depth. *Folia Biol (Praha)* **51**, 103-108.

80. Elder, S.H., Kimura, J.H., Soslowsky, L.J., Lavagnino, M. & Goldstein, S.A. (2000) Effect of compressive loading on chondrocyte differentiation in agarose cultures of chick limb-bud cells. *J Orthop Res* **18**, 78-86.

81. Enders, J.T., Otto, T.J., Peters, H.C., Wu, J., Hardouin, S., Moed, B.R. & Zhang, Z. (2010) A model for studying human articular cartilage integration in vitro. *J Biomed Mater Res A* **94**, 509-514.

82. Falah, M., Nierenberg, G., Soudry, M., Hayden, M. & Volpin, G. (2010) Treatment of articular cartilage lesions of the knee. *Int Orthop* **34**, 621-630.

83. Fan, J., Varshney, R.R., Ren, L., Cai, D. & Wang, D.A. (2009) Synovium-derived mesenchymal stem cells: a new cell source for musculoskeletal regeneration. *Tissue Eng Part B Rev* **15**, 75-86.

84. Farhan-Alanie, M.M. & Hall, A.C. (2014) Temperature changes and chondrocyte death during drilling in a bovine cartilage model and chondroprotection by modified irrigation solutions. *Int Orthop*.

85. Farndale, R.W., Buttle, D.J. & Barrett, A.J. (1986) Improved quantitation and discrimination of sulphated glycosaminoglycans by use of dimethylmethylene blue. *Biochim Biophys Acta* **883**, 173-177.

86. Farndale, R.W., Sayers, C.A. & Barrett, A.J. (1982) A direct spectrophotometric microassay for sulfated glycosaminoglycans in cartilage cultures. *Connect Tissue Res* **9**, 247-248.

87. Fassler, R., Schnegelsberg, P.N., Dausman, J., Shinya, T., Muragaki, Y., McCarthy, M.T., Olsen, B.R. & Jaenisch, R. (1994) Mice lacking alpha 1 (IX) collagen develop noninflammatory degenerative joint disease. *Proc Natl Acad Sci U S A* **91**, 5070-5074.

88. Fernandes, J.C., Martel-Pelletier, J. & Pelletier, J.P. (2002) The role of cytokines in osteoarthritis pathophysiology. *Biorheology* **39**, 237-246.

89. Fitzgerald, J.B., Jin, M., Dean, D., Wood, D.J., Zheng, M.H. & Grodzinsky, A.J. (2004) Mechanical compression of cartilage explants induces multiple time-dependent gene expression patterns and involves intracellular calcium and cyclic AMP. *J Biol Chem* **279**, 19502-19511.

90. Forsey, R.W., Tare, R., Oreffo, R.O. & Chaudhuri, J.B. (2012) Perfusion bioreactor studies of chondrocyte growth in alginate-chitosan capsules. *Biotechnol Appl Biochem* **59**, 142-152.

91. Fransen, M., McConnell, S. & Bell, M. (2002) Therapeutic exercise for people with osteoarthritis of the hip or knee. A systematic review. *J Rheumatol* **29**, 1737-1745.

92. Frenkel, S.R., Clancy, R.M., Ricci, J.L., Di Cesare, P.E., Rediske, J.J. & Abramson, S.B. (1996) Effects of nitric oxide on chondrocyte migration, adhesion, and cytoskeletal assembly. *Arthritis Rheum* **39**, 1905-1912.

93. Fukumoto, T., Sperling, J.W., Sanyal, A., Fitzsimmons, J.S., Reinholz, G.G., Conover, C.A. & O'Driscoll, S.W. (2003) Combined effects of insulin-like growth factor-1 and transforming growth factor-beta1 on periosteal mesenchymal cells during chondrogenesis in vitro. *Osteoarthritis Cartilage* **11**, 55-64.

94. Furukawa, T., Eyre, D.R., Koide, S. & Glimcher, M.J. (1980) Biochemical studies on repair cartilage resurfacing experimental defects in the rabbit knee. *J Bone Joint Surg Am* **62**, 79-89.

95. Gabriel, N., Innes, J.F., Caterson, B. & Vaughan-Thomas, A. (2010) Development of an in vitro model of feline cartilage degradation. *J Feline Med Surg* **12**, 614-620.

96. Galois, L., Etienne, S., Grossin, L., Cournil, C., Pinzano, A., Netter, P., Mainard, D. & Gillet, P. (2003) Moderate-impact exercise is associated with decreased severity of experimental osteoarthritis in rats. *Rheumatology (Oxford)* **42**, 692-693; author reply 693-694.

97. Galois, L., Etienne, S., Grossin, L., Watrin-Pinzano, A., Cournil-Henrionnet, C., Loeuille, D., Netter, P., Mainard, D. & Gillet, P. (2004) Dose-response relationship for exercise on severity of experimental osteoarthritis in rats: a pilot study. *Osteoarthritis Cartilage* **12**, 779-786.

98. Garcia, A.M., Frank, E.H., Grimshaw, P.E. & Grodzinsky, A.J. (1996) Contributions of fluid convection and electrical migration to transport in cartilage: relevance to loading. *Arch Biochem Biophys* **333**, 317-325.

99. Garcia, A.M., Lark, M.W., Trippel, S.B. & Grodzinsky, A.J. (1998) Transport of tissue inhibitor of metalloproteinases-1 through cartilage: contributions of fluid flow and electrical migration. *J Orthop Res* **16**, 734-742.

100. Garcia, M. & Knight, M.M. (2010) Cyclic loading opens hemichannels to release ATP as part of a chondrocyte mechanotransduction pathway. *J Orthop Res* **28**, 510-515.

101. Gelse, K., Poschl, E. & Aigner, T. (2003) Collagens - structure, function, and biosynthesis. *Advanced Drug Delivery Review* **55**, 1531-1546.

102. Gemmiti, C.V. & Guldberg, R.E. (2009) Shear stress magnitude and duration modulates matrix composition and tensile mechanical properties in engineered cartilaginous tissue. *Biotechnol Bioeng* **104**, 809-820.

103. Getgood, A., Bhullar, T.P.S. & Rushton, N. (2009) Current concepts in articular cartilage repair. *Orthop. Trauma* **23**, 189-200.

104. Glowacki, J., Mizuno, S. & Greenberger, J.S. (1998) Perfusion enhances functions of bone marrow stromal cells in three-dimensional culture. *Cell Transplant* **7**, 319-326.

105. Glowacki, J., Trepman, E. & Folkman, J. (1983) Cell shape and phenotypic expression in chondrocytes. *Proc Soc Exp Biol Med* **172**, 93-98.

106. Gosiewska, A., Rezania, A., Dhanaraj, S., Vyakarnam, M., Zhou, J., Burtis, D., Brown, L., Kong, W., Zimmerman, M. & Geesin, J.C. (2001) Development of a three-dimensional transmigration assay for testing cell--polymer interactions for tissue engineering applications. *Tissue Eng* **7**, 267-277.

107. Grad, S., Eglin, D., Alini, M. & Stoddart, M.J. (2011) Physical stimulation of chondrogenic cells in vitro: a review. *Clin Orthop Relat Res* **469**, 2764-2772.

108. Grad, S., Gogolewski, S., Alini, M. & Wimmer, M.A. (2006a) Effects of simple and complex motion patterns on gene expression of chondrocytes seeded in 3D scaffolds. *Tissue Eng* **12**, 3171-3179.

109. Grad, S., Lee, C.R., Wimmer, M.A. & Alini, M. (2006b) Chondrocyte gene expression under applied surface motion. *Biorheology* **43**, 259-269.

110. Grenier, S., Bhargava, M.M. & Torzilli, P.A. (2014) An in vitro model for the pathological degradation of articular cartilage in osteoarthritis. *J Biomech* **47**, 645-652.

111. Gruber, J., Vincent, T.L., Hermansson, M., Bolton, M., Wait, R. & Saklatvala, J. (2004) Induction of interleukin-1 in articular cartilage by explantation and cutting. *Arthritis Rheum* **50**, 2539-2546.

112. Grumbles, R.M., Howell, D.S., Howard, G.A., Roos, B.A., Setton, L.A., Mow, V.C., Ratcliffe, A., Muller, F.J. & Altman, R.D. (1995) Cartilage metalloproteases in disuse atrophy. *J Rheumatol Suppl* **43**, 146-148.

113. Guilak, F., Awad, H.A., Fermor, B., Leddy, H.A. & Gimble, J.M. (2004) Adipose-derived adult stem cells for cartilage tissue engineering. *Biorheology* **41**, 389-399.

114. Guilak, F., Meyer, B.C., Ratcliffe, A. & Mow, V.C. (1994) The effects of matrix compression on proteoglycan metabolism in articular cartilage explants. *Osteoarthritis Cartilage* **2**, 91-101.

115. Guingamp, C., Gegout-Pottie, P., Philippe, L., Terlain, B., Netter, P. & Gillet, P. (1997) Mono-iodoacetate-induced experimental osteoarthritis: a dose-response study of loss of mobility, morphology, and biochemistry. *Arthritis Rheum* **40**, 1670-1679.

116. Gunsilius, E., Petzer, A., Stockhammer, G., Nussbaumer, W., Schumacher, P., Clausen, J. & Gastl, G. (2000) Thrombocytes are the major source for soluble vascular endothelial growth factor in peripheral blood. *Oncology* **58**, 169-174.

117. Haapala, J., Arokoski, J.P., Hyttinen, M.M., Lammi, M., Tammi, M., Kovanen, V., Helminen, H.J. & Kiviranta, I. (1999) Remobilization does not fully restore immobilization induced articular cartilage atrophy. *Clin Orthop Relat Res*, 218-229.

118. Hall, A.C., Urban, J.P. & Gehl, K.A. (1991) The effects of hydrostatic pressure on matrix synthesis in articular cartilage. *J Orthop Res* **9**, 1-10.

119. Hangody, L., Kish, G., Modis, L., Szerb, I., Gaspar, L., Dioszegi, Z. & Kendik, Z. (2001) Mosaicplasty for the treatment of osteochondritis dissecans of the talus: two to seven year results in 36 patients. *Foot Ankle Int* **22**, 552-558.

120. Hardingham, T.E. & Fosang, A.J. (1995) The structure of aggrecan and its turnover in cartilage. *J Rheumatol Suppl* **43**, 86-90.

121. Harris, J.D., Siston, R.A., Pan, X. & Flanigan, D.C. (2010) Autologous chondrocyte implantation: a systematic review. *J Bone Joint Surg Am* **92**, 2220-2233.

122. Hayashi, K., Thabit, G., 3rd, Massa, K.L., Bogdanske, J.J., Cooley, A.J., Orwin, J.F. & Markel, M.D. (1997) The effect of thermal heating on the length and histologic properties of the glenohumeral joint capsule. *Am J Sports Med* **25**, 107-112.

123. Heath, C.A. & Magari, S.R. (1996) Mini-review: Mechanical factors affecting cartilage regeneration in vitro. *Biotechnol Bioeng* **50**, 430-437.

124. Heimer, R., Sporer, R., Molinaro, L., Hansen, L. & Laposata, E. (1992) Normal human synovial fluid and articular cartilage contain similar intact proteoglycans. *Lab Invest* **66**, 701-707.

125. Helmark, I.C., Mikkelsen, U.R., Borglum, J., Rothe, A., Petersen, M.C., Andersen, O., Langberg, H. & Kjaer, M. (2010) Exercise increases interleukin-10 levels both intraarticularly and peri-synovially in patients with knee osteoarthritis: a randomized controlled trial. *Arthritis Res Ther* **12**, R126.

126. Helminen, H.J., Kiraly, K., Pelttari, A., Tammi, M.I., Vandenberg, P., Pereira, R., Dhulipala, R., Khillan, J.S., Ala-Kokko, L., Hume, E.L. & et al. (1993) An inbred line of transgenic mice expressing an internally deleted gene for type II procollagen (COL2A1). Young mice have a variable phenotype of a chondrodysplasia and older mice have osteoarthritic changes in joints. *J Clin Invest* **92**, 582-595.

127. Henrotin, Y.E., Bruckner, P. & Pujol, J.P. (2003) The role of reactive oxygen species in homeostasis and degradation of cartilage. *Osteoarthritis Cartilage* **11**, 747-755.

128. Hildebrand, A., Romaris, M., Rasmussen, L.M., Heinegard, D., Twardzik, D.R., Border, W.A. & Ruoslahti, E. (1994) Interaction of the small interstitial proteoglycans biglycan, decorin and fibromodulin with transforming growth factor beta. *Biochem J* **302 (Pt 2)**, 527-534.

129. Hodge, W.A., Fijan, R.S., Carlson, K.L., Burgess, R.G., Harris, W.H. & Mann, R.W. (1986) Contact pressures in the human hip joint measured in vivo. *Proc Natl Acad Sci U S A* **83**, 2879-2883.

130. Hoemann, C.D., Sun, J., Chrzanowski, V. & Buschmann, M.D. (2002) A multivalent assay to detect glycosaminoglycan, protein, collagen, RNA, and DNA content in milligram samples of cartilage or hydrogel-based repair cartilage. *Anal Biochem* **300**, 1-10.

131. Holmdahl, D.E. & Ingelmark, B.E. (1951) The contact between the articular cartilage and the medullary cavities of the bones. *Acta Anat (Basel)* **12**, 341-349.

132. Huang, F.S., Simonian, P.T., Norman, A.G. & Clark, J.M. (2004) Effects of small incongruities in a sheep model of osteochondral autografting. *Am J Sports Med* **32**, 1842-1848.

133. Huang, J.S. & Huang, S.S. (1985) Role of growth factors in oncogenesis: growth factor-proto-oncogene pathways of mitogenesis. *Ciba Found Symp* **116**, 46-65.

134. Huber, M., Trattnig, S. & Lintner, F. (2000) Anatomy, biochemistry, and physiology of articular cartilage. *Invest Radiol* **35**, 573-580.

135. Humphries, J.D., Byron, A. & Humphries, M.J. (2006) Integrin ligands at a glance. *J Cell Sci* **119**, 3901-3903.

136. Hunter, C.J., Imler, S.M., Malaviya, P., Nerem, R.M. & Levenston, M.E. (2002) Mechanical compression alters gene expression and extracellular matrix synthesis by chondrocytes cultured in collagen I gels. *Biomaterials* **23**, 1249-1259.

137. Hunter, C.J., Mouw, J.K. & Levenston, M.E. (2004) Dynamic compression of chondrocyte-seeded fibrin gels: effects on matrix accumulation and mechanical stiffness. *Osteoarthritis Cartilage* **12**, 117-130.

138. Huntley, J.S., Bush, P.G., McBirnie, J.M., Simpson, A.H. & Hall, A.C. (2005) Chondrocyte death associated with human femoral osteochondral harvest as performed for mosaicplasty. *J Bone Joint Surg Am* **87**, 351-360.

139. Hunziker, E.B. (2001) Growth-factor-induced healing of partial-thickness defects in adult articular cartilage. *Osteoarthritis Cartilage* **9**, 22-32.

140. Hunziker, E.B. (2002) Articular cartilage repair: basic science and clinical progress. A review of the current status and prospects. *Osteoarthritis Cartilage* **10**, 432-463.

141. Hunziker, E.B. (2009) The elusive path to cartilage regeneration. *Adv Mater* **21**, 3419-3424.

142. Hunziker, E.B. & Kapfinger, E. (1998) Removal of proteoglycans from the surface of defects in articular cartilage transiently enhances coverage by repair cells. *J Bone Joint Surg Br* **80**, 144-150.

143. Hunziker, E.B., Kapfinger, E. & Geiss, J. (2007) The structural architecture of adult mammalian articular cartilage evolves by a synchronized process of tissue resorption and neoformation during postnatal development. *Osteoarthritis Cartilage* **15**, 403-413.

144. Hunziker, E.B. & Quinn, T.M. (2003) Surgical removal of articular cartilage leads to loss of chondrocytes from cartilage bordering the wound edge. *J Bone Joint Surg Am* **85-A Suppl 2**, 85-92.

145. Hurtig, M., Pearce, S., Warren, S., Kalra, M. & Miniaci, A. (2001) Arthroscopic mosaic arthroplasty in the equine third carpal bone. *Vet Surg* **30**, 228-239.

146. Hutmacher, D.W. (2001) Scaffold design and fabrication technologies for engineering tissues--state of the art and future perspectives. *J Biomater Sci Polym Ed* **12**, 107-124.

147. Hynes, R.O. (2002) Integrins: bidirectional, allosteric signaling machines. *Cell* **110**, 673-687.

148. Imhof, H., Breitenseher, M., Kainberger, F., Rand, T. & Trattnig, S. (1999) Importance of subchondral bone to articular cartilage in health and disease. *Top Magn Reson Imaging* **10**, 180-192.

149. Jackson, D.W., Lalor, P.A., Aberman, H.M. & Simon, T.M. (2001) Spontaneous repair of full-thickness defects of articular cartilage in a goat model. A preliminary study. *J Bone Joint Surg Am* **83-a**, 53-64.

150. Jamieson, A.M., Blackwell, J., Reihanian, H., Ohno, H., Gupta, R., Carrino, D.A., Caplan, A.I., Tang, L.H. & Rosenberg, L.C. (1987) Thermal and solvent stability of proteoglycan aggregates by quasielastic laser light-scattering. *Carbohydr Res* **160**, 329-341.

151. Jansen, M.J., Viechtbauer, W., Lenssen, A.F., Hendriks, E.J. & de Bie, R.A. (2011) Strength training alone, exercise therapy alone, and exercise therapy with passive manual mobilisation each reduce pain and disability in people with knee osteoarthritis: a systematic review. *J Physiother* **57**, 11-20.

152. Jeffery, A.K., Blunn, G.W., Archer, C.W. & Bentley, G. (1991) Three-dimensional collagen architecture in bovine articular cartilage. *J Bone Joint Surg Br* **73**, 795-801.

153. Jeffrey, J.E. & Aspden, R.M. (2006) The biophysical effects of a single impact load on human and bovine articular cartilage. *Proc Inst Mech Eng H* **220**, 677-686.

154. Jeffrey, J.E., Gregory, D.W. & Aspden, R.M. (1995) Matrix damage and chondrocyte viability following a single impact load on articular cartilage. *Arch Biochem Biophys* **322**, 87-96.

155. Jelic, M., Pecina, M., Haspl, M., Kos, J., Taylor, K., Maticic, D., McCartney, J., Yin, S., Rueger, D. & Vukicevic, S. (2001) Regeneration of articular cartilage chondral defects by osteogenic protein-1 (bone morphogenetic protein-7) in sheep. *Growth Factors* **19**, 101-113.

156. Jim, B., Steffen, T., Moir, J., Roughley, P. & Haglund, L. (2011) Development of an intact intervertebral disc organ culture system in which degeneration can be induced as a prelude to studying repair potential. *Eur Spine J* **20**, 1244-1254.

157. Jin, M., Frank, E.H., Quinn, T.M., Hunziker, E.B. & Grodzinsky, A.J. (2001) Tissue shear deformation stimulates proteoglycan and protein biosynthesis in bovine cartilage explants. *Arch Biochem Biophys* **395**, 41-48.

158. Jordan, K.M., Arden, N.K., Doherty, M., Bannwarth, B., Bijlsma, J.W., Dieppe, P., Gunther, K., Hauselmann, H., Herrero-Beaumont, G., Kaklamanis, P., Lohmander, S., Leeb, B., Lequesne, M., Mazieres, B., Martin-Mola, E., Pavelka, K., Pendleton, A., Punzi, L., Serni, U., Swoboda, B., Verbruggen, G., Zimmerman-Gorska, I. & Dougados, M. (2003) EULAR Recommendations 2003: an evidence based approach to the management of knee osteoarthritis: Report of a Task Force of the Standing Committee for International Clinical Studies Including Therapeutic Trials (ESCISIT). *Ann Rheum Dis* **62**, 1145-1155.

159. Julkunen, P., Iivarinen, J., Brama, P.A., Arokoski, J., Jurvelin, J.S. & Helminen, H.J. (2010) Maturation of collagen fibril network structure in tibial and femoral cartilage of rabbits. *Osteoarthritis Cartilage* **18**, 406-415.

160. Jurgensen, K., Aeschlimann, D., Cavin, V., Genge, M. & Hunziker, E.B. (1997) A new biological glue for cartilage-cartilage interfaces: tissue transglutaminase. *J Bone Joint Surg Am* **79**, 185-193.

161. Jurvelin, J., Kiviranta, I., Tammi, M. & Helminen, J.H. (1986) Softening of canine articular cartilage after immobilization of the knee joint. *Clin Orthop Relat Res*, 246-252.

162. Karsdal, M.A., Byrjalsen, I., Henriksen, K., Riis, B.J., Lau, E.M., Arnold, M. & Christiansen, C. (2010) The effect of oral salmon calcitonin delivered with 5-CNAC on bone and cartilage degradation in osteoarthritic patients: a 14-day randomized study. *Osteoarthritis Cartilage* **18**, 150-159.

163. Kelly, T.A., Ng, K.W., Wang, C.C., Ateshian, G.A. & Hung, C.T. (2006) Spatial and temporal development of chondrocyte-seeded agarose constructs in free-swelling and dynamically loaded cultures. *J Biomech* **39**, 1489-1497.

164. Kiani, C., Chen, L., Wu, Y.J., Yee, A.J. & Yang, B.B. (2002) Structure and function of aggrecan. *Cell Res* **12**, 19-32.

165. Kim, H.K., Moran, M.E. & Salter, R.B. (1991) The potential for regeneration of articular cartilage in defects created by chondral shaving and subchondral abrasion. An experimental investigation in rabbits. *J Bone Joint Surg Am* **73**, 1301-1315.

166. Kim, W., Vacanti, J.P., Mooney, D., Upton, J., Ibarra, C. & Vacanti, C.A. (1996) Functional Viability of Chondrocytes Stored at 4 degrees C. *Tissue Eng* **2**, 75-81.

167. Kisiday, J.D., Frisbie, D.D., McIlwraith, C.W. & Grodzinsky, A.J. (2009) Dynamic compression stimulates proteoglycan synthesis by mesenchymal stem cells in the absence of chondrogenic cytokines. *Tissue Eng Part A* **15**, 2817-2824.

168. Kisiday, J.D., Jin, M., DiMicco, M.A., Kurz, B. & Grodzinsky, A.J. (2004) Effects of dynamic compressive loading on chondrocyte biosynthesis in self-assembling peptide scaffolds. *J Biomech* **37**, 595-604.

169. Kiviranta, I., Tammi, M., Jurvelin, J., Arokoski, J., Saamanen, A.M. & Helminen, H.J. (1992) Articular cartilage thickness and glycosaminoglycan distribution in the canine knee joint after strenuous running exercise. *Clin Orthop Relat Res*, 302-308.

170. Kiviranta, I., Tammi, M., Jurvelin, J., Saamanen, A.M. & Helminen, H.J. (1988) Moderate running exercise augments glycosaminoglycans and thickness of articular cartilage in the knee joint of young beagle dogs. *J Orthop Res* **6**, 188-195.

171. Kock, L., van Donkelaar, C.C. & Ito, K. (2012) Tissue engineering of functional articular cartilage: the current status. *Cell Tissue Res* **347**, 613-627.

172. Kon, E., Gobbi, A., Filardo, G., Delcogliano, M., Zaffagnini, S. & Marcacci, M. (2009) Arthroscopic second-generation autologous chondrocyte implantation compared with microfracture for chondral lesions of the knee: prospective nonrandomized study at 5 years. *Am J Sports Med* **37**, 33-41.

173. Korecki, C.L., MacLean, J.J. & Iatridis, J.C. (2007) Characterization of an in vitro intervertebral disc organ culture system. *Eur Spine J* **16**, 1029-1037.

174. Krishnan, R., Kopacz, M. & Ateshian, G.A. (2004) Experimental verification of the role of interstitial fluid pressurization in cartilage lubrication. *J Orthop Res* **22**, 565-570.

175. Kubota, K., Iseki, S., Kuroda, S., Oida, S., Iimura, T., Duarte, W.R., Ohya, K., Ishikawa, I. & Kasugai, S. (2002) Synergistic effect of fibroblast growth factor-4 in ectopic bone formation induced by bone morphogenetic protein-2. *Bone* **31**, 465-471.

176. Kurz, B., Jin, M., Patwari, P., Cheng, D.M., Lark, M.W. & Grodzinsky, A.J. (2001) Biosynthetic response and mechanical properties of articular cartilage after injurious compression. *J Orthop Res* **19**, 1140-1146.

177. Laprell, H. & Petersen, W. (2001) Autologous osteochondral transplantation using the diamond bone-cutting system (DBCS): 6-12 years' follow-up of 35 patients with osteochondral defects at the knee joint. *Arch Orthop Trauma Surg* **121**, 248-253.

178. Lee, C., Grad, S., Wimmer, M. & Alini, M. (2006a) The influence of mechanical stimuli on articular cartilage tissue engineering. *Tissue Engineering* **2**, 1-20.

179. Lee, C.M., Kisiday, J.D., McIlwraith, C.W., Grodzinsky, A.J. & Frisbie, D.D. (2013) Development of an in vitro model of injury-induced osteoarthritis in cartilage explants from adult horses through application of single-impact compressive overload. *Am J Vet Res* **74**, 40-47.

180. Lee, C.R., Iatridis, J.C., Poveda, L. & Alini, M. (2006b) In vitro organ culture of the bovine intervertebral disc: effects of vertebral endplate and potential for mechanobiology studies. *Spine* **31**, 515-522.

181. Lee, K., Silva, E.A. & Mooney, D.J. (2011a) Growth factor delivery-based tissue engineering: general approaches and a review of recent developments. *J R Soc Interface* **8**, 153-170.

182. Lee, T.J., Bhang, S.H., La, W.G., Yang, H.S., Seong, J.Y., Lee, H., Im, G.I., Lee, S.H. & Kim, B.S. (2011b) Spinner-flask culture induces redifferentiation of de-differentiated chondrocytes. *Biotechnol Lett* **33**, 829-836.

183. Leong, D.J., Hardin, J.A., Cobelli, N.J. & Sun, H.B. (2011) Mechanotransduction and cartilage integrity. *Ann N Y Acad Sci* **1240**, 32-37.

184. Lewis, P.N., Pinali, C., Young, R.D., Meek, K.M., Quantock, A.J. & Knupp, C. (2010) Structural interactions between collagen and proteoglycans are elucidated by three-dimensional electron tomography of bovine cornea. *Structure* **18**, 239-245.

185. Lewis, R.J., MacFarland, A.K., Anandavijayan, S. & Aspden, R.M. (1998) Material properties and biosynthetic activity of articular cartilage from the bovine carpo-metacarpal joint. *Osteoarthritis Cartilage* **6**, 383-392.

186. Li, D., Yuan, Q. & Wang, W. (2012a) The role of telomeres in musculoskeletal diseases. *J Int Med Res* **40**, 1242-1250.

187. Li, K.W., Wang, A.S. & Sah, R.L. (2003) Microenvironment regulation of extracellular signal-regulated kinase activity in chondrocytes: effects of culture configuration, interleukin-1, and compressive stress. *Arthritis Rheum* **48**, 689-699.

188. Li, X., Ellman, M.B., Kroin, J.S., Chen, D., Yan, D., Mikecz, K., Ranjan, K.C., Xiao, G., Stein, G.S., Kim, S.G., Cole, B., van Wijnen, A.J. & Im, H.J. (2012b) Species-specific biological effects of FGF-2 in articular cartilage: implication for distinct roles within the FGF receptor family. *J Cell Biochem* **113**, 2532-2542.

189. Lin, G., Garcia, M., Ning, H., Banie, L., Guo, Y.L., Lue, T.F. & Lin, C.S. (2008) Defining stem and progenitor cells within adipose tissue. *Stem Cells Dev* **17**, 1053-1063.

190. Lin, S.J., Hsiao, C.Y., Sun, Y., Lo, W., Lin, W.C., Jan, G.J., Jee, S.H. & Dong, C.Y. (2005) Monitoring the thermally induced structural transitions of collagen by use of second-harmonic generation microscopy. *Opt Lett* **30**, 622-624.

191. Lincoln, C.K. & Gabridge, M.G. (1998) Cell culture contamination: sources, consequences, prevention, and elimination. *Methods Cell Biol* **57**, 49-65.

192. Lindahl, U. & Hook, M. (1978) Glycosaminoglycans and their binding to biological macromolecules. *Annu Rev Biochem* **47**, 385-417.

193. Lindhorst, E., Vail, T.P., Guilak, F., Wang, H., Setton, L.A., Vilim, V. & Kraus, V.B. (2000) Longitudinal characterization of synovial fluid biomarkers in the canine meniscectomy model of osteoarthritis. *J Orthop Res* **18**, 269-280.

194. Loening, A.M., James, I.E., Levenston, M.E., Badger, A.M., Frank, E.H., Kurz, B., Nuttall, M.E., Hung, H.H., Blake, S.M., Grodzinsky, A.J. & Lark, M.W. (2000) Injurious mechanical compression of bovine articular cartilage induces chondrocyte apoptosis. *Arch Biochem Biophys* **381**, 205-212.

195. Lotz, M. (2012) Osteoarthritis year 2011 in review: biology. *Osteoarthritis Cartilage* **20**, 192-196.

196. Lotz, M., Hashimoto, S. & Kuhn, K. (1999) Mechanisms of chondrocyte apoptosis. *Osteoarthritis Cartilage* **7**, 389-391.

197. Lotz, M. & Loeser, R.F. (2012) Effects of aging on articular cartilage homeostasis. *Bone* **51**, 241-248.

198. Lovett, M., Rockwood, D., Baryshyan, A. & Kaplan, D.L. (2010) Simple modular bioreactors for tissue engineering: a system for characterization of oxygen gradients, human mesenchymal stem cell differentiation, and prevascularization. *Tissue Eng Part C Methods* **16**, 1565-1573.

199. Luo, Z.J. & Seedhom, B.B. (2007) Light and low-frequency pulsatile hydrostatic pressure enhances extracellular matrix formation by bone marrow mesenchymal cells: an in-vitro study with special reference to cartilage repair. *Proc Inst Mech Eng H* **221**, 499-507.

200. Malaviya, P. & Nerem, R.M. (2002) Fluid-induced shear stress stimulates chondrocyte proliferation partially mediated via TGF-beta1. *Tissue Eng* **8**, 581-590.

201. Malinin, T. & Ouellette, E.A. (2000) Articular cartilage nutrition is mediated by subchondral bone: a long-term autograft study in baboons. *Osteoarthritis Cartilage* **8**, 483-491.

202. Mankin, H.J. & Buckwalter, J.A. (1996) Restoration of the osteoarthrotic joint. *J Bone Joint Surg Am* **78**, 1-2.

203. Mankin, H.J., Mow, V.C., Buckwalter, J.A., Iannotti, J.P. & Ratcliffe, A. (1994) Form and function of articular cartilage. *American Academy of Orthopaedic Surgeons, Columbus, OH.*, 1-44.

204. Mankin, J.H., Jennings, C., Treadwell, B.V. & Trippel, S.B. (1991) Growth factors and articular cartilage. *J Rheumatol Suppl* **27**, 66-67.

205. Marcus, R.E. (1973) The effect of low oxygen concentration on growth, glycolysis, and sulfate incorporation by articular chondrocytes in monolayer culture. *Arthritis Rheum* **16**, 646-656.

206. Maroudas, A. (1979) Physico-chemical properties of articular cartilage. *Adult articular cartilage*, 215-290.

207. Maroudas, A., Bayliss, M.T., Uchitel-Kaushansky, N., Schneiderman, R. & Gilav, E. (1998) Aggrecan turnover in human articular cartilage: use of aspartic acid racemization as a marker of molecular age. *Arch Biochem Biophys* **350**, 61-71.

208. Maroudas, A. & Bullough, P. (1968) Permeability of articular cartilage. *Nature* **219**, 1260-1261.

209. Maroudas, A., Popper, O. & Grushko, G. (1992) Partition coefficients of IGF-1 between cartilage and external medium in the presence and absence of FCS. *Trans Am Orthop Res Soc* **16**, 398.

210. Martel-Pelletier, J., Boileau, C., Pelletier, J.P. & Roughley, P.J. (2008) Cartilage in normal and osteoarthritis conditions. *Best Pract Res Clin Rheumatol* **22**, 351-384.

211. Martel-Pelletier, J. & Pelletier, J.P. (2010) Is osteoarthritis a disease involving only cartilage or other articular tissues? *Joint diseases and related surgery* **21**, 2-14.

212. Martin, J.A. & Buckwalter, J.A. (2001) Roles of articular cartilage aging and chondrocyte senescence in the pathogenesis of osteoarthritis. *Iowa Orthop J* **21**, 1-7.

213. Martin, J.A. & Buckwalter, J.A. (2002a) Aging, articular cartilage chondrocyte senescence and osteoarthritis. *Biogerontology* **3**, 257-264.

214. Martin, J.A. & Buckwalter, J.A. (2002b) Aging, articular cartilage chondrocyte senescence and osteoarthritis. *Biogerontology* **3**, 257-264.

215. Matsiko, A., Levingstone, T.J. & O'Brien, F.J. (2013) Advanced Strategies for Articular Cartilage Defect Repair. *Materials* **6**, 637-668.

216. Mauck, R.L., Byers, B.A., Yuan, X. & Tuan, R.S. (2007) Regulation of cartilaginous ECM gene transcription by chondrocytes and MSCs in 3D culture in response to dynamic loading. *Biomech Model Mechanobiol* **6**, 113-125.

217. Mayne, R., Vail, M.S., Mayne, P.M. & Miller, E.J. (1976) Changes in type of collagen synthesized as clones of chick chondrocytes grow and eventually lose division capacity. *Proc Natl Acad Sci U S A* **73**, 1674-1678.

218. McGuire-Goldring, M.B., Meats, J.E., Wood, D.D., Ihrie, E.J., Ebsworth, N.M. & Russell, R.G. (1984) In vitro activation of human chondrocytes and synoviocytes by a human interleukin-1-like factor. *Arthritis Rheum* **27**, 654-662.

219. Mendler, M., Eich-Bender, S.G., Vaughan, L., Winterhalter, K.H. & Bruckner, P. (1989) Cartilage contains mixed fibrils of collagen types II, IX, and XI. *J Cell Biol* **108**, 191-197.

220. Micheli, L.J., Browne, J.E., Erggelet, C., Fu, F., Mandelbaum, B., Moseley, J.B. & Zurakowski, D. (2001) Autologous chondrocyte implantation of the knee: multicenter experience and minimum 3-year follow-up. *Clin J Sport Med* **11**, 223-228.

221. Mikic, B., Isenstein, A.L. & Chhabra, A. (2004) Mechanical modulation of cartilage structure and function during embryogenesis in the chick. *Ann Biomed Eng* **32**, 18-25.

222. Millward-Sadler, S.J., Khan, N.S., Bracher, M.G., Wright, M.O. & Salter, D.M. (2006) Roles for the interleukin-4 receptor and associated JAK/STAT proteins in human articular chondrocyte mechanotransduction. *Osteoarthritis Cartilage* **14**, 991-1001.

223. Minns, R.J. & Steven, F.S. (1977) The collagen fibril organization in human articular cartilage. *J Anat* **123**, 437-457.

224. Mital, M.A. & Millington, P.F. (1970) Osseous pathway of nutrition to articular cartilage of the human femoral head. *Lancet* **1**, 842.

225. Mithoefer, K., McAdams, T., Williams, R.J., Kreuz, P.C. & Mandelbaum, B.R. (2009) Clinical efficacy of the microfracture technique for articular

cartilage repair in the knee: an evidence-based systematic analysis. *Am J Sports Med* **37**, 2053-2063.

226. Mizrahi, J., Maroudas, A., Lanir, Y., Ziv, I. & Webber, T.J. (1986) The "instantaneous" deformation of cartilage: effects of collagen fiber orientation and osmotic stress. *Biorheology* **23**, 311-330.

227. Mobasheri, A., Lewis, R., Maxwell, J.E., Hill, C., Womack, M. & Barrett-Jolley, R. (2010) Characterization of a stretch-activated potassium channel in chondrocytes. *J Cell Physiol* **223**, 511-518.

228. Mollenhauer, J., Bee, J.A., Lizarbe, M.A. & von der Mark, K. (1984) Role of anchorin CII, a 31,000-mol-wt membrane protein, in the interaction of chondrocytes with type II collagen. *J Cell Biol* **98**, 1572-1579.

229. Moo, E.K., Osman, N.A. & Pingguan-Murphy, B. (2011) The metabolic dynamics of cartilage explants over a long-term culture period. *Clinics (Sao Paulo)* **66**, 1431-1436.

230. Morales, T.I. (2007) Chondrocyte moves: clever strategies? *Osteoarthritis Cartilage* **15**, 861-871.

231. Moseley, J.B., Jr., Wray, N.P., Kuykendall, D., Willis, K. & Landon, G. (1996) Arthroscopic treatment of osteoarthritis of the knee: a prospective, randomized, placebo-controlled trial. Results of a pilot study. *Am J Sports Med* **24**, 28-34.

232. Moskalewski, S. & Bator, S. (1985) Regenerating rib cartilage tentatively used as a source of chondrocytes for transplantation. *Arch Immunol Ther Exp (Warsz)* **33**, 685-692.

233. Mow, V.C., Holmes, M.H. & Lai, W.M. (1984) Fluid transport and mechanical properties of articular cartilage: a review. *J Biomech* **17**, 377-394.

234. Mow, V.C. & Lai, W.M. (1974) Some surface characteristics of articular cartilage. I. A scanning electron microscopy study and a theoretical model for the dynamic interaction of synovial fluid and articular cartilage. *J Biomech* **7**, 449-456.

235. Mow, V.C., Ratcliffe, A. & Poole, A.R. (1992) Cartilage and diarthrodial joints as paradigms for hierarchical materials and structures. *Biomaterials* **13**, 67-97.

236. Murata, M., Bonassar, L.J., Wright, M., Mankin, H.J. & Towle, C.A. (2003) A role for the interleukin-1 receptor in the pathway linking static mechanical compression to decreased proteoglycan synthesis in surface articular cartilage. *Arch Biochem Biophys* **413**, 229-235.

237. Murphy, C.M., Matsiko, A., Haugh, M.G., Gleeson, J.P. & O'Brien, F.J. (2012) Mesenchymal stem cell fate is regulated by the composition and mechanical properties of collagen-glycosaminoglycan scaffolds. *J Mech Behav Biomed Mater* **11**, 53-62.

238. Nakano, T., Thompson, J.R., Christopherson, R.J. & Aherne, F.X. (1986) Blood flow distribution in hind limb bones and joint cartilage from young growing pigs. *Can J Vet Res* **50**, 96-100.

239. Nastase, M.V., Young, M.F. & Schaefer, L. (2012) Biglycan: a multivalent proteoglycan providing structure and signals. *J Histochem Cytochem* **60**, 963-975.

240. Nicodemus, G.D. & Bryant, S.J. (2008) The role of hydrogel structure and dynamic loading on chondrocyte gene expression and matrix formation. *J Biomech* **41**, 1528-1536.

241. Nugent-Derfus, G.E., Takara, T., O'Neill J, K., Cahill, S.B., Gortz, S., Pong, T., Inoue, H., Aneloski, N.M., Wang, W.W., Vega, K.I., Klein, T.J., Hsieh-Bonassera, N.D., Bae, W.C., Burke, J.D., Bugbee, W.D. & Sah, R.L. (2007) Continuous passive motion applied to whole joints stimulates chondrocyte biosynthesis of PRG4. *Osteoarthritis Cartilage* **15**, 566-574.

242. Ogawa, R., Mizuno, S., Murphy, G.F. & Orgill, D.P. (2009) The effect of hydrostatic pressure on three-dimensional chondroinduction of human adipose-derived stem cells. *Tissue Eng Part A* **15**, 2937-2945.

243. Osborn, K.D., Trippel, S.B. & Mankin, H.J. (1989) Growth factor stimulation of adult articular cartilage. *J Orthop Res* **7**, 35-42.

244. Otterness, I.G., Eskra, J.D., Bliven, M.L., Shay, A.K., Pelletier, J.P. & Milici, A.J. (1998) Exercise protects against articular cartilage degeneration in the hamster. *Arthritis Rheum* **41**, 2068-2076.

245. Owens, B.D., Stickles, B.J., Balikian, P. & Busconi, B.D. (2002) Prospective analysis of radiofrequency versus mechanical debridement of isolated patellar chondral lesions. *Arthroscopy* **18**, 151-155.

246. Pacifici, M., Koyama, E., Shibukawa, Y., Wu, C., Tamamura, Y., Enomoto-Iwamoto, M. & Iwamoto, M. (2006) Cellular and molecular mechanisms of synovial joint and articular cartilage formation. *Ann N Y Acad Sci* **1068**, 74-86.

247. Pallante, A.L., Bae, W.C., Chen, A.C., Gortz, S., Bugbee, W.D. & Sah, R.L. (2009) Chondrocyte viability is higher after prolonged storage at 37 degrees C than at 4 degrees C for osteochondral grafts. *Am J Sports Med* **37 Suppl 1**, 24s-32s.

248. Palmoski, M., Perricone, E. & Brandt, K.D. (1979) Development and reversal of a proteoglycan aggregation defect in normal canine knee cartilage after immobilization. *Arthritis Rheum* **22**, 508-517.

249. Palmoski, M.J., Colyer, R.A. & Brandt, K.D. (1980) Joint motion in the absence of normal loading does not maintain normal articular cartilage. *Arthritis Rheum* **23**, 325-334.

250. Parkkinen, J.J., Ikonen, J., Lammi, M.J., Laakkonen, J., Tammi, M. & Helminen, H.J. (1993) Effects of cyclic hydrostatic pressure on proteoglycan synthesis in cultured chondrocytes and articular cartilage explants. *Arch Biochem Biophys* **300**, 458-465.

251. Peterson, L., Vasiliadis, H.S., Brittberg, M. & Lindahl, A. (2010) Autologous chondrocyte implantation: a long-term follow-up. *Am J Sports Med* **38**, 1117-1124.

252. Ponticiello, M.S., Schinagl, R.M., Kadiyala, S. & Barry, F.P. (2000) Gelatin-based resorbable sponge as a carrier matrix for human mesenchymal stem cells in cartilage regeneration therapy. *J Biomed Mater Res* **52**, 246-255.

253. Poole, A.R., Pidoux, I., Reiner, A. & Rosenberg, L. (1982) An immunoelectron microscope study of the organization of proteoglycan monomer, link protein, and collagen in the matrix of articular cartilage. *J Cell Biol* **93**, 921-937.

254. Posey, K.L. & Hecht, J.T. (2008) The role of cartilage oligomeric matrix protein (COMP) in skeletal disease. *Curr Drug Targets* **9**, 869-877.

255. Pun, S.Y., Teng, M.S. & Kim, H.T. (2006) Periodic rewetting enhances the viability of chondrocytes in human articular cartilage exposed to air. *J Bone Joint Surg Br* **88**, 1528-1532.

256. Rajpurohit, R., Koch, C.J., Tao, Z., Teixeira, C.M. & Shapiro, I.M. (1996) Adaptation of chondrocytes to low oxygen tension: relationship between hypoxia and cellular metabolism. *J Cell Physiol* **168**, 424-432.

257. Ramage, L., Nuki, G. & Salter, D.M. (2009) Signalling cascades in mechanotransduction: cell-matrix interactions and mechanical loading. *Scand J Med Sci Sports* **19**, 457-469.

258. Redler, I., Mow, V.C., Zimny, M.L. & Mansell, J. (1975) The ultrastructure and biomechanical significance of the tidemark of articular cartilage. *Clin Orthop Relat Res*, 357-362.

259. Redman, S.N., Dowthwaite, G.P., Thomson, B.M. & Archer, C.W. (2004) The cellular responses of articular cartilage to sharp and blunt trauma. *Osteoarthritis Cartilage* **12**, 106-116.

260. Redman, S.N., Oldfield, S.F. & Archer, C.W. (2005) Current strategies for articular cartilage repair. *Eur Cell Mater* **9**, 23-32; discussion 23-32.

261. Reginster, J.Y., Badurski, J., Bellamy, N., Bensen, W., Chapurlat, R., Chevalier, X., Christiansen, C., Genant, H., Navarro, F., Nasonov, E., Sambrook, P.N., Spector, T.D. & Cooper, C. (2013) Efficacy and safety of strontium ranelate in the treatment of knee osteoarthritis: results of a double-blind, randomised placebo-controlled trial. *Ann Rheum Dis* **72**, 179-186.

262. Responte, D.J., Lee, J.K., Hu, J.C. & Athanasiou, K.A. (2012) Biomechanics-driven chondrogenesis: from embryo to adult. *Faseb j* **26**, 3614-3624.

263. Roach, H.I. (1997) New aspects of endochondral ossification in the chick: chondrocyte apoptosis, bone formation by former chondrocytes, and acid phosphatase activity in the endochondral bone matrix. *J Bone Miner Res* **12**, 795-805.

264. Roach, H.I., Aigner, T. & Kouri, J.B. (2004) Chondroptosis: a variant of apoptotic cell death in chondrocytes? *Apoptosis* **9**, 265-277.

265. Roddy, K.A., Prendergast, P.J. & Murphy, P. (2011) Mechanical influences on morphogenesis of the knee joint revealed through morphological, molecular and computational analysis of immobilised embryos. *PLoS One* **6**, e17526.

266. Rogers, B.A., Murphy, C.L., Cannon, S.R. & Briggs, T.W. (2006) Topographical variation in glycosaminoglycan content in human articular cartilage. *J Bone Joint Surg Br* **88**, 1670-1674.

267. Rolauffs, B., Muehleman, C., Li, J., Kurz, B., Kuettner, K.E., Frank, E. & Grodzinsky, A.J. (2010) Vulnerability of the superficial zone of immature articular cartilage to compressive injury. *Arthritis Rheum* **62**, 3016-3027.

268. Roos, E.M. & Juhl, C.B. (2012) Osteoarthritis 2012 year in review: rehabilitation and outcomes. *Osteoarthritis Cartilage* **20**, 1477-1483.

269. Roughley, P.J., Nguyen, Q. & Mort, J.S. (1991) Mechanisms of proteoglycan degradation in human articular cartilage. *J Rheumatol Suppl* **27**, 52-54.

270. Ryu, J., Towle, C.A. & Treadwell, B.V. (1982) Characterisation of human articular cartilage link proteins from normal and osteoarthritic cartilage. *Ann Rheum Dis* **41**, 164-167.

271. Saamanen, A.M., Tammi, M., Kiviranta, I., Jurvelin, J. & Helminen, H.J. (1987) Maturation of proteoglycan matrix in articular cartilage under increased and decreased joint loading. A study in young rabbits. *Connect Tissue Res* **16**, 163-175.

272. Sah, R.L., Kim, Y.J., Doong, J.Y., Grodzinsky, A.J., Plaas, A.H. & Sandy, J.D. (1989) Biosynthetic response of cartilage explants to dynamic compression. *J Orthop Res* **7**, 619-636.

273. Salter, D.M., Millward-Sadler, S.J., Nuki, G. & Wright, M.O. (2001) Integrin-interleukin-4 mechanotransduction pathways in human chondrocytes. *Clin Orthop Relat Res*, S49-60.

274. Saris, D.B., Vanlauwe, J., Victor, J., Almqvist, K.F., Verdonk, R., Bellemans, J. & Luyten, F.P. (2009) Treatment of symptomatic cartilage defects of the knee: characterized chondrocyte implantation results in better clinical outcome at 36 months in a randomized trial compared to microfracture. *Am J Sports Med* **37 Suppl 1**, 10s-19s.

275. Sawaji, Y., Hynes, J., Vincent, T. & Saklatvala, J. (2008) Fibroblast growth factor 2 inhibits induction of aggrecanase activity in human articular cartilage. *Arthritis Rheum* **58**, 3498-3509.

276. Saxne, T. & Heinegard, D. (1992) Cartilage oligomeric matrix protein: a novel marker of cartilage turnover detectable in synovial fluid and blood. *Br J Rheumatol* **31**, 583-591.

277. Schmid, T.M. & Linsenmayer, T.F. (1985) Immunohistochemical localization of short chain cartilage collagen (type X) in avian tissues. *J Cell Biol* **100**, 598-605.

278. Schulz, R.M. & Bader, A. (2007) Cartilage tissue engineering and bioreactor systems for the cultivation and stimulation of chondrocytes. *Eur Biophys J* **36**, 539-568.

279. Schulze-Tanzil, G., de Souza, P., Villegas Castrejon, H., John, T., Merker, H.J., Scheid, A. & Shakibaei, M. (2002) Redifferentiation of dedifferentiated human chondrocytes in high-density cultures. *Cell Tissue Res* **308**, 371-379.

280. Schulze-Tanzil, G., Zreiqat, H., Sabat, R., Kohl, B., Halder, A., Muller, R.D. & John, T. (2009) Interleukin-10 and articular cartilage: experimental therapeutical approaches in cartilage disorders. *Curr Gene Ther* **9**, 306-315.

281. Seol, D., McCabe, D.J., Choe, H., Zheng, H., Yu, Y., Jang, K., Walter, M.W., Lehman, A.D., Ding, L., Buckwalter, J.A. & Martin, J.A. (2012) Chondrogenic progenitor cells respond to cartilage injury. *Arthritis Rheum* **64**, 3626-3637.

282. Shapiro, F., Koide, S. & Glimcher, M.J. (1993) Cell origin and differentiation in the repair of full-thickness defects of articular cartilage. *J Bone Joint Surg Am* **75**, 532-553.

283. Smith, I.D., Winstanley, J.P., Milto, K.M., Doherty, C.J., Czarniak, E., Amyes, S.G., Simpson, A.H. & Hall, A.C. (2013) Rapid in situ chondrocyte

death induced by Staphylococcus aureus toxins in a bovine cartilage explant model of septic arthritis. *Osteoarthritis Cartilage* **21**, 1755-1765.

284. Smith, R.L., Donlon, B.S., Gupta, M.K., Mohtai, M., Das, P., Carter, D.R., Cooke, J., Gibbons, G., Hutchinson, N. & Schurman, D.J. (1995) Effects of fluid-induced shear on articular chondrocyte morphology and metabolism in vitro. *J Orthop Res* **13**, 824-831.

285. Sohn, D.H., Lottman, L.M., Lum, L.Y., Kim, S.G., Pedowitz, R.A., Coutts, R.D. & Sah, R.L. (2002) Effect of gravity on localization of chondrocytes implanted in cartilage defects. *Clin Orthop Relat Res*, 254-262.

286. Steinmeyer, J., Ackermann, B. & Raiss, R.X. (1997) Intermittent cyclic loading of cartilage explants modulates fibronectin metabolism. *Osteoarthritis Cartilage* **5**, 331-341.

287. Stevens, M.M., Marini, R.P., Schaefer, D., Aronson, J., Langer, R. & Shastri, V.P. (2005) In vivo engineering of organs: the bone bioreactor. *Proc Natl Acad Sci U S A* **102**, 11450-11455.

288. Stockwell, R.A. (1967) The cell density of human articular and costal cartilage. *J Anat* **101**, 753-763.

289. Stokes, D.G., Liu, G., Coimbra, I.B., Piera-Velazquez, S., Crowl, R.M. & Jimenez, S.A. (2002) Assessment of the gene expression profile of differentiated and dedifferentiated human fetal chondrocytes by microarray analysis. *Arthritis Rheum* **46**, 404-419.

290. Strangeways, T. (1920) The nutrition of articular cartilage. *Brit Med J*, 661-663.

291. Suh, J.K., Baek, G.H., Aroen, A., Malin, C.M., Niyibizi, C., Evans, C.H. & Westerhausen-Larson, A. (1999) Intermittent sub-ambient interstitial hydrostatic pressure as a potential mechanical stimulator for chondrocyte metabolism. *Osteoarthritis Cartilage* **7**, 71-80.

292. Suzuki, T., Fujikura, K., Higashiyama, T. & Takata, K. (1997) DNA staining for fluorescence and laser confocal microscopy. *J Histochem Cytochem* **45**, 49-53.

293. Sztrolovics, R., White, R.J., Roughley, P.J. & Mort, J.S. (2002) The mechanism of aggrecan release from cartilage differs with tissue origin and the agent used to stimulate catabolism. *Biochem J* **362**, 465-472.

294. Takahashi, I., Nuckolls, G.H., Takahashi, K., Tanaka, O., Semba, I., Dashner, R., Shum, L. & Slavkin, H.C. (1998) Compressive force promotes sox9, type II collagen and aggrecan and inhibits IL-1beta expression resulting in chondrogenesis in mouse embryonic limb bud mesenchymal cells. *J Cell Sci* **111 (Pt 14)**, 2067-2076.

295. Takebe, T., Kobayashi, S., Kan, H., Suzuki, H., Yabuki, Y., Mizuno, M., Adegawa, T., Yoshioka, T., Tanaka, J., Maegawa, J. & Taniguchi, H. (2012) Human elastic cartilage engineering from cartilage progenitor cells using rotating wall vessel bioreactor. *Transplant Proc* **44**, 1158-1161.

296. Tew, S.R., Kwan, A.P., Hann, A., Thomson, B.M. & Archer, C.W. (2000) The reactions of articular cartilage to experimental wounding: role of apoptosis. *Arthritis Rheum* **43**, 215-225.

297. Tierney, C.M., Jaasma, M.J. & O'Brien, F.J. (2009) Osteoblast activity on collagen-GAG scaffolds is affected by collagen and GAG concentrations. *J Biomed Mater Res A* **91**, 92-101.

298. Torzilli, P.A. & Grigiene, R. (1998) Continuous cyclic load reduces proteoglycan release from articular cartilage. *Osteoarthritis Cartilage* **6**, 260-268.

299. Toyoda, T., Seedhom, B.B., Yao, J.Q., Kirkham, J., Brookes, S. & Bonass, W.A. (2003) Hydrostatic pressure modulates proteoglycan metabolism in chondrocytes seeded in agarose. *Arthritis Rheum* **48**, 2865-2872.

300. Ueno, T., Kagawa, T., Mizukawa, N., Nakamura, H., Sugahara, T. & Yamamoto, T. (2001) Cellular origin of endochondral ossification from grafted periosteum. *Anat Rec* **264**, 348-357.

301. Ulrich-Vinther, M., Maloney, M.D., Schwarz, E.M., Rosier, R. & O'Keefe, R.J. (2003) Articular cartilage biology. *J Am Acad Orthop Surg* **11**, 421-430.

302. Ulstein, S., Aroen, A., Rotterud, J.H., Loken, S., Engebretsen, L. & Heir, S. (2014) Microfracture technique versus osteochondral autologous transplantation mosaicplasty in patients with articular chondral lesions of the knee: a prospective randomized trial with long-term follow-up. *Knee Surg Sports Traumatol Arthrosc*.

303. Urban, J.P. (1994) The chondrocyte: a cell under pressure. *Br J Rheumatol* **33**, 901-908.

304. Urban, J.P., Hall, A.C. & Gehl, K.A. (1993) Regulation of matrix synthesis rates by the ionic and osmotic environment of articular chondrocytes. *J Cell Physiol* **154**, 262-270.

305. van Susante, J.L., Buma, P., Schuman, L., Homminga, G.N., van den Berg, W.B. & Veth, R.P. (1999) Resurfacing potential of heterologous chondrocytes suspended in fibrin glue in large full-thickness defects of femoral articular cartilage: an experimental study in the goat. *Biomaterials* **20**, 1167-1175.

306. Vanwanseele, B., Lucchinetti, E. & Stussi, E. (2002) The effects of immobilization on the characteristics of articular cartilage: current concepts and future directions. *Osteoarthritis Cartilage* **10**, 408-419.

307. Vasan, N.S. & Lash, J.W. (1977) Heterogeneity of proteoglycans in developing chick limb cartilage. *Biochem J* **164**, 179-183.

308. Vasan, N.S. & Lash, J.W. (1979) Monomeric and aggregate proteoglycans in the chondrogenic differentiation of embryonic chick limb buds. *J Embryol Exp Morphol* **49**, 47-59.

309. Villanueva, I., Weigel, C.A. & Bryant, S.J. (2009) Cell-matrix interactions and dynamic mechanical loading influence chondrocyte gene expression and bioactivity in PEG-RGD hydrogels. *Acta Biomater* **5**, 2832-2846.

310. Vincent, T., Hermansson, M., Bolton, M., Wait, R. & Saklatvala, J. (2002) Basic FGF mediates an immediate response of articular cartilage to mechanical injury. *Proc Natl Acad Sci U S A* **99**, 8259-8264.

311. Vincent, T. & Saklatvala, J. (2006) Basic fibroblast growth factor: an extracellular mechanotransducer in articular cartilage? *Biochem Soc Trans* **34**, 456-457.

312. Vincent, T.L., McLean, C.J., Full, L.E., Peston, D. & Saklatvala, J. (2007) FGF-2 is bound to perlecan in the pericellular matrix of articular cartilage, where it acts as a chondrocyte mechanotransducer. *Osteoarthritis Cartilage* **15**, 752-763.

313. von der Mark, K., Gauss, V., von der Mark, H. & Muller, P. (1977) Relationship between cell shape and type of collagen synthesised as chondrocytes lose their cartilage phenotype in culture. *Nature* **267**, 531-532.

314. von Steyern, F.V., Kristiansson, I., Jonsson, K., Mannfolk, P., Heinegard, D. & Rydholm, A. (2007) Giant-cell tumour of the knee: the condition of the cartilage after treatment by curettage and cementing. *J Bone Joint Surg Br* **89**, 361-365.

315. Wada, T. & Akizuki, S. (1987) An ultrastructural study of solid matrix in articular cartilage uner unisxial tensile stress. *J. Jpn Orthop Assn*, 61.

316. Wakitani, S., Goto, T., Young, R.G., Mansour, J.M., Goldberg, V.M. & Caplan, A.I. (1998) Repair of large full-thickness articular cartilage defects with allograft articular chondrocytes embedded in a collagen gel. *Tissue Eng* **4**, 429-444.

317. Waldman, S.D., Couto, D.C., Grynpas, M.D., Pilliar, R.M. & Kandel, R.A. (2007) Multi-axial mechanical stimulation of tissue engineered cartilage: review. *Eur Cell Mater* **13**, 66-73; discussion 73-64.

318. Wang, J.H. & Thampatty, B.P. (2006) An introductory review of cell mechanobiology. *Biomech Model Mechanobiol* **5**, 1-16.

319. Wann, A.K., Zuo, N., Haycraft, C.J., Jensen, C.G., Poole, C.A., McGlashan, S.R. & Knight, M.M. (2012) Primary cilia mediate mechanotransduction through control of ATP-induced Ca2+ signaling in compressed chondrocytes. *Faseb j* **26**, 1663-1671.

320. Watt, F.E., Ismail, H.M., Didangelos, A., Peirce, M., Vincent, T.L., Wait, R. & Saklatvala, J. (2013) Src and fibroblast growth factor 2 independently regulate signaling and gene expression induced by experimental injury to intact articular cartilage. *Arthritis Rheum* **65**, 397-407.

321. Weed, J.L. & Raber, J.M. (2005) Balancing Animal Research with Animal Well-being: Establishmen of Goals and Harmonization of Approaches. *ILAR J.* **46**, 118-128.

322. Wieland, H.A., Michaelis, M., Kirschbaum, B.J. & Rudolphi, K.A. (2005) Osteoarthritis - an untreatable disease? *Nat Rev Drug Discov* **4**, 331-344.

323. Wilk, K.E., Escamilla, R.F., Fleisig, G.S., Barrentine, S.W., Andrews, J.R. & Boyd, M.L. (1996) A comparison of tibiofemoral joint forces and electromyographic activity during open and closed kinetic chain exercises. *Am J Sports Med* **24**, 518-527.

324. Wilusz, R.E., Zauscher, S. & Guilak, F. (2013) Micromechanical mapping of early osteoarthritic changes in the pericellular matrix of human articular cartilage. *Osteoarthritis Cartilage*, 1-9.

325. Wimmer, M.A., Grad, S., Kaup, T., Hanni, M., Schneider, E., Gogolewski, S. & Alini, M. (2004) Tribology approach to the engineering and study of articular cartilage. *Tissue Eng* **10**, 1436-1445.

326. Wohl, G., Goplen, G., Ford, J., Novak, K., Hurtig, M., McPherson, R., McGann, L., Schachar, N. & Zernicke, R.F. (1998) Mechanical integrity of subchondral bone in osteochondral autografts and allografts. *Can J Surg* **41**, 228-233.

327. Wong, M., Wuethrich, P., Eggli, P. & Hunziker, E. (1996) Zone-specific cell biosynthetic activity in mature bovine articular cartilage: a new method using confocal microscopic stereology and quantitative autoradiography. *J Orthop Res* **14**, 424-432.

328. Wotton, S.F. & Duance, V.C. (1994) Type III collagen in normal human articular cartilage. *Histochem J* **26**, 412-416.

329. Wright, M., Jobanputra, P., Bavington, C., Salter, D.M. & Nuki, G. (1996) Effects of intermittent pressure-induced strain on the electrophysiology of

cultured human chondrocytes: evidence for the presence of stretch-activated membrane ion channels. *Clin Sci (Lond)* **90**, 61-71.

330. Yates, K.E., Allemann, F. & Glowacki, J. (2005) Phenotypic analysis of bovine chondrocytes cultured in 3D collagen sponges: effect of serum substitutes. *Cell Tissue Bank* **6**, 45-54.

331. Youn, I., Choi, J.B., Cao, L., Setton, L.A. & Guilak, F. (2006) Zonal variations in the three-dimensional morphology of the chondron measured in situ using confocal microscopy. *Osteoarthritis Cartilage* **14**, 889-897.

332. Zhang, Z., McCaffery, J.M., Spencer, R.G. & Francomano, C.A. (2005) Growth and integration of neocartilage with native cartilage in vitro. *J Orthop Res* **23**, 433-439.